

# Synthesis of Diverse Degradable Polymers by Redox-Switchable Iron-Based Catalysis:

Author: Ashley B. Biernesser

Persistent link: <http://hdl.handle.net/2345/bc-ir:107403>

This work is posted on [eScholarship@BC](#),  
Boston College University Libraries.

---

Boston College Electronic Thesis or Dissertation, 2017

Copyright is held by the author, with all rights reserved, unless otherwise noted.

# SYNTHESIS OF DIVERSE DEGRADABLE POLYMERS BY REDOX-SWITCHABLE IRON-BASED CATALYSIS

Ashley B. Biernesser

A dissertation  
submitted to the Faculty of  
the department of Chemistry  
in partial fulfillment  
of the requirements for the degree of  
Doctor of Philosophy

Boston College

Morrissey College of Arts and Sciences  
Graduate School

December 2016



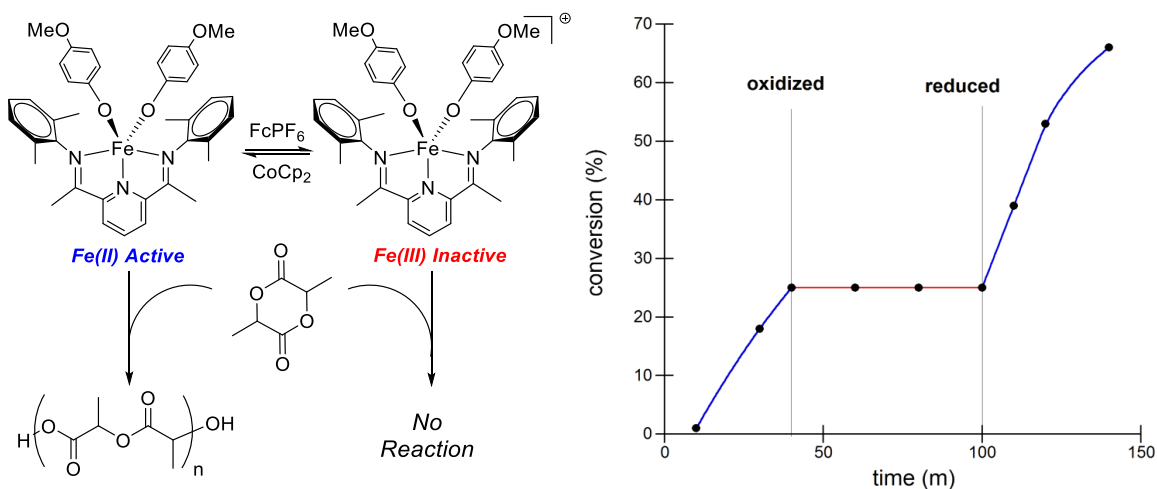
# **SYNTHESIS OF DIVERSE DEGRADABLE POLYMERS BY REDOX-SWITCHABLE IRON-BASED CATALYSIS**

Ashley B. Biernesser

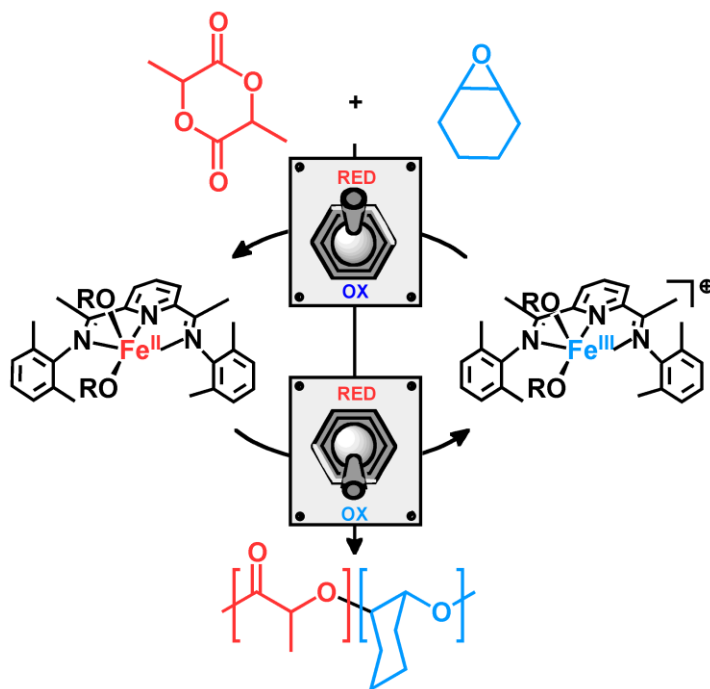
Advisor: Jeffery A. Byers

**Chapter 1.** Poly(lactic acid) (PLA) is a biodegradable polymer derived from renewable resources that has garnered much interest in recent years as an environmentally friendly substitute to conventional petroleum-derived engineering polymers. PLA has many applications in textiles, packaging, compostable consumables, and biomedical devices, as PLA displays excellent biocompatibility. This polymer is primarily produced from the ring-opening polymerization of lactide, a cyclic dimer of lactic acid. This introductory chapter highlights mechanistic features of this ring-opening polymerization reaction as well as metal-based catalysts that have been reported for lactide polymerization. In addition, switchable catalysis is an emerging field that has gained interest with polymer chemists for the potential of creating original polymer compositions and architectures. The utilization of redox-switchable catalysis to control lactide polymerization is discussed in this chapter.

**Chapter 2.** Bis(imino)pyridine iron bis(alkoxide) complexes have been synthesized and utilized in the polymerization of (*rac*)-lactide. The activities of the catalysts were particularly sensitive to the identity of the initiating alkoxide with more electron-donating alkoxides resulting in faster polymerization rates. The reaction displayed characteristics of a living polymerization with production of polymers that exhibited low molecular weight distributions, linear relationships between molecular weight and conversion, and polymer growth observed for up to fifteen sequential additions of lactide monomer to the polymerization reaction. Mechanistic experiments revealed that iron bis(aryloxy) catalysts initiate polymerization with one alkoxide ligand, while iron bis(alkylalkoxide) catalysts initiate polymerization with both alkoxide ligands. Oxidation of an iron(II) catalyst precursor lead to a cationic iron(III) bis(alkoxide) complex that was completely inactive towards lactide polymerization. When redox reactions were carried out during lactide polymerization, catalysis could be switched off and turned back on upon oxidation and reduction of the iron catalyst, respectively. In addition, preliminary investigations of copolymerization reactions of lactide with ethylene are reported.



**Chapter 3.** A cationic iron(III) complex is active for the polymerization of various epoxides, whereas the analogous neutral iron(II) complex is inactive. Cyclohexene oxide polymerization could be "switched off" upon *in situ* reduction of the Fe(III) complex and "switched on" upon *in situ* oxidation, which is orthogonal to what was observed previously for lactide polymerization. Conducting copolymerization reactions in the presence of both monomers resulted in block copolymers whose identity can be controlled by the oxidation state of the complex: selective lactide polymerization was observed in the iron(II) oxidation state and selective epoxide polymerization was observed in the iron(III) oxidation state. Evidence for the formation of block copolymers was obtained from solubility differences, GPC, and DOSY-NMR studies.



**Chapter 4.** Formally iron(I) bis(imino)pyridine monoalkoxide complexes were synthesized through protonolysis of a bis(imino)pyridine iron alkyl species with *p*-methoxyphenol or neopentyl alcohol. The resulting complexes were characterized by X-ray crystallography,  $^1\text{H}$  NMR, EPR, and Mössbauer spectroscopy, and preliminary characterization of the electronic structure of these complexes is discussed. These iron complexes were found to be highly active catalysts for the polymerization of various cyclic esters and carbonates, with the iron mono(neopentoxide) complex being much more active and giving more narrow molecular weight distributions than the mono(aryloxide) complex. The bis(imino)pyridine iron neopentoxide complex was highly active in particular for the polymerization of  $\epsilon$ -caprolactone (CL), giving full conversion within 10 minutes at room temperature in toluene, making it one of the most active iron complexes reported for this transformation ( $[\text{Fe}]:[\text{CL}] = 1:2000$ ). Comparison of the polymerization activity of these iron mono(alkoxide) complexes with the analogous iron(II) bis(alkoxide) complexes is reported.

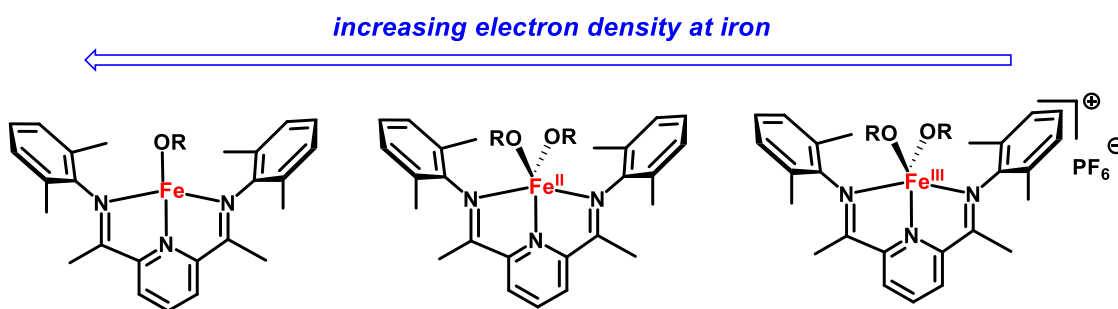


## Table of Contents

Chapter 1: Introduction .....	1
1.1 Introduction to Poly(lactic acid) and its Applications .....	1
1.2 Mechanistic Features of the Ring-Opening Polymerization of Lactide .....	3
1.2.1 Coordination-Insertion Mechanism .....	3
1.2.2 Activated-Monomer Mechanism .....	5
1.2.3 Transesterification Reactions .....	6
1.2.4 Living and Immortal Polymerization .....	7
1.3 Catalytic Systems for the Ring-Opening Polymerization of Lactide .....	9
1.3.1 Aluminum-Based Complexes .....	9
1.3.2 Zinc-Based Complexes .....	12
1.3.3 Group 2 Metal-Based Complexes .....	16
1.3.4 Gallium and Indium-Based Complexes .....	21
1.3.5 Group 14-Based Complexes .....	22
1.3.6 Transition Metal-Based Complexes .....	24
1.3.6.1 Group IV-Based Complexes .....	24
1.3.6.2 Copper-Based Complexes .....	27
1.3.6.3 Iron-Based Complexes .....	28
1.4 Switchable Polymerization Catalysis .....	31
1.4.1 Overview .....	31
1.4.2 Redox-Switchable Polymerization of Lactide .....	31
Chapter 2: Redox-Switchable Polymerization of Lactide Catalyzed by Bis(imino)pyridine Iron Bis(alkoxide) Complexes .....	42
2.1 Introduction .....	42
2.2 Synthesis of Bis(imino)pyridine) Iron Bis(alkoxide) Complexes .....	45
2.3 Lactide Polymerization with Iron(II) Bis(Imino)Pyridine Iron Alkoxide Complexes .....	51
2.4 Mechanistic Studies of Lactide Polymerization .....	54
2.4.1 Living Polymerization Studies .....	54
2.4.2 Identity of the Active Species .....	58



2.5	Redox-Controlled Lactide Polymerization.....	66
2.6	Efforts Toward Copolymerization of Lactide and Ethylene .....	71
2.6.1	Investigation of Lactide Interaction with Methylaluminoxane (MAO).....	72
2.6.2	Polymerization of Ethylene with Iron Bis(imino)pyridine Complexes in the Presence of Lactide.....	75
2.6.3	Preliminary Investigations of Transformations Necessary for Lactide-Ethylene Copolymerization .....	79
2.7	Conclusions .....	81
2.8	Experimental .....	83
Chapter 3: Redox-Switchable Copolymerization of Lactide and Epoxides Catalyzed by Bis(imino)pyridine Iron(II/III) Bis(alkoxide) Complexes .....		92
3.1	Introduction .....	92
3.2	Epoxide Polymerization with Iron(III) Bis(imino)pyridine Bis(alkoxide) Complexes.....	93
3.2.1	Epoxide Monomer Scope.....	93
3.2.2	Redox-Switchable Epoxide Polymerization .....	95
3.3	Redox-Switchable Diblock Copolymerization of Lactide and Cyclohexene Oxide .....	97
3.4	Evidence for Block Copolymer Formation .....	112
3.5	Conclusions .....	116
3.6	Experimental .....	118
Chapter 4: Exploration of Formally Iron(I) Bis(imino)pyridine Mono(alkoxide) Complexes.....		126
4.1	Introduction .....	126
4.2	Synthesis and Characterization of Bis(imino)pyridine Iron Mono(alkoxide) Complexes.....	129
4.3	Polymerization Activity of Bis(imino)pyridine Iron Aryloxide Complexes Toward Various Cyclic Esters.....	136
4.3.1	Polymerization of Lactide.....	136
4.3.2	Polymerization of $\epsilon$ -Caprolactone .....	138
4.4	Polymerization Activity of Bis(imino)pyridine Iron Neopentoxide Complexes Toward Various Cyclic Esters.....	139
4.4.1	Polymerization of Lactide.....	139
4.4.2	Polymerization of $\epsilon$ -Caprolactone .....	141

4.4.3 Polymerization of other Lactones .....	144
4.4.4 Polymerization of Cyclic Carbonates .....	146
4.5 Copolymerization of cyclic esters with bis(imino)pyridine mono(alkoxide) complexes.....	147
4.6 Conclusions .....	152
4.7 Experimental .....	155
Appendix A: X-ray Crystal Structure Data.....	166
A.1 X-ray crystal structure data from Chapter 2.....	166
A.2 X-ray crystal structure data from Chapter 4.....	173
Appendix B: NMR and $^{57}\text{Fe}$ Mössbauer Spectra.....	181
B.1 NMR Spectra from Chapter 2 .....	181
B.2 NMR Spectra from Chapter 4 .....	185
Appendix C: Additional Polymer Molecular Weight Data.....	186
C.1 Cyclohexene oxide polymerization molecular weight data from Chapter 3 .....	186
C.2 Lactide-epoxide copolymerization data from Chapter 3 .....	187
C.3 Copolymerization molecular weight data from Chapter 3 .....	191

## List of tables

<b>Table 2.1.</b> Comparison of selected bond lengths and angles for complexes <b>2.4a</b> and <b>2.5</b> . .....	50
<b>Table 2.2.</b> ( <i>rac</i> )-Lactide polymerization catalyzed by iron bis(imino)pyridine complexes. <sup>a</sup> .....	51
<b>Table 2.3.</b> Lactide Polymerization Catalyzed by <b>2.3</b> in the Presence of Various Alcohol Initiators. <sup>a</sup> .....	52
<b>Table 2.4.</b> Attempted immortal polymerization of lactide with complex <b>2.3</b> and alcohol initiators. ....	57
<b>Table 2.5.</b> Ethylene polymerization at 10 bar in the presence of lactide. ....	76
<b>Table 2.6.</b> Ethylene polymerization at 1 atm in the presence of lactide. ....	77
<b>Table 2.7.</b> Ethylene polymerization with MMAO as activator in the presence of lactide. .....	78
<b>Table 2.8.</b> Investigation of <b>2.3/4</b> -methoxyphenol as a catalyst system for ethylene polymerization.....	80
<b>Table 3.1.</b> Polymerization of epoxides catalyzed by <b>3.2</b> <sup>a</sup> .....	94
<b>Table 3.2.</b> Epoxide polymerization with various reaction conditions in attempt to achieve original reaction rate in chlorobenzene. ....	101
<b>Table 3.3.</b> Redox-controlled diblock copolymerization of ( <i>rac</i> )-lactide (L) and cyclohexene oxide (CHO) (1:1). ....	102
<b>Table 3.4.</b> Comparison of cyclohexene oxide (CHO) polymerization initiated with FcPF <sub>6</sub> and <b>3.2</b> . <sup>a</sup> .....	105
<b>Table 3.5.</b> Cyclohexene oxide polymerization initiated by various oxidants in CH <sub>2</sub> Cl <sub>2</sub> . .....	106
<b>Table 3.6.</b> Redox-controlled diblock copolymerization of ( <i>rac</i> )-lactide (L) and cyclohexene oxide (CHO) (1:1). ....	109
<b>Table 3.7.</b> Diffusion coefficients determined by DOSY-NMR for copolymers and blend of homopolymers. <sup>a</sup> .....	113
<b>Table 3.8.</b> Separation of a blend of homo-PLA and homo-PCHO by precipitation. <sup>a</sup> ....	115
<b>Table 4.1.</b> Zero-field <sup>57</sup> Fe Mössbauer parameters for synthesized iron complexes. <sup>a</sup> ....	134
<b>Table 4.2.</b> Polymerization of lactide (L) with <b>4.1a</b> and <b>4.2a</b> in chlorobenzene. <sup>a</sup> .....	137
<b>Table 4.3.</b> Polymerization of ε-caprolactone with complexes <b>4.1a</b> and <b>4.2a</b> <sup>a</sup> .....	139
<b>Table 4.4.</b> Polymerization of lactide with complexes <b>4.1b</b> and <b>4.2b</b> . ....	140
<b>Table 4.5.</b> Polymerization of ε-caprolactone (CL) with complexes <b>4.1b</b> and <b>4.2b</b> . ....	142
<b>Table 4.6.</b> Polymerization of β-butyrolactone (βBL) with complex <b>4.1b</b> . <sup>a</sup> .....	144
<b>Table 4.7.</b> Polymerization of δ-valerolactone (VL) with complexes <b>4.1b</b> and <b>4.2b</b> . <sup>a</sup> ...	145
<b>Table 4.8.</b> Polymerization of trimethylene carbonate (TMC) with complex <b>4.1b</b> . ....	146
<b>Table 4.9.</b> Attempted copolymerization of lactide (L) and ε-caprolactone (CL) in one pot. <sup>a</sup> .....	148
<b>Table 4.10.</b> Copolymerization of ε-caprolactone (CL) and δ-valerolactone (VL) with complex <b>4.1b</b> in one pot. ....	150

<b>Table A.1.</b> Crystal data and structure refinement for $[\text{Fe}(\text{PDI})(4\text{-methoxyphenoxide})_2]^+\text{PF}_6^-$ ( <b>2.5</b> ). .....	166
<b>Table A.2.</b> Bond lengths [ $\text{\AA}$ ] and angles [ $^\circ$ ] for $[\text{Fe}(\text{PDI})(4\text{-methoxyphenoxide})_2]^+\text{PF}_6^-$ ( <b>2.5</b> ) .....	167
<b>Table A.3.</b> Crystal data and structure refinement for $\text{Fe}(\text{PDI})(\text{neopentoxide})$ ( <b>4.1b</b> ) ....	173
<b>Table A.4.</b> Bond lengths [ $\text{\AA}$ ] and angles [ $^\circ$ ] for $\text{Fe}(\text{PDI})(\text{neopentoxide})$ ( <b>4.1b</b> ) .....	174
<b>Table C.1.</b> Molecular weight and dispersities over time for redox-switching cyclohexene oxide (CHO) polymerization .....	186
<b>Table C.2.</b> Lactide-epoxide copolymerization data with a 1:1 monomer ratio <sup>a</sup> ( <b>Table 3.3</b> , entry 1) .....	187
<b>Table C.3.</b> Lactide-epoxide copolymerization data with a 5:1 [L]:[CHO] ratio <sup>a</sup> ( <b>Table 3.3</b> , entry 3) .....	188
<b>Table C.4.</b> Lactide-epoxide copolymerization data with a 1:1 monomer ratio where the lactide polymerization is switched off before full conversion is reached <sup>a</sup> ( <b>Table 3.3</b> , entry 4) .....	189
<b>Table C.5.</b> Sequential lactide-epoxide copolymerization data with a 1:1 monomer ratio <sup>a</sup> ( <b>Table 3.3</b> , entry 2) .....	190
<b>Table C.6.</b> Lactide-Epoxide Copolymer molecular weight data by GPC and $^1\text{H}$ NMR	190
<b>Table C.7.</b> Epoxide-lactide copolymerization data with a 1:1 monomer ratio <sup>a</sup> ( <b>Table 3.6</b> , entry 1) .....	191
<b>Table C.8.</b> Epoxide-lactide copolymerization data with a 5:1 [L]:[CHO] ratio <sup>a</sup> ( <b>Table 3.6</b> , entry 3) .....	192
<b>Table C.9.</b> Epoxide-lactide copolymerization data with a 5:1 [L]:[CHO] ratio where the lactide polymerization is switched off before full conversion is reached <sup>a</sup> ( <b>Table 3.6</b> , entry 4) .....	193
<b>Table C.10.</b> Sequential epoxide-lactide copolymerization data with a 1:1 monomer ratio <sup>a</sup> ( <b>Table 3.6</b> , entry 2) .....	194
<b>Table C.11.</b> Copolymer molecular weight data by GPC and $^1\text{H}$ NMR .....	194

## List of figures

<b>Figure 1.1.</b> Coordination-insertion mechanism for the ring-opening polymerization of lactide. ....	4
<b>Figure 1.2.</b> Activated monomer mechanism for the ring-opening polymerization of lactide. A = Brønsted or Lewis acid. ....	5
<b>Figure 1.3.</b> Transesterification reactions compete with chain propagation, and can occur intramolecularly or intermolecularly. ....	6
<b>Figure 1.4.</b> Immortal polymerization of lactide. ....	8
<b>Figure 1.5.</b> Examples of aluminum initiators for lactide polymerization. ....	11
<b>Figure 1.6.</b> Representative zinc complexes used as catalysts for lactide polymerization. ....	13
<b>Figure 1.7.</b> Examples of magnesium complexes used for lactide polymerization. ....	18
<b>Figure 1.8.</b> Examples of calcium, strontium, and barium complexes used for lactide polymerization. ....	20
<b>Figure 1.9.</b> Representative germanium and indium complexes used for lactide polymerization. ....	22
<b>Figure 1.10.</b> Examples of group 14-based complexes for lactide polymerization. ....	23
<b>Figure 1.11.</b> Examples of group 4 metal-based complexes for lactide polymerization. ....	25
<b>Figure 1.12.</b> Representative copper-based catalyst used for lactide polymerization. ....	28
<b>Figure 1.13.</b> Examples of iron-based complexes used for lactide polymerization. ....	30
<b>Figure 1.14.</b> a) First report catalyst system for the redox-controlled polymerization of lactide. b) Plot of conversion vs. time for redox-controlled polymerization of lactide with <b>1.41</b> . c) Titanium complex <b>1.42</b> demonstrates more complete redox-switching compared to <b>1.41</b> . ....	32
<b>Figure 1.15.</b> a) Yttrium and indium complexes used for the redox-switchable polymerization of lactide. b) Plot of conversion versus time for the redox-switchable polymerization of lactide with <b>1.43a</b> . ....	33
<b>Figure 1.16.</b> Complexes that undergo redox-switchable lactide polymerization at the metal center that is also the site for catalysis. ....	34
<b>Figure 2.1.</b> Iron bis(imino)pyridine complexes have been used as catalysts for a diverse range of reactions. ....	43
<b>Figure 2.2.</b> <sup>1</sup> H NMR spectra from: a) bis(imino)pyridine iron bis(alkyl) <b>2.3</b> , b) <b>2.3</b> + 0.5 equiv. neopentyl alcohol, c) <b>2.3</b> + 1 equiv. neopentyl alcohol, d) <b>2.3</b> + 1.5 equiv. neopentyl alcohol, e) <b>2.3</b> + 2 equiv. neopentyl alcohol ( <b>2.4c</b> ). ....	47
<b>Figure 2.3.</b> X-ray structure of <b>2.4a</b> with thermal ellipsoids represented at the 50% probability level. ....	48
<b>Figure 2.4.</b> X-ray structure of <b>2.5</b> with thermal ellipsoids represented at the 50% probability level. ....	49
<b>Figure 2.5.</b> Proposed mechanism for the initiation of lactide polymerization by an iron hydride species. ....	53
<b>Figure 2.6.</b> Bis(amidinato)- <i>N</i> -heterocyclic carbene iron bis(alkoxide) complex used as a catalyst for lactide polymerization. ....	54
<b>Figure 2.7.</b> Number average molecular weight ( $M_n$ ) versus conversion for lactide polymerizations catalyzed by <b>2.3</b> /4-methoxyphenol. ....	55

<b>Figure 2.8.</b> Sequential addition of lactide to give polymers with increased molecular weight.....	56
<b>Figure 2.9.</b> Reaction rate comparison between lactide polymerizations catalyzed by 4/4-methoxyphenol (■) and Fe(py) <sub>2</sub> (CH <sub>2</sub> SiMe <sub>3</sub> ) <sub>2</sub> /4-methoxyphenol (●).....	59
<b>Figure 2.10.</b> Comparison of experimental and theoretical molecular weights with one initiating alkoxide or two initiating alkoxides per iron center. ....	60
<b>Figure 2.11.</b> Polymer propagation with a) one polymer chain and one spectator alkoxide (R = aryl) and b) two polymer chains per metal center (R = alkyl). ....	61
<b>Figure 2.12.</b> a) Methine region of the <sup>1</sup> H- <sup>1</sup> H homodecoupled NMR spectrum of poly(lactic acid) initiated by <b>2.3</b> /( <i>R</i> )-(+)-1-phenylethanol. b) Methine region of the <sup>1</sup> H- <sup>1</sup> H homodecoupled NMR spectrum of poly(lactic acid) initiated by <b>2.3</b> /neopentyl alcohol.....	63
<b>Figure 2.13.</b> Stereoselective polymerization of lactide with silanols as initiators with complex <b>2.3</b> .....	65
<b>Figure 2.14.</b> Cyclic voltammogram of complex <b>2.4a</b> . ....	68
<b>Figure 2.15.</b> Polymerization of ( <i>rac</i> )-lactide in the presence of <b>2.4a</b> over time. At the time points labeled 40 min. and 60 min., ferrocenium hexafluorophosphate and cobaltocene were added to the reaction to oxidize and reduce the metal center, respectively. ....	69
<b>Figure 2.16.</b> Polymerization of ( <i>rac</i> )-lactide in the presence of <b>2.3</b> /4-methoxyphenol with three redox switches of the catalyst.. ....	70
<b>Figure 2.17.</b> a) Conversion of lactide vs. time in the presence of 5 equivalents solid MAO (♦) or 10 wt.% MAO solution (▲) in toluene. b) Conversion of lactide vs. time in the presence of 5 equivalents (♦) or 20 equivalents (●) solid MAO.....	73
<b>Figure 2.18.</b> Lactide concentration monitored against internal standard ferrocene by <sup>1</sup> H NMR after addition of 5 equivalents MAO solution. ....	74
<b>Figure 3.1.</b> Redox-controlled polymerization of cyclohexene oxide in PhCl (0.91M) with complex <b>3.2</b> (2 mol%).....	96
<b>Figure 3.2.</b> Comparison of lactide polymerization conversion vs. time in the presence (blue) and absence (red) of cyclohexene oxide (1 equiv. relative to lactide) in PhCl (0.17M) at 24°C. ....	99
<b>Figure 3.3.</b> Representative <sup>1</sup> H NMR spectra (CDCl <sub>3</sub> ) of lactide-cyclohexene oxide diblock copolymerization.....	103
<b>Figure 3.4.</b> Representative GPC traces (RI detector) for lactide-cyclohexene oxide copolymerization.....	104
<b>Figure 3.5.</b> Representative <sup>1</sup> H NMR spectra (CDCl <sub>3</sub> ) of cyclohexene oxide-lactide diblock copolymerization.....	110
<b>Figure 3.6.</b> Representative GPC traces (RI detector) for cyclohexene oxide-lactide copolymerization .....	111
<b>Figure 3.7.</b> DOSY-NMR spectra in CDCl <sub>3</sub> of a) lactide-epoxide block copolymer b) blend of homopolymers with similar M <sub>n</sub> and [PLA]:[PCHO] and c) epoxide-lactide block copolymer.....	114
<b>Figure 3.8.</b> Complexes used by the Diaconescu group for redox-controlled copolymerization reactions. ....	118

<b>Figure 4.1.</b> Different reactivities of iron bis(imino)pyridine alkoxide complexes in different oxidation states and exploitation of complementary reactivity of lactide and epoxide polymerization for the synthesis of redox-controlled copolymers. ....	127
<b>Figure 4.2.</b> Picture of complex <b>4.1b</b> in a 0.0035M toluene solution (left) compared to complex <b>4.2b</b> in 0.0035M toluene solution (right). ....	130
<b>Figure 4.3.</b> Frozen-toluene EPR spectrum of complex <b>4.1a</b> (unpurified) in black showing simulated spectrum in red with the parameters given in the text and a Gaussian line broadening of 15 Hz. ....	131
<b>Figure 4.4.</b> Zero-field $^{57}\text{Mössbauer}$ spectra at 90K for complexes a) <b>4.1a</b> and b) <b>4.1b</b> . ..	132
<b>Figure 4.5.</b> Zero-field $^{57}\text{Mössbauer}$ spectra at 90K for complexes a) <b>4.2a</b> and b) <b>4.2b</b> . ..	133
<b>Figure 4.6.</b> X-ray crystal structure of bis(imino)pyridine iron mono(neopentoxide) complex <b>4.1b</b> . ....	135
<b>Figure 4.7.</b> Molecular weight ( $M_n$ ) vs. conversion for lactide polymerization catalyzed by <b>4.1b</b> . ....	141

## ACKNOWLEDGEMENTS

I would like to express my gratitude to those who enabled my participation in the Ph.D. program at Boston College – first, to the National Science Foundation Graduate Research Fellowship and the LaMattina Family Fellowship for Chemical Synthesis for funding my research; second, to the faculty and staff of the Boston College chemistry department; and finally, to my advisor Prof. Jeff Byers for the unique experience to be one of his first students. I have had the privilege of watching the Byers' Lab group grow, develop, and mature over the past few years into a group of talented individuals I am happy to have the opportunity to know. I particularly acknowledge Kayla Delle Chiaie, who has been an amazing friend, co-worker/author, and an integral support in both my professional and personal life. For never-ending support and encouragement, I thank my parents and my sister. Finally, to Matt Wilding, whose knowledge, love, and emotional support bolstered my research, my perseverance, and my well-being, I freely share an overwhelming feeling of gratitude.



## ABBREVIATIONS

$ \Delta E $	quadrupole splitting (Mössbauer)
$\mathcal{D}$	dispersity
$\beta$ BL	$\beta$ -butyrolactone
$\delta$	chemical shift (NMR); isomer shift (Mössbauer)
$\mu$ B	Bohr magneton
Å	angstrom
Ac	acetyl
acac	acetylacetonyl
Ar	aryl
Bu	butyl
CHO	cyclohexene oxide
CL	$\epsilon$ -caprolactone
conv	conversion
Cp	cyclopentadienyl
EPR	electron paramagnetic resonance
equiv	equivalents(s)
Et	ethyl
Fc	ferrocene
FTIR	fourier transform infrared spectroscopy
g	gram(s)
GC	gas chromatography
GPC	gel permeation chromatography
h	hour(s)
HRMS	high resolution mass spectrometry
<i>i</i> Pr	isopropyl
L	liter(s); lactide

M	molarity (mol/L)
m	milli; multiplet (NMR)
MAO	methylaluminoxane
Me	methyl
Mes	2,4,6-trimethylphenyl
min	minute(s)
MMAO	modified MAO
M <sub>n</sub>	number average molecular weight
mol	mole(s)
M <sub>w</sub>	weight average molecular weight
NMR	nuclear magnetic resonance
p	para
PCL	Poly(caprolactone)
PDI	Pyridyl diimine
Ph	phenyl
PLA	poly(lactic acid)
pyr	pyridine
RI	refractive index
s	singlet (NMR)
S	spin
SPS	solvent purification system
<sup>t</sup> Bu	<i>tert</i> -butyl
THF	tetrahydrofuran
TMC	Trimethylene carbonate
TMS	trimethylsilyl
VL	δ-valerolactone
v/v	volume/volume

# **Chapter 1: Introduction**

## **1.1 Introduction to Poly(lactic acid) and its Applications**

The increasing concern over waste disposal, environmental pollution and the depletion of petroleum resources has driven efforts to develop biodegradable alternatives to conventional petroleum-based polymers. A leading candidate in this regard is poly(lactic acid) (PLA). Derived from renewable resources such as corn and rice, PLA can degrade by hydrolytic cleavage of the ester bonds of the polymer backbone, and subsequently break down into water and carbon dioxide.<sup>1</sup>

In early stages of development, poly(lactic acid) was limited to use in biomedical devices due to high cost of production and limited polymer molecular weights.<sup>2,3</sup> The good biocompatibility of PLA makes it suitable for use in a variety of medical applications. Poly(lactic acid) medical devices can degrade slowly in the body after they fulfill their function, avoiding the need for surgery to remove implants. Many different biomedical devices have been formulated from poly(lactic acid), including dissolvable sutures, stents, and bone fixation devices. Poly(lactic acid) has also been utilized as a drug delivery agent, and its long degradation time compared to other biodegradable polymers makes it ideal for long-term controlled drug release applications.<sup>2,4</sup>

In the past two decades, technological developments have allowed for the economical production of poly(lactic acid) in high volumes and molecular weights. Enabled by these recent advancements, applications of poly(lactic acid) have been

extended to many other fields. PLA fibers have great potential to replace traditional petroleum-derived fibers and textiles due to their good dyeability, hydrophilicity, low flammability, and weather resistance. PLA has also been widely used in packaging and film applications, and for compostable consumables such as bottles, beverage cups, and utensils.<sup>2</sup> Global production capacity of poly(lactic acid) has grown drastically in recent years, and is projected to reach over 800,000 tons/year by 2020.<sup>5</sup> In addition, the global demand for poly(lactic acid) is rising rapidly, in part due to increased environmental awareness of the public.<sup>2,3</sup>

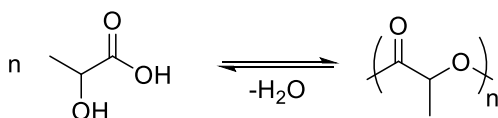
However, it should be noted that poly(lactic acid) has some drawbacks that limit its use for certain applications; mainly its brittle nature and poor thermal stability. Modifications to poly(lactic acid) have been made by adding plasticizers or blending with other polymers, but these tend to leach out from PLA during use due to poor miscibility.<sup>2,6</sup> The copolymerization of poly(lactic acid) with other monomers has also been utilized as a strategy to alter the physical properties of poly(lactic acid), as well as modify its degradation rate.<sup>1,6</sup>

The most direct synthesis of poly(lactic acid) is from the self-condensation of lactic acid in a step growth polymerization reaction (**Scheme 1.1a**).<sup>1</sup> However, it is difficult to drive these reactions to completion due to the formation of water when a lactic acid unit is added to the polymer chain, which can readily react with the lactate ester products. This can be overcome by carrying out the self-condensation reactions under neat conditions and at elevated temperatures, but typically result in low molecular weight polymer with low yields.<sup>7</sup> In addition, since all of these reactions are step growth

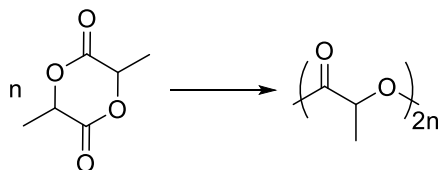
polymerizations, they are not suitable for applications that require control over molecular weight and molecular weight distributions (such as block copolymerization reactions).

**Scheme 1.1.** Methods for the synthesis of poly(lactic acid).

a) *condensation polymerization*



b) *ring-opening polymerization*



Poly(lactic acid) is primarily produced by the ring-opening polymerization of lactide, a cyclic dimer of lactic acid (**Scheme 1.1b**). Unlike the self-condensation of lactic acid, the ring-opening polymerization of lactide is a chain growth polymerization that does not liberate an equivalent of water after every insertion. Moreover, the reaction is driven towards the polymer from release of ring strain that is inherent to cyclic diesters. As a result, high molecular weight poly(lactic acid) is achievable in a controlled fashion.

## 1.2 Mechanistic Features of the Ring-Opening Polymerization of Lactide

### 1.2.1 Coordination-Insertion Mechanism

Many well-defined transition metal and main group metal catalysts proceed through a coordination-insertion mechanism for the ring-opening polymerization of lactide.<sup>1</sup> In this mechanism, coordination of lactide by a Lewis acidic metal (typically a metal alkoxide) results in electrophilic activation of the lactide for attack by the nucleophilic alkoxide group on the metal (**1.1, Figure 1.1**). This results in the formation of an intermediate that is similar to the tetrahedral intermediate commonly observed in

organic chemistry during the interconversion of carboxylic acid derivatives (**1.2**). Ring opening then occurs by collapse of this intermediate to reform an alkoxide that incorporates one unit of lactide (**1.3**). Propagation occurs by subsequent lactide coordination and alkoxide insertion until the metal-alkoxide bond is cleaved by a termination reaction.

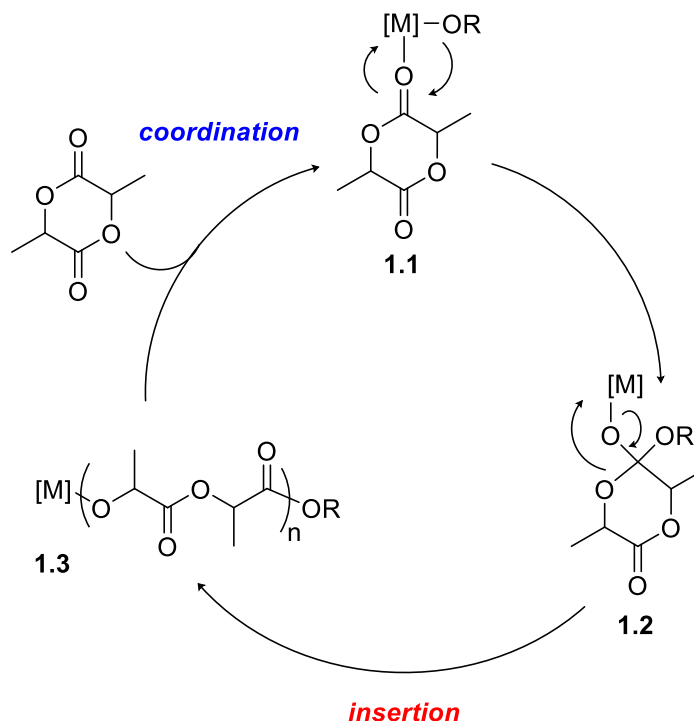


**Figure 1.1.** Coordination-insertion mechanism for the ring-opening polymerization of lactide.

As a consequence of this mechanism, poly(lactic acid) obtains an ester end group derived from the initiator. The first experimental evidence for a coordination-insertion mechanism for the ring-opening of lactide was reported by Kricheldorf<sup>8</sup> and nearly simultaneously by Dubois and coworkers.<sup>9</sup> These researchers analyzed polymer end groups by  $^1H$  and  $^{13}C$  NMR spectroscopy and utilized polymer characterization by IR

spectroscopy to confirm that the lactide ring opens through ester cleavage, and the lactide monomer inserts into the metal-alkoxide bond. A feature common to many polymerizations that proceed through a coordination-insertion mechanism is excellent control over polymer molecular weight. Many catalysts also demonstrate evidence for living polymerization or even immortal polymerization, when an excess of alcohol is used (see section 1.2.4).

### 1.2.2 Activated-Monomer Mechanism

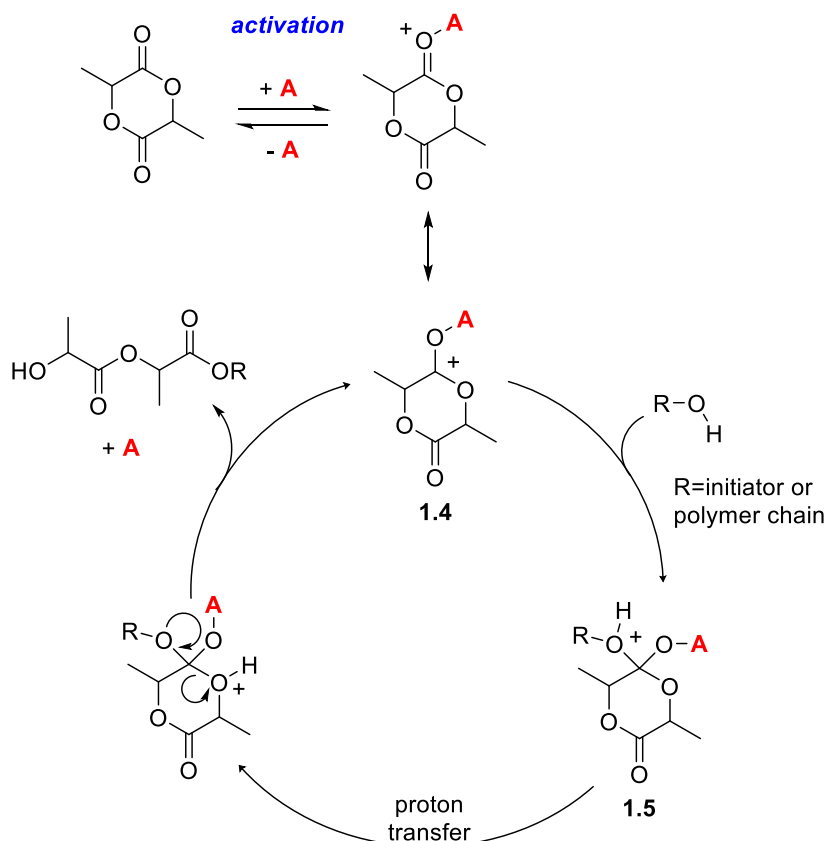


**Figure 1.2.** Activated monomer mechanism for the ring-opening polymerization of lactide. A = Brønsted or Lewis acid.

Other than the coordination-insertion mechanism, the most common mechanism invoked for lactide polymerization reactions is the activated monomer mechanism (**Figure 1.2**).<sup>10</sup> This mechanism begins with the electrophilic activation of lactide with either a Brønsted acid initiator or a Lewis acidic catalyst. Either way, an oxo-carbenium ion intermediate **1.4** is formed that serves as the activated monomer poised for nucleophilic attack. At this stage, either the initiator or the growing polymer chain attacks this oxo-carbenium ion forming the tetrahedral intermediate **1.5**. After proton transfer, collapse of this intermediate results in ring opening and incorporation of a lactide unit into the growing polymer chain. In addition to traditional Lewis acid and Brønsted acid catalysts, the activated monomer mechanisms are also proposed for guanidine type organocatalysts where hydrogen bonding to the monomer is thought to be the primary source of monomer activation.<sup>11</sup>

### 1.2.3 Transesterification Reactions

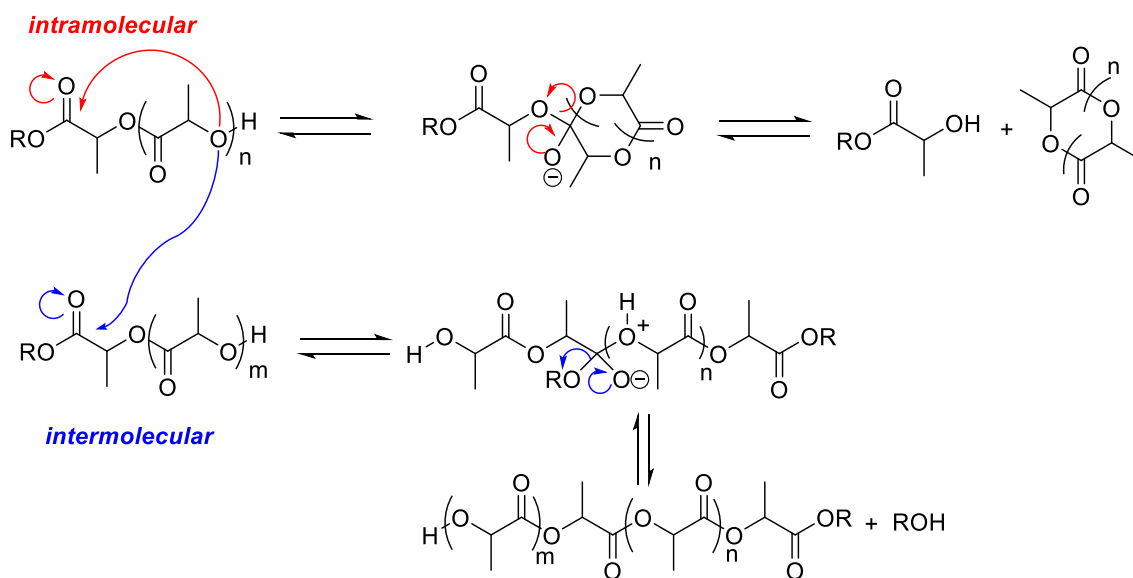


**Figure 1.3.** Transesterification reactions compete with chain propagation, and can occur intramolecularly or intermolecularly.



Side reactions that commonly occur for many lactide polymerization reactions are transesterification reactions, which predominate at high conversions and compete with chain propagation (**Figure 1.3**).<sup>1</sup> These reactions typically arise due to electrophilic activation of esters along the polymer chain rather than in the lactide monomer. Intramolecular transesterification is often called backbiting, and results in a cyclic polymeric species (or lactide, if  $n=1$ ). Intermolecular transesterification can also occur when the end of one polymer chain attacks another polymer chain that has been activated by the catalyst. The products from this side reaction are linear polymer chains of different lengths. A measurable consequence of these side reactions is polymer compositions with broad dispersities and molecular weights that do not coincide with catalyst to monomer ratios.

#### *1.2.4 Living and Immortal Polymerization*

In polymerizations where transesterification events are minimal, there is opportunity for the polymerization reaction to demonstrate living behavior.<sup>1, 12</sup> Characteristics of a living polymerization include narrow dispersity, a linear correlation between conversion and number average molecular weight, and a predictable molecular weight that is based on the monomer to catalyst ratio and the conversion of the reaction. The living characteristics that many lactide polymerization reactions demonstrate make them amenable for sequential addition of monomers, which provides a convenient way to synthesize block copolymers when lactide polymerization is combined with the ring-opening polymerization of other cyclic monomers.

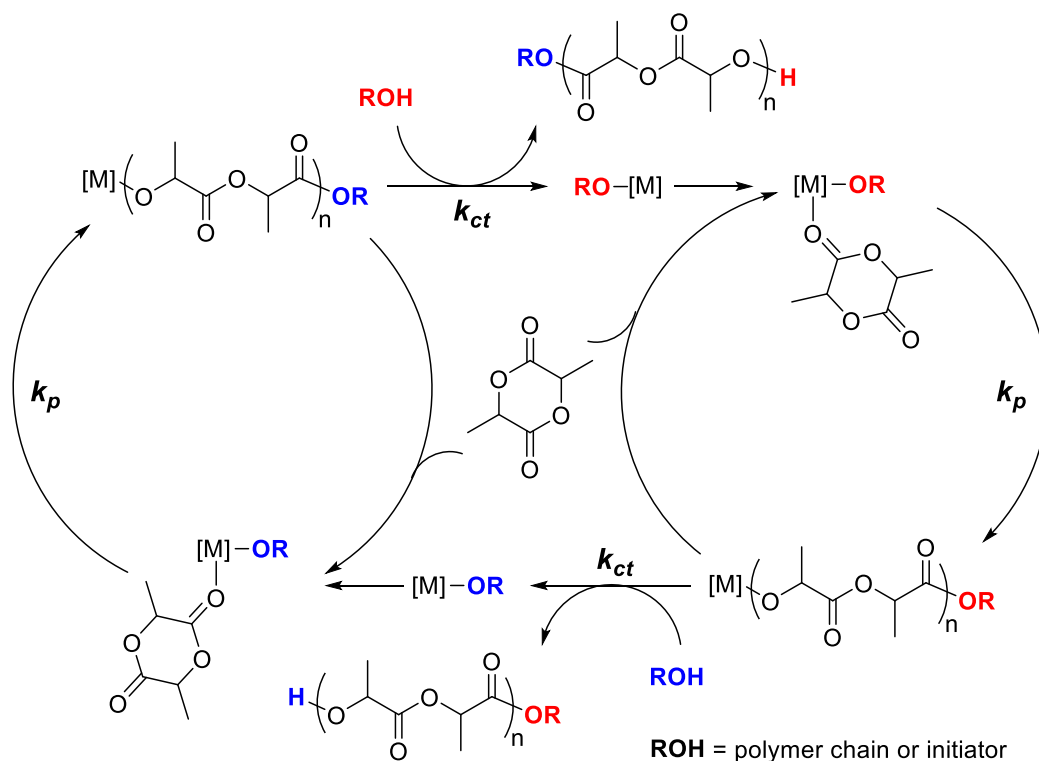


**Figure 1.4.** Immortal polymerization of lactide. More than one growing polymer chain is obtainable per metal center if chain transfer ( $k_{ct}$ ) is faster than chain propagation ( $k_p$ ).

In a living polymerization system, for every active catalyst or initiator site there is one growing polymer chain. While this feature provides excellent control over polymer molecular weight and molecular weight distribution, it limits the number of polymer molecules that can be synthesized to the number of catalyst molecules in the reaction. However, many lactide polymerization catalysts also demonstrate immortal polymerization when carried out with an excess of alcohol initiator. These reactions demonstrate molecular weights that are linearly related to the ratio between the initiator and monomer rather than the catalyst and monomer. This behavior is made possible because the alcohol initiator can undergo chain transfer reactions that liberate a polymer chain with an alcohol end group, which can enter the polymerization cycle (**Figure 1.4**).

An important requirement for immortal polymerization is that the rate of chain transfer ( $k_{ct}$ ) must be significantly faster than the rate of lactide propagation ( $k_p$ ) so as to ensure that polymers are produced with narrow dispersities.<sup>13</sup>

### 1.3 Catalytic Systems for the Ring-Opening Polymerization of Lactide

The most common commercially used catalyst for the ring-opening polymerization of lactide is tin(II) octanoate ( $\text{Sn}(\text{Oct})_2$ ). Although this complex is relatively insensitive to environmental factors, such as the presence of oxygen, it requires elevated temperatures and neat conditions to give high molecular weight polymer. Moreover, toxicity concerns remain with  $\text{Sn}(\text{Oct})_2$ .<sup>14</sup> Although the compound is approved by the U.S. Food and Drug Administration, its toxicity makes it allowable in less than 1% by weight in the polymer.<sup>15</sup> Finally, lactide polymerization catalyzed by  $\text{Sn}(\text{Oct})_2$  proceeds without control over polymer tacticity, which is important in affecting polymer properties and degradation profiles.<sup>16</sup> As a result, there has been significant effort in developing catalysts that are more active, more selective, and less toxic than the  $\text{Sn}(\text{Oct})_2$  that remains the industry standard. Many of these systems are metal-containing catalysts, of which representative and noteworthy examples are highlighted in this section. There are also many organic catalysts reported and commonly used for the polymerization of lactide that will not be discussed in this chapter.<sup>1</sup>

#### 1.3.1 Aluminum-Based Complexes

Dubois and coworkers reported the first controlled synthesis of high molecular weight poly(lactic acid) with common and widely available aluminum triisopropoxide ( $\text{Al}(\text{O}^i\text{Pr})_3$ ).<sup>17</sup> Although elevated temperatures (70 °C) were required, living

characteristics for the polymerization of (*rac*)-lactide were observed with evidence for a coordination-insertion mechanism. From the molecular weight of the polymer obtained, it was determined that each  $\text{Al}(\text{O}^i\text{Pr})_3$  initiates three poly(lactic acid) chains per metal center. Although controlled polymerization was observed, it was limited to  $M_n < 90$  kg/mol and  $[\text{lactide}]:[\text{Al}] < 1600$ , beyond which transesterification and backbiting reactions became significant. These transesterification reactions caused the dispersity to increase over time and became more prevalent as the temperature was raised. Use of  $\text{Al}(\text{O}^i\text{Pr})_3$  to initiate lactide polymerization had many advantages compared to  $\text{Sn}(\text{Oct})_2$  because it is a living polymerization rather than poorly controlled and had well-defined chain-end groups. In addition, poly(lactic acid) obtained from  $\text{Al}(\text{O}^i\text{Pr})_3$  initiator had increased thermal stability compared to poly(lactic acid) initiated by  $\text{Sn}(\text{Oct})_2$  when lactide was polymerized in the bulk. The reason for the difference is that residual aluminum decreased transesterification reactions compared to tin. While it is unclear why transesterification is slower for aluminum compared to tin, some possible reasons include more favorable interaction between the polymeric ester carbonyls and the larger tin ion, better freedom for the tin catalyst to activate the esters on the polymer chain due to it not being covalently bound to the polymer chain end, and residual octanoic acid in the tin catalyst that can serve as a Brønsted acid catalyst for the transesterification reaction.<sup>18</sup>

Because aluminum alkoxides initiated lactide polymerization with good molecular weight control, aluminum alkoxide complexes bearing different ancillary ligands were investigated to further alter polymerization characteristics. Wide success was achieved with aluminum complexes ligated with salen derivatives (e.g., **1.6**, **1.7**, **1.8**), which

resulted in controlled polymerization that occurred with enhanced reaction rates and with good stereocontrol depending on the identity of the salen ligand (**Figure 1.5**).

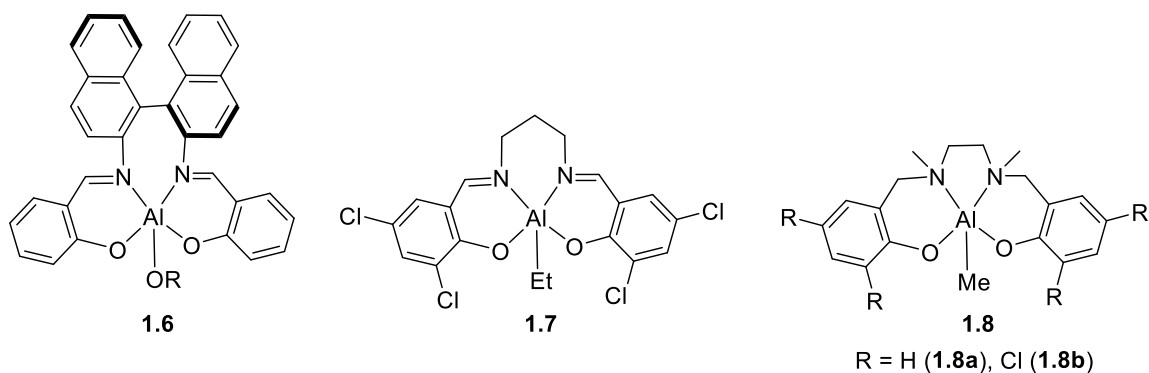


**Figure 1.5.** Examples of aluminum initiators for lactide polymerization.

Following on an initial report from Nomura,<sup>19</sup> Gibson and coworkers further delineated the structural features that salen ligands had on the rate and stereoselectivity of (*rac*)-lactide polymerization with a systematic investigation with various aluminum complexes containing salen ancillary ligands.<sup>20</sup> In general, lactide polymerization activities were enhanced with electron-withdrawing substituents (Cl, Br) installed on the phenoxide donor and with a flexible three-carbon linker between the imino donors (**1.7**); whereas lower activities were observed with sterically demanding (<sup>t</sup>Bu) substituents installed in the position ortho to oxygen in the phenoxide donor. Regarding stereochemistry, increased isoselectivity was observed with a combination of a flexible three-carbon linker between imino-nitrogen donors and a large ortho-phenoxy substituent.

A different class of tetradentate aminophenoxide ligands known as salan-type ligands were utilized by Gibson and coworkers for lactide polymerization when ligated to aluminum (**1.8, Figure 1.5**).<sup>21</sup> These aluminum complexes were colorless unlike the

highly conjugated salen-type complexes, which could be advantageous for commercial production of polymers. When combined with benzyl alcohol as an initiator, complex **1.8** was found to polymerize (*rac*)-lactide with living characteristics, and the rate of polymerization as well as the resulting microstructure could be altered by changing the substituents on the salen ligand. Changes to the phenoxide and amino moieties resulted in poly(lactic acid) ranging from highly isotactic to highly heterotactic. For example, when the phenoxide ligand was unsubstituted (**1.8a**), isotactic poly(lactic acid) was observed ( $P_m = 0.79$ ) and with 3,5-dichloro substituted phenoxide ligand (**1.8b**), heterotactic poly(lactic acid) was observed ( $P_r = 0.96$ ). This is the first time a significant change in poly(lactic acid) tacticity was observed by altering remote ligand substituents.

Although aluminum complexes have been successfully employed for lactide polymerization, elevated aluminum concentrations have been linked to Alzheimer's and other neurodegenerative diseases,<sup>22</sup> which may be problematic for poly(lactic acid) used in biomedical applications. Moreover, they are less desirable because most catalysts require elevated temperatures to achieve high reaction rates. For these reasons, more biocompatible and non-toxic metals have been sought out.

### 1.3.2 Zinc-Based Complexes

Outside of tin and aluminum-based complexes, zinc-based complexes are the most common metal-based catalyst employed for the ring opening polymerization of lactide.<sup>23</sup> Zinc(II)-based complexes are attractive due to their low toxicity, high Lewis acidity, and high stability. As a result, some of the most active catalysts that have been developed are zinc-based complexes.

By far the most common zinc-based complexes are those that incorporate mono-anionic ligands (**Figure 1.6**). Chisholm and coworkers were among the first to report discrete zinc complexes capable of undergoing the ring opening polymerization of lactide by showing that four coordinate zinc complexes supported by tris(pyrazolyl)borate ligands could be effective catalysts for L-lactide polymerization.<sup>24</sup> Sterically encumbered complexes such as **1.9** led to 90% consumption of L-lactide in 6 days at room temperature when [lactide]:[Zn] = 500:1. Molecular weights were well controlled and molecular weight distributions were narrow and consistent with a living polymerization reaction.

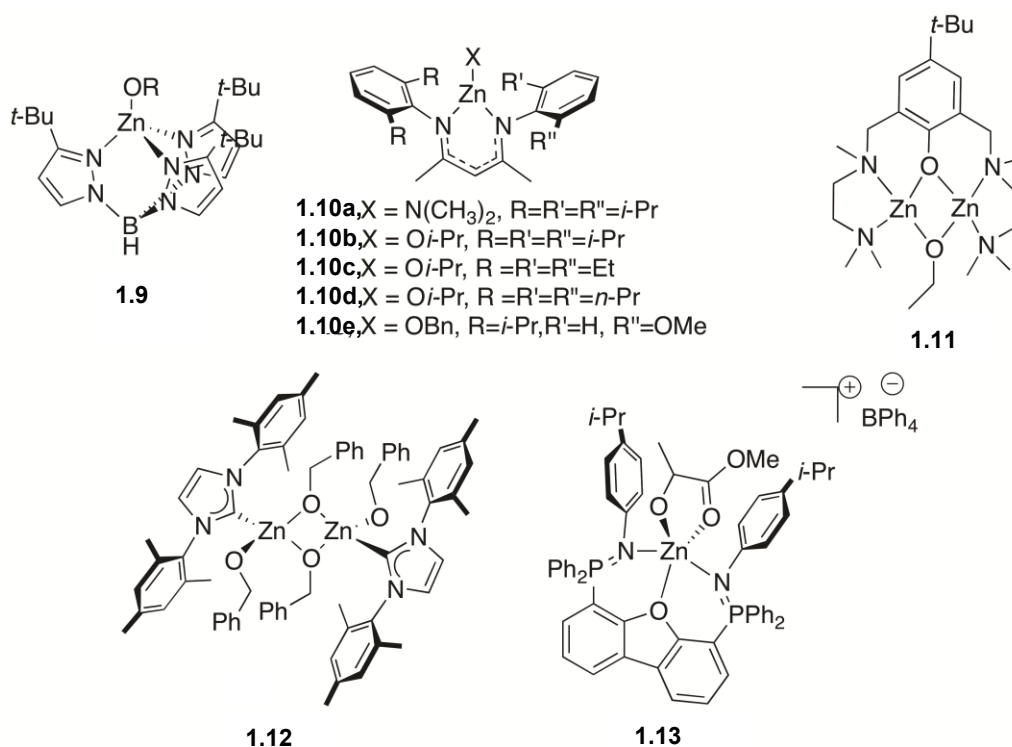


**Figure 1.6.** Representative zinc complexes used as catalysts for lactide polymerization.

Another pioneering system discovered by Coates and coworkers were zinc complexes supported by  $\beta$ -diketiminato ligands featuring a sterically encumbered 2,6-

diisopropyl aryl substituents. These ligands support three coordinate zinc(II) alkoxides or amides (**1.10**) that are in equilibrium with dimeric zinc complexes. These coordinatively unsaturated complexes proved to be good catalysts for (*rac*)-lactide polymerization.<sup>25</sup> While reaction rates with zinc amide **1.10a** were slow, the polymerization of lactide with zinc isopropoxide **1.10b** was complete in 20 minutes at room temperature at [lactide]:[Zn] = 200:1 (**Figure 1.6**). Although absolute polymer molecular weights were higher than theoretical molecular weights based on [lactide]:[Zn] and conversion, molecular weights were linearly correlated with molecular weight and dispersities were narrow ( $M_w/M_n = 1.10$ ), consistent with a living polymerization. The higher molecular weights than expected can be attributed to slower initiation relative to propagation. Further studies revealed that activity for the complex was acutely sensitive to the steric environment of the ligand with zinc complexes containing sterically less demanding  $\beta$ -diketiminato ligands giving significantly slower reaction rates. For example, zinc complex **1.10c** with a 2,6-diethylaryl substituted  $\beta$ -diketiminato ligand was one order of magnitude slower compared to **1.10b**. Nevertheless, the relationship between sterics and activity are not necessarily linearly correlated as complexes bearing 2,6-dipropylaryl substituted  $\beta$ -diketiminato ligands (**1.10d**) were slower than **1.10c**.<sup>26</sup> Further demonstrating the sophisticated relationship between stereoelectronic properties of the ligand and the activity of the catalyst was the finding that zinc complexes containing unsymmetrically substituted, electron-rich  $\beta$ -diketiminato ligands were more much more efficient catalysts. In the presence of zinc complex **1.10e**, (*rac*)-lactide underwent complete reaction in three minutes when [lactide]:[Zn] = 100:1, while maintaining excellent control over molecular weight and molecular weight distributions ( $M_w/M_n =$



1.17).<sup>27</sup> The authors hypothesized that the increased reactivity for the electron-rich ligands were due to greater liability of the alkoxide ligand thereby making it more nucleophilic for its addition to lactide.

Inspired by hydrolytic enzymes, Tollman, Hillmyer, and coworkers have developed dimeric zinc complexes containing tridentate diamine phenoxide ligands (**1.11**, **Figure 1.6**). These complexes were efficient for the polymerization of (*rac*)-lactide, leading to 90% conversion within 30 minutes at room temperature and with 300 equivalents of lactide relative to zinc.<sup>28</sup> The reactions demonstrated evidence for living polymerization and proceeded with excellent control over polymer molecular weight distributions ( $M_w/M_n = 1.19$ ). The authors carried out some kinetic studies, and favored a propagation mechanism that requires both zinc metals but could not rule out a mechanism involving one metal.

Many more mono-anionic ligands have been appended to zinc(II) to form complexes capable of undergoing the ring opening polymerization of lactide,<sup>23</sup> but less common are complexes that incorporate neutral ancillary ligands. Two systems have emerged as particularly active catalysts. The first are neutral zinc complexes that are supported by N-heterocyclic carbene ligands.<sup>29</sup> The dimeric zinc complex **1.12** (**Figure 1.6**) demonstrated excellent activity for the polymerization of (*rac*)-lactide, resulting in 98% conversion of 130 equivalents of monomer in 20 minutes at room temperature. The reaction resulted in heterotactic-biased polymer that had a different tacticity compared to analogous reactions catalyzed by free carbene. Although not conclusive, this outcome suggested that the NHC-ligand remains bound to zinc and that the reaction was not catalyzed by the free carbene. With the thinking that cationic zinc complexes would be

more Lewis acidic and therefore more reactive, Hayes and Wheaton developed cationic zinc complexes that incorporate a bis(phosphinimine) dibenzofuran ligand (Complex **1.13**, **Figure 1.6**).<sup>30</sup> These complexes proved to be efficient for the polymerization of (*rac*)-lactide leading to 90% conversion of 200 equivalents of the monomer in 50 minutes. At these catalyst loadings, the molecular weight of the polymer was predictable from [lactide]:[Zn] and conversion and molecular weight distributions were narrow ( $M_w/M_n = 1.15$ ). Molecular weights were lower than expected at lower catalyst loadings, which was attributed to chain transfer events that occur from small impurities in the monomer. On the other hand, at high catalyst loadings, significant transesterification reactions occurred, which led to characteristics inconsistent with a living polymerization such as broad dispersities and molecular weights that were not linearly correlated with the conversion of the reactions.

### 1.3.3 Group 2 Metal-Based Complexes

Complexes based on group 2 metals of magnesium, calcium, strontium, and barium have been extensively investigated for lactide polymerization because they are colorless, readily available, inexpensive, and low in toxicity.<sup>31</sup> Calcium and magnesium are biocompatible and essential for life, making them attractive candidates for lactide polymerization catalysts for the production of polymers that can be utilized for biomedical applications. Chisholm and coworkers reported well-defined magnesium complexes with tris(pyrazolyl)borate and tris(indazolyl)borate ligands for the polymerization of lactide at room temperature in dichloromethane to give 90% conversion in 60 minutes with [lactide]:[Mg] = 500:1. The polymerizations demonstrated

good control over molecular weight with linear relationships between molecular weight and monomer conversion and dispersities of 1.1-1.25.<sup>24</sup>

Magnesium complexes with  $\beta$ -diketiminate ligands have also been successfully utilized for lactide polymerization. Complex **1.14** was highly active for (*rac*)-lactide polymerization, giving full conversion within 2 minutes at 20 °C to afford atactic poly(lactic acid) with [lactide]:[Mg] = 200:1 (**Figure 1.7**).<sup>32</sup> Although the system was much more active than the analogous zinc complexes, the dispersities in this system were somewhat broad (1.59) and molecular weights were higher compared to the theoretical value based on [lactide]:[Mg] and conversion. Fortunately, the addition of 2-propanol with catalyst **1.14** also showed high activity and gave more narrow molecular weight distributions (1.2-1.35) and molecular weights more closely aligned with expected values. A magnesium tetraborohydrate  $\beta$ -diketiminate complex (**1.15**) afforded over 85% conversion of lactide in THF after 5 minutes. This polymerization showed characteristics of a living polymerization but back-biting reactions prevailed at higher conversions. The analogous calcium tetraborohydrate complex was less active (91% conversion after 90 min.).<sup>33</sup> Magnesium compounds with amino-phenolate ligands (**1.16**) were found to be active for the living polymerization of L-lactide.<sup>34</sup> Full conversion of 50 equiv. L-lactide was observed in 15 minutes in toluene at room temperature. Polymers with narrow dispersities (1.10-1.12) were obtained and a coordination-insertion mechanism was implicated. Magnesium silylamido complexes, such as **1.17** show remarkable activities, promoting the polymerization of 10,000 equivalents of (*rac*)-lactide within 15 minutes at room temperature in toluene.<sup>35</sup> High molecular weight poly(lactic acid) (>100 kg/mol)

was attainable with these low catalyst loadings, resulting in polymer with relatively narrow dispersities.

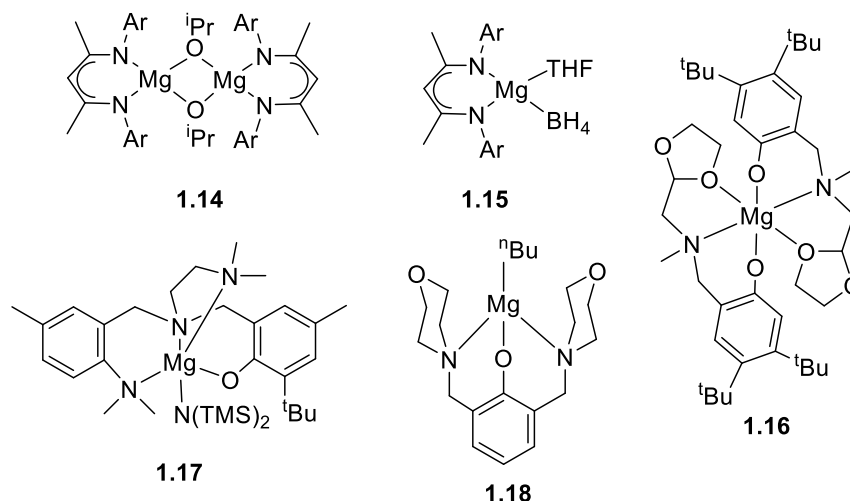


**Figure 1.7.** Examples of magnesium complexes used for lactide polymerization. Ar = 2,6-diisopropylphenyl.

The first documented example of an immortal polymerization with a magnesium catalyst was reported by Carpentier and coworkers, who utilized a bulky bis(morphalinomethyl)phenoxy ligand (**1.18**, **Figure 1.7**) to demonstrate this mode of reactivity.<sup>23</sup> With the addition of alcohol initiators, this complex demonstrated high activity. For example, the addition of 10 equivalents of isopropanol resulted in the polymerization of 1000 equivalents of L-lactide within 6 minutes in toluene at 60 °C without sacrificing the living characteristics of the polymerization reaction as was evident by the low dispersity (**1.14**).

Feijen and coworkers were among the first to have developed calcium complexes for lactide polymerization. A calcium alkoxide system generated *in situ* from  $\text{Ca}(\text{THF})_2(\text{NTMS}_2)_2$  and an alcohol proved to be an excellent route to form active

catalysts.<sup>36</sup> With isopropanol as the added alcohol, full conversion of 100 equivalents of L-lactide was observed in 35 minutes at room temperature in THF, resulting in poly(lactic acid) with a dispersity of 1.05. Due to the success of tris(pyrazolyl)borate and  $\beta$ -diketiminato complexes of magnesium for lactide polymerization, Chisholm investigated well-defined analogous calcium complexes for lactide polymerization.<sup>37</sup> With the calcium  $\beta$ -diketiminato complexes, over 90% conversion of 200 equivalents of (*rac*)-lactide was obtained within 2 hours to afford atactic poly(lactic acid) in THF at room temperature; analogous magnesium complexes gave heterotactic poly(lactic acid) within 5 minutes. Since calcium is larger than magnesium, these results suggest that the  $\beta$ -diketiminato ligand does not provide efficient steric crowding to engender stereocontrol. With the bulky tris(pyrazolyl)borate ligands, calcium complexes (**1.19**, **Figure 1.8**) were found to be highly active for lactide polymerization, with a rapid reaction rate (90% conversion within 5 minutes), albeit with broader dispersities ( $M_w/M_n = 1.7$ ).

Calcium 2,6-di-*tert*-butyl-4-methylphenoxide complexes (**1.20**, **Figure 1.8**) are highly active catalysts for the polymerization of L-lactide in toluene at room temperature when benzyl alcohol is used as an initiator.<sup>38</sup> These calcium complexes gave full conversion of lactide within a few minutes with narrow dispersities (1.08-1.17). Contrasting the  $\beta$ -diketiminato complexes, the calcium complexes afforded faster polymerization rates compared to their magnesium counterparts. For example, with [lactide]:[**1.20**]:[BnOH] = 100:0.3:1, 83% conversion was obtained after 1 minute with the calcium complex, whereas after 60 minutes, only 15% was observed with the magnesium complex.

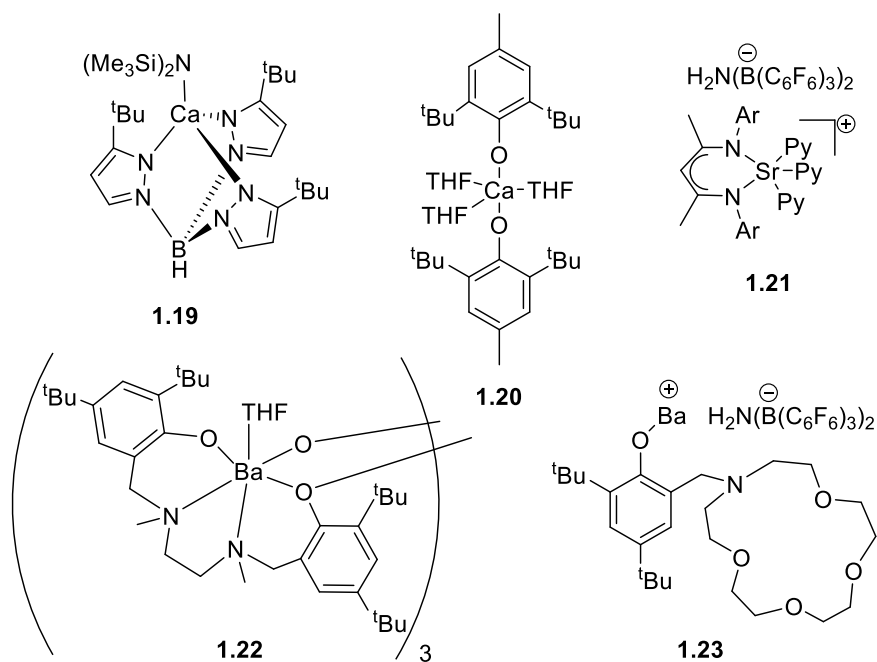


**Figure 1.8.** Examples of calcium, strontium, and barium complexes used for lactide polymerization.

There are fewer examples of lactide polymerization catalysts for the larger group 2 metals than with magnesium and calcium. This trend is in part due to the difficulty in isolating stable heteroleptic complexes of these metals, which possess Schlenk equilibria that favor homoleptic complexes. Nevertheless, a handful of examples of strontium and barium complexes have demonstrated lactide polymerization activity.  $\text{Sr}(\text{O}i\text{-Pr})(\text{NH}_2)$  was found to be an effective initiator for L-lactide polymerization at 80 °C in toluene.<sup>39</sup> Nearly full monomer conversion was obtained within three hours with dispersities of 1.57-2.26. The  $\beta$ -diketiminato class of ligands has been successful for strontium-catalyzed lactide polymerization as well. A cationic strontium  $\beta$ -diketiminato complex (**1.21**, **Figure 1.8**) was highly active for the immortal ring-opening polymerization of L-lactide with benzyl alcohol initiator.<sup>40</sup> In toluene at 30 °C with  $[\text{lactide}]:[\text{Sr}]:[\text{BnOH}] =$

1000:1:10, 82% conversion of lactide was observed in 10 minutes, with a dispersity of 1.19. If the polymerization was carried out to high conversions, the dispersity of the polymer broadened, indicating deleterious transesterification reactions. The strontium complex was much more active than the calcium analog (66% conversion in three hours), which is posited to be due to the high electrophilicity and accessibility of the larger metal center.

A trinuclear barium complex with a bulky amine bis(phenolate) ligand (**1.22**, **Figure 1.8**) was isolated and showed moderate activity for the polymerization of lactide in the melt. With [lactide]:[Ba] = 900:1, 60% conversion was observed after 3.5 hours producing polymer with a dispersity of 1.57.<sup>41</sup> A series of well-defined, cationic barium complexes (**1.23**) were investigated by Sarazin and coworkers, which showed good activity for the ring-opening polymerization of L-lactide with various nucleophilic additives.<sup>42</sup> At room temperature in dichloromethane, over 90% conversion was achieved in 30 minutes with [lactide]:[Sr] = 1000:1.

#### 1.3.4 Gallium and Indium-Based Complexes

Besides aluminum, complexes based on other group 13 metals such as gallium and indium have also shown good activity for lactide polymerization. A dialkyl gallium N-heterocyclic carbene (NHC) complex (**1.24**, **Figure 1.9**) was found to initiate the polymerization of L-lactide and (*rac*)-lactide rapidly at -20 °C in dichloromethane to afford 97% conversion in 30 minutes with a dispersity of 1.1 ([lactide]:[Ga] = 50:1).<sup>43</sup>

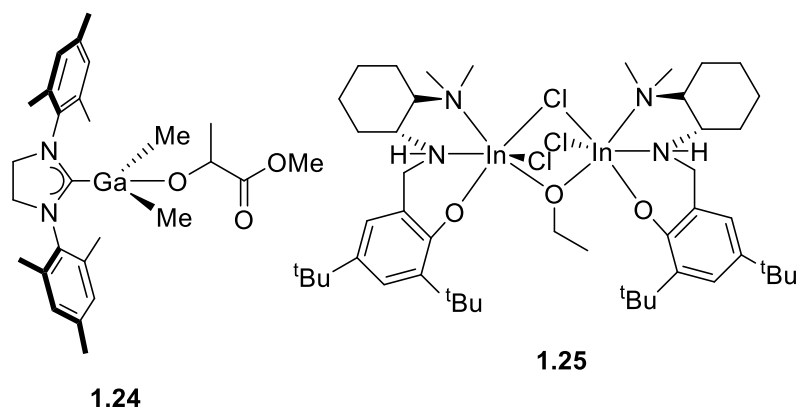


**Figure 1.9.** Representative germanium and indium complexes used for lactide polymerization.

Compared to gallium, there has been significant effort in the development of indium-based catalysts. Mehrkhodavandi and coworkers reported the first example of an indium initiator for the living polymerization of (*rac*)-lactide with a chiral dinuclear indium complex (**1.25**) that afforded good molecular weight control and rapid polymerization (>90% conversion in 30 min., [lactide]:[**1.25**] = 200:1).<sup>44</sup> Further mechanistic studies with this family of chiral dinuclear indium complexes showed that the indium complex remains dinuclear during lactide polymerization.<sup>45</sup>

### 1.3.5 Group 14-Based Complexes

Besides the industrial standard lactide polymerization catalyst  $\text{Sn}(\text{Oct})_2$ , many simple tin salts<sup>46</sup> as well as several well-defined tin complexes have been reported for lactide polymerization. Tin(II) complexes supported by  $\beta$ -diketiminato, salicylaldiminato ligands, and amidinate ligands showed living characteristics for the polymerization of (*rac*)-lactide, albeit with modest activities.<sup>47</sup> The immortal ring-opening polymerization of lactide was reported with tin complexes supported by bulky amino-ether phenolate



ligands (**1.26**, **Figure 1.10**) with isopropanol as a cocatalyst.<sup>48</sup> At 60 °C in toluene, over 80% conversion could be achieved in 90 minutes with good molecular weight control (PDI = 1.09, [lactide]:[Sn]:[iPrOH] = 1000:1:10).

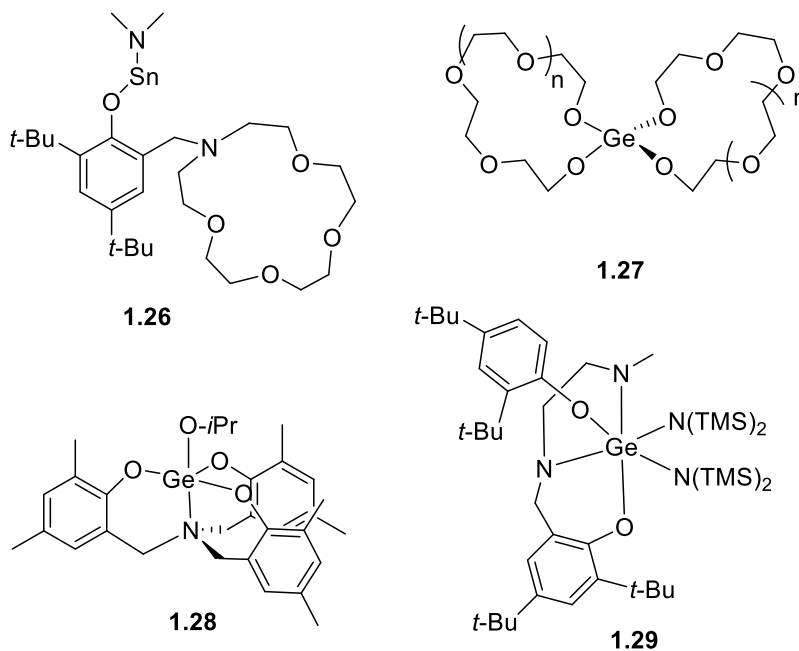


**Figure 1.10.** Examples of group 14-based complexes for lactide polymerization.

Examples of germanium complexes for lactide polymerizations are quite rare, despite germanium's enhanced electrophilicity with respect to tin and its low toxicity. Spirocyclic germanium complexes (**1.27**, **Figure 1.10**) were found to initiate L-lactide polymerization in chlorobenzene at 120 °C; however, reaction times of several days were required to reach 90% conversion.<sup>49</sup> The first reported single-site germanium alkoxide imitator for lactide polymerization is a germanium amine tris(phenolate) complex (**1.28**).<sup>50</sup> This germanium initiator showed moderate activity for the bulk polymerization of (*rac*)-lactide at 130 °C (85% conversion after 24 hours with [lactide]:[Ge] = 300:1) and afforded high selectivities for the formation of heterotactic poly(lactic acid) ( $P_r$  = 0.78-0.82). Germanium(IV) amide complexes (**1.29**) were highly active for lactide

polymerization, giving 96% conversion of lactide in 2 minutes with [LA]:[**1.31**] = 200:1, although with somewhat broad dispersities (1.4-1.9).<sup>51</sup> Interestingly, Ge(O<sup>i</sup>Pr)<sub>4</sub> showed no polymerization activity under the same conditions.

### 1.3.6 Transition Metal-Based Complexes

Of the transition metals, only group IV metals, copper, and iron-based complexes have been established as catalysts for lactide polymerization. Complexes based on manganese,<sup>52,53</sup> cobalt,<sup>52,54,55</sup> nickel,<sup>55,56</sup> chromium,<sup>57</sup> tantalum,<sup>58</sup> silver,<sup>59</sup> and gold<sup>60</sup> exist, but these systems are less studied and require further development for activities and selectivities to be on par with the other metal-based complexes for lactide polymerization.

#### 1.3.6.1 Group IV-Based Complexes

Because of their Lewis acidic properties, titanium complexes have recently drawn interest as catalysts for lactide polymerization. The first titanium alkoxide catalyst that was reported as an initiator was the tetranuclear titanium alkoxide complex (MeC(CH<sub>2</sub>-μ<sub>3</sub>-O)(CH<sub>2</sub>-μ-O)<sub>2</sub>)<sub>2</sub>Ti<sub>4</sub>(O<sup>i</sup>Pr)<sub>10</sub> that was effective for bulk and solution polymerization of (*rac*)-lactide and L-lactide.<sup>61</sup> In bulk polymerization conditions at 130 °C, nearly full conversion was achieved in 30 minutes, but transesterification reactions led to broad dispersities. Carrying out the reactions in toluene at room temperature resulted in better control over molecular weight, but required prolonged reaction times. Verkade and coworkers investigated a series of titanium alkoxides for lactide polymerization with well-defined ligand environments including amine-tris(phenolate) ligands that appeared

to operate by a coordination-insertion mechanism (**1.30**, **Figure 1.11**).<sup>62</sup> Nevertheless, the complexes were not very active, leading to long reaction times.

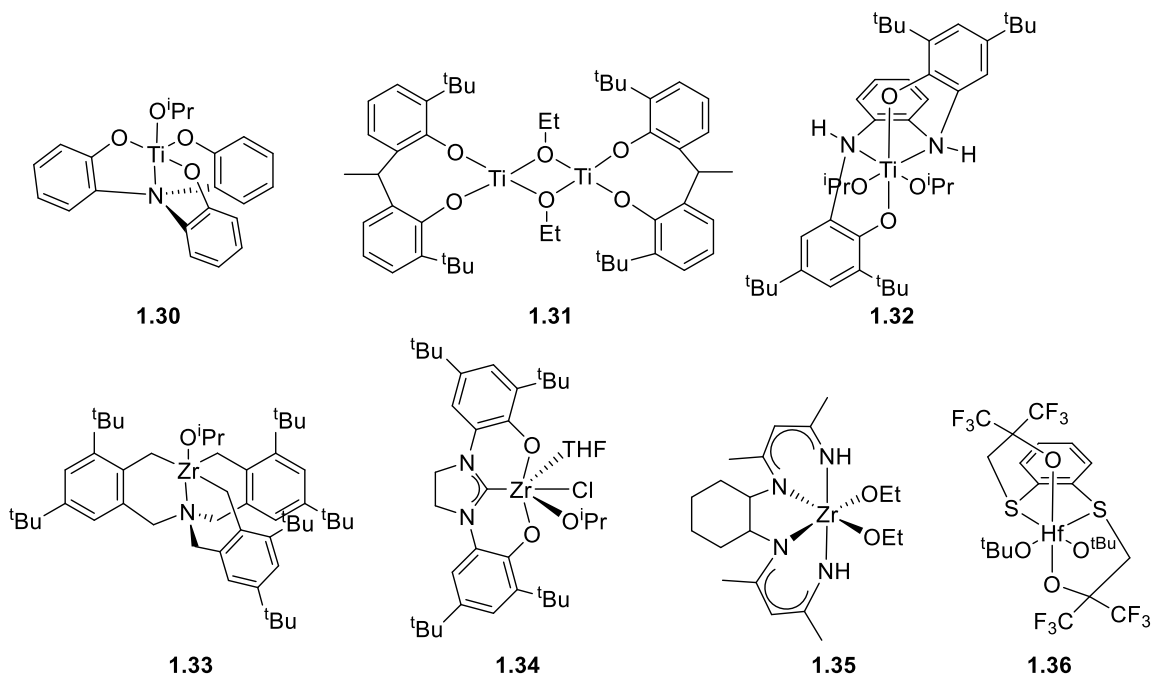


**Figure 1.11.** Examples of group 4 metal-based complexes for lactide polymerization.

Bis(aryl-oxo) titanium complexes were shown to be active for the controlled polymerization of lactide in toluene at 70 °C.<sup>63</sup> When  $[\text{Ti}_2(\mu\text{-OEt})_2(\text{edbp})_2(\text{OEt})_2]$  (**1.31**) (edbp = 2,2'-ethylenebis(4,6-*tert*-butylphenol)) was used as a catalyst, 90% conversion of lactide within 2.5 hours was observed with  $[\text{Ti}]:[\text{LA}] = 1:100$  resulting in polymer with excellent control over molecular weight distributions ( $M_w/M_n = 1.06$ ). Complex  $[\text{Ti}(\text{edbp})(\text{O}^i\text{Pr})_2]$  also gave nearly monodisperse poly(lactic acid) with slightly faster polymerization rate (98% conversion in 72 minutes). Both polymerization reactions demonstrated evidence for a coordination-insertion mechanism. Compared to other titanium complexes, titanium diamine-diphenolate complex **1.32** is one of the most active catalysts reported for the bulk polymerization of (*rac*)-lactide. Full conversion was achieved in around one minute with  $[\text{Ti}]:[\text{lactide}] = 1:300$ .<sup>64</sup>

Compared to titanium complexes, analogous zirconium and hafnium complexes often exhibit superior activities and stereoselectivities. This trend may be due to the larger ionic radius of these metals allowing for a more open coordination sphere compared to titanium. Additionally, zirconium and hafnium alkoxides may be more nucleophilic because these metals are more electropositive than titanium.<sup>65</sup>

Zirconium and hafnium salen complexes are active for bulk lactide polymerization at 140 °C, giving full conversion of 200 equivalents of lactide within an hour.<sup>66</sup> The polymerizations demonstrated living characteristics with narrow dispersities of 1.01-1.05 and a linear relationship between molecular weight and monomer conversion being observed. Zirconium and hafnium amine tris(phenolate) complexes (**1.33**) showed high reactivity and stereoselectivity for the polymerization of (*rac*)-lactide in the bulk at 130 °C.<sup>67</sup> With 300 equivalents of lactide, 95% conversion was achieved in 30 minutes. The polymerization showed living characteristics and showed promise for industrial applications where solvent-free conditions are required.

A bis-aryloxy N-heterocyclic carbene zirconium alkoxide complex (**1.34**) was found to initiate (*rac*)-lactide polymerization in dichloromethane at room temperature to give polymer with narrow dispersity ( $M_w/M_n = 1.02-1.10$ ) and high stereoselectivity ( $P_r > 0.95$ ).<sup>68</sup> Notably, the polymerization could be performed with commercial (*rac*)-lactide without purification, unlike many other lactide polymerization catalysts. Further highlighting the robustness of the zirconium complex is the ability for the catalyst to proceed in an immortal fashion. For example, benzyl alcohol added in excess of the catalyst resulted in rapid chain transfer so that up to ten polymer chains were grown per zirconium center without any detriment to polymer molecular weight distributions.

Ligands based on the popular  $\beta$ -diketiminato class of ligands have also been utilized to support zirconium for the formation of alkoxide complex **1.35**, which resulted in a highly active lactide polymerization catalyst.<sup>69</sup> In THF at room temperature, 95% monomer conversion was observed within 5 minutes ( $[\text{Zr}]:[\text{lactide}] = 1:300$ ), making it one of the most active group 4 complexes reported for lactide polymerization. Despite being active, this catalyst suffered from low stability under polymerization conditions, which resulted in the formation of bimodal molecular weight distributions.

Compared to zirconium- and titanium-based complexes, hafnium-based variants are less frequently explored. Nevertheless, hafnium dithiodiolate complexes (**1.36**) are particularly notable because they were found to be highly active for polymerization of (*rac*)-lactide in the melt. These complexes led to full consumption of 300 equivalents of lactide within one minute and consumption of 3000 equivalents of lactide within 5 minutes in melt polymerization reactions.<sup>70</sup> The hafnium-based complexes were significantly more active compared to analogous titanium and zirconium complexes.

#### 1.3.6.2 Copper-Based Complexes

Only a handful of copper complexes have been studied for lactide polymerization, but most of them provide good molecular weight control. On the other hand, many are not very active, requiring high temperatures and prolonged reaction times to reach full conversion.<sup>55,71</sup> An exception to this trend has been copper(II)  $\beta$ -diketiminato alkoxide complexes (**1.37**, **Figure 1.12**), which polymerized (*rac*)-lactide in dichloromethane at room temperature within one minute.<sup>72</sup> In addition to being active, these polymerization reactions demonstrated good control with dispersities of 1.04-1.08 and could achieve

molecular weights up to 480 kg/mol. Under immortal conditions, isopropanol acted as a chain transfer agent to give narrow dispersity polymer close to expected molecular weights. To probe the role that ligand sterics and electronics play, a series of N-alkyl and N-aryl Cu(II) diketiminate complexes were studied.<sup>73</sup> Sterically unencumbered N-alkyl ligands allowed for the synthesis of heteroleptic complexes that were highly active for lactide polymerization, giving full conversion within a few minutes and dispersities below 1.1 even under immortal conditions.

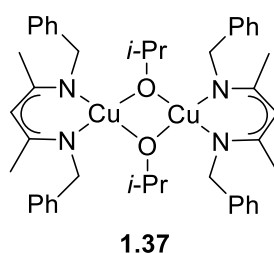


**Figure 1.12.** Representative copper-based catalyst used for lactide polymerization.

#### 1.3.6.3 Iron-Based Complexes

It is often difficult to completely remove residual catalyst from the polymer product. Therefore, it would be ideal if the catalyst residue was nontoxic and bioresorbable, especially for poly(lactic acid) used for medical and food packaging applications. Compared to many other transition metal compounds, iron can be regarded as less harmful, making it an attractive catalyst for this process.<sup>74</sup> Simple iron(III) salts such as iron acetate, iron oxides, and iron porphyrins have been shown to polymerize lactide in the melt with modest activity.<sup>75</sup> However, these reactions require prolonged reaction times and high temperatures, which can cause racemization of the lactide

monomer. Moreover, mechanistic analysis is challenging because the precatalyst structure is unknown.

The groups of Hillymer and Tolman synthesized a discrete ferric alkoxide  $\text{Fe}_5(\mu_5\text{-O})(\text{OEt})_3$  for use as a lactide polymerization catalyst.<sup>76</sup> This complex was active for the polymerization of (*rac*)-lactide in toluene at 70°C, giving 97% conversion of 450 equivalents of lactide in 21 minutes. The polymerization had living characteristics with narrow dispersities (1.17), and molecular weights that agreed with  $[\text{Fe}]:[\text{lactide}]$ . The presence of ethoxy-ester end groups by  $^1\text{H}$  NMR gave evidence for a coordination-insertion mechanism and polymerization of L-lactide produced enantiomerically enriched poly(L-lactic acid), showing that racemization of lactide does not occur. The homoleptic complex  $\text{Fe}_2(\text{OCMe}_2\text{Ph})_6$  was also highly active for lactide polymerization but gave broader dispersities (1.6).

In related examples, simple ferric alkoxides  $\text{Fe}(\text{OR})_3$  ( $\text{R} = \text{Et}, \text{Pr}, \text{iPr}, \text{OBu}$ ) were found to have modest activity for ring opening polymerization of lactide in the bulk at 130 °C.<sup>77</sup> Unlike other simple iron salts, no racemization occurred for the polymerization of L-lactide to poly(L-lactic acid). Somewhat broad dispersities were observed (1.6-1.9) with larger alkoxide ligands leading to lower molecular weights and higher molecular weight distributions. Bis-anionic Fe(II) complexes **1.38a** and **1.38b** were also found to be effective initiators for the polymerization of lactide but unlike the neutral iron(III) compounds, the reactions could be carried out at room temperature (**Figure 1.13**).<sup>78</sup> Compound **1.38a** gave 81% conversion in 60 min. with  $[\text{Fe}]:[\text{lactide}] = 200:1$  with good molecular weight control. Linear relationship between  $M_n$  and conversion and dispersities of 1.3 were observed until prolonged reaction times and higher conversions, upon which

transesterification reactions caused the molecular weight to decrease and dispersity to increase. Addition of an exogenous alcohol (EtOH) resulted in immortal polymerization behavior. Addition of carboxylic acid (PhCO<sub>2</sub>H) slowed the reaction, but simultaneously narrowed molecular weight distributions. Compound **1.38b** was also active for lactide polymerization at room temperature, but suffered from poor molecular weight control and reproducibility.

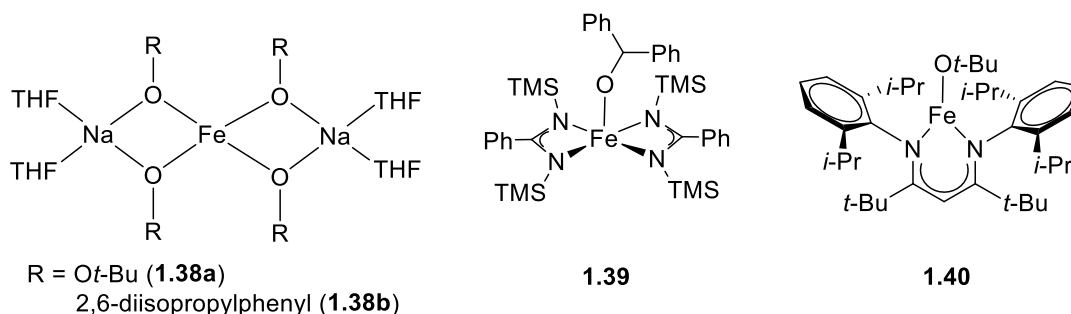


**Figure 1.13.** Examples of iron-based complexes used for lactide polymerization.

To make the iron-based complexes more tunable, several groups have investigated complexes that contained ancillary ligands. Hillmyer and Tolman have synthesized iron(III) amidinate complexes (**1.39**) that proved to be active catalysts at 70°C, polymerizing 1000 equivalents of lactide in 77 minutes. Reactions demonstrated good control over molecular weight and molecular weight distributions ( $M_w/M_n = 1.29$ ).<sup>79</sup> Gibson and coworkers reported a three-coordinate iron(II) alkoxide **1.40** with a  $\beta$ -diketiminate ligand that was highly active for lactide polymerization at room temperature in toluene, giving 94% conversion of 100 equivalents of monomer to atactic poly(lactic acid) in 20 minutes at room temperature.<sup>80</sup> The polymerization was well-controlled with dispersities of 1.12. A drawback of this system is that at high conversions (>95%), broadening of dispersity resulted from transesterification side reactions.



## 1.4 Switchable Polymerization Catalysis

### 1.4.1 Overview

The macroscopic properties of polymeric materials are highly dependent on their microstructure, including their architecture, tacticity, and composition. Although there are many techniques available to synthesize polymers of many functionalities, switchable catalysis is an emerging field in recent years that could provide access to original polymer structures. Switchable catalysis involves an external trigger that is able to “switch” the activity of a catalyst *in situ* to control its activity.<sup>81</sup>

The temporal control provided by switchable catalysts allows for many high-valued applications such as coatings, thermosets, adhesives, dental resins, and photolithography. In order for switchable catalysis to be viable, a catalyst needs to be able to switch between active and dormant states quickly and reversibly, show qualities of living polymerization in the active state, not compromise the polymerization rate after switching, and be tolerable to a wide variety of monomers and functional groups.<sup>81c</sup> A variety of external stimuli have been utilized to control the activity of polymerization catalysts, including allosteric control,<sup>82</sup> redox control,<sup>83,87-90,92,93</sup> chemical control,<sup>84</sup> electrochemical control,<sup>85</sup> and photochemical control.<sup>86</sup>

### 1.4.2 Redox-Switchable Polymerization of Lactide

Because lactide polymerization can be well controlled and show living characteristics with metal alkoxide complexes, significant effort has been devoted to controlling the activity of lactide polymerization by switchable catalysis. Particularly successful in this regard has been the development of redox-controlled polymerization of

lactide where the addition of oxidants and reductants results in reversible catalyst activation and deactivation.

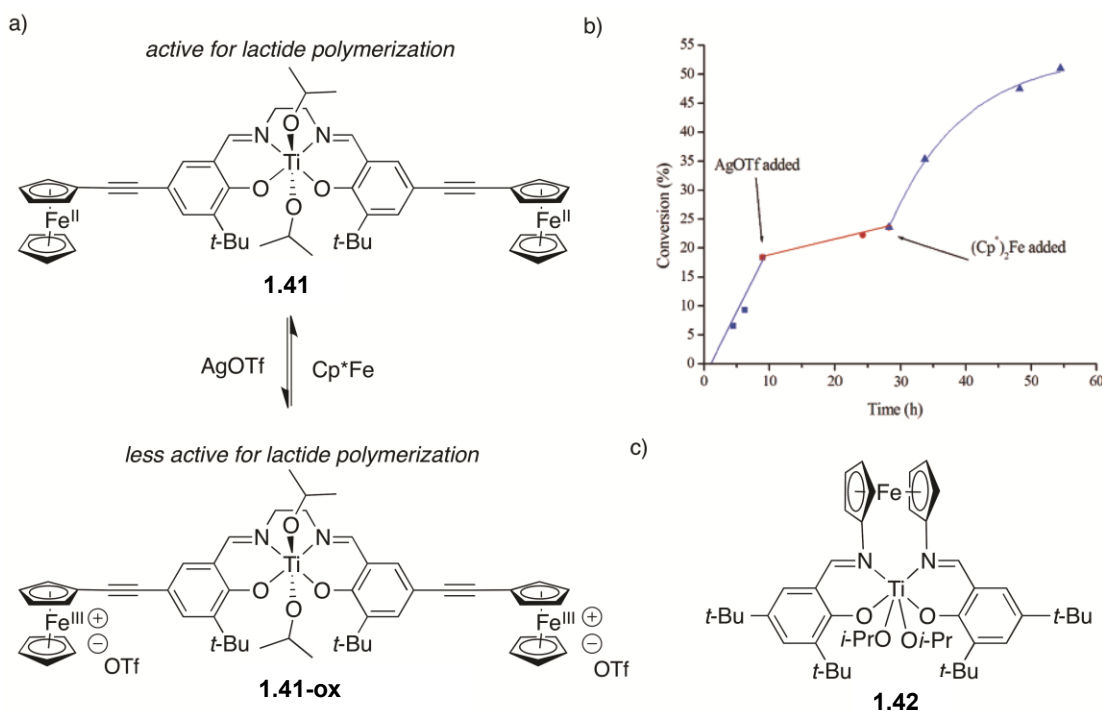


**Figure 1.14.** a) First report catalyst system for the redox-controlled polymerization of lactide. b) Plot of conversion vs. time for redox-controlled polymerization of lactide with **1.41**. Reprinted with permission from Gregson, C.K.A.; Gibson, V.C.; Long, N.J.; Marshall, E.L.; Oxford, P.J.; White, A.J.P. *J. Am. Chem. Soc.* **2006**, *128*, 7410-7411. Copyright 2006 American Chemical Society. c) Titanium complex **1.42** demonstrates more complete redox-switching compared to **1.41**.

The first example of redox-controlled polymerization was reported by Gibson and Long in 2006 who utilized titanium complex **1.41**, which features a salen ligand derivative containing a redox-active ferrocene moiety (**Figure 1.14a**).<sup>87</sup> The activity of the complex for lactide polymerization is sensitive to the oxidation state of the ferrocene moieties of the ligand. The reduced form of the catalyst catalyzed lactide polymerization approximately 30 times faster than the oxidized form, allowing for redox-switching experiments to be performed *in situ* with the addition of AgOTf oxidant to switch off the

polymerization, and decamethylferrocene reductant to resume the polymerization (**Figure 1.14b**). Although the polymerization could not be completely switched off upon oxidation of the catalyst, this seminal report inspired subsequent researchers to investigate redox-controlled lactide polymerization through the use of complexes with appended ferrocene groups. Long *et al.* investigated this further with the titanium salen complex **1.42** (**Figure 1.14c**) that positions the ferrocenyl moiety closer to the metal center showed a much more prominent redox-switch when activated for polymerization in the presence of lactide.<sup>88</sup>

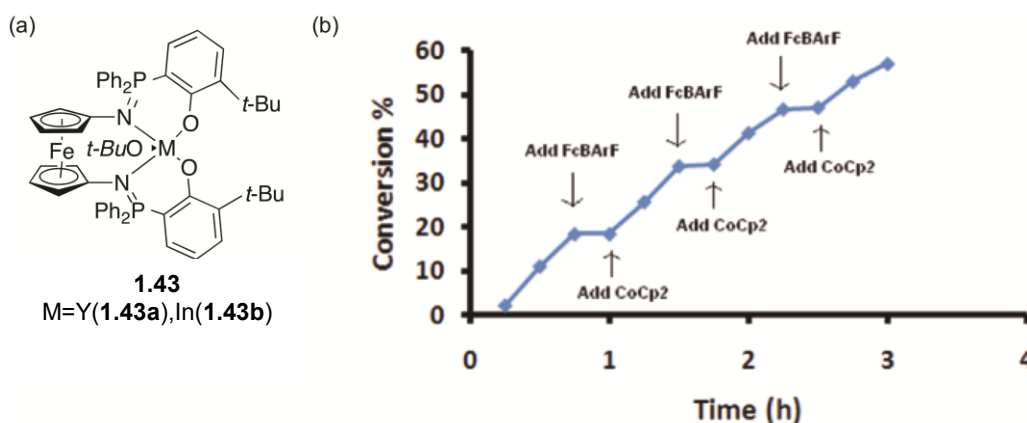


**Figure 1.15.** a) Yttrium and indium complexes used for the redox-switchable polymerization of lactide. b) Plot of conversion versus time for the redox-switchable polymerization of lactide with **1.43a**. Reprinted with permission from Broderick, E.M.; Guo, N.; Vogel, C.S.; Xu, C.; Sutter, J.; Miller, J.T.; Meyer, K.; Mehrkhodovandi, P.; Diaconescu, P.L. *J. Am. Chem. Soc.* **2011**, *133*, 9278-9281. Copyright 2011 American Chemical Society.

The Diaconescu group examined yttrium catalyst **1.43a** for redox-controlled lactide polymerization utilizing a phosfen ligand in which ferrocene was once again incorporated into the ligand backbone (**Figure 1.15**).<sup>89</sup> Lactide polymerization remained controlled after several oxidations and reductions of the catalyst *in situ*, with the active catalyst in the reduced state and inactive catalyst in the oxidized state. Oxidation of the

catalyst resulted in complete deactivation of the lactide polymerization, while subsequent catalyst reductions led to full reactivation of the polymerization catalyst. Interestingly, when the analogous indium complex was used (**1.43b**) the catalyst demonstrated the opposite reactivity, being active in the oxidized state and inactive in the reduced state.

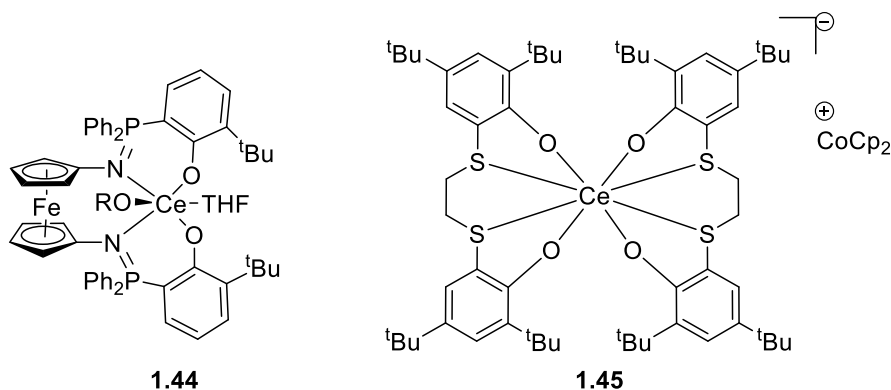


**Figure 1.16.** Complexes that undergo redox-switchable lactide polymerization at the metal center that is also the site for catalysis.

Besides altering the redox-state of the ligand to control the activity in lactide polymerization, there are a few examples where redox-switchable lactide polymerization has been observed by altering the redox state of the metal that is also the active site for polymerization catalysis (**Figure 1.16**). Several cerium-based complexes are efficient for the redox-switchable polymerization of lactide where the cerium(III) center is active for polymerization and its oxidized cerium(IV) form is deactivated for polymerization. Diaconescu et al. showed that complex **1.44** underwent oxidation at the cerium center rather than the iron center through X-ray absorption near-edge structure and Mössbauer spectroscopic studies.<sup>90</sup> The cerium complex **1.45** without a ferrocene-containing ligand was also proficient for the redox-controlled polymerization of lactide, but broader dispersities were observed ( $M_w/M_n = 2.2\text{-}2.6$ ) compared to **1.44**.<sup>91</sup> In addition, we have

developed a class of iron-based complexes for redox-switchable lactide polymerization which will be discussed in the following chapter.

---

## **References**

1. a) Dove, A.P. *Chem. Commun.* **2008**, 48, 6446-6470. b) Dechy-Cabaret, O.; Martin-Vaca, B.; Bourissou, D. *Chem. Rev.* **2004**, 104, 6147-6176. c) Mehta, R.; Kumar, V.; Bhunia, H.; Upadhyay, S.N. *J. Macromol. Sci. Polymer Rev.* **2005**, 45, 325-349.
2. Chen, Y.; Geever, L.M.; Killion, J.A.; Lyones, J.G.; Higginbotham, C.L.; Devine, D.M. *Polym. Plast. Technol. Eng.* **2016**, 55, 1057-1075.
3. Lim, L.-T.; Auras, R.; Rubino, M. *Progr. Polym. Sci.* **2008**, 33, 820-852.
4. Lasprilla, A.J.R.; Martinez, G.A.R.; Lunelli, B.H.; Jardini, A.L.; Filho, R.M. *Biotechnol. Adv.* **2012**, 1, 321-328.
5. Growth in PLA bioplastics: a production capacity of over 800,000 tonnes expected by 2020, *Bioplastics Magazine*, **2012** [Online]. Available: [http://www.bioplasticsmagazine.com/en/news/meldungen/PLA\\_Growth.php](http://www.bioplasticsmagazine.com/en/news/meldungen/PLA_Growth.php) (Accessed November 11, 2016).
6. Rasal, R.M.; Janorkar, A.V.; Hirt, D.E.. *Progr. Poly. Sci.* **2010**, 3, 338-356.
7. a) Chen, G.-X.; Kim, H.-S.; Kim, E.-S.; Yoon, J.-S. *Eur. Polym. J.* **2006**, 42, 468-472. b) Moon, S.I.; Lee, C.W.; Miyamoto, M.; Kimura, Y. *J. Polym. Sci. A Polym. Chem.* **2000**, 38, 1673-1679.
8. Kricheldorf, H.R.; Berl, M.; Scharnagl, N. *Macromolecules* **1988**, 21, 286-293.
9. Dubois, P.; Jacobs, C.; Jerome, R.; Teyssie, P. *Macromolecules* **1991**, 24, 2266-2270.
10. a) Gupta, A.P.; Kumar, V. *Eur. Polym. J.* **2007**, 43, 4053-4074. b) Garlotta, D. *J. Polym. Env.* **2001**, 9, 63-84. c) Bourissou, D.; Martin-Vaca, B.; Dumitrescu, A.; Graullier, M.; Lacombe, F. *Macromolecules* **2005**, 38, 9993-9998.
11. Chuma, A.; Horn, H.W.; Swope, W.C.; Pratt, R.C.; Zhang, L.; Lohmeijer, B.G.G.; Wade, C.G.; Waymouth, R.M.; Hedrick, J.L.; Rice, J.E. *J. Am. Chem. Soc.* **2008**, 130, 6749-6754.
12. Penczek, S.; Szymanski, R.; Duda, A.; Baran, J. *Macromol. Symp.* **2003**, 201, 261-269.

- 
13. a) Inoue, S. *J. Poly. Sci. Polym. Chem.* **2000**, *38*, 2861-2871. b) Ajellal, N.; Carpentier, J.-F.; Guillaume, C.; Guillaume, S.M.; Helou, M.; Poirier, V.; Sarazin, Y.; Trifonov, A. *Dalton Trans.* **2010**, *39*, 8362-8376.
  14. Álvarez-Chávez, C.R.; Edwards, S.; Moure-Eraso, R.; Geiser, K. *Journal of Cleaner Production*, **2012**, *23*, 47-56.
  15. CFR - Code of Federal Regulations Title 21. **(2015)** U.S. Food and Drug Administration.
  16. a) Middleton, J.C.; Tipton, A.J. *Biomaterials*, **2000**, *21*, 2335-2346. b) Chile, L.-E.; Mehrkhodavandi, P.; Hatzikiriakos, S.G. *Macromolecules*, **2016**, *49*, 909-919. c) Perego, G.; Cella, G.D. **(2010)** Mechanical Properties. In: Poly(Lactic Acid). John Wiley & Sons, Inc., pp 141-153. d) Dorgan, J.R. **(2010)** Rheology of Poly(Lactic Acid). In: Poly(Lactic Acid). John Wiley & Sons, Inc., pp 125-139.
  17. Dubois, P.; Jacobs, C.; Jerome, R.; Teyssie, P. *Macromolecules*, **1991**, *24*, 2266-2270.
  18. Degée, P.; Dubois, P.; Jérôme, R. *Macromol. Chem. Phys.* **1997**, *198*, 1985-1995.
  19. Nomura, N.; Ishii, R.; Akakura, M.; Aoi, K. *J. Am. Chem. Soc.* **2002**, *124*, 5938-5939.
  20. Hormnirun, P.; Marshall, E.L.; Gibson, V.C.; Pugh, R.I.; White, A.J.P. *Proc. Natl. Acad. Sci.* **2006**, *103*, 15343-15348.
  21. Hormnirun, P.; Marshall, E.L.; Gibson, V.C.; White, A.J.P.; Williams, D.J. *J. Am. Chem. Soc.* **2004**, *126*, 2688-2689.
  22. Kawahara, M.; Kato-Negishi, M. *Int. J. Alzheimers.* **2011**, 276393.
  23. Poirier, V.; Roisnel, T.; Carpentier, J.-F.; Sarazin, Y. *Dalton Trans.* **2009**, *44*, 9820-9827.
  24. Chisholm, M.H.; Eilerts, N.W.; Huffman, J.C.; Iyer, S.S.; Pacold, M.; Phomphrai, K. *J. Am. Chem. Soc.* **2000**, *122*, 11845-11854.
  25. Cheng, M.; Attygalle, A.B.; Lobkovsky, E.; Coates, G.W. *J. Am. Chem. Soc.* **1999**, *121*, 11583-11584.
  26. Chamberlain, B.M.; Cheng, M.; Moore, D.R.; Ovitt, T.M.; Lobkovsky, E.B.; Coates, G.W. *J. Am. Chem. Soc.* **2001**, *123*, 3229-3238.

- 
27. a) Chen, H.-Y.; Peng, Y.-L.; Huang, T.-H.; Sutar, A.K.; Miller, S.A.; Lin, C.-C. *J. Mol. Catal. A-Chem.* **2011**, 339, 61-71. b) Dove, A.P.; Gibson, V.C.; Marshall, E.L.; White, A.J.P.; Williams, D.J. *Dalton Trans.* **2004**, 570-578.
28. Williams, C.K.; Brooks, N.R.; Hillmyer, M.A.; Tolman, W.B. *Chem. Commun.* **2002**, 2132-2133.
29. Jensen, T.R.; Breyfogle, L.E.; Hillmyer, M.A.; Tolman, W.B. *Chem. Commun.* **2004**, 2504-2505.
30. Wheaton, C.A.; Hayes, P.G. *Chem. Commun.* **2010**, 46, 8404-8406.
31. Wu, J.; Yu, T.-L.; Chen, C.-T.; Lin, C.-C. *Coord. Chem. Rev.* **2006**, 250, 602-626.
32. Chamberlain, B.M.; Cheng, M.; Moore, D.R.; Ovitt, T.M.; Lobkovsky, E.B.; Coates, G.W. *J. Am. Chem. Soc.* **2001**, 123, 3229-3238.
33. Collins, R.A.; Unruangsri, J.; Mountford, P. *Dalton Trans.* **2013**, 42, 759-769.
34. Ejfler, J.; Kobylka, M.; Jerzykiewicz, L.B.; Sobota, P. *Dalton Trans.* **2005**, 11, 2047-2050.
35. Wang, L.; Ma, H. *Macromolecules* **2010**, 43, 6535-6537.
36. Zhong, Z.; Dijkstra, P.J.; Birg, C.; Westerhausen, M.; Feijen, J. *Macromolecules* **2001**, 34, 3863-3868.
37. Chisholm, M.H.; Gallucci, J.C.; Phomphrai, K. *Inorg. Chem.* **2004**, 43, 6717-6725.
38. Chen, H.-Y.; Mialon, L.; Abboud, K.A.; Miller, S.A. *Organometallics* **2012**, 43, 6717-6725.
39. Tang, Z.; Chen, X.; Liang, Q.; Bian, X.; Yang, L.; Piao, L.; Jing, X. *J. Polym. Sci. Pol. Chem.* **2003**, 41, 1934-1941.
40. Liu, B.; Dorcet, V.; Maron, L.; Carpentier, J.-F.; Sarazin, Y. *Eur. J. Inorg. Chem.* **2012**, 18, 3023-3031.
41. Davidson, M.G.; O'Hara, C.T.; Jones, M.D.; Keir, C.G.; Mahon, M.F.; Kociok-Kohn, G. *Inorg. Chem.* **2007**, 46, 7686-7688.
42. Liu, B.; Roisnel, T.; Sarazin, Y. *Inorg. Chim. Acta* **2012**, 380, 2-13.
43. Horeglad, P.; Szczepaniak, G.; Dranka, M.; Zachara, J. *Chem. Commun.* **2012**, 48, 1171-1173.

- 
44. Douglas, A.F.; Patrick, B.O.; Mehrkhodavandi, P. *Angew. Chem.* **2008**, *120*, 2322-2325.
45. Yu, I.; Acosta-Ramarez, A.; Mehrkhodavandi, P. *J. Am. Chem. Soc.* **2012**, *134*, 12758-12773.
46. a) Kowalski, A.; Libiszowski, J.; Duda, A.; Penczek, S. *Macromolecules* **2000**, *33*, 1964-1971. b) Kricheldorf, H.R.; Sumbel, M. *Eur. Polym. J.* **1989**, *25*, 585-591.
47. a) Dove, A.P.; Gibson, V.C.; Marshall, E.L.; Rzepa, H.S.; White, A.J.P.; Williams, D.J. *J. Am. Chem. Soc.* **2006**, *128*, 9834-9843. b) Nimitsiriwat, N.; Marshall, E.L.; Gibson, V.C.; Elsegood, M.R.J.; Dale, S.H. *J. Am. Chem. Soc.* **2004**, *126*, 13598-13599. c) Aubrecht, K.B.; Hillmyer, M.A.; Tolman, W.B. *Macromolecules* **2002**, *35*, 644-650.
48. Poirier, V.; Roisnel, T.; Sinbandhit, S.; Bochmann, M.; Carpentier, J.-F.; Sarazin, Y. *Chem. Eur. J.* **2012**, *18*, 2998-3013.
49. Finne, A.; Reema, Albertsson, A.-C. *J. Polym. Sci. Pol. Chem.* **2003**, *41*, 3074-3082.
50. Chmura, A.J.; Chuck, C.J.; Davidson, M.G.; Jones, M.D.; Lunn, M.D.; Bull, S.D.; Mahon, M.F. *Angew. Chem.* **2007**, *119*, 2330-2333.
51. Guo, J.; Haquette, P.; Martin, J.; Salim, K.; Thomas, C.M. *Angew. Chem. Int. Ed.* **2013**, *52*, 13584-13587.
52. Rajashekhar, B.; Chakraborty, D. *Polym. Bull.* **2014**, *71*, 2185-2203.
53. a) Idage, B.B.; Idage, S.B.; Kasegaonkar, A.S.; Jadhav, R.V. *Mater. Sci. Eng. B-Adv.* **2010**, *168*, 193-198. b) Daneshmand, P.; Schaper, F. *Dalton Trans.* **2015**, *44*, 20449-20458.
54. Breyfogle, L.E.; Williams, C.K.; Young, J.V.G.; Hillmyer, M.A.; Tolman, W.B. *Dalton Trans.* **2006**, 928-936.
55. Sun, J.; Shi, W.; Chen, D.; Liang, C. *J. Appl. Polym. Sci.* **2002**, *86*, 3312-3315.
56. Ding, L.; Jin, W.; Chu, Z.; Chen, L.; L X.; Yuan, G.; Song, J.; Fan, D.; Bao, F. *Inorg. Chem. Commun.* **2011**, *14*, 1274-1278.
57. Balasanthiran, V.; Chatterjee, C.; Chisholm, M.H.; Harrold, N.D.; RajanBabu, T.V.; Warren, G.A. *J. Am. Chem. Soc.* **2015**, *137*, 1786-1789.
58. Kim, Y.; Kapoor, P.N.; Verkade, J.G. *Inorg. Chem.* **2002**, *41*, 4834-4838.



- 
59. Samantaray, M.K.; Katiyar, V.; Pang, K.; Nanavati, H.; Ghosh, P. *J. Organomet. Chem.* **2007**, *692*, 1672-1682.
60. Ray, L.; Katiyar, V.; Barman, S.; Raihan, M.J.; Nanavati, H.; Shaikh, M.M.; Ghosh, P. *J. Organomet. Chem.* **2007**, *692*, 4259-4269.
61. Kim, Y.; Verkade, J.G. *Macromol. Rapid Comm.* **2002**, *23*, 917-921.
62. Kim, Y.; Verkade, J.G. *Macromol. Symp.* **2005**, *224*, 105-118.
63. Ejfler, J.; Kobylka, M.; Jerzykiewicz, L.B.; Sobota, P. *J. Mol. Catal. A-Chem.* **2006**, *257*, 105-111.
64. Zelikoff, A.L.; Kopilov, J.; Goldberg, I.; Coates, G.W.; Kol, M. *Chem. Commun.* **2009**, *44*, 6804-6806.
65. Sauer, A.; Kapelski, A.; Fliedel, C.; Dagorne, S.; Kol, M.; Okuda, J. *Dalton Trans.* **2012**, *42*, 9007-9023.
66. Saha, T.K.; Ramkumar, V.; Chakraborty, D. *Inorg. Chem.* **2011**, *50*, 2720-2722.
67. Chmura, A.J.; Davidson, M.G.; Frankis, C.J.; Jones, M.D.; Lunn, M.D. *Chem. Commun.* **2008**, *11*, 1293-1295.
68. Romain, C.; Heinrich, B.; Laponnaz, S.B.; Dagorne, S. *Chem. Commun.* **2012**, *48*, 2213-2215.
69. El-Zoghbi, I.; Whitehorne, T.J.J.; Schaper, F. *Dalton Trans.* **2013**, *42*, 9376-9387.
70. Sergeeva, E.; Kopilov, J.; Goldberg, I.; Kol, M. *Inorg. Chem.* **2010**, *49*, 3977-3979.
71. a) Gowda, R.R.; Chakraborty, D. *J. Mol. Catal. A-Chem.* **2011**, *349*, 86-93. b) Chen, L.-L.; Ding, L.-Q.; Zeng, C.; Long, Y.; Lü, X.-Q.; Song, J.-R.; Fan, D.-D.; Jin, W.-J. *Appl. Organomet. Chem.* **2011**, *25*, 310-316. c) John, A.; Katiyar, V.; Pang, K.; Shaikh, M.M.; Nanavati, H.; Ghosh, P. *Polyhedron* **2007**, *26*, 4033-4044.
72. Whitehorne, T.J.J.; Schaper, F. *Chem. Commun.* **2012**, *48*, 10334-10336.
73. Whitehorne, T.J.J.; Schaper, F. *Inorg. Chem.* **2013**, *52*, 13612-13622.
74. Hoppe, J.O.; Agnew Marcelli, M.G.; Tainter, M.L. *Am. J. Med. Sci.* **1955**, *230*, 558-571.

- 
75. a) Stolt, M.; Sodergard, A. *Macromolecules* **1999**, *32*, 6412-6417. b) Södergård, A.; Stolt, M. *Macromol. Symp.* **1998**, *130*, 393-402. c) Arvanitoyannis, I.; Nakayama, A.; Psomiadou, E.; Kawasaki, N.; Yamamoto, N. *Polymer* **1996**, *37*, 651-660. d) Kricheldorf, H.R.; Boettcher, C. *Die Makromol. Chem.* **1993**, *194*, 463-473. e) Kricheldorf, H.R.; Damrau, D.-O. *Macromol. Chem. Phys.* **1997**, *198*, 1767-1774.
76. O'Keefe, B.J.; Monnier, S.M.; Hillmyer, M.A.; Tolman, W.B. *J. Am. Chem. Soc.* **2000**, *123*, 339-340.
77. Wang, X.; Liao, K.; Quan, D.; Wu, Q. *Macromolecules* **2005**, *38*, 4611-4617.
78. McGuinness, D.S.; Marshall, E.L.; Gibson, V.C.; Steed, J.W. *J. Polym. Sci. A-Pol. Chem.* **2003**, *41*, 3798-3803.
79. O'Keefe, B.J.; Breyfogle, L.E.; Hillmyer, M.A.; Tolman, W.B. *J. Am. Chem. Soc.* **2002**, *124*, 4384-4393.
80. Gibson, V.C.; Marshall, E.L.; Navarro-Llobet, D.; White, A.J.P.; Williams, D.J. *J. Chem. Soc. Dalton Trans.* **2002**, *23*, 4321-4322.
81. a) Blanco, V.; Leigh, D.A.; Marcos, V. *Chem. Soc. Rev.* **2015**, *44*, 5341. b) Guillame, S.; Kirillov, E.; Sarazin, Y.; Carpentier, J.-F. *Chem. Eur. J.* **2015**, *21*, 7988. c) Leibfarth, F.A.; Mattson, K.M.; Fors, B.P.; Collins, H.A.; Hawker, C.J. *Angew. Chem. Int. Ed.* **2013**, *52*, 199.
82. Yoon, H.J.; Kuwabara, J.; Kim, J.-H.; Mirkin, C.A. *Science*, **2010**, *330*, 66.
83. Fang, Y.-Y.; Gong, W.-J.; Shang, X.-S.; Li, H.-X.; Gao, J.; Lang, J.P. *Dalton Trans.* **2014**, *43*, 8282..
84. a) Coulembier, O.; Moins, S.; Todd, R.; Dubois, P. *Macromolecules*, **2014**, *47*, 486. b) Romain, C.; C.K. Williams, *Angew. Chem. Int. Ed.*, **2014**, *53*, 1607.
85. a) Magenau, A.J.D.; Strandwitz, N.C.; Gennaro, A.; Matyjaszewski, K. *Science*, **2011**, *332*, 82. b) Plamper, F.A. *Colloid Polym. Sci.* **2014**, *292*, 777. c) Park, S.; Cho, H.Y.; Wegner, K.B.; Burdynska, J.; Magenau, A.J.D.; Paik, H.; Jurga, S.; Matyjaszewski, K. *Macromol*, **2013**, *46*, 5856. d) Li, B.; Yu, B.; Huck, W.T.S.; Liu, W.; Zhou, F. *J. Am. Chem. Soc.* **2013**, *135*, 1708.
86. a) B.P. Fors, C.J. Hawker, *Angew. Chem. Int. Ed.* **2012**, *51*, 8850. b) J.E. Poelma, B.P. Fors, C.J. Hawker et al. *Angew. Chem. Int. Ed.* **2013**, *52*, 6844. c) Xu, J.; Jung, K.; Atme, A.; Shanmugam, S.; Boyer, C. *J. Am. Chem. Soc.* **2014**, *136*, 5508. d) B. M. Neilson, C. W. Bielawski, *Chem. Commun.* **2013**, *49*, 5453.
87. Gregson, C.K.A.; Gibson, V.C.; Long, N.J.; Marshall, E.L.; Oxford, P.J.; White, A.J.P. *J. Am. Chem. Soc.* **2006**, *128*, 7410-7411.

- 
88. Brown, L.A.; Rhinehart, J.L.; Long, B.K. *ACS Catal.* **2015**, *5*, 6057-6060.
  89. Broderick, E.M.; Guo, N.; Vogel, C.S.; Xu, C.; Sutter, J.; Miller, J.T.; Meyer, K.; Mehrkhodovandi, P.; Diaconescu, P.L. *J. Am. Chem. Soc.* **2011**, *133*, 9278-9281.
  90. Broderick, E.M.; Guo, N.; Wu, T.; Vogel, C.S.; Xu, C.; Sutter, J.; Miller, J.T.; Meyer, K.; Cantat, T.; Diaconescu, P.L. *Chem. Commun.* **2011**, *47*, 9897-9899.
  91. Sauer, A.; Buffet, J.-C.; Spaniol, T.P.; Nagae, H.; Mashima, K.; Okuda, J. *ChemCatChem* **2013**, *5*, 1088-1091.

## **Chapter 2: Redox-Switchable Polymerization of Lactide Catalyzed by Bis(imino)pyridine Iron Bis(alkoxide) Complexes<sup>1</sup>**

### **2.1 Introduction**

Millions of tons of largely biologically inert polymeric materials are produced and disposed of annually. The growing amount of waste created by this practice has generated concern about the environmental impact that results from releasing large quantities of slowly degrading materials into the environment. In response to these concerns, recent research efforts have been devoted to the development of biodegradable alternatives to the useful engineering polymers used today. A leading candidate in this regard is poly(lactic acid). Derived from renewable resources such as corn starch, poly(lactic acid) (PLA) can degrade by hydrolytic cleavage of the ester bonds of the polymer backbone. This property has been exploited for several applications including textiles, fibers, packaging, and for a variety of medical materials.<sup>2</sup>

As discussed in Chapter 1.3, the ring-opening polymerization of lactide is typically catalyzed or initiated by Lewis acidic metal alkoxide complexes of tin, zinc, and aluminum. There are also several excellent nucleophilic organocatalysts, specifically those that involve N-heterocyclic carbenes.<sup>3</sup> Compared to several other transition metal catalysts, the biocompatibility and low toxicity of iron complexes makes them ideal as catalysts for this process, especially when the products are used for food packaging or as

degradable devices in the biomedical industry.<sup>4</sup> Additionally, the redox activity of iron complexes is unique compared to other catalysts typically used for lactide polymerization. Considering recent reports demonstrating how lactide polymerization can be controlled by the electronic nature of the catalyst (discussed in section 1.4),<sup>5,6,7</sup> the ability to modulate the electronic properties of the catalyst through redox reactions at the metal center provides an additional dimension for the design of active and selective catalysts. Despite these advantages, there are only a few reports documenting iron catalysts for lactide polymerization (see section 1.3.6.3), none of which address the sensitivity of the polymerization reaction to the oxidation state of iron.

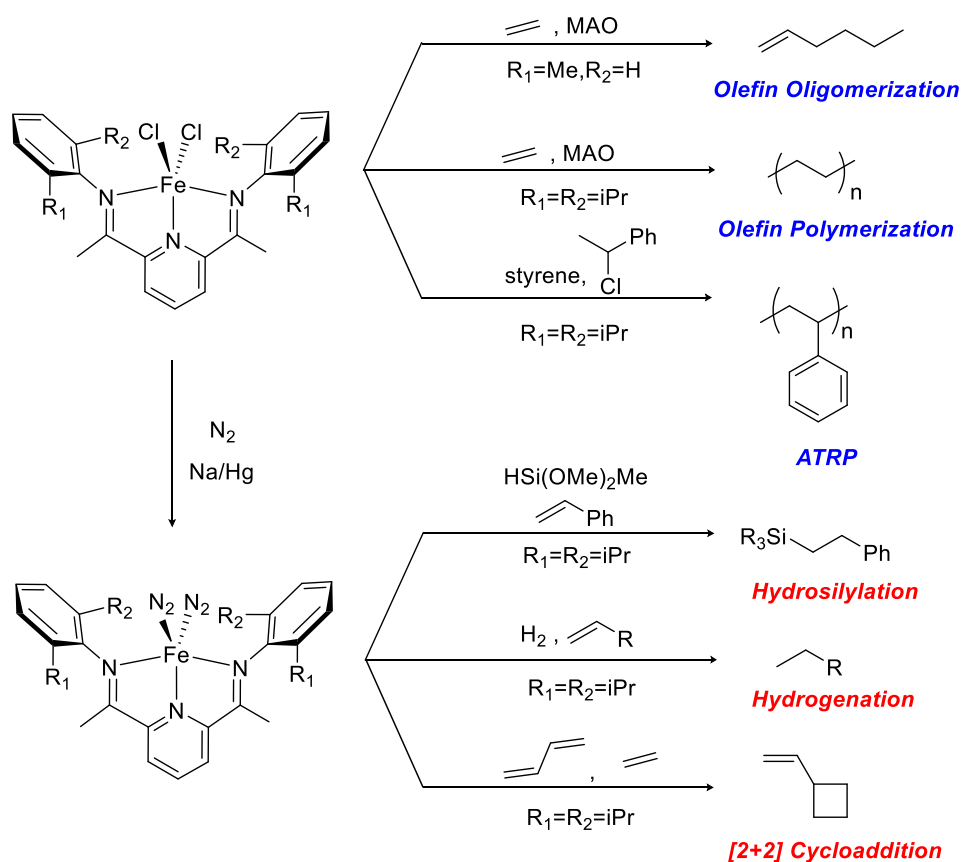
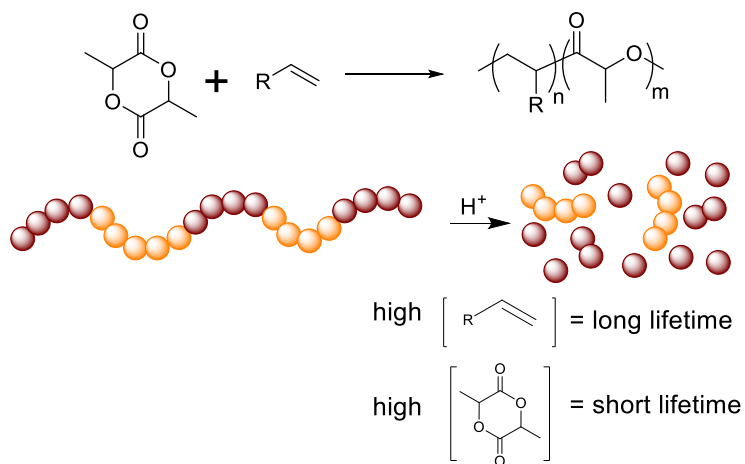


**Figure 2.1.** Iron bis(imino)pyridine complexes have been used as catalysts for a diverse range of reactions.

Considering that iron bis(imino)pyridine complexes have the ability to catalyze a wide variety of transformations including ethylene polymerization and oligomerization,<sup>8</sup> atom transfer radical polymerization,<sup>9</sup> hydrogenation and hydrosilation of alkenes,<sup>10</sup> and intermolecular [2+2] cycloadditions of alkenes,<sup>11</sup> we reasoned that they would also be good candidates as lactide polymerization catalysts (**Figure 2.1**). Due to their ability to stabilize multiple oxidation states, we also reasoned that bis(imino)pyridine complexes would be ideally suited to investigate the sensitivity of lactide polymerization to iron oxidation state. To date, no other transition metal complex containing bis(imino)pyridine ligands had ever been used as a catalyst for the ring-opening polymerization of lactide or any other cyclic ester. We report the synthesis of iron(II) bis(imino)pyridine alkoxide complexes and, for the first time, the application of a transition metal catalyst for lactide polymerization that contains this versatile class of ligand.

**Scheme 2.1.** Proposed copolymerization of lactide and  $\alpha$ -olefins.



Because these complexes have a wide range of reactivity, most notably for the polymerization of ethylene, we were also interested in these catalyst systems for the potential to synthesize copolymers of poly(lactic acid). Copolymerization of lactide with

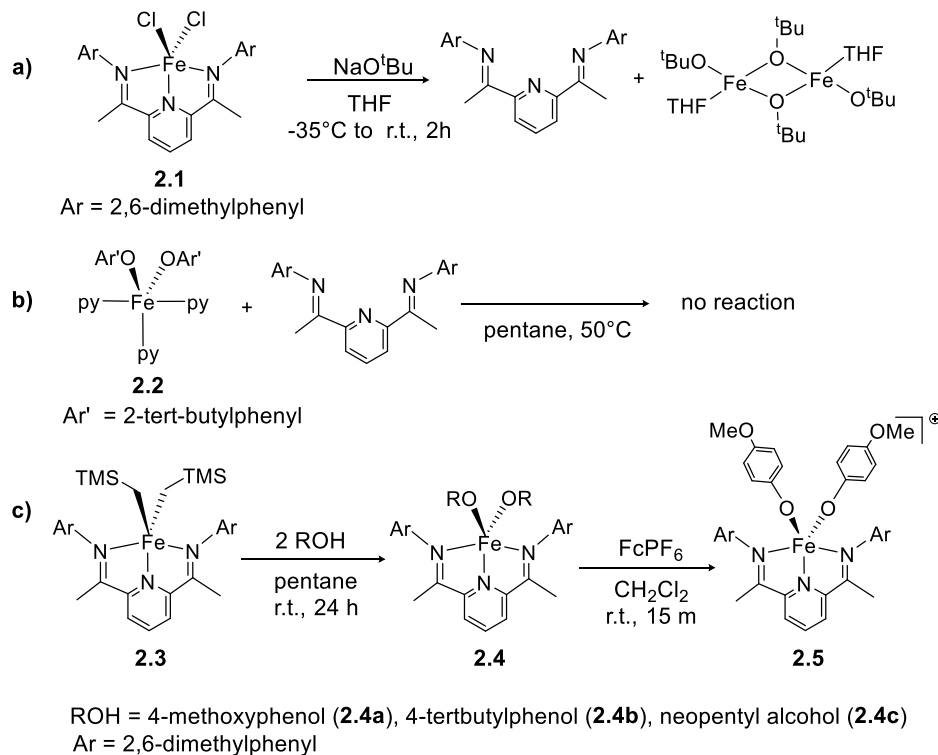
low-cost  $\alpha$ -olefins could provide a novel degradable polyolefin material. By varying the comonomer feed, polymer lifetimes could be tuned, with copolymers containing higher concentrations of lactide displaying shorter polymer lifetimes (**Scheme 2.1**). This would allow the degradation rate to be adjusted for the desired application of the polymer. In addition, this new polymer may gain some beneficial mechanical properties similar to polyolefins. Preliminary investigations into the feasibility of these types of copolymerization reactions are reported.

## 2.2 Synthesis of Bis(imino)pyridine) Iron Bis(alkoxide) Complexes

The majority of lactide polymerization catalysts are metal alkoxide complexes that produce polymer by a coordination-insertion mechanism for the enchainment of lactide monomers. Initiation typically occurs from a metal alkoxide precursor that acts simultaneously as a Lewis acid to activate the lactide monomer and as a nucleophile to initiate ring opening. Due to this precedence, we targeted bis(imino)pyridine iron bis(alkoxides) as useful precatalysts for lactide polymerization. We initially envisioned that these complexes could be synthesized through salt metathesis reactions between a bis(imino) pyridine iron dichloride complex<sup>12</sup> (**2.1**) and alkaline or alkaline earth alkoxides. However, these reactions typically lead to loss of the bis(imino)pyridine ligand and the formation of bridging alkoxide species (**Scheme 2.2a**). We also attempted to synthesize bis(imino) pyridine iron bis(alkoxide) complexes through ligand substitution reactions between the known iron alkoxide complex **2.2**<sup>13</sup> and free bis(imino)pyridine ligand (**Scheme 2.2b**). To our surprise, **2.2** was found to be largely

inert to ligand substitution reactions even after prolonged heating (24 h) at 50 °C in *n*-pentane or THF.

**Scheme 2.2.** Synthesis of Iron Bis(imino)pyridine alkoxide complexes



Ultimately we discovered that protonolysis reactions of the dialkyl complex **2.3** with various alcohols allowed for the synthesis of bis(imino)pyridine iron(II) alkoxide complexes (**2.4**) (**Scheme 2.2c**). The protonolysis reaction was general for a variety of aromatic and aliphatic alcohols producing bis(alkoxide) complexes **2.4** in high yields (86-96%). Attempts to crystallize **2.4** were unsuccessful, but some insight into the structure of the new complexes could be obtained by following the progress of the protonation reactions by <sup>1</sup>H NMR spectroscopy. Titration of an alcohol such as neopentyl alcohol into a C<sub>6</sub>D<sub>6</sub> solution of iron dialkyl **2.3** lead to the clean formation of a new paramagnetic complex after two equivalents of alcohol were added (**Scheme 2.2**). Diagnostic peaks



appeared at -174 ppm, -20 ppm, and 60 ppm (shifted from -149 ppm, -17 ppm, and 58 ppm, respectively). Concomitant with the appearance of this new species was the formation of tetramethylsilane that resulted from the protonolysis reaction (not shown in **Scheme 2.2**). Integration of the tetramethylsilane relative to the *m*-pyridine protons of the bis(imino)pyridine ligand revealed that two equivalents of tetramethylsilane were liberated upon addition of two equivalents of alcohol. These results suggested that the new species was a bis(imino)pyridine iron bis(alkoxide) iron complex **2.4c**. Solution magnetic moment measurements by means of Evans' method were in line with a high spin iron(II) complex ( $\mu_{\text{eff}} = 5.2 \mu_{\text{B}}$ ), as expected in analogy to the reported bis(imino)pyridine iron dichloride complex.

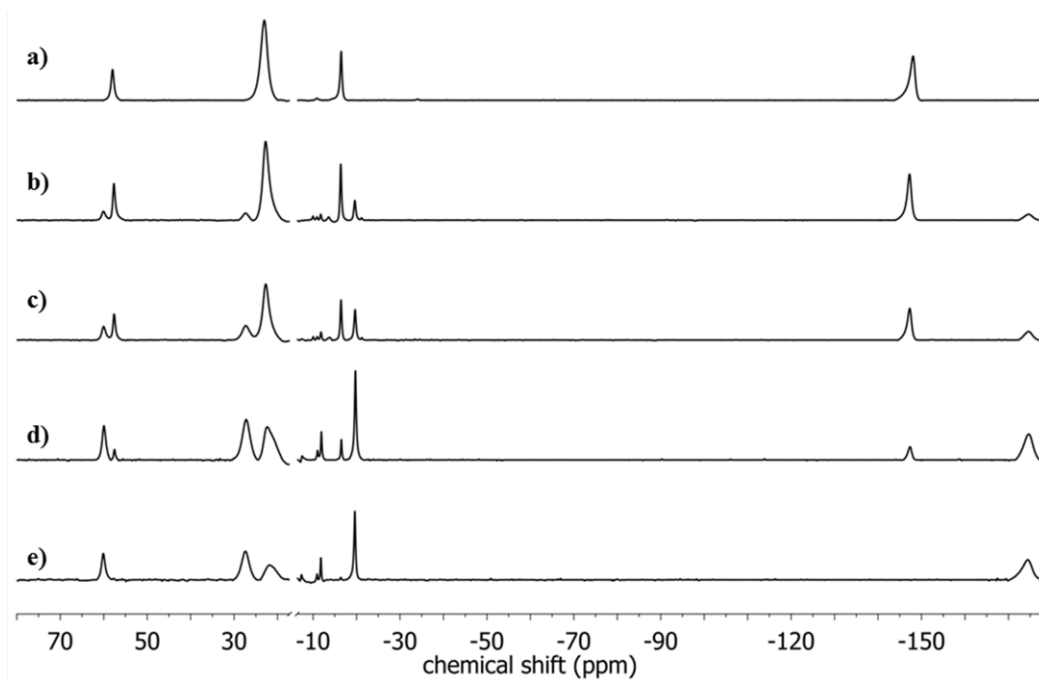


**Figure 2.2.**  $^1\text{H}$  NMR spectra from: a) bis(imino)pyridine iron bis(alkyl) **2.3**, b) **2.3** + 0.5 equiv. neopentyl alcohol, c) **2.3** + 1 equiv. neopentyl alcohol, d) **2.3** + 1.5 equiv. neopentyl alcohol, e) **2.3** + 2 equiv. neopentyl alcohol (**2.4c**). The region of the NMR spectra between -10 and 20 ppm is omitted for clarity.

Although the protonolysis reaction proceeded cleanly to a new species as monitored by NMR spectroscopy, the paramagnetic nature of these complexes make NMR analysis difficult. In addition to NMR data, X-ray crystallography was utilized in order to determine unambiguously that an iron(bis) alkoxide complex was formed. Crystallization of complex **2.4a** from a dichloromethane solution layered with pentane by Julia Curley resulted in crystallized material suitable for X-ray diffraction. The complex is a five coordinate species with distorted trigonal bipyramidal geometry at the iron center where the imine moieties comprise the axial positions of the trigonal bipyramid (Figure 2.3).

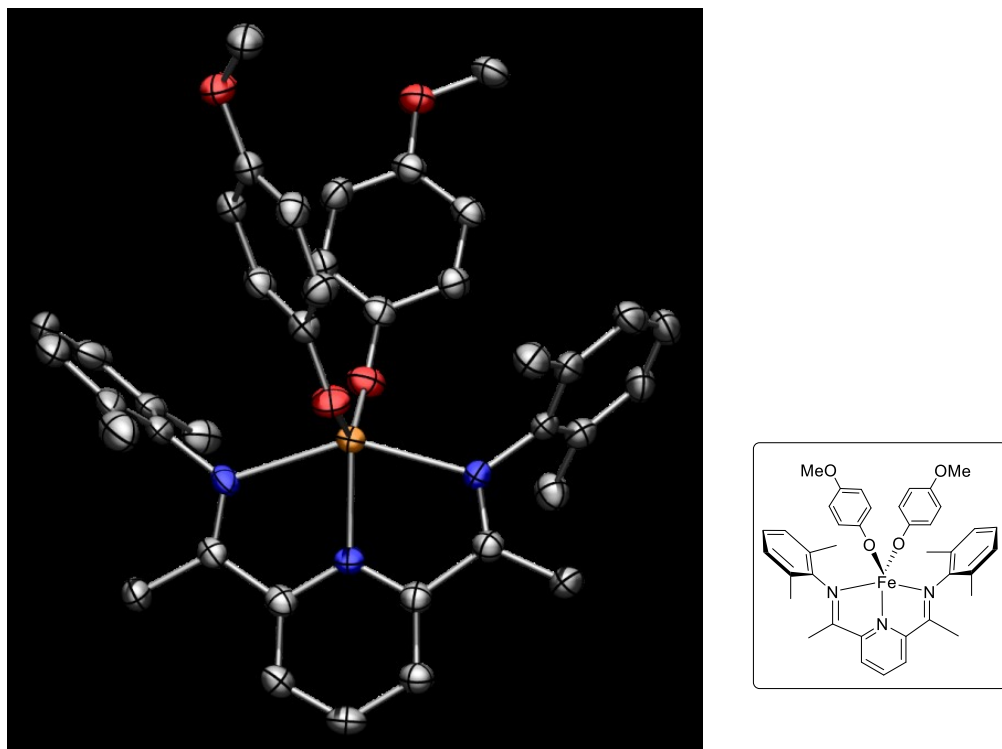


**Figure 2.3.** X-ray structure of **2.4a** with thermal ellipsoids represented at the 50% probability level. Hydrogen atoms, solvent ( $\text{CH}_2\text{Cl}_2$ ), and free 4-methoxyphenol are omitted for clarity.

As we were also interested in the polymerization ability of Fe(III) alkoxide complexes, oxidation of the iron(II) alkoxide **2.4a** was performed with ferrocenium (Fc) hexafluorophosphate (Scheme 2.2c). This reaction proceeded cleanly to give a cationic iron(III) species (**2.5**), which could be crystallized from benzene to give X-ray quality crystals. The molecular structure of this complex appears in Figure 2.4 and is a five coordinate iron species that is best described as a distorted trigonal bipyramidal complex, with similar geometry to complex **2.4a**.

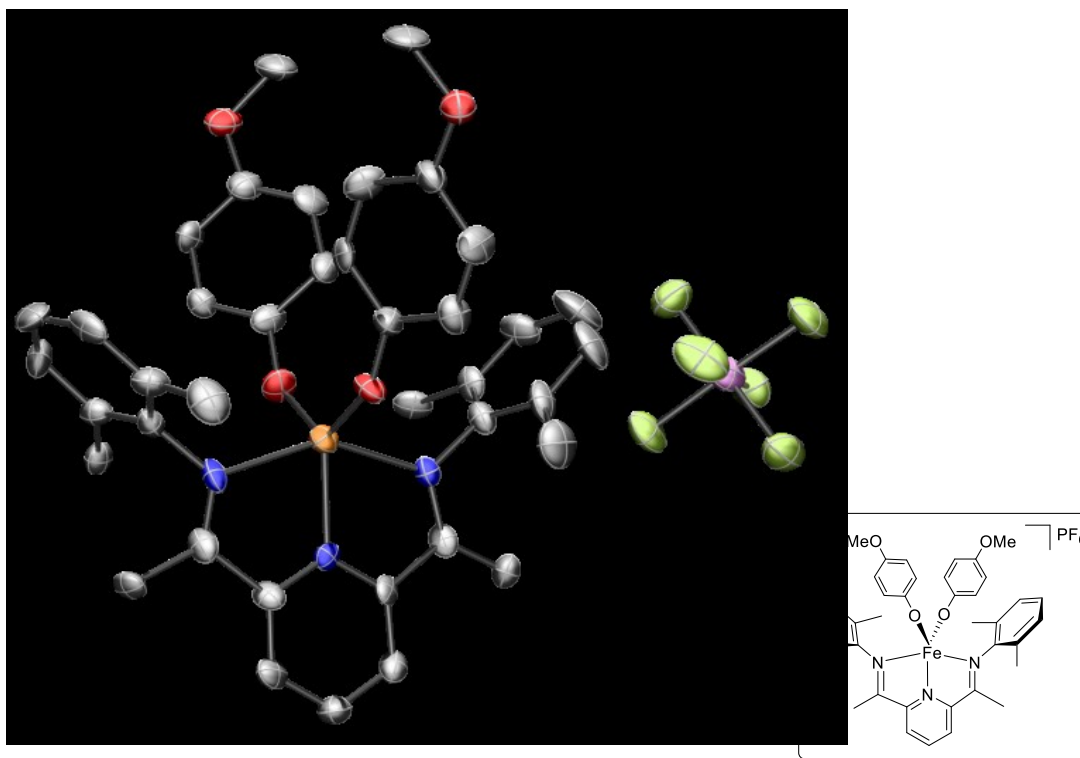
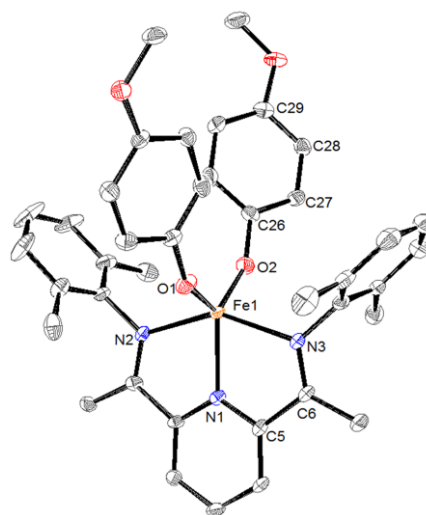


**Figure 2.4.** X-ray structure of **2.5** with thermal ellipsoids represented at the 50% probability level. Hydrogen atoms and solvent (benzene) are omitted for clarity. See appendix A for further crystallographic data.

A comparison of crystal structure bond metrics for the iron(II) and iron(III) bis(alkoxide) complexes is shown in **Table 2.1**. The iron-oxygen and iron-nitrogen bond distances are generally shorter for the cationic iron(III) complex **2.5** compared to iron(II) complex **2.4a** (entries 1-4). The bis(imino)pyridine and phenol ligand bond metrics can be examined to determine whether the oxidation event occurred at one of the two potentially redox-active ligands or at the metal center. Bond distances for the bis(imino)pyridine ligand (entries 5-6) as well as for the *p*-methoxyphenoxide ligand (entries 7-9) are typical for neutral ligands<sup>14</sup> and are not significantly different from the bond metrics of the ligands in complex **2.4a**, which suggests that oxidation occurred at the iron center. This assignment was supported by the magnetic moment of the complex, which was measured at 5.9  $\mu_B$ , a typical value for a high spin iron(III) complex.

**Table 2.1.** Comparison of selected bond lengths and angles for complexes **2.4a** and **2.5**.

Entry		Bond Lengths (Å)	
		Complex <b>2.4a</b>	Complex <b>2.5</b>
<b>1</b>	Fe-O <sub>1</sub>	2.006	1.820
<b>2</b>	Fe-O <sub>2</sub>	1.894	1.815
<b>3</b>	Fe-N <sub>1</sub>	2.091	2.089
<b>4</b>	Fe-N <sub>2</sub>	2.295	2.172
<b>5</b>	N <sub>2</sub> -C <sub>6</sub>	1.286	1.283
<b>6</b>	C <sub>5</sub> -C <sub>6</sub>	1.492	1.495
<b>7</b>	O <sub>2</sub> -C <sub>26</sub>	1.345	1.350
<b>8</b>	C <sub>26</sub> -C <sub>27</sub>	1.388	1.385
<b>9</b>	C <sub>27</sub> -C <sub>28</sub>	1.381	1.378
Bond Angles (°)			
<b>10</b>	N <sub>2</sub> -Fe <sub>1</sub> -N <sub>3</sub>	146.89	147.05
<b>11</b>	N <sub>2</sub> -Fe <sub>1</sub> -N <sub>1</sub>	73.32	71.73



## 2.3 Lactide Polymerization with Iron(II) Bis(Imino)Pyridine Iron Alkoxide Complexes

Iron bis(imino)pyridine bis(alkoxide) complexes were next investigated for their catalytic activity toward the polymerization of (*rac*)-lactide. At a monomer to catalyst ratio of 50:1, iron(II) bis(alkoxide) complex **2.4a** was active for the polymerization of lactide at room temperature, giving 93% conversion of lactide after 3 hours. The polymer obtained from this reaction was analyzed by gel permeation chromatography (GPC), and, relative to polystyrene standards, revealed a number average molecular weight ( $M_n$ ) of 6.8 kg/mol and a narrow dispersity ( $\mathcal{D}$ ) (entry 1, **Table 2.2**). For example, when **2.3** (2 mol%) was treated with 4-methoxyphenol (4 mol%) and exposed to lactide, similar results were obtained compared to the preformed catalyst species (cf. entry 1 to entry 2, **Table 2.2**). This result suggests that the bis(alkoxide) could be successfully formed *in situ*.

**Table 2.2.** (*rac*)-Lactide polymerization catalyzed by iron bis(imino)pyridine complexes.<sup>a</sup>

Entry	Time (h)	Cat.	[LA]:[cat.]: [ <i>p</i> -OMePh] <sup>b</sup>	$M_n$ (kg/mol)	$\mathcal{D}$	Conv. (%)
<b>1</b>	3	<b>2.4a</b>	50:1:0	6.8	1.16	93
<b>2</b>	3	<b>2.3</b>	50:1:2	6.2	1.18	88
<b>3</b>	24	<b>2.3</b>	100:1:2	9.6	1.09	62
<b>4</b>	24	<b>2.3</b>	200:1:2	1.9	1.06	5
<b>5</b>	24	<b>2.3</b>	50:1:0	15.6	1.45	14

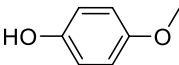
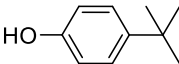
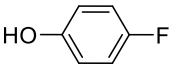
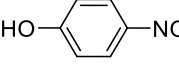
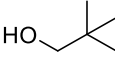
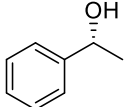
<sup>a</sup> Reactions were performed in dichloromethane (0.25M) for 3 h at room temperature. Conversion was determined by <sup>1</sup>H NMR with 1,3,5-trimethoxybenzene as an internal standard. Molecular weights were determined by GPC relative to polystyrene standards. <sup>b</sup> LA = lactide.

Increasing the monomer to catalyst ratio resulted in polymers with increased molecular weights, but at the expense of slower monomer conversion. Efficient reactions could still be obtained at a monomer to catalyst ratio of 100:1 (entry 3, **Table 2.2**), but

further increasing the ratio to 200:1 lead to reactions that were too slow to be practical at room temperature (entry 4).

As is common for lactide polymerization reactions, the efficacy of the polymerization was sensitive to the identity of the initiating species.<sup>2, 15</sup> For polymerizations catalyzed by the iron bis(alkyl) complex **2.3**, high molecular weight polymer was obtained but the reaction was sluggish (entry 5, **Table 2.2**). This result could be explained with slower initiation rates and/or lower concentration of the active species in the reaction mixture.

**Table 2.3.** Lactide Polymerization Catalyzed by **2.3** in the Presence of Various Alcohol Initiators.<sup>a</sup>

Entry	Initiator	Time (h)	M <sub>n</sub> (kg/mol)	Đ	Conv. (%)
1		3	6.2	1.18	88
2		24	7.2	1.18	95
3		24	6.2	1.21	93
4		24	1.1	1.27	6
5		24	--	--	0
6		2	4.1	1.27	96
7		24	4.0	1.33	96
8		24	3.6	1.21	88

<sup>a</sup> Reactions were performed in dichloromethane (0.25M) at room temperature with 2 mol% **2.3** and 4 mol% initiator. Conversion was determined by <sup>1</sup>H NMR with 1,3,5-trimethoxybenzene as internal standard. Molecular weight was determined by GPC relative to polystyrene standards. The average of three trials is reported.

Because the catalytically active bis(alkoxide) species could be generated *in situ*, the sensitivity of the polymerization to the identity of the initiator for lactide polymerization

was investigated (**Table 2.3**). These studies revealed that the initiator has a dramatic effect on the activity of the polymerization catalyst. Electron-donating phenols were found to serve as better initiators (entries 1-3), while electron-withdrawing initiators resulted in little to no activity (entries 4-5). Aliphatic alcohols were tolerated in addition to phenols (entries 6-8). In fact, neopentyl alcohol was found to be the most efficient initiator of all that were studied (entry 6), although this initiator resulted in significantly lower molecular weight polymer. End group analysis of all of the polymers revealed alkyl or aryl ester end groups even for polymerizations initiated by neopentyl alcohol where formyl end groups may be expected as a result of  $\beta$ -hydride elimination and initiation by an iron hydride (**Figure 2.5**).

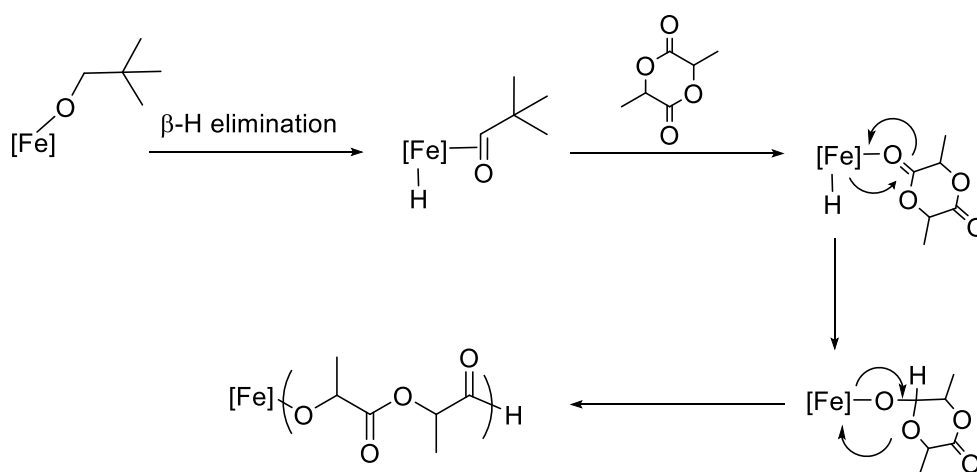


**Figure 2.5.** Proposed mechanism for the initiation of lactide polymerization by an iron hydride species. We do not observe these formyl end groups in our polymerization reactions, suggesting this process is not occurring.

The finding that a more electron-rich iron center gave faster lactide polymerization rates led to the subsequent investigation of Drs. Cesar Manna and Hilan Kaplan on the polymerization of lactide with a bis(amidinato)-*N*-heterocyclic carbene iron bis(alkoxide) complex (**Figure 2.6**).<sup>16</sup> These complexes afforded the synthesis of

high molecular weight poly(lactic acid) with faster reaction rates compared to the analogous bis(imino)pyridine complexes in the conditions studied. This is hypothesized to be due to the better  $\sigma$ -donating capabilities of the *N*-heterocyclic carbene moiety compared to pyridine.

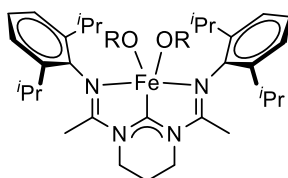


**Figure 2.6.** Bis(amidinato)-*N*-heterocyclic carbene iron bis(alkoxide) complex used as a catalyst for lactide polymerization. R = *p*-OMePh.

## 2.4 Mechanistic Studies of Lactide Polymerization

### 2.4.1 Living Polymerization Studies

In order to get a better understanding of the mechanism for the polymerization reactions and to help identify the active species, we decided to carry out a time course study on the polymerization of lactide. Treatment of **2.3** (2 mol%) with 4-methoxyphenol (4 mol%) generated **2.4a** as a pre-catalyst, which was subsequently exposed to a 0.25 M solution of lactide in dichloromethane. A plot of the number average molecular weight ( $M_n$ ) versus conversion was linearly correlated, which suggests that the polymerization reaction is a living polymerization (**Figure 2.7**). However, the dispersities observed in the reactions, while narrow, are slightly broader than what is typically observed for living polymerization. Nevertheless, the linear plots of  $M_n$  vs. conversion and the narrow dispersities observed for the polymerization demonstrate good control over molecular weight and are consistent with little termination or transesterification events.



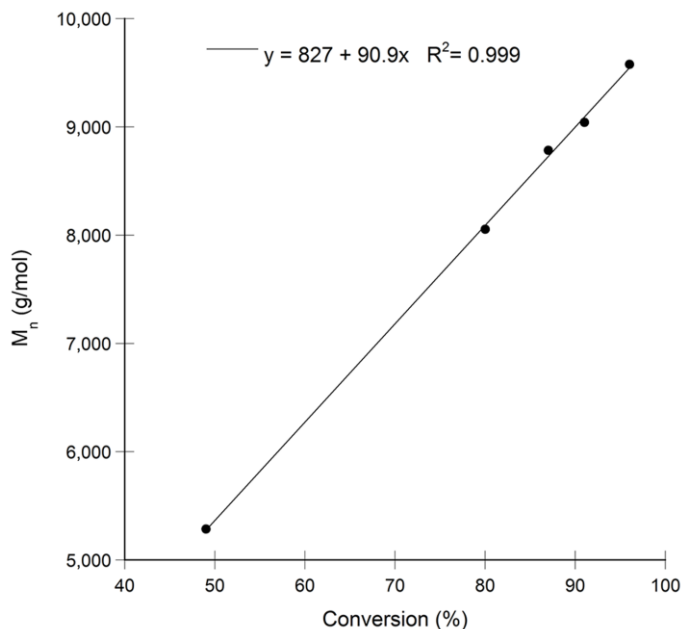


**Figure 2.7.** Number average molecular weight ( $M_n$ ) versus conversion for lactide polymerizations catalyzed by 2,3/4-methoxyphenol.

Extrapolation of the  $M_n$  vs. conversion plot to zero conversion did not go through the origin (**Figure 2.7**), which is consistent with several possibilities including: a) small amounts of impurity in the lactide that promote chain transfer, b) inefficient initiation of the polymerization, or c) significant amounts of polymer backbiting resulting in unexpectedly low molecular weight at high monomer conversion.<sup>17</sup> We can rule out this last possibility because little broadening in the dispersity of the polymer was observed at high monomer conversion (cf. entries 2 to 1 and 7 to 6, **Table 2.3**). This observation is consistent with minimal transesterification reactions, which are more prevalent at high monomer conversions.<sup>2</sup> This property of the catalyst is particularly noteworthy because many lactide polymerization catalysts suffer from competing transesterification reactions at high monomer conversions.<sup>18</sup> It is likely that the bulky 2,6-dimethyl-aryl substituted

bis(imino)pyridine ligand restricts access to the transition metal center for extended chain ester moieties on the polymer but are accessible to the sterically less encumbered cyclic monomer unit.

The living characteristics of the reaction are further highlighted by the sequential addition of lactide to the polymerization, which lead to a linear increase in molecular weight for up to fifteen sequential additions (**Figure 2.8**). High molecular weight polymer (>75 kg/mol) could be obtained in this fashion with little loss in molecular weight control as is evidenced by the low dispersities of the polymer.

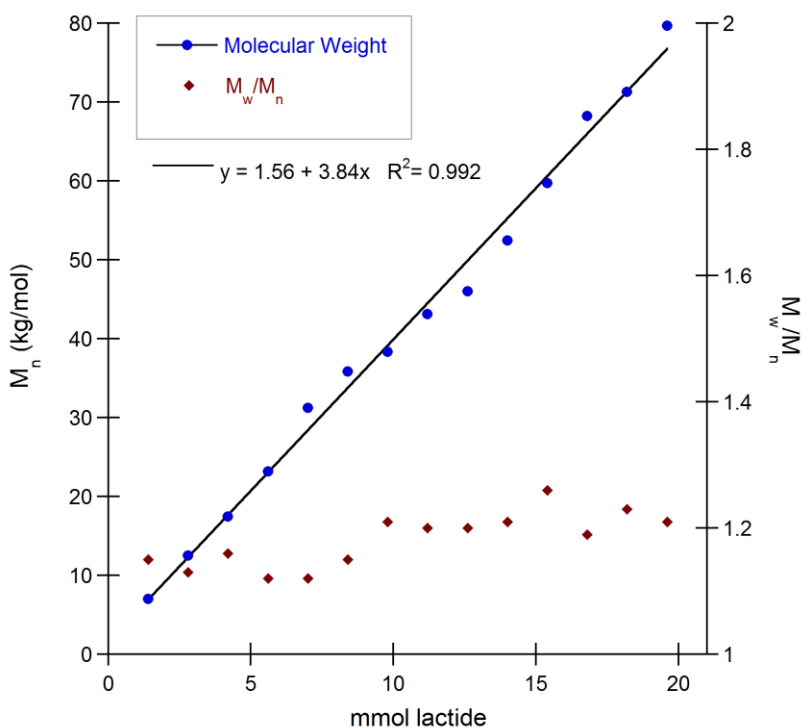
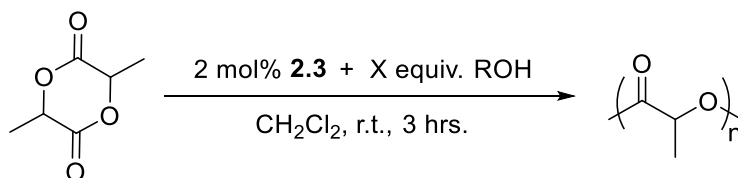


**Figure 2.8.** Sequential addition of lactide to give polymers with increased molecular weight.

To determine whether immortal polymerization reactions could be performed with our catalyst system, lactide polymerization was performed with complex **2.3** and an

excess concentration of alcohol initiator relative to **2.3** (Table 2.4). As described in section 1.2.4, in an immortal polymerization the ultimate polymer molecular weight is dictated by the lactide to alcohol initiator ratio. Previously, reactions were carried out with two equivalents of the alcohol relative to complex **2.3** in order to form the iron bis(alkoxide) species *in situ*. When polymerization was carried out with five equivalents of 4-methoxyphenol or neopentyl alcohol, no significant differences in the PLA molecular weights were observed. This suggests that the alcohol initiator does not undergo chain transfer reactions, which is unlike most catalyst systems for lactide polymerization. When a larger excess of 4-methoxyphenol was added to complex **2.3** (40 equivalents), no polymerization activity was observed.

**Table 2.4.** Attempted immortal polymerization of lactide with complex **2.3** and alcohol initiators.



ROH	Equiv.	Conv. (%)	$M_n$ (kg/mol)	PDI
	2	94	7.6	1.19
	5	96	6.1	1.23
	40	0	--	--
	2	96	3.8	1.44
	5	97	4.4	1.38

### 2.4.2 Identity of the Active Species

Considering the propensity for iron alkoxides to form multinuclear species with expulsion of the bis(imino) pyridine ligand (*vide supra*), we considered the possibility that the bis(imino) pyridine iron alkoxide complexes were precursors to multinuclear iron alkoxides that form under the polymerization conditions. To determine whether the bis(imino)pyridine ligand remained coordinated to iron during the polymerization reaction, we compared polymerizations initiated by **2.3** and 4-methoxyphenol to those initiated by  $\text{Fe}(\text{py})_2(\text{CH}_2\text{SiMe}_3)_2$  and 4-methoxyphenol. We anticipated that if the tridentate bis(imino)pyridine ligand in **2.3** was being replaced by alkoxide ligands to form multinuclear alkoxide species, a similar phenomenon would occur for the substitutionally more labile monodentate pyridine ligands in  $\text{Fe}(\text{py})_2(\text{CH}_2\text{SiMe}_3)_2$ . Consequently, similar reaction rate, polymer molecular weight, and dispersity would be observed for both catalyst compositions. In the event, much slower and less reproducible reaction rates were observed for  $\text{Fe}(\text{py})_2(\text{CH}_2\text{SiMe}_3)_2$  /4-methoxyphenol ( $k_{\text{obs}} = 0.73 \times 10^{-4} \pm 0.6 \times 10^{-4} \text{ s}^{-1}$ ) than with **2.3**/4-methoxyphenol ( $k_{\text{obs}} = 1.66 \times 10^{-4} \pm 0.08 \times 10^{-4} \text{ s}^{-1}$ ) (**Figure 2.9**). Additionally, the molecular weight of the polymer for reactions catalyzed by  $\text{Fe}(\text{py})_2(\text{CH}_2\text{SiMe}_3)_2$ /4-methoxyphenol was lower ( $M_n = 4.9 \text{ kg/mol}$ ) compared to **2.3**/4-methoxyphenol ( $M_n = 6.2 \text{ kg/mol}$ ). These results demonstrate that the catalytically active species in  $\text{Fe}(\text{py})_2(\text{CH}_2\text{SiMe}_3)_2$ /4-methoxyphenol is different compared to **2.3**/4-methoxyphenol, and suggests that the bis(imino)pyridine ligand remains coordinated to iron during polymerization reactions catalyzed by **2.3** with various alcohol initiators.

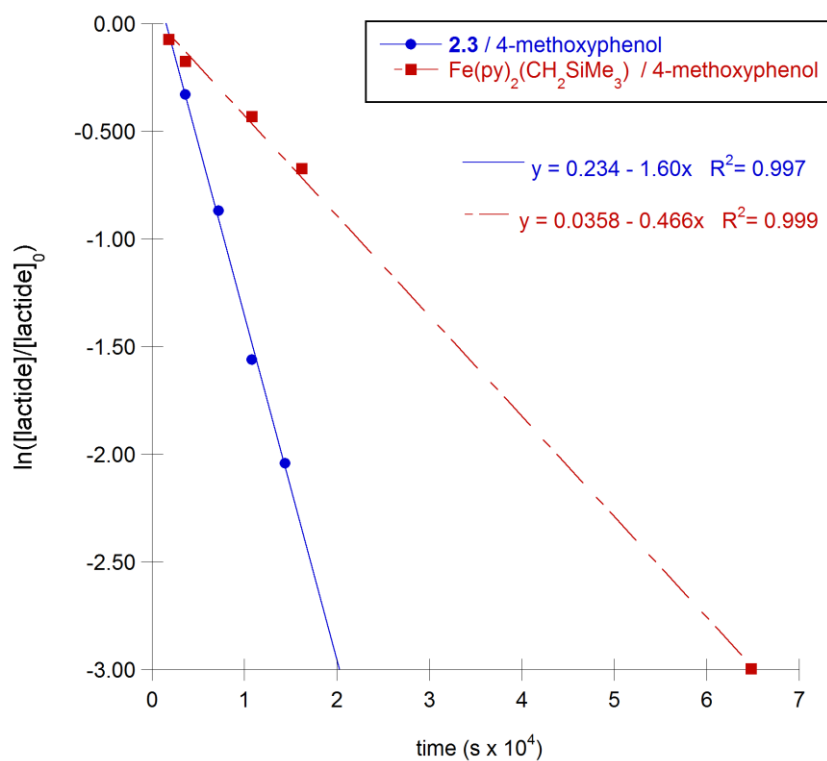


**Figure 2.9.** Reaction rate comparison between lactide polymerizations catalyzed by 4/4-methoxyphenol (■) and Fe(py)<sub>2</sub>(CH<sub>2</sub>SiMe<sub>3</sub>)<sub>2</sub>/4-methoxyphenol (●).

To characterize the identity of the active species further, we addressed the issue of whether one or both alkoxide ligands can act as initiators for lactide polymerization. The dramatic effect that the identity of the initiator has on the catalyst activity suggests that only one alkoxide is involved in lactide polymerization while the other remains as an ancillary ligand for the catalyst. However, assuming the bis(imino)pyridine remains tridentate, this possibility would involve an unusual six-coordinate iron complex containing a bis(imino)pyridine ligand. As an alternative explanation, the identity of the alkoxide may affect the initiation rate without significantly altering propagation rates.

To gain insight regarding this issue, we analyzed the molecular weight data that resulted from the polymerization reactions. Since the molecular weight of the polymer

increases linearly with conversion, a theoretical  $M_n$  can be predicted given the conversion of the reaction, the monomer to catalyst ratio, and the number of initiating alkoxides.<sup>17</sup> If one alkoxide were initiating the polymerization reaction carried out by **2.3/4**-methoxyphenol, a theoretical  $M_n$  of 6.8 kg/mol is expected. This compares favorably with the observed  $M_n$  of 7.2 kg/mol and suggests that only one phenol is used as an initiator in the polymerization reaction (**Figure 2.10**). A similar conclusion can be made for lactide polymerizations initiated by **2.3/4-tert-butylphenol**.

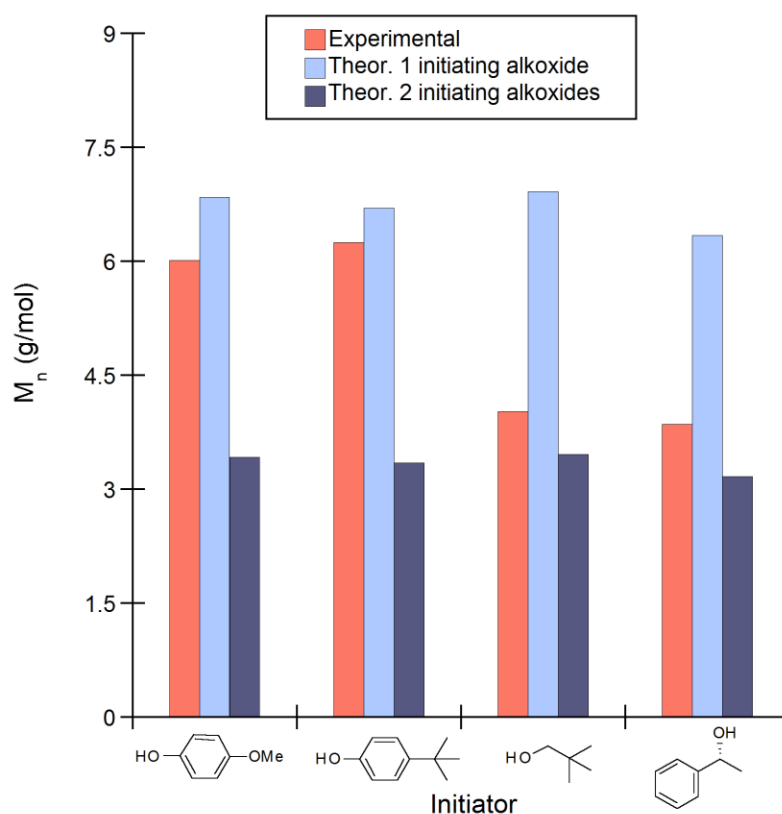


**Figure 2.10.** Comparison of experimental and theoretical molecular weights with one initiating alkoxide or two initiating alkoxides per iron center.

In a case where two growing polymer chains initiate per metal center, the molecular weight of the polymers observed should be lower (half the value compared to

one initiating chain per metal center), since the ultimate molecular weight in a living polymerization reaction is dictated by the ratio of monomer to active propagation sites. The observed  $M_n$  for polymerization reactions initiated by **2.3**/neopentyl alcohol (4.0 kg/mol) is much closer to the theoretical  $M_n$  predicted by a catalyst that uses two initiating alcohols ( $M_n = 3.5$  kg/mol). Therefore, it appears that for the phenols, one initiating alkoxide is used during the polymerization reaction whereas for the aliphatic alcohols, both alkoxide ligands are used as initiating species (**Figure 2.10**).

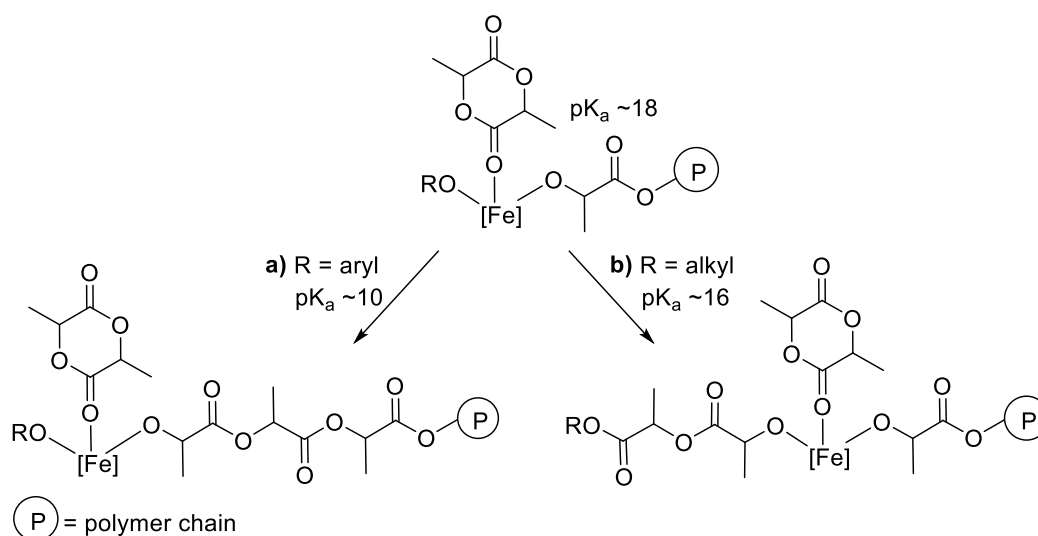


**Figure 2.11.** Polymer propagation with a) one polymer chain and one spectator alkoxide (R = aryl) and b) two polymer chains per metal center (R = alkyl).

These results can be rationalized by realizing that the identity of the propagating species is electronically more similar to neopentyl alcohol as compared to 4-methoxyphenol. For example, the pK<sub>a</sub> for neopentyl alcohol and the alcohol of lactic acid is ~16 and 18, respectively, whereas the pK<sub>a</sub> for *p*-methoxyphenol is 10.2, which is considerably more acidic. If pK<sub>a</sub> and nucleophilicity are directly correlated, when a lactide monomer coordinates to a catalyst containing neopentoxide and a growing

polymer chain, insertions from the neopentoxide ligand occur at about the same rate as insertions from the growing polymer chain (pathway b, **Figure 2.11**). In contrast, lactide insertion for a catalyst containing an aryloxide ligand and a growing polymer chain favors insertion from the growing polymer chain because the aryloxide ligand is significantly less nucleophilic than the propagating polymer chain (pathway a, **Figure 2.11**).

To assess whether one or two alkoxide ligands are involved in the polymerization reaction, we carried out the polymerization of lactide initiated by the chiral secondary alcohol (*R*)-1-phenylethanol. We reasoned that if both alkoxides were to initiate the polymerization of lactide, the propagating species would be similar to the reactions carried out with neopentyl alcohol. As such, we predicted that there would be little difference in tacticity for the resulting polymer. However, if one alkoxide remains as an ancillary ligand during the polymerization, then a difference in tacticity might be observed for the reactions initiated with (*R*)-1-phenylethanol compared to neopentyl alcohol due to different amounts of stereoinduction resulting from enantiomorphic site control.<sup>19</sup> Analysis of the polymer tacticity from polymerizations initiated by both (*R*)-1-phenylethanol and neopentyl alcohol were found to produce atactic polymer ( $P_r = 0.49$  and  $0.51$ ) with nearly the same relative concentrations of stereoerrors (**Figure 2.12**).<sup>20</sup> This result provides further support that both alkoxides bound to iron are initiating lactide polymerization.



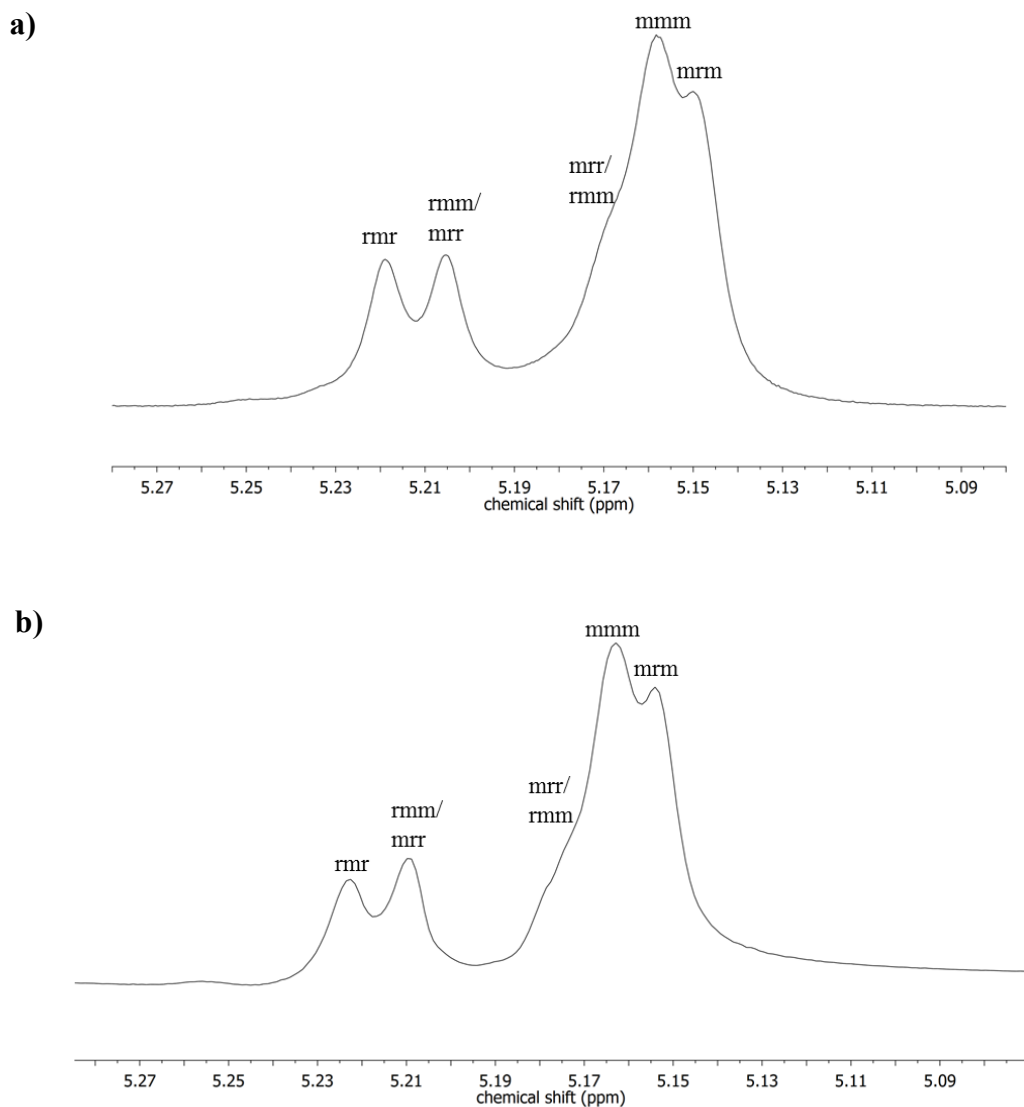


**Figure 2.12.** a) Methine region of the  $^1\text{H}$ - $^1\text{H}$  homodecoupled NMR spectrum of poly(lactic acid) initiated by **2.3**/*(R)*-(+)-1-phenylethanol. b) Methine region of the  $^1\text{H}$ - $^1\text{H}$  homodecoupled NMR spectrum of poly(lactic acid) initiated by **2.3**/neopentyl alcohol.

The low stereoselectivity observed in the polymerization reactions regardless to the identity of the initiating alcohol species is noteworthy ( $P_r = 0.50$  when 4-methoxyphenol is used as the initiator). This outcome is to be expected for a catalyst that contains an achiral ancillary ligand such as the bis(imino)pyridine ligands when there is minimal

stereoiduction from chain-end control. Therefore, under the reaction conditions investigated, it appears that the chiral polymer chain end has minimal stereochemical influence on subsequent insertions of lactide monomer when bis(imino)pyridine ligands are used as ancillary ligands on iron. In addition, polymerization reactions carried out with L-lactide showed no epimerization of the lactide and yielded isotactic poly(L-lactide). The bis(imino)pyridine iron bis(alkoxide) catalyst system is unusual for lactide polymerization because there is an option for one or two alkoxide ligands to initiate lactide polymerization. Most catalysts consist of an anionic ancillary ligand and one alkoxide to initiate polymerization.<sup>2</sup> However, the bis(imino)pyridine is a neutral ligand, allowing for the coordination of two anionic alkoxide ligands to iron. Either or both of these alkoxide ligands can participate in the ring opening polymerization reaction.

The ability for one alkoxide ligand to remain ancillary during polymerization was successfully exploited for stereocontrol over poly(lactic acid) through the use of silanols as initiators by other members of the Byers group. Treatment of complex **2.3** with silanol additives as initiators led to the stereoselective polymerization of (*meso*)-lactide to give syndiotactic polymer ( $P_s = 0.92$  when silanol is  $\text{Et}_3\text{SiOH}$ ) and of (*rac*)-lactide to afford heterotactic polymer ( $P_s = 0.75$  when silanol is  $\text{MePh}_2\text{SiOH}$ ).<sup>21,22</sup> Although the catalysts and additives are achiral, NMR analysis of the resulting polymer suggested that an enantiomorphic site control mechanism was more likely as opposed to a chain end control mechanism. This can be rationalized with a mechanism that involves desymmetrization of the catalyst so as to yield intermediates that are stereogenic at iron, since one siloxide initiates lactide polymerization and the other remains as a spectator ligand bound to the iron center (**Figure 2.13**).

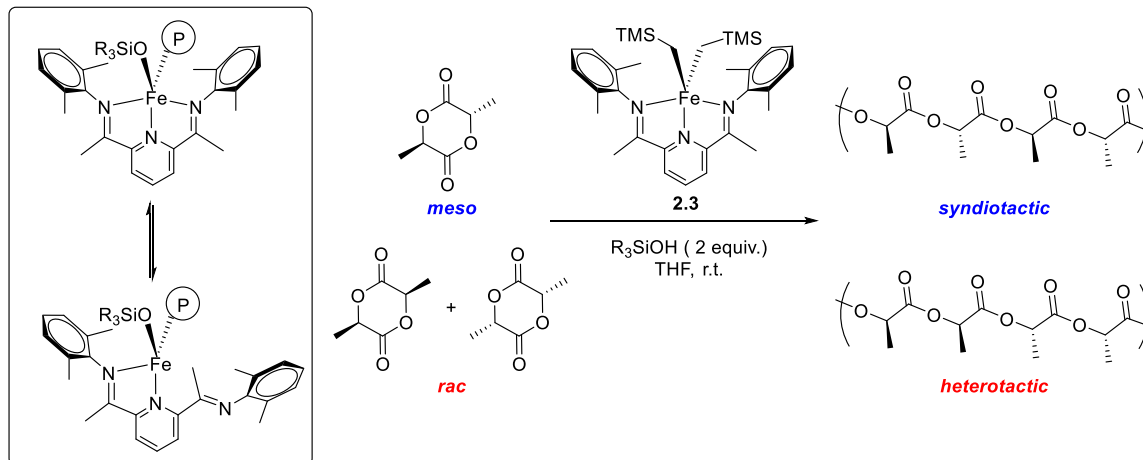
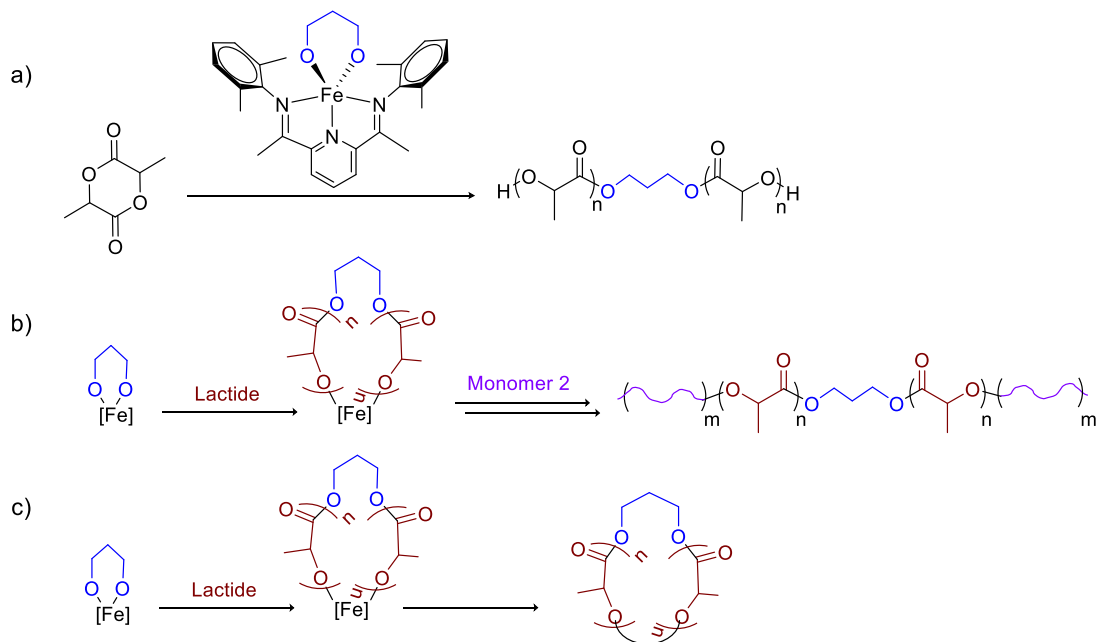


**Figure 2.13.** Stereoselective polymerization of lactide with silanols as initiators with complex **2.3**.

The ability to have two propagating poly(lactic acid) chains per metal center allows for the possibility of telechelic polymerization, or propagating polymerization from both chain ends, when a linked diol initiator is utilized. If both alkoxide groups on the coordinated diol initiate lactide polymerization, as they should when alkyl alkoxide initiators are used, then the resulting polymer would be linked in the center by the diol initiator (**Scheme 2.3a**). During preliminary studies on lactide polymerization catalyzed by **2.3** in the presence of various alcohols, 1,4-butanediol was found to be an effective initiator for lactide polymerization. Dr. Cesar Manna further showed that many diols could act as initiators with precatalyst **2.3** to polymerize lactide. This telechelic polymerization strategy could be utilized to form block copolymers of type A-B-A if a second monomer feed is introduced into the reaction sequentially (**Scheme 2.3b**). Additionally, this strategy could be used to synthesize cyclic poly(lactic acid) if the two chain ends could be linked (**Scheme 2.3c**). Dr. Cesar Manna and Dr. Aman Kaur investigated routes to cyclize the poly(lactic acid) and preliminary results suggested that

cyclic poly(lactic acid) could be synthesized by simply heating the reaction, but characterization was complicated by a mixture of linear and cyclic polymers being formed in the reaction.

**Scheme 2.3.** Telechelic polymerization of lactide with a dialkoxide initiator.



## 2.5 Redox-Controlled Lactide Polymerization

Since we had access to the iron(III) bis(alkoxide) complex **2.5**, we decided to investigate its competency as a lactide polymerization catalyst. Previous studies have shown the ability to control lactide polymerization by oxidation and reduction reactions of ferrocene ligands attached to metals such as titanium,<sup>5</sup> indium,<sup>6</sup> or cerium.<sup>7</sup> The activity of the catalyst can be “switched” off and on by reversibly oxidizing or reducing the ferrocene ligands. Less common are examples where lactide polymerization is controlled by oxidation and reduction of the metal that is also the active site for polymerization, although there are two reports detailing examples of this with cerium as

the metal catalyst.<sup>7</sup> Despite the fact that many iron(II/III) redox processes are accessible and reversible, redox switchable lactide polymerization had never been demonstrated previously for an iron catalyst. In fact, a direct comparison between iron(II) and iron(III) lactide polymerization catalysts with the same ancillary ligand set had never been performed. Despite the enhanced Lewis acidity of **2.5** compared to **2.4a**, complex **2.5** did not show any activity for lactide polymerization after 24 hours at room temperature. This result was somewhat expected due to the acute electronic dependence observed for the iron(II) complexes where an electron-donating initiator was required for enhanced catalytic activity (*vide supra*). Oxidation of the neutral iron(II) bis(alkoxide) **2.4a** to the cationic iron(III) bis(alkoxide) **2.5** results in a significantly less electron rich metal center, so much so that lactide polymerization is completely thwarted. The reversibility of the redox reactions were demonstrated with stoichiometric reactions followed by <sup>1</sup>H NMR spectroscopy. Although low signal to noise complicated quantitative electrochemical analysis of **2.4a**, reversible redox behavior was identifiable in the cyclic voltammogram of **2.4a** in dichloromethane (**Figure 2.14**) with **2.4a** demonstrating a redox potential of approximately -0.71 V relative to Fc/Fc<sup>+</sup>. Later studies carried out by Miao Qi in our group showed that this redox event is completely reversible electrochemically in dichloromethane.

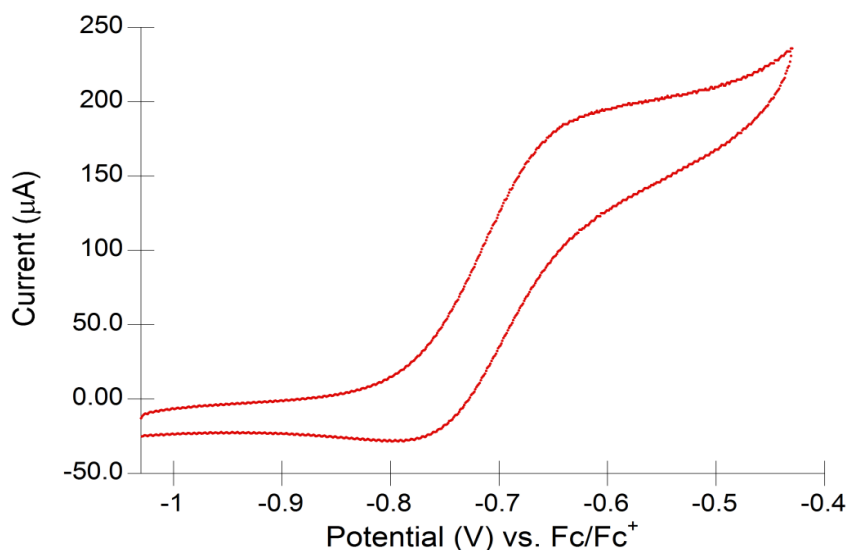


**Figure 2.14.** Cyclic voltammogram of complex **2.4a**. Conditions: 0.005M dichloromethane solution of the analyte, 0.1M *n*Bu<sub>4</sub>NPF<sub>6</sub> as supporting electrolyte, platinum mesh as working electrode, platinum wire as counter electrode, scan rate of 50 mV/s.

Considering the reversibility of the redox reaction and the complete inactivity of the iron(III) complex **2.5**, we then decided to see if our lactide polymerization catalysts could be controlled by changing the oxidation state of the metal center (**Figure 2.15**). The polymerization was performed with complex **2.4a** (2 mol%) until 25% conversion had been achieved. At this point, ferrocenium hexafluorophosphate (2 mol%) was added to the reaction mixture to oxidize the complex to the iron(III) species (**2.5**) *in situ*. The polymerization was completely shut down and no further conversion or change in polymer molecular weight (**Figure 2.15**) or molecular weight distribution was observed until cobaltocene (CoCp<sub>2</sub>, 2 mol%) was added to the reaction mixture to reduce the complex back to iron(II). At this point, the polymerization resumed with a comparable rate to that initially observed for complex **2.4a** ( $k_{obs} = 1.5 \times 10^{-4} \text{ s}^{-1}$  before addition of FcPF<sub>6</sub> and  $2.2 \times 10^{-4} \text{ s}^{-1}$  after addition of cobaltacene).

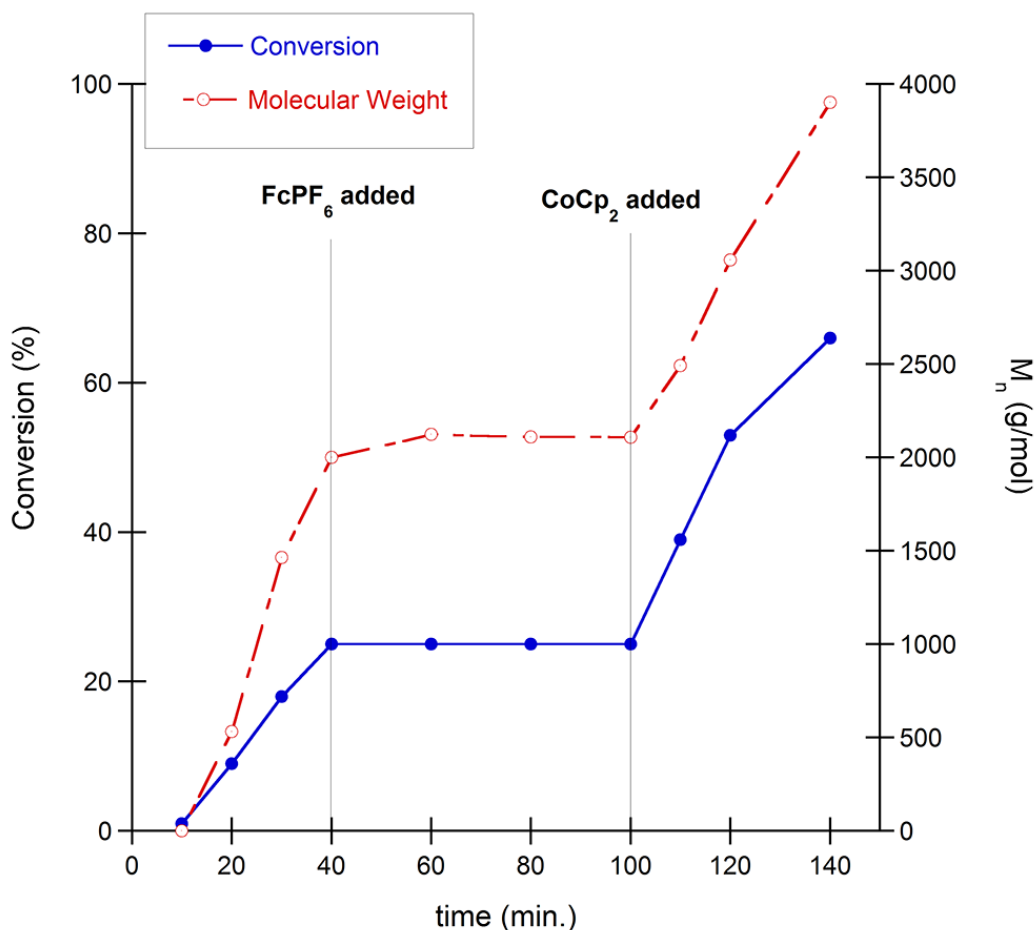


**Figure 2.15.** Polymerization of (*rac*)-lactide in the presence of **2.4a** over time. At the time points labeled 40 min. and 60 min., ferrocenium hexafluorophosphate and cobaltocene were added to the reaction to oxidize and reduce the metal center, respectively.

The veracity of the redox switching capabilities was further demonstrated by performing multiple redox switches without decreasing catalyst activity and with minimal impact on the polymer molecular weight distribution (**Figure 2.16**). These results demonstrate the reversible nature of the redox event occurring at the iron center and the sensitivity of the lactide polymerization to the oxidation state of the metal center.

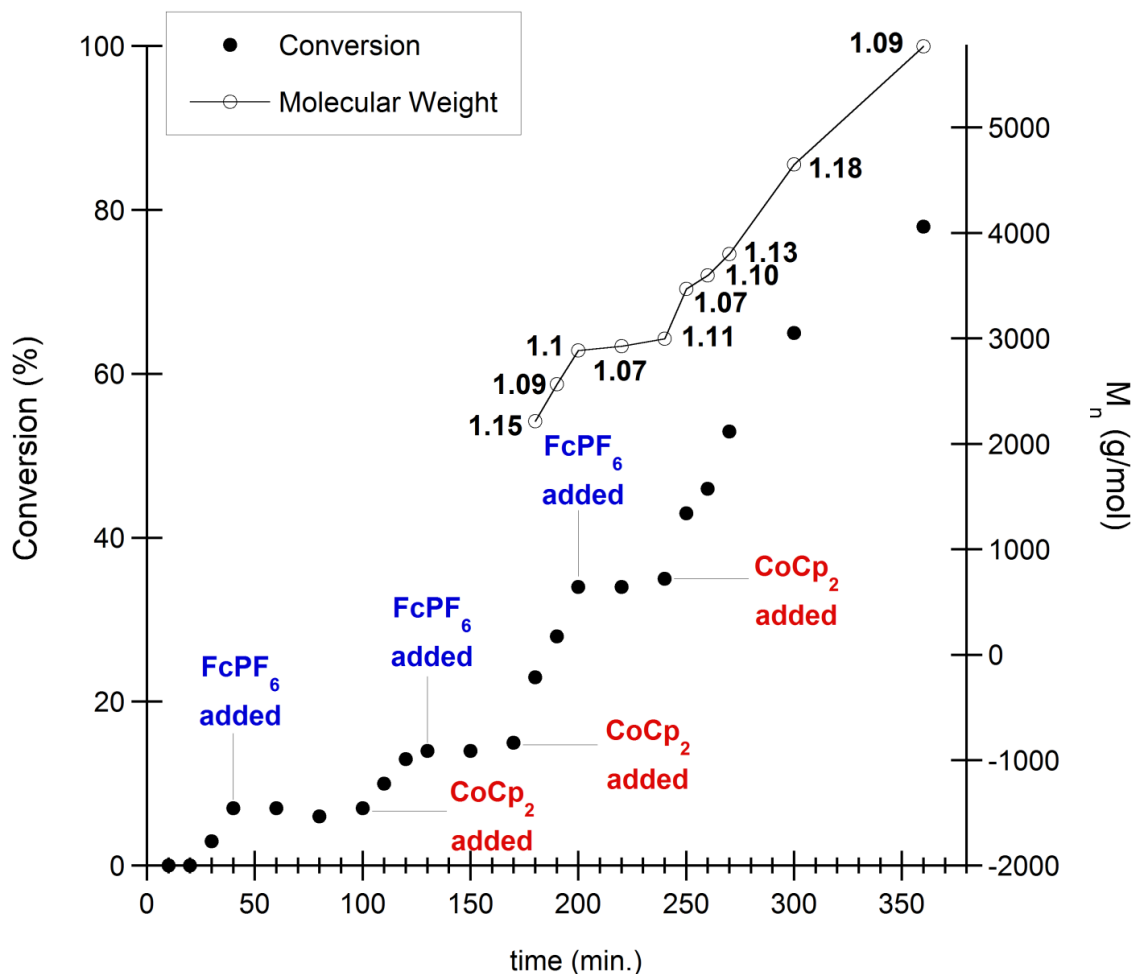


**Figure 2.16.** Polymerization of (*rac*)-lactide in the presence of 2,3/4-methoxyphenol with three redox switches of the catalyst. Add the time points  $t = 40$  min., 130 min., and 220 min., ferrocenium hexafluorophosphate ( $\text{FcPF}_6$ ) was added to the reaction mixture to oxidize the complex, and at time points  $t = 100$  min., 170 min., and 240 min., cobaltocene ( $\text{CoCp}_2$ ) was added to the reaction mixture to reduce the complex. Molecular weight data is shown for the last redox switch, with dispersities displayed next to each time point. Molecular weight was determined by GPC relative to polystyrene standards. Molecular weight data at lower conversion was complicated by the low molecular weight polymer obtained.

The bis(imino)pyridine iron catalyst system provides some distinct advantages compared to other catalysts that have demonstrated redox switchable polymerization. First, catalysis is completely shut down upon oxidation of the iron center to iron(III), whereas some redox switchable catalysts demonstrate only a lowering in reaction rate

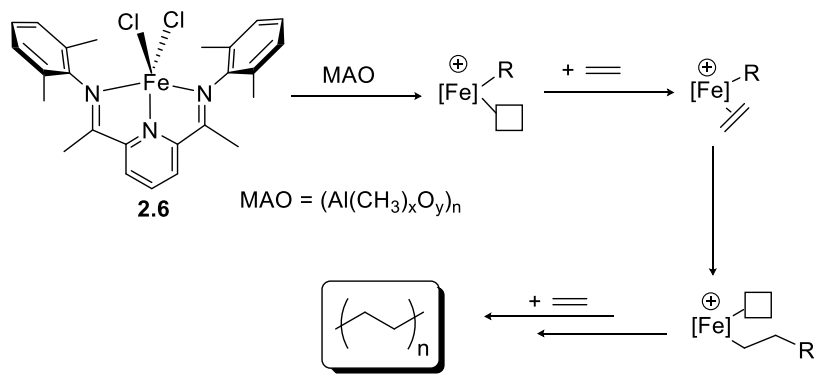


upon catalyst oxidation.<sup>5</sup> Second, the bis(imino)pyridine ligands are easier to synthesize and modify compared to the ferrocene-based ligands that are commonly employed for redox switchable polymerization.<sup>5,6,7a</sup> Finally, among the catalysts where redox switching occurs upon oxidation and reduction at the active site of polymerization,<sup>7</sup> the bis(imino)pyridine iron complexes display the most control over molecular weight. Whereas the cerium complexes reported by Diaconescu and coworkers demonstrate some broadening in molecular weight distribution upon redox switching,<sup>7a</sup> **2.4a** resulted in polymer with the same molecular weight and molecular weight distribution whether or not redox switching was employed.

## 2.6 Efforts Toward Copolymerization of Lactide and Ethylene

The most prominent use of iron bis(imino)pyridine complexes for catalysis is for the polymerization of ethylene. These complexes are known to polymerize ethylene with high efficiency upon activation with methylaluminoxane (MAO) as a cocatalyst.<sup>8</sup> The iron bis(imino)pyridine dichloride precatalyst is believed to form a cationic iron alkyl species upon exposure to MAO, which is the active species for coordination-insertion propagation (**Scheme 2.4**).

**Scheme 2.4.** Ethylene polymerization mechanism with precatalyst **2.6**.



### 2.6.1 Investigation of Lactide Interaction with Methylaluminoxane (MAO)

Aluminum alkoxides are known to be active polymerization catalysts for lactide (See Chapter 1.3.1). However, use of methylaluminoxane as a catalyst for ring opening polymerization of lactide has never been reported. For our envisioned copolymerization, a large excess of MAO relative to iron complex is required to activate the iron complex toward ethylene polymerization. For this reason, we found it imperative to investigate the reactivity of MAO with lactide to determine how the presence of MAO in our system will affect lactide polymerization.

Small amounts of MAO (10 mol%) added to a solution of lactide in toluene resulted in no conversion of lactide after several days. However, when an excess of MAO was added (5 or 20 equivalents relative to lactide), full conversion of lactide was observed by GC (**Figure 2.17**). No new features were observed in the GC trace after the reaction was complete, which suggested that MAO was binding to lactide and formed an insoluble adduct undetectable by GC.

The control experiments were also performed with solid MAO rather than the commercial solution (10 wt.% in toluene). The commercial MAO solution contains a small amount of trimethyl aluminum, which could lead to detrimental side reactions with lactide. MAO solution was placed under vacuum for prolonged periods to remove all volatile materials, including trimethyl aluminum. When solid MAO was exposed to a solution of lactide in toluene, conversion of lactide was still observed, but occurred at a slower rate than with MAO solution (**Figure 2.17**).

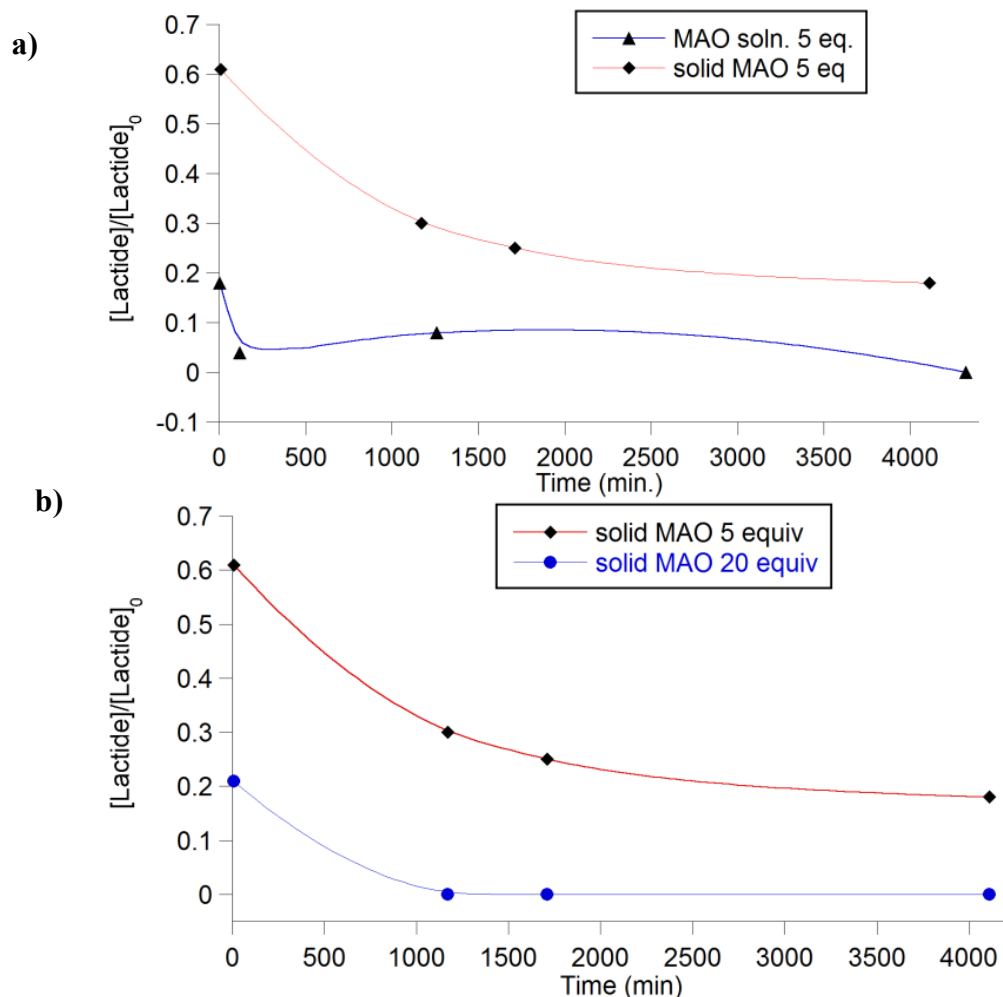


**Figure 2.17.** a) Conversion of lactide vs. time in the presence of 5 equivalents solid MAO (♦) or 10 wt.% MAO solution (▲) in toluene. b) Conversion of lactide vs. time in the presence of 5 equivalents (♦) or 20 equivalents (●) solid MAO. The reactions were monitored at room temperature in toluene. [lactide]/[lactide]<sub>0</sub> determined by GC with tetradecane as internal standard.

To better understand how MAO interacts with lactide, NMR experiments were performed with lactide and varying equivalents of MAO solution in C<sub>6</sub>D<sub>6</sub>. When up to 20 equivalents of MAO are added relative to lactide, no shift is seen in the lactide resonances by <sup>1</sup>H NMR. An interesting observation is that resonances associated with MAO are not observed in the <sup>1</sup>H NMR spectrum. Monitoring lactide concentration with

ferrocene as an internal standard in the presence of MAO solution showed a decrease in lactide concentration over time (**Figure 2.18**). This result also suggests MAO is binding to lactide to form an insoluble species which does not appear by  $^1\text{H}$  NMR.

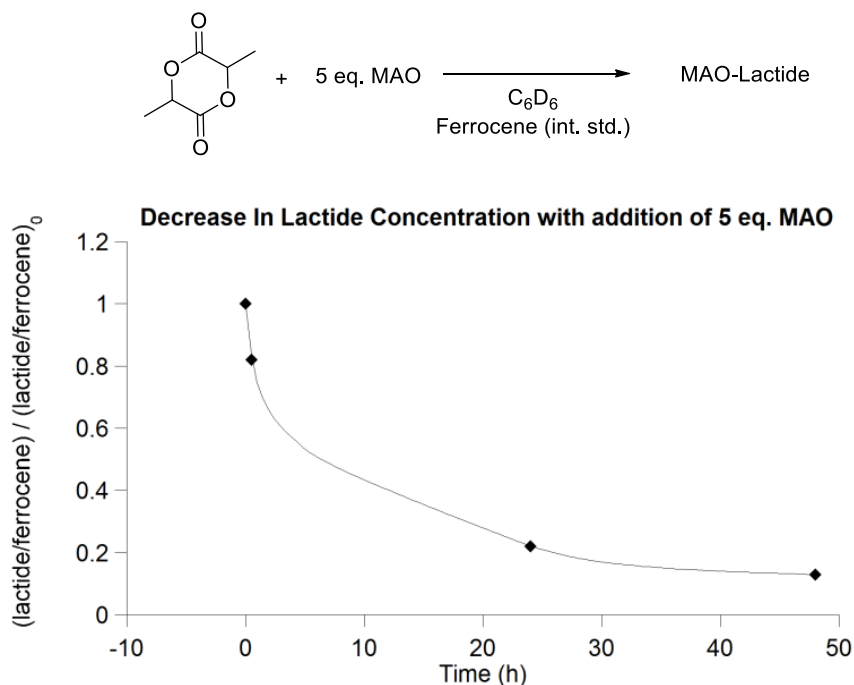


**Figure 2.18.** Lactide concentration monitored against internal standard ferrocene by  $^1\text{H}$  NMR after addition of 5 equivalents MAO solution.

These control experiments were carried out to determine whether lactide reacts with aluminum alkyl compounds. The presence of trimethyl aluminum in the MAO solution may be contributing to lactide conversion, as less conversion is observed with solid MAO. Also, if bulkier aluminum compounds are used, this may sterically block the binding of lactide. When monitored by NMR, addition of  $\text{AlMe}_3$  (1 or 5 equivalents relative to lactide) to a solution of lactide in  $\text{C}_6\text{D}_6$  resulted in complete conversion of lactide to ring-opened products. In the case of  $\text{Al}(\text{iBu})_3$ , no additional resonances were

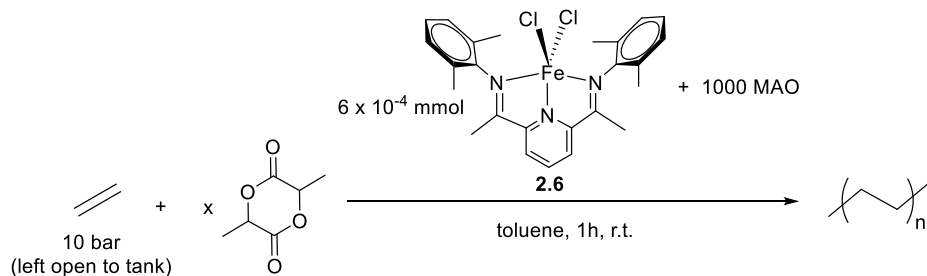
observed in the NMR spectrum upon addition to a C<sub>6</sub>D<sub>6</sub> solution of lactide, suggesting the Al(iBu)<sub>3</sub> is binding to the lactide to form an insoluble complex.

### *2.6.2 Polymerization of Ethylene with Iron Bis(imino)pyridine Complexes in the Presence of Lactide*

Although it seemed as though MAO cocatalyst may not be compatible with lactide, some preliminary ethylene-lactide polymerization studies were carried out. Early transition metal ethylene polymerization catalysts are highly sensitive to oxygen-containing functionalities, and are not be able to perform ethylene polymerization in the presence of polar monomers.<sup>23</sup> Therefore, it is important to determine whether ethylene polymerization with iron bis(imino)pyridine dichloride complex **2.6** can proceed in the presence of a polar monomer such as lactide.

Ethylene polymerization was performed in the presence of lactide to determine whether the reaction would be inhibited and whether any lactide would be incorporated into the polymer chain. The control reaction without lactide present gave an activity of 183 g/mmol·h·bar (**Table 2.5**, entry 1). When large amounts of lactide (2200 equiv. relative to **2.6**) were added to the reaction, no polyethylene was observed (**Table 2.5**, entry 2). This could be due to the lactide binding to MAO to form an insoluble complex, which was discussed in section 2.6.1. There was an excess of lactide relative to MAO (2.2 equiv.) in the reaction, so it is possible that all of the MAO was bound to lactide in solution so that the precatalyst was not able to be activated. When smaller amounts of lactide (1 equiv. relative to **2.6**) were added, the reaction still produced polyethylene, although with lower activity (**Table 2.5**, entry 3). Regardless of the lower activity, the ability to polymerize ethylene in the presence of lactide is a promising result.

**Table 2.5.** Ethylene polymerization at 10 bar in the presence of lactide.



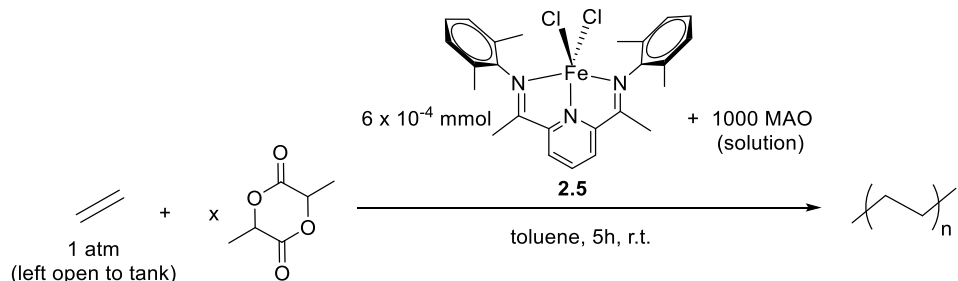
Entry	Equiv. Lactide (relative to 2.6)	Yield (g)	Activity (g/mmol·h·bar)
1	--	1.1	183
2	2200	0	0
3	1	0.4	60

Ethylene polymerization in the presence of lactide was also carried out at 1 atm instead of high pressures. In order to obtain a sufficient amount of polymer to characterize, the reaction time was increased to 5 hours. To investigate the limit of how much added lactide will shut down the reaction, the polymerization was performed with varying amounts of lactide (**Table 2.6**).

Up to 1000 equivalents lactide (equimolar to MAO) were able to be added without shutting down the polymerization. The activity may have decreased slightly, but there was no clear trend in activity with increasing amount of lactide added. This could be attributed to difficulty in measuring accurate amounts of MAO, since it is purchased as a solution that is not homogenous and it is difficult to know the exact structure of this poorly defined material. However, it is important to note that lactide does not shut down ethylene polymerization at concentrations equal to or less than the amount of MAO in the reaction. This shows one of the advantages of iron bis(imino)pyridine catalysts for the

copolymerization over early transition metals – they are more versatile and much more functional group tolerant.

**Table 2.6.** Ethylene polymerization at 1 atm in the presence of lactide.



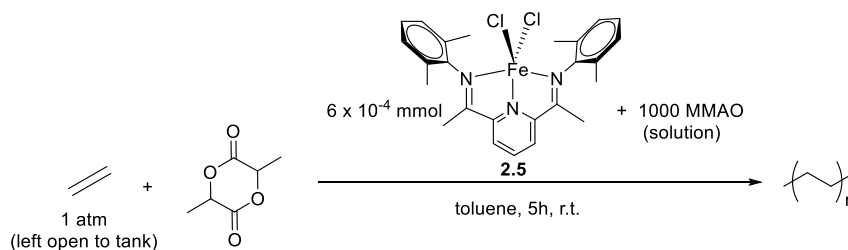
Entry	Equiv. Lactide (relative to 2.5)	Polymer mass (g)	Activity (g/mmol·h·bar)
1	0	0.387	129
2	1	0.414	138
3	10	0.590	197
4	100	0.191	64
5	500	0.708	236
6	1000	0.124	41

To determine whether any lactide units inserted into the polyethylene chain, IR and NMR spectroscopy were utilized to analyze the polymer products. Although the polymerizations performed in the presence of lactide showed slightly different IR spectra than pure polyethylene (peaks around 3300 and 1630cm<sup>-1</sup>), they were not consistent with the presence of ester peaks, and may have been due to the presence of water. High temperature (120°C) NMR in 1,1,2,2-tetrachloroethane-d<sub>2</sub> showed only linear polyethylene with no presence of polyester signals.

It has been shown that the identity of the cocatalyst in ethylene polymerization can have strong effects on the outcome of polymerization.<sup>24</sup> Modified MAO (MMAO) is the most commonly used activator for ethylene polymerization. Ethylene polymerizations with MMAO as the activator were performed in the presence of lactide (**Table 2.7**). With

500 or 1000 equivalents of lactide relative to **2.5**, the polymerization was shut down and no polyethylene was isolated (entries 1-2). With a smaller amount of lactide (100 equiv.), ethylene polymerization proceeded with similar activity as in the absence of lactide (entry 3). It is likely that MMAO is binding to lactide to form an insoluble adduct, which does not allow for proper activation of the iron precatalyst. An experiment was carried out where lactide (300 equiv.) was added prior to catalyst activation, and polymerization was not deactivated (entry 4). This should be repeated with 500 or 1000 equivalents of lactide for a direct comparison to determine whether polymerization shuts down due to the insufficient activation of the precatalyst.

**Table 2.7.** Ethylene polymerization with MMAO as activator in the presence of lactide.



Entry	[Lactide]:[2.5]	Polymer mass (g)	Activity (g/mmol·h·bar)
1	1000	No polymer isolated	0
2	500	No polymer isolated	0
3	100	0.864	289
4	300 <sup>a</sup>	0.354	118

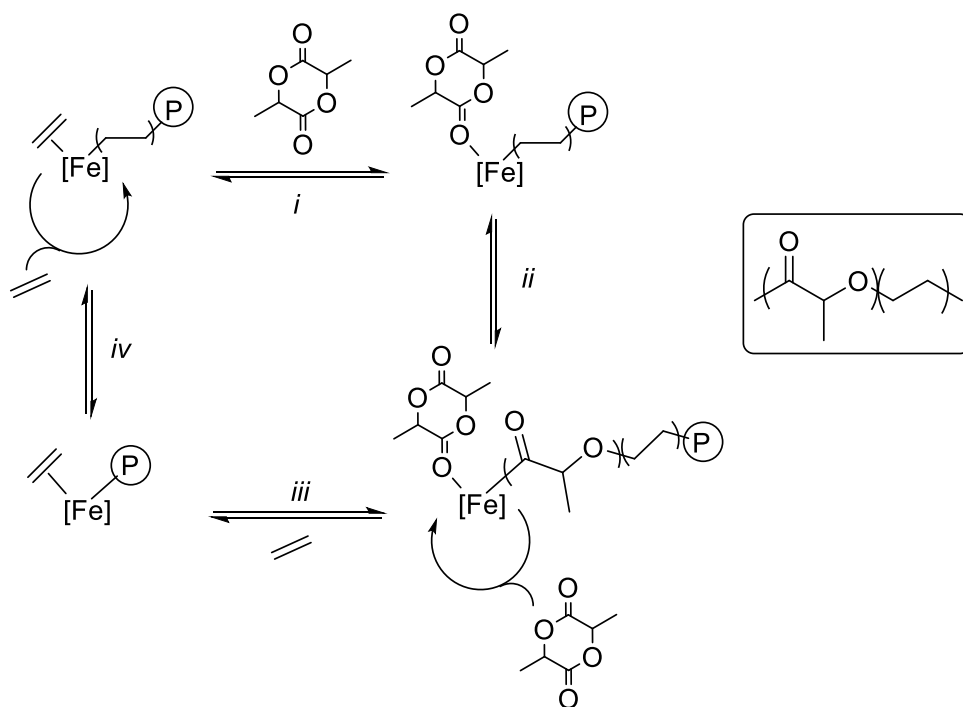
<sup>a</sup>Lactide was added after complex was activated with MMAO.



### 2.6.3 Preliminary Investigations of Transformations Necessary for Lactide-Ethylene Copolymerization

Synthesizing a copolymer of lactide and ethylene is challenging as the efficient polymerization of each monomer requires orthogonal polymerization mechanisms. To crossover from ethylene to lactide polymerization, an iron alkyl species will need to insert into lactide (*ii*, **Scheme 2.5**). In order to switch from lactide polymerization to ethylene polymerization, an iron alkoxide species must insert into a bound olefin (*iv*). In order to copolymerize lactide and ethylene, the interconversion from one polymerization mechanism to the other must be feasible.

**Scheme 2.5.** Envisioned copolymerization of lactide and ethylene. P = growing (co)polymer chain.

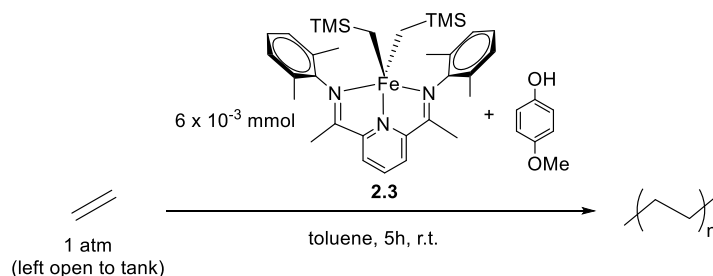


In order to investigate whether an iron alkoxide can insert into a bound olefin, 2,3/4-methoxyphenol was investigated as a catalyst system for ethylene polymerization

(Table 2.8). Although no polymer was observed in the absence of an activator, **2.3**/4-methoxyphenol was a successful precatalyst for ethylene polymerization in the presence of 100 equiv. MAO. Unfortunately,  $^1\text{H}$  NMR spectra of the resulting polymer did not show phenol end groups; only alkene end groups were observed. This suggests that polymerization was not initiated by an alkoxide. An iron alkyl species was most likely formed upon the addition of MAO which initiated the polymerization.

In order to crossover from ethylene polymerization to lactide polymerization, a cationic iron alkyl must insert into lactide. To investigate this crossover reaction, **2.6**/MAO and **2.6**/MMAO were utilized as catalysts for lactide polymerization. If lactide polymerization occurred, this would show that lactide polymerization can be initiated by the cationic alkyl complex formed *in situ* when precatalyst **2.6** is activated with aluminoxanes.

**Table 2.8.** Investigation of **2.3**/4-methoxyphenol as a catalyst system for ethylene polymerization.



	Polymer mass (g)	Activity (g/mmol·h·bar)
Without MAO	--	0
With 100 eq. MAO (relative to [ <b>2.3</b> ])	0.388	13

During the polymerization reaction, the mixture turned red in color, suggesting the cationic iron alkyl species had formed. No poly(lactic acid) was observed after 24 hours in toluene at room temperature. These results do not show that lactide polymerization

cannot be catalyzed by cationic iron alkyl complexes, but rather that aluminum activators are probably not suitable for the copolymerization reaction, which has also been suggested by control experiments with lactide and MAO. These copolymerization studies should be further investigated in the future with borane activators (such as  $\text{B}(\text{C}_6\text{F}_5)_3$ )<sup>25</sup> as alternatives to aluminoxane activators. Also, stoichiometric NMR studies of these fundamental crossover transformations necessary for the copolymerization reaction should be examined, such as the addition of stoichiometric  $\alpha$ -olefins to iron alkoxide species.

## 2.7 Conclusions

Synthesis of iron(II) bis(alkoxides) supported by bis(imino)pyridine ligands was achieved by treating the bis(alkyl) iron(II) complex **2.3** to a variety of aliphatic and aromatic alcohols. A cationic iron(III) bis(alkoxide) complex **2.5** was also synthesized and structurally characterized by oxidation of **2.4a** with ferrocenium hexafluorophosphate.

The iron(II) complexes were found to be effective catalysts for the polymerization of (*rac*)-lactide both as the discrete iron(II) bis(alkoxide) species or through *in situ* activation from **2.3** and the appropriate alcohol. Activity for lactide polymerization was found to be sensitive to the identity of the initiating alcohol with electron rich alcohols initiating lactide polymerization much more efficiently than the electron poor alcohols. Poly(lactic acid) with narrow molecular weight distributions was obtained within a few hours at room temperature, and the catalysis demonstrated several hallmarks of a living polymerization system such as the linear dependence of  $M_n$  on conversion, narrow

molecular weight distributions, and linear polymer growth upon sequential addition of lactide monomer. Mechanistic experiments revealed that only one alkoxide ligand serves as an initiator for lactide polymerizations initiated by aromatic alcohols whereas both alkoxide ligands participate as initiators for catalysts initiated by aliphatic alcohols.

The iron(III) bis(alkoxide) complex **2.5** was found to be completely inactive for lactide polymerization. However, the lactide polymerization reaction could be “switched” on and off by reversibly reducing and oxidizing the metal center, respectively. It is our belief that the versatility of this catalyst system is due in large part to the special properties of iron complexes supported by bis(imino) pyridine ligands. While we have no evidence for the participation of the known redox activity of the bis(imino) pyridine ligands in the polymerization of (*rac*)-lactide, we believe that the electronic and steric flexibility provided by these ancillary ligands will be useful for a variety of polymerization and copolymerization reactions.

Preliminary studies were performed to investigate the feasibility of the copolymerization of lactide and  $\alpha$ -olefins with bis(imino)pyridine iron complexes. Ethylene polymerization catalyzed by **2.6**/MAO was able to proceed in the presence of lactide of equal or less concentration to that of MAO cocatalyst. The iron bis(alkoxide) complex **2.4a** (formed *in situ*) is able to polymerize ethylene upon activation with MAO, although  $^1\text{H}$  NMR indicates polymerization was not initiated by an alkoxide, but rather an iron alkyl species. Precatalyst **2.6** activated with MAO or MMAO was not active for lactide polymerization. These results, along with NMR studies, indicate that aluminum activators should not be utilized for a lactide/ethylene copolymerization. MAO and MMAO likely bind to lactide, which can cause the precatalyst to not be properly

activated. In the future, borane activators should instead be investigated for the copolymerization of ethylene and lactide.

## 2.8 Experimental

**General Considerations.** Unless stated otherwise, all reactions were carried out in oven-dried glassware in nitrogen-filled glove box or with standard Schlenk line techniques.<sup>26</sup> Solvents were used after passage through a solvent purification system under a blanket of argon and then degassed briefly by exposure to vacuum. Nuclear magnetic resonance (NMR) spectra were recorded at ambient temperature on spectrometers operating at 500 MHz. The line listing for the NMR spectra are reported as: chemical shift in ppm (peak width at half-height in Hz, number of protons, proton assignment). Peak width at half-height is reported for paramagnetic complexes. NMR assignments were made in analogy to assignments made for **2.3**.<sup>27</sup> Infrared (IR) spectra were recorded on an attenuated total reflectance infrared spectrometer. Magnetic moments were determined by Evans' method<sup>28</sup> in THF by means of a procedure published by Gibson and coworkers.<sup>29</sup> High-resolution mass spectra were obtained at the Boston College Mass Spectrometry Facility. Gel permeation chromatography (GPC) was performed on an Agilent GPC220 in THF at 40°C with three PL gel columns (10 $\mu$ m) in series and recorded with a refractive index detector. Molecular weights and molecular weight distributions were determined from the signal response of the RI detector relative to polystyrene standards. Cyclic voltammetry was carried out with 0.1 M tetrabutylammonium hexafluorophosphate as the electrolyte in dichloromethane. The sample solution was 0.005 M with respect to the analyte. The working electrode was a

platinum mesh, the counter electrode was a platinum wire, and the reference electrode was a nonaqueous  $\text{Ag}/\text{Ag}^+/\text{I}^-$  electrode. Cyclic voltammograms were measured with scan rates of  $50 \text{ mV s}^{-1}$  and were referenced to  $\text{Fc}/\text{Fc}^+$ . (*rac*)-Lactide was obtained from Purac Biomaterials and was recrystallized from ethyl acetate followed by recrystallization from toluene and dried *in vacuo* prior to polymerization.  $\text{Fe}(\text{py})_2(\text{CH}_2\text{TMS})_2$ ,<sup>27,30</sup> complex **2.2**,<sup>31</sup> complex **2.3**,<sup>27,30</sup> and complex **2.6**<sup>8b</sup> were synthesized as described previously.

**Synthesis of  $\text{Fe}(\text{PDI})(4\text{-methoxyphenoxy})_2$ ,  $\text{PDI} = 2,6\text{-(2,6-Me}_2\text{-C}_6\text{H}_3\text{N=CMe)}_2\text{C}_5\text{H}_3\text{N}$  (2.4a)** At room temperature in a 20 mL vial, a solution of **2.3** (0.10 g, 0.17 mmol) in *n*-pentane (5 mL) was added to a slurry of 4-methoxyphenol (0.042 g, 0.34 mmol) in *n*-pentane (5 mL). After stirring at room temperature for one hour, the solvent was removed to yield a dark purple powder (0.10 g, 88%).  $\mu_{\text{eff}} = 5.2 \mu_{\text{B}}$  at 25°C.  $^1\text{H NMR}$  ( $\text{C}_6\text{D}_6$ ): 50.4 (193, 2H, *m*-pyr), 22.3 (466, 4H), 13.3 (239, 2H), -19.5 (200, 2H, *p*-CH<sub>ar</sub>), -162.4 (502, 6H,  $\text{CH}_3\text{CN}$ ) ppm. IR(neat): 3361, 2944, 2831, 1645, 1593, 1509, 1495, 1465, 1439, 1366, 1295, 1224, 1177, 1122, 1098, 1034, 826, 760, 733, 705, 519  $\text{cm}^{-1}$ . HRMS ( $\text{ESI}^+$ ): calc'd for  $\text{C}_{39}\text{H}_{41}\text{FeN}_3\text{O}_2$  671.24465, found 671.24468.

**Synthesis of  $\text{Fe}(\text{PDI})(4\text{-tert-butylphenoxy})_2$  (2.4b)** At room temperature, a solution of **2.3** (0.10 g, 0.17 mmol) in *n*-pentane (5 mL) was added to a slurry of 2-*tert*-butylphenol (0.051 g, 0.34 mmol) in *n*-pentane (5 mL) in a 20 mL vial. After the solution was allowed to stir at room temperature for one hour, the solvent was removed and a brown powder resulted (0.12g, 96%).  $\mu_{\text{eff}} = 5.1 \mu_{\text{B}}$  at 25°C.  $^1\text{H NMR}$  ( $\text{C}_6\text{D}_6$ ): 53.4 (244, 2H, *m*-pyr), 50.0 (169, 1H), 23.1 (371, 6H), 13.16 (205, 2H), -19.9 (109, 2H, *p*-CH<sub>ar</sub>), -164.2 (85, 6H,  $\text{CH}_3\text{CN}$ ) ppm. IR(neat): 2951, 1643, 1593, 1502, 1362, 1263, 1204, 1175,

1093, 831, 762, 692, 549  $\text{cm}^{-1}$ . HRMS (ESI<sup>+</sup>): calc'd for  $\text{C}_{45}\text{H}_{53}\text{FeN}_3\text{O}_2$  723.34872, found 723.34523.

**Synthesis of  $\text{Fe}(\text{PDI})(\text{neopentoxide})_2$  (2.4c)** At room temperature, a solution of neopentyl alcohol (0.030 g, 0.34 mmol) in *n*-pentane (5 mL) was added slowly to a solution of **4** (0.10 g, 0.17 mmol) in *n*-pentane (5 mL) in a 20 mL vial. After the mixture was allowed to stir at room temperature for one hour, the solvent was removed and a green powder resulted (0.088 g, 86%).  $\mu_{\text{eff}} = 5.1 \mu_{\text{B}}$  at 25°C.  $^1\text{H}$  NMR ( $\text{C}_6\text{D}_6$ ): 60.3 (463, 2H, *m*-pyr), 27.8 (287, 6H), 21.4 (342, 4H), 14.4 (680, 4H), 11.98 (233, 18H), -19.7 (158, 2H, *p*-CH<sub>ar</sub>), -174.9 (71.3, 6H,  $\text{CH}_3\text{CN}$ ) ppm. IR(neat): 2948, 1643, 1592, 1468, 1362, 1247, 1025, 1061, 1018, 840, 762, 693, 558, 495, 429  $\text{cm}^{-1}$ .

**Synthesis of  $[\text{Fe}(\text{PDI})(4\text{-methoxyphenoxide})_2]^+\text{PF}_6^-$  (2.5).** In a 20 mL vial, a solution of ferrocenium hexafluorophosphate (0.074g, 0.22mmol) in dichloromethane (5 mL) was added dropwise to a solution of **2.4a** (0.15g, 0.22mmol) in dichloromethane (5 mL). The blue solution was allowed to stir at room temperature for 15 minutes and the solvent was removed. The resulting blue powder was washed with *n*-pentane and dried *in vacuo* (0.15g, 84%). Crystallization by slow evaporation in benzene afforded crystals suitable for X-ray analysis.  $\mu_{\text{eff}} = 5.9 \mu_{\text{B}}$  at 25°C.  $^1\text{H}$  NMR ( $\text{C}_6\text{D}_6$ ): 28.5 (296), 6.6 (16.4), 6.3 (19.4), 4.1 (280), 3.5 (29.1), 3.1 (9.22), 1.2 (37.0), 0.8 (19.4) ppm. IR(neat): 1630, 1593, 1509, 1494, 1231, 1178, 1031, 825, 771, 732, 556  $\text{cm}^{-1}$ . HRMS (ESI<sup>+</sup>): calc'd for  $\text{C}_{39}\text{H}_{41}\text{FeN}_3\text{O}_2$  671.24465, found 671.24504.

**Generic procedure for the polymerization of (*rac*)-lactide with iron bis(alkoxide).** At room temperature in a glove box, iron bis(alkoxide) complex **2.4a** (0.0186g, 0.028 mmol) in dichloromethane (3.6 mL) was added to a 20 mL vial

containing (*rac*)-lactide (0.20g, 1.4 mmol) and 1,3,5-trimethoxybenzene (0.020g, 0.12 mmol) in dichloromethane (2.0 mL). Aliquots were removed periodically from the reaction mixture and terminated by exposing them to air. Solvent was removed *in vacuo* and conversion was determined by  $^1\text{H}$  NMR in DMSO- $\text{d}_6$  by integrating the methine peak of the remaining lactide versus the methoxy peak of the 1,3,5-trimethoxybenzene internal standard. The aliquots were also analyzed by GPC to determine molecular weight and molecular weight distribution of the polymers.

**Generic procedure for the polymerization of (*rac*)-lactide with iron bis(alkoxides) formed *in situ*.** A similar procedure was adopted as for the pre-formed iron bis(alkoxide) complexes except the bis(alkoxide) complex was formed without isolation by exposing iron alkyl complex **2.3** (0.0168 g, 0.028 mmol) to an alcohol initiator (0.055 mmol) in dichloromethane (3.6 mL) for five minutes prior to addition to lactide.

**Sequential addition of lactide to form higher molecular weight polymers.** At room temperature in a glove box, iron alkyl complex **2.3** (0.0168g, 0.028 mmol) and 4-methoxyphenol (0.0068g, 0.055 mmol) in dichloromethane (3.6 mL) were added to a 20 mL vial containing (*rac*)-lactide (0.20g, 1.4 mmol) and 1,3,5-trimethoxybenzene (0.020g, 0.12 mmol) in dichloromethane (2.0 mL). After the initial lactide was consumed, additional lactide (0.20g, 1.4 mmol) was added to the reaction mixture. This was repeated for a total of 15 additions (21 mmol), with 3-16 hours between additions. Molecular weight was determined by GPC relative to polystyrene standards.

**Redox switchable polymerization of lactide.** Iron alkyl complex **2.3** (0.0168 g, 0.028 mmol) and 4-methoxyphenol (0.0068 g, 0.055 mmol) in dichloromethane (3.6 mL)



were added to a 20 mL vial containing (*rac*)-lactide (0.20 g, 1.4 mmol) and 1,3,5-trimethoxybenzene (0.020 g, 0.12 mmol) in dichloromethane (2.0 mL). After 40 min., ferrocenium hexafluorophosphate (0.0093 g, 0.028 mmol) was added to the reaction mixture and the color changed from purple-brown to blue. At  $t = 100$  min., cobaltocene (0.0053 g, 0.028 mmol) was added and the mixture turned back to purple-brown in color. Aliquots were removed periodically from the reaction mixture and terminated by exposing them to air. Solvent was removed in vacuo and conversion was determined by  $^1\text{H}$  NMR in  $\text{DMSO-d}_6$  by integrating the methine peak of the remaining lactide versus the methoxy peak of the 1,3,5-trimethoxybenzene internal standard. The aliquots were also analyzed by GPC to determine molecular weight and molecular weight distribution of the polymers.

**General procedure for ethylene polymerization at high pressures in the presence of lactide.** The desired amount of lactide was added to a Fisher-Porter tube equipped with a stir bar and dissolved in toluene (25 ml). Methylaluminoxane solution in toluene (10 wt.%, 0.40ml, 0.6 mmol) was added. The apparatus was sealed and removed from a glove box. The tube was pressurized to 50psi ethylene and vented three times. The tube was then pressurized to 145psi ethylene and allowed to stir 1 hour. In a glove box, **2.6** (0.37mg,  $6 \times 10^{-4}$  mmol) was suspended in toluene (0.6 ml). The Fisher-Porter tube was depressurized and kept under positive pressure of  $\text{N}_2$  while the catalyst solution was injected. The reaction was pressurized to 145psi ethylene and the needle valve was left open to the ethylene tank. The reaction turned cloudy immediately (unless inhibited by lactide) and it was allowed to stir 1 hour at room temperature. The vessel was depressurized, exposed to air, and the mixture was poured into stirring MeOH (200 ml)

and stirred overnight to precipitate white solid. The polymer was collected by filtration and dried in vacuum.

**General procedure for ethylene polymerization at atmospheric pressure in the presence of lactide.** The desired amount of lactide was added to a polymerization flask equipped with a stir bar and dissolved in toluene (25 ml). Methylaluminoxane solution in toluene (10 wt.%, 0.40ml, 0.60 mmol) was added. The flask was sealed, fitted with a septum on the side arm, and removed from a glove box. It was placed on the Schlenk line under 1 atm ethylene and allowed to stir 1 hour. In a glove box, **2.6** (0.37mg,  $6 \times 10^{-4}$  mmol) was suspended in toluene (0.6 ml), and this mixture was injected through the side arm of the polymerization flask. The mixture became cloudy after a few minutes (unless inhibited by lactide), and was allowed to stir at room temperature for 5 hours. The reaction was then exposed to air and poured into stirring MeOH (200 ml) and stirred overnight to precipitate white solid. The polymer was collected by filtration and dried in vacuum.

**General Procedure for Lactide Control Experiments with MAO.** Lactide (0.10g, 0.69mmol) was dissolved in toluene (5mL) and stirred for 1h to dissolve all lactide. Tetradecane (0.025g, 0.06mmol) was added to the solution as an internal standard. A 0-time aliquot was then removed. To the lactide solution was added the aluminum reagent (MAO, AlMe<sub>3</sub>, or Al(iBu)<sub>3</sub>). The reaction was monitored by GC to determine lactide conversion. The reaction mixtures were then poured into HCl/MeOH for 1h and then solvent was removed. <sup>1</sup>H NMR of the residue was taken in CDCl<sub>3</sub>.

---

## **References**

1. Adapted with permission from Biernesser, A.B.; Li, B.; Byers, J.A. *J. Am. Chem. Soc.*, **2013**, *135*, 16553-16560. Copyright 2013 American Chemical Society.
2. a) Mehta, R.; Kumar, V.; Bhunia, H.; Upadhyay, S. N. *J. Macromol. Sci., Polym. Rev.* **2005**, *45*, 325-349. b) Dechy-Cabaret, O.; Martin-Vaca, B.; Bourissou, D. *Chem. Rev.* **2004**, *104*, 6147-6176. c) Dove, A. P. *Chem. Commun.* **2008**, 6446-6470.
3. a) Dove, A. P.; Li, H.; Pratt, R. C.; Lohmeijer, B. G. G.; Culkin, D. A.; Waymouth, R. M.; Hedrick, J. L. *Chem. Commun.* **2006**, 2881-2883. b) Dove, A. P.; Pratt, R. C.; Lohmeijer, B. G. G.; Culkin, D. A.; Hagberg, E. C.; Nyce, G. W.; Waymouth, R. M.; Hedrick, J. L. *Polymer* **2006**, *47*, 4018-4025.
4. Hoppe, J. O.; Agnew Marcelli, M. G.; Tainter, M. L. *Am. J. Med. Sci.* **1955**, *230*, 558-571.
5. Gregson, C. K. A.; Gibson, V. C.; Long, N. J.; Marshall, E. L.; Oxford, P. J.; White, A. J. P. *J. Am. Chem. Soc.* **2006**, *128*, 7410-7411.
6. Broderick, E. M.; Guo, N.; Vogel, C. S.; Xu, C.; Sutter, J. r.; Miller, J. T.; Meyer, K.; Mehrkhodavandi, P.; Diaconescu, P. L. *J. Am. Chem. Soc.*, **2011**, *133*, 9278-9281.
7. a) Broderick, E. M.; Guo, N.; Wu, T.; Vogel, C. S.; Xu, C.; Sutter, J.; Miller, J. T.; Meyer, K.; Cantat, T.; Diaconescu, P. L. *Chem. Commun.*, **2011**, *47*, 9897-9899. b) Sauer, A.; Buffet, J.-C.; Spaniol, T. P.; Nagae, H.; Mashima, K.; Okuda, J. *J. ChemCatChem*, **2013**, *5*, 1088-1091.
8. a) Small, B. L.; Brookhart, M.; Bennett, A. M. A. *J. Am. Chem. Soc.* **1998**, *120*, 4049-4050. b) Britovsek, G. J. P.; Bruce, M.; Gibson, V. C.; Kimberley, B. S.; Maddox, P. J.; Mastroianni, S.; McTavish, S. J.; Redshaw, C.; Solan, G. A.; Strömberg, S.; White, A. J. P.; Williams, D. J. *J. Am. Chem. Soc.* **1999**, *121*, 8728-8740.
9. O'Reilly, R.K.; Gibson, V.C.; White, A.J.P.; Williams, D.J. *Polyhedron* **2004**, *17*, 2921-2928.
10. a) Trovitch, R. J.; Lobkovsky, E.; Bill, E.; Chirik, P. J. *Organometallics* **2008**, *27*, 1470-1478; Monfette, S.; b) Turner, Z. R.; Semproni, S. P.; Chirik, P. J. *J. Am. Chem. Soc.*, **2012**, *134*, 4561-4564; c) Tondreau, A. M.; Atienza, C. C. H.; Weller, K. J.; Nye, S. A.; Lewis, K. M.; Delis, J. G. P.; Chirik, P. J. *Science*, **2012**, *335*, 567-570.

- 
11. Russell, S. K.; Lobkovsky, E.; Chirik, P. J. *J. Am. Chem. Soc.*, **2011**, *133*, 8858-8861.
  12. Britovsek, G. J. P.; Bruce, M.; Gibson, V. C.; Kimberley, B. S.; Maddox, P. J.; Mastroianni, S.; McTavish, S. J.; Redshaw, C.; Solan, G. A.; Strömberg, S.; White, A. J. P.; Williams, D. J. *J. Am. Chem. Soc.* **1999**, *121*, 8728-8740.
  13. Boyle, T. J.; Ottley, L. A. M.; Apblett, C. A.; Stewart, C. A.; Hoppe, S. M.; Hawthorne, K. L.; Rodriguez, M. A. *Inorg. Chem.*, **2011**, *50*, 6174-6182.
  14. a) Bart, S. C.; Chlopek, K.; Bill, E.; Bouwkamp, M. W.; Lobkovsky, E.; Neese, F.; Wieghardt, K.; Chirik, P. J. *J. Am. Chem. Soc.* **2006**, *128*, 13901-13912. b) Sokolowski, A.; Bothe, E.; Bill, E.; Weyhermuller, T.; Wieghardt, K. *Chem. Commun.* **1996**, 1671-1672.
  15. Zhang, X.; MacDonald, D. A.; Goosen, M. F. A.; McAuley, K. B. *J. Polym. Sci. A Polym. Chem.* **1994**, *32*, 2965-2970.
  16. Manna, C.M.; Kaplan, H.Z.; Li, B.; Byers, J.A. *Polyhedron* **2014**, *84*, 160-167.
  17. O'Keefe, B. J.; Breyfogle, L. E.; Hillmyer, M. A.; Tolman, W. B. *J. Am. Chem. Soc.* **2002**, *124*, 4384-4393.
  18. McGuinness, D. S.; Marshall, E. L.; Gibson, V. C.; Steed, J. W. *J. Polym. Sci. A Polym. Chem.* **2003**, *41*, 3798-3803.
  19. Similar tacticities observed for both polymers does not definitively rule out a mechanism involving one alkoxide as an initiator because the secondary alcohol could be poor at inducing chirality in the growing polymer chain.
  20. a) Chamberlain, B. M.; Cheng, M.; Moore, D. R.; Ovitt, T. M.; Lobkovsky, E. B.; Coates, G. W. *J. Am. Chem. Soc.* **2001**, *123*, 3229-3238. b) Kasperczyk, J. E. *Macromolecules* **1995**, *28*, 3937-3939. c) Kean, R. T.; Hall, E. S.; Kolstad, J. J.; Lindgren, T. A.; Doscotch, M. A.; Siepmann, J. I.; Munson, E. J. *Macromolecules* **1997**, *30*, 2422-2428. d) Thakur, K. A. M.; Kean, R. T.; Hall, E. S.; Kolstad, J. J.; Munson, E. J. *Macromolecules* **1998**, *31*, 1487-1494.
  21.  $P_s$  refers to the probability of syndiotactic enchainment.
  22. Manna, C.M.; Kaur, A.; Yablon, L.M.; Haeffner, F.; Li, B.; Byers, J.A. *J. Am. Chem. Soc.* **2015**, *137*, 14232-14235.
  23. Johnson, L.K.; Mecking, S.; Brookhart, M. *J. Am. Chem. Soc.* **1996**, *118*, 267.
  24. Chen, E.Y.-X.; Marks, T.J. *Chem. Rev.* **2000**, *100*, 1391.

- 
25. Bouwkamp, M.W.; Lobkovsky, E.; Chirik, P.J. *J. Am. Chem. Soc.* **2005**, *127*, 9660-9661.
26. Burger, B. J.; Bercaw, J. E. *New Developments in the Synthesis, Manipulation and Characterization of Organometallic Compounds*; Wayda, A.L., Darensbourg, M.Y., Eds.; American Chemical Society: Washington D.C., 1987.
27. Cámpora, J.; Naz, A. M.; Palma, P.; Álvarez, E.; Reyes, M. L. *Organometallics* **2005**, *24*, 4878-4881.
28. a) Evans, D. F. *J. Chem. Soc.* **1959**, 2003-2005. b) Schubert, E. M. *J. Chem. Educ.* **1992**, *69*, 62.
29. Britovsek, G. J. P.; Gibson, V. C.; Spitzmesser, S. K.; Tellmann, K. P.; White, A. J. P.; Williams, D. J. *J. Chem. Soc., Dalton Trans.* **2002**, 1159-1171.
30. Fernández, I.; Trovitch, R. J.; Lobkovsky, E.; Chirik, P. J. *Organometallics* **2007**, *27*, 109-118.
31. Boyle, T. J.; Ottley, L. A. M.; Apblett, C. A.; Stewart, C. A.; Hoppe, S. M.; Hawthorne, K. L.; Rodriguez, M. A. *Inorg. Chem.*, **2011**, *50*, 6174-6182.

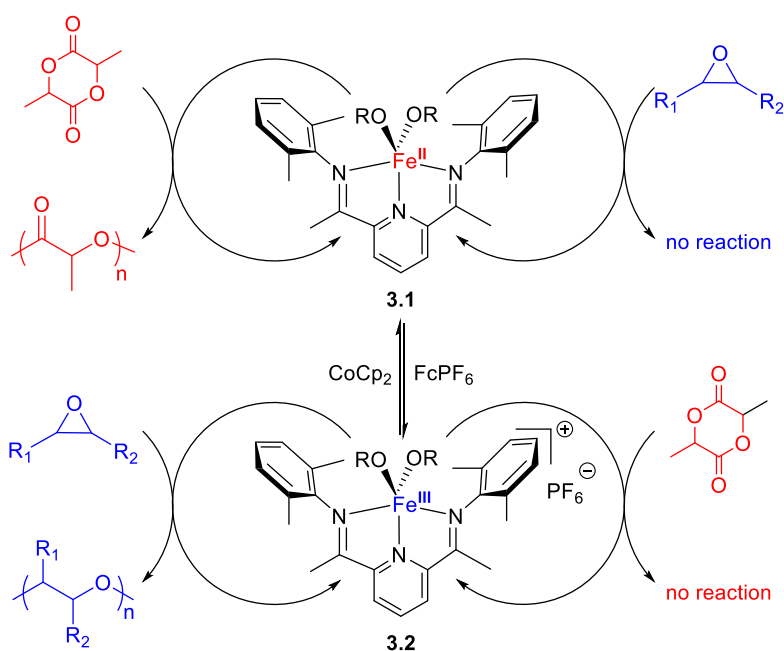
## Chapter 3: Redox-Switchable Copolymerization of Lactide and Epoxides Catalyzed by Bis(imino)pyridine Iron(II/III) Bis(alkoxide) Complexes<sup>1</sup>

### 3.1 Introduction

Recently, several reports have emerged that describe the ability to reversibly activate and deactivate chemical reactions with the addition of exogenous redox reagents, which have applications in sequence controlled polymerization reactions, chemical sensing, chemotherapy, information storage, and for coatings technologies.<sup>2</sup> The ability to control lactide ring-opening polymerization by oxidizing and reducing catalysts that are either supported by redox active ligands<sup>3,4</sup> or that utilize redox-active metals<sup>5,6</sup> as catalytically active species has been particularly successful. In Chapter 2, we reported a bis(imino)pyridine iron complex (**3.1**) was described that undergoes lactide polymerization in the iron(II) oxidation state but is dormant in the iron(III) oxidation state (See Chapter 2.5, **Scheme 3.1**).<sup>5</sup> Sequential catalyst oxidation and reduction resulted in the ability to deactivate and activate polymerization, respectively, without evidence for detrimental side reactions.

We hypothesized that the different reactivity of iron(II) and iron(III) complexes would be amenable to developing a chemoselective block copolymerization with a second monomer that has orthogonal reactivity to lactide. In this way, we could synthesize a variety of microstructures from the same monomer feedstock by switching

the oxidation state of the catalyst to dictate which monomer polymerizes. We discovered that epoxides have such reactivity and utilized the complementary reactivity of epoxides and lactide for the synthesis of block copolymers. In these reactions, iron(II) serves as the active oxidation state for lactide polymerization, while iron(III) is the active oxidation state for epoxide polymerization. This synthetic methodology provides rapid access to block copolymers that are promising candidates for drug delivery devices<sup>7</sup> and as biodegradable thermoplastic elastomers.<sup>8</sup>



**Scheme 3.1.** Orthogonal reactivity of lactide and epoxide monomers.

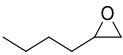
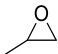


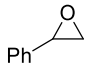
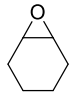
## 3.2 Epoxide Polymerization with Iron(III) Bis(imino)pyridine Bis(alkoxide) Complexes

### 3.2.1 Epoxide Monomer Scope

During preliminary investigations, we were pleased to find that while the iron(II) alkoxide **3.1** is completely inactive for hexene oxide polymerization, exposing small

amounts of the cationic iron(III) alkoxide **3.2** (0.2 mol%) to neat hexene oxide lead to polymer with a number average molecular weight of 6.5 kg/mol and a dispersity ( $\bar{D}$ ) of 2.0 after 24 hours (**Table 3.1**, entry 1). In addition to hexene oxide, iron(III) alkoxide **3.2** was a good catalyst to polymerize a variety of other epoxide monomers. Monosubstituted, 1,2-disubstituted (entry 4), and 1,1-disubstituted epoxides (entry 3) were competent substrates for the polymerization reaction although polymerization of isoprene oxide led to low yields of low molecular weight polymer (entry 3). Compared to the other monomers examined, styrene oxide demonstrated broader dispersities as a consequence of a bimodal molecular weight distribution observed in the GPC trace (entry 5).

**Table 3.1.** Polymerization of epoxides catalyzed by **3.2**<sup>a</sup>

	epoxide	$M_n^b$	$\bar{D}$	%Yield <sup>c</sup>
1		6.5	2.0	57
2		4.6	1.7	69
3		1.9	1.7	28
4		22.1	1.9	36
5		12.7/0.7 <sup>d</sup>	1.3/1.5	51
6 <sup>e</sup>		22.6	2.3	81

<sup>a</sup>Neat epoxide with 0.2 mol% **2** for 24 h at 24 °C. <sup>b</sup>kg/mol; determined by GPC relative to polystyrene standards. <sup>c</sup>determined by mass. <sup>d</sup>bimodal distribution. <sup>e</sup>In PhCl (2.1 M).

Iron(III) alkoxide **3.2** proved to be a particularly active catalyst for the polymerization of cyclohexene oxide. Attempted polymerization of this substrate in neat



epoxide resulted in a significant exotherm and the rapid formation of a viscous solution that could not be stirred. The use of chlorobenzene as a solvent was required to mitigate the significant exotherm observed during neat epoxide polymerization reactions (entry 6). Importantly, when CHO was treated with the iron(II) complex **3.1**, no polymerization occurred.

### 3.2.2 Redox-Switchable Epoxide Polymerization

The redox-switchable polymerization of cyclohexene oxide was next demonstrated (**Figure 3.1**). A polymerization reaction in chlorobenzene was allowed to proceed to 40% conversion, at which time cobaltocene ( $\text{Cp}_2\text{Co}$ ) was added to the reaction to reduce the complex to the inactive iron(II) state. The conversion of cyclohexene oxide stopped upon addition of  $\text{Cp}_2\text{Co}$ , and after 40 minutes, the reaction was reinitiated by oxidizing the complex with ferrocenium hexafluorophosphate ( $\text{FcPF}_6$ ). After oxidation, the reaction proceeded at a similar rate ( $k_{\text{obs}} = 1.23 \times 10^{-4} \text{ s}^{-1}$ ) as initially observed ( $k_{\text{obs}} = 2.54 \times 10^{-4} \text{ s}^{-1}$ ), which suggested the catalyst was dormant when in the iron(II) oxidation state.

The polymerization reaction did not reach full conversion, but we do not believe this to be a detrimental effect of the redox-switching because we have found that ultimate conversion of the epoxide is dependent on its concentration. To support this assertion, we note that the overall conversion observed in the redox-switching experiment is identical to the ultimate conversion obtained from epoxide polymerization catalyzed by **3.2** at the same initial concentration of cyclohexene oxide.

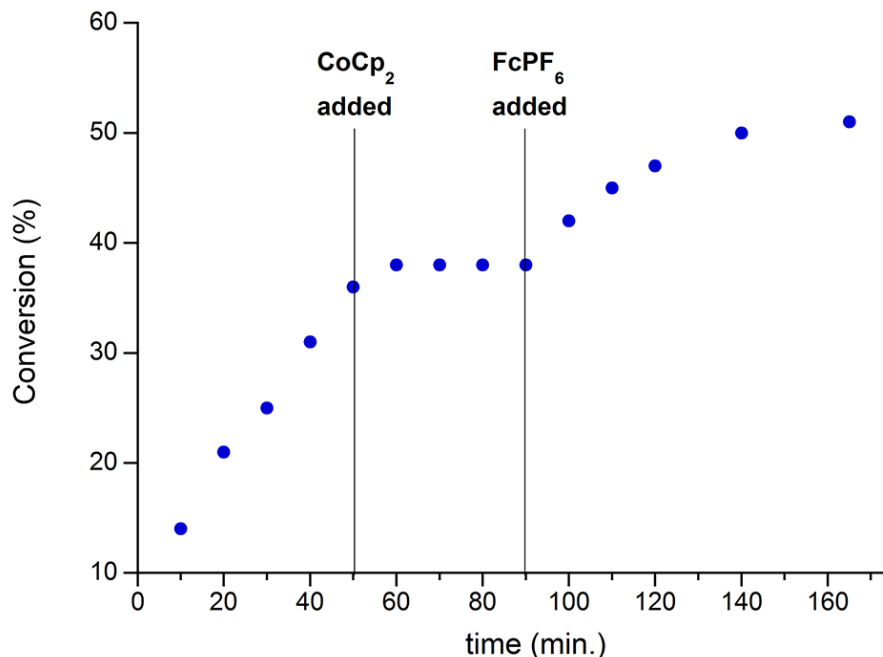


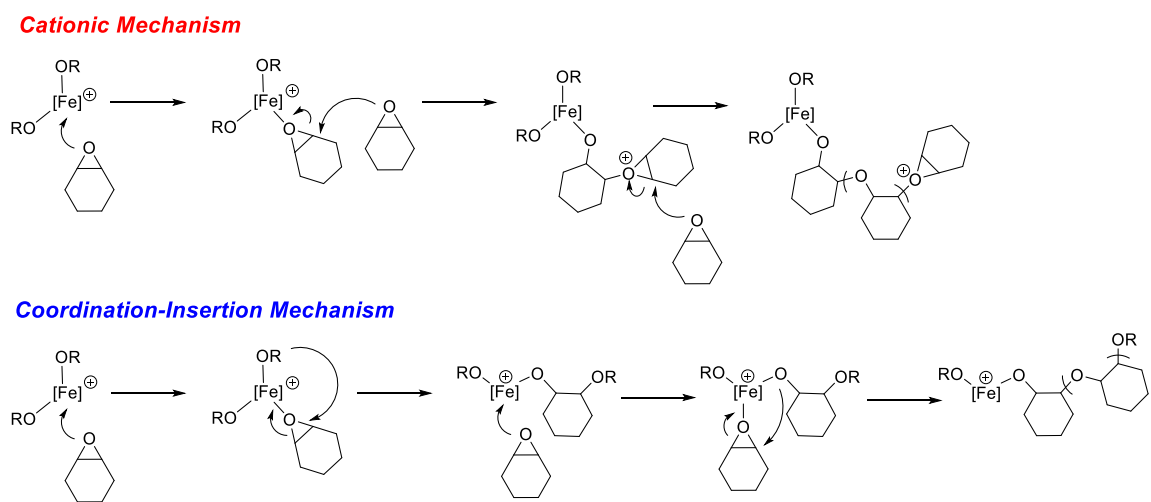
**Figure 3.1.** Redox-controlled polymerization of cyclohexene oxide in PhCl (0.91M) with complex **3.2** (2 mol%). At the time points labeled 50 and 90 min., cobaltocene and ferrocenium hexafluorophosphate were added to the reaction to reduce and oxidize the complex, respectively.

Previously reported bond metrics obtained from an X-ray crystal structure of **3.2** (see Chapter 2.2) suggest that the redox reactions reported here occur at the metal center rather than at one of the two potentially redox active ligands.<sup>5</sup> The ability to control epoxide polymerization by oxidizing and reducing the metal center has interesting mechanistic implications. We considered whether the epoxide polymerization was occurring by a cationic or coordination-insertion mechanism ( In this case, propagation directly involves the iron center, and alteration of the oxidation state of the iron center could deactivate the polymerization.

**Scheme 3.2).** For a cationic polymerization mechanism, a bound epoxide would be attacked by a second epoxide monomer to form a cationic epoxonium intermediate

that would propagate polymerization. Since chain propagation does not involve iron but rather an epoxonium intermediate, reduction of the iron complex would not alter chain propagation rates. Therefore, results obtained thus far are more consistent with a coordination insertion mechanism (although a monometallic mechanism is shown, a mechanism that involves two iron centers is also possible and has precedence<sup>9</sup>). In this case, propagation directly involves the iron center, and alteration of the oxidation state of the iron center could deactivate the polymerization.

**Scheme 3.2.** Two common mechanisms proposed for epoxide polymerization.



### 3.3 Redox-Switchable Diblock Copolymerization of Lactide and Cyclohexene Oxide

Currently, the epoxide polymerization reactions do not demonstrate characteristics of a living polymerization, as somewhat broad dispersities are observed and the molecular weight obtained is not in line for theoretical values based on the catalyst to monomer ratio. However, the complementary reactivity of cyclohexene oxide and lactide made redox-switchable block copolymerization reactions possible.

Many optimization experiments were performed for the copolymerization reactions due to encountered issues with reproducibility. When the copolymerization experiments were performed in dichloromethane, irreproducible reaction rates of the epoxide polymerization were observed. Because epoxide polymerization proceeded as usual in neat conditions, and was slower than observed previously even when control reactions were performed with  $\text{FcPF}_6$  as the catalyst, it was concluded that the solvent was the source of these inconsistencies and may be contaminated.

The dichloromethane solvent that had been used for the epoxide polymerization and copolymerization reactions was degassed solvent from our solvent purification system (SPS). Suspecting that our dichloromethane keg may be contaminated, we decided to use solvent from another SPS instead; however, similar results were obtained (70% conversion after 24 hours compared to previously observed full conversion within 3 hours). Dichloromethane that was treated with  $\text{K}_2\text{CO}_3$  to remove any acid impurities and then vacuum transferred, as well as a purchased bottle of sureseal anhydrous dichloromethane that did not have to pass through the SPS did not improve the slow polymerization rates that were being observed.

This led us to investigate alternative solvents for the epoxide polymerization and copolymerization reactions. Diethyl ether and 1,2-dichloroethane were suitable solvents for cyclohexene oxide polymerization, but were not successful for lactide polymerization (no conversion was observed). Benzene seemed like a promising choice because both lactide and epoxide polymerization could be conducted in this solvent, but cyclohexene oxide polymerization was sluggish and would require several days of reaction time. Chlorobenzene was promising choice as epoxide polymerization proceeded to 65%

conversion within three hours in this solvent. It was also discovered that the rate of lactide polymerization is much faster in chlorobenzene than it is in dichloromethane; lactide polymerization in the absence of cyclohexene oxide reached over 90% conversion in 20 minutes in chlorobenzene, compared to three hours in dichloromethane (**Figure 3.2**).

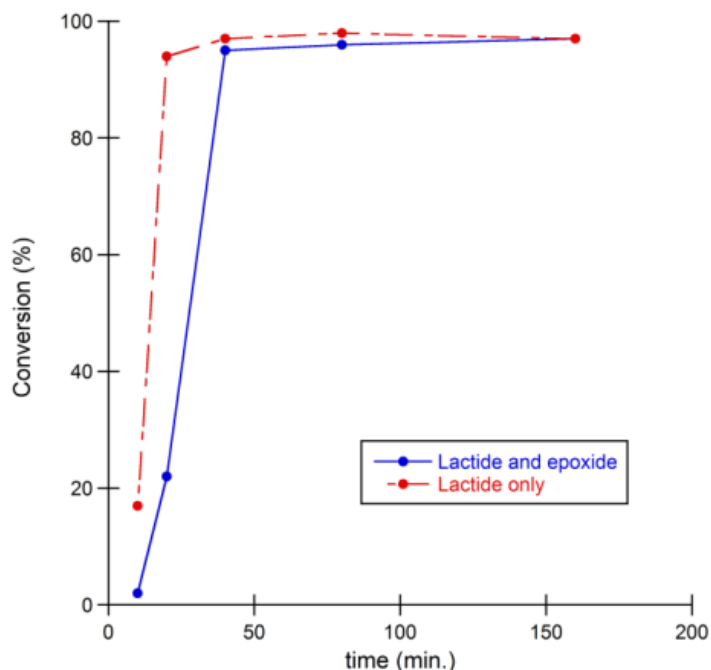


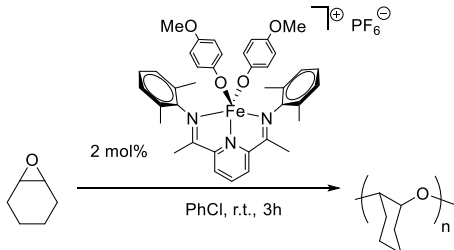
**Figure 3.2.** Comparison of lactide polymerization conversion vs. time in the presence (blue) and absence (red) of cyclohexene oxide (1 equiv. relative to lactide) in PhCl (0.17M) at 24°C.

In the presence of one equivalent of cyclohexene oxide, the lactide polymerization reached over 90% conversion in 40 minutes (**Figure 3.2**). The only drawback observed with chlorobenzene is that transesterification of poly(lactic acid) became an issue at prolonged reaction times (>3h), leading to broader dispersities, but this can be avoided by quenching the reactions once full conversion of lactide is reached.

However, after performing the polymerization reactions in chlorobenzene for a few months and seeing consistent results, the epoxide polymerization rate suddenly became much slower. Instead of observing around 70% conversion of the epoxide in three hours, less than 50% conversion occurred (sometimes as little as 15%) and did not reach full conversion with prolonged reaction times. To determine the source of the impurity causing inhibition of the reaction, several reaction conditions were varied. First, it was suspected that the complex contained impurities, so new batches of complex were synthesized and used for the reaction. In each case, slow polymerization rates were observed with only 15-30% epoxide conversion after 3 hours, suggesting that the complex was not the source of the impurity.

Because we previously had issues with the solvent when we were using dichloromethane, it seemed likely that the solvent was also the culprit for these slower reaction rates. The chlorobenzene in a glove box was degassed again to remove any oxygen and passed through alumina to remove any water, and gave improved polymerization rates (**Table 3.2**, 47% after 3h, Entry 2), although reactions were not restored to the original rate. Fresh chlorobenzene was purified by washing it with sulfuric acid,  $\text{NaHCO}_3$ , and water, dried over  $\text{K}_2\text{CO}_3$  and  $\text{P}_2\text{O}_5$ , and then vacuum transferred. This chlorobenzene gave even slower epoxide polymerization rates (entry 3). Storing the chlorobenzene over molecular sieves did not have an effect on the reaction rate.

**Table 3.2.** Epoxide polymerization with various reaction conditions in attempt to achieve original reaction rate in chlorobenzene.

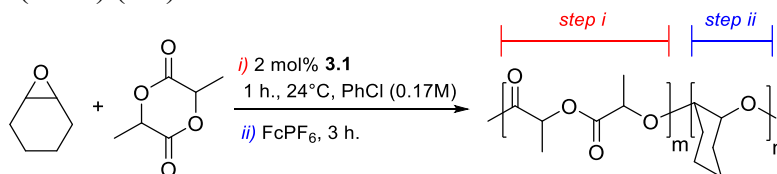


Entry	Reaction conditions	Conv. (%)
1	Original results	68
2	Re-degassed PhCl passed thru Al <sub>2</sub> O <sub>3</sub>	47
3	Freshly purified, distilled PhCl (washed with H <sub>2</sub> SO <sub>4</sub> )	7
4	Vials washed with DI H <sub>2</sub> O before drying and brand new stir bar	22
5	PhCl dried over CaH <sub>2</sub> and distilled	45
6	Anhydrous sureseal PhCl passed through SiO <sub>2</sub>	60

Suspecting that the reaction vials may be contaminated, we took extra measures to rid them of contaminants. Chloride counterions were found to have negative effects on the reaction, so it is possible that some chloride salts were present on the reaction vials. The vials and pipets were rinsed with deionized water and oven-dried before use. A brand new stir bar was also used in case the Teflon stir bars contained detrimental contaminants. This did not help the reaction; a 22% conversion of epoxide was observed (**Table 3.2**, Entry 4). Distilling the chlorobenzene after drying over CaH<sub>2</sub> did not improve the poly(cyclohexene oxide yield) (**Table 3.2**, entry 5). Finally, consistent results were obtained when the chlorobenzene was passed through SiO<sub>2</sub> before use in polymerization reactions (**Table 3.2**, entry 6). Moving forward, all epoxide homo- and copolymerization reactions were performed in chlorobenzene that had been passed through SiO<sub>2</sub>. It is still unclear what impurities the SiO<sub>2</sub> removed that interfered with the epoxide polymerization reactions.

Satisfyingly, when a 1:1 mixture of cyclohexene oxide and lactide in chlorobenzene (that had been passed through SiO<sub>2</sub>) at 24 °C was exposed to **3.1**, clean polymerization of lactide was observed without any incorporation of cyclohexene oxide (entry 1, **Table 3.3**). The chemoselectivity of the reaction was apparent from the absence of polyether resonances in the <sup>1</sup>H NMR spectrum of the polymer (**Figure 3.3b**). Although only PLA was observed when the complex was in the iron(II) oxidation state, oxidation of the complex to iron(III) with FcPF<sub>6</sub> led to clear evidence for the formation of poly(cyclohexene oxide) (PCHO) in the <sup>1</sup>H NMR spectrum (**Figure 3.3c**).

**Table 3.3.** Redox-controlled diblock copolymerization of (*rac*)-lactide (L) and cyclohexene oxide (CHO) (1:1).



After step <i>i</i>					After step <i>ii</i> and precipitation <sup>a</sup>					
	M <sub>n</sub> <sup>b</sup>	Đ	% CHO <sup>c</sup>	% L <sup>c</sup>	M <sub>n</sub> <sup>b</sup>	Đ	% CHO <sup>c</sup>	% L <sup>c</sup>	m:n <sup>c</sup>	% Copolym. <sup>d</sup>
<b>1</b>	11.9	1.2	0	98	10.2 (37.5)	1.5	69	98	7:1	67
<b>2<sup>e</sup></b>	11.2 (12.1)	1.2	0	98	9.2 (27.2)	1.5	89	98	7:1	65
<b>3<sup>f</sup></b>	10.0	1.2	0	99	3.5 (20.1)	1.4	71	98	5:1	23
<b>4<sup>g</sup></b>	4.5	1.3	0	35	1.7 (27.0)	2.0	32	36	4:1	68

<sup>a</sup>Isolated by precipitation from acetone and hexanes. <sup>b</sup>kg/mol, determined by GPC with RI detector relative to polystyrene standards; values in parentheses from LS detector. <sup>c</sup> percent conversion determined by <sup>1</sup>H NMR. <sup>d</sup> percent copolymer determined from mass of isolated copolymer/mass of total polymer. <sup>e</sup>Epoxide added in second step after oxidant. <sup>f</sup>[CHO]:[L] = 5:1 ([CHO] = 0.80M). <sup>g</sup>Step *i* carried out for 15 min.



The molecular weight obtained from this reaction after the first step (11.9 kg/mol, **Table 3.3** entry 1) was identical to the molecular weight of poly(lactic acid) (PLA) in the absence of cyclohexene oxide.<sup>10</sup> However, a slightly slower reaction rate was observed for lactide polymerization in the presence of cyclohexene oxide (**Figure 3.2**), which likely arises from competitive binding of cyclohexene oxide and lactide to the iron complex.

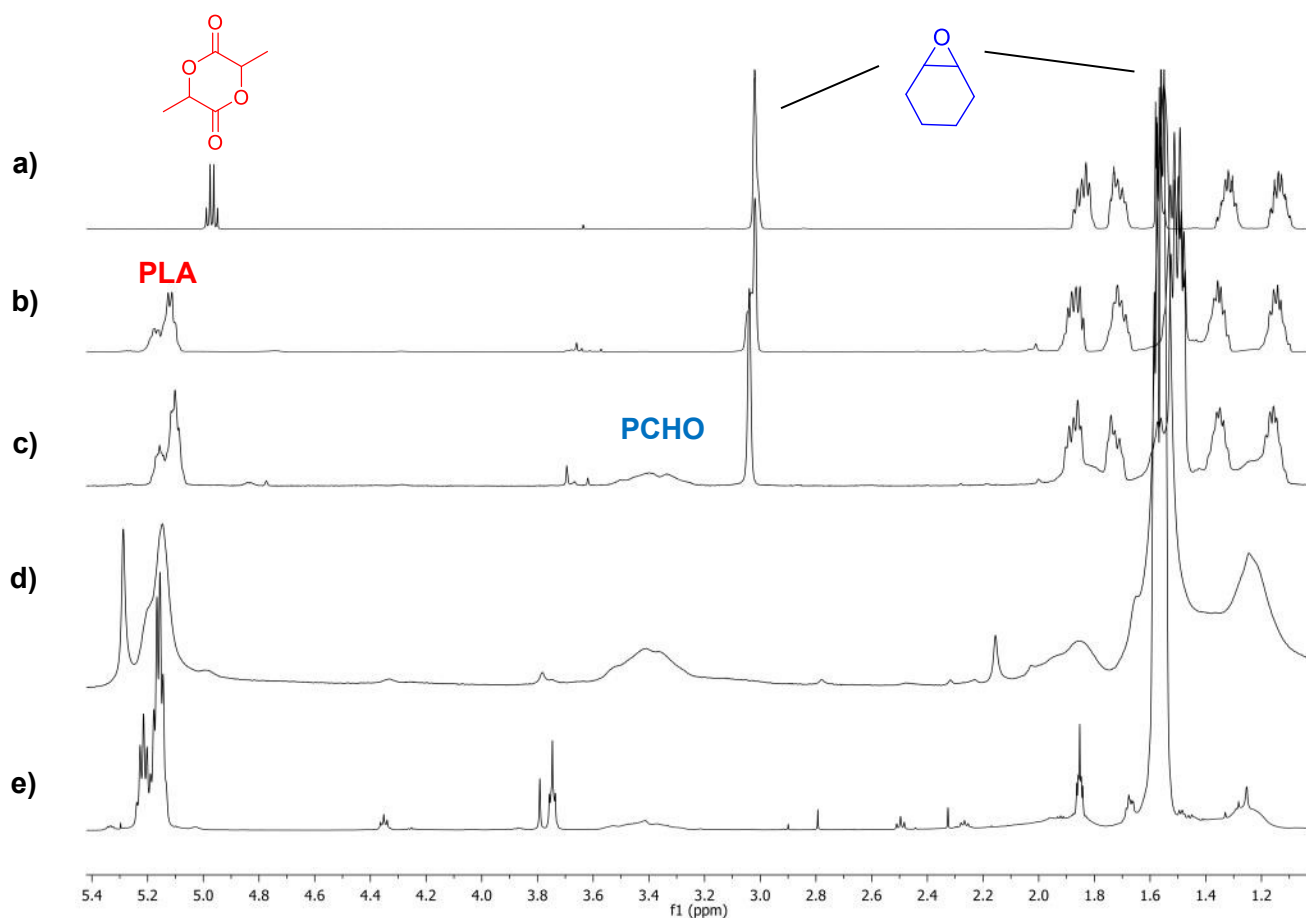


**Figure 3.3.** Representative <sup>1</sup>H NMR spectra (CDCl<sub>3</sub>) of lactide-cyclohexene oxide diblock copolymerization (**Table 3.3**, entry 1) showing a) a 1:1 mixture of lactide and cyclohexene oxide for reference b) reaction mixture after step *i* (t = 1 h) c) reaction mixture after step *ii* (t = 4 h) d) acetone precipitation filtrate containing copolymer e) isolated copolymer from hexanes precipitation.

Molecular weight analysis of the resulting diblock copolymer after step *ii* of the reaction by gel permeation chromatography (GPC) revealed a broad dispersity ( $M_w/M_n = 2.2$ ), which led us to believe the copolymer contained some polyether homopolymer. Fortunately, isolation of the copolymer was possible through sequential polymer precipitation in acetone and hexanes (see Section 3.4). This procedure resulted in 70% yield of copolymer, based on the mass of recovered polymer products (copolymer and homopolyether). GPC analysis of the isolated copolymer demonstrated a single peak with a dispersity of 1.5, but a decrease in molecular weight was observed from the first to second step when analyzed with a refractive index (RI) detector calibrated relative to polystyrene standards (entry 1, **Table 3.3** and **Figure 3.4**).

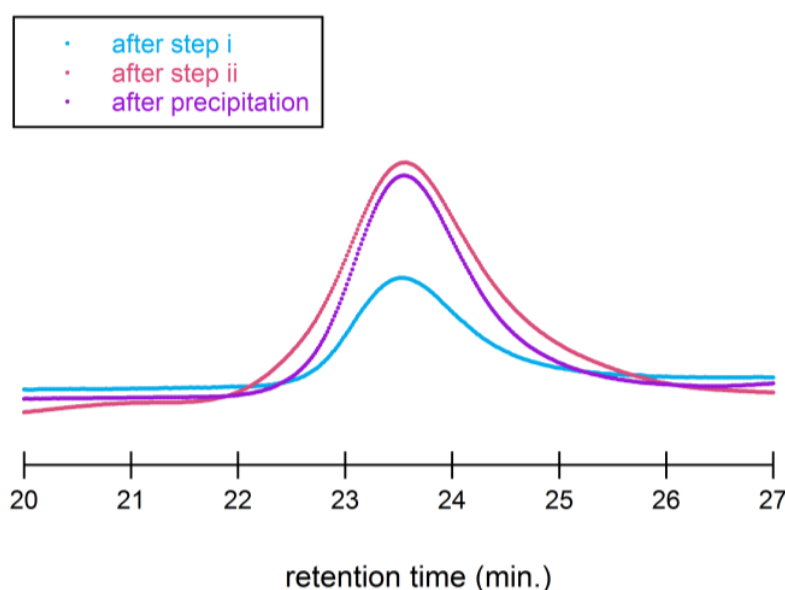


**Figure 3.4.** Representative GPC traces (RI detector) for lactide-cyclohexene oxide copolymerization (**Table 3.3**, entry 1) after step *i* (lactide polymerization), step *ii* (epoxide polymerization), and precipitation to isolate the block copolymer.

This result was not surprising considering the significantly different hydrodynamic volume expected for the copolymers compared to polystyrene. Therefore,

GPC analysis with a light scattering (LS) detector was carried out, which showed comparable values with the RI detector for PLA in the first step, but higher molecular weight for the copolymer product ( $M_n = 37.5$  kg/mol, **Table 3.3** entry 1). These results are consistent with the formation of a diblock copolymer.

Control experiments revealed that the  $\text{FcPF}_6$  oxidant was also a competent catalyst for the polymerization of cyclohexene oxide, although at a much slower rate and with lower polymer molecular weights and broader dispersities compared to **3.2** (**Table 3.4**). Cobaltocene is inactive for lactide and epoxide polymerization and ferrocene is inactive for epoxide polymerization.

**Table 3.4.** Comparison of cyclohexene oxide (CHO) polymerization initiated with  $\text{FcPF}_6$  and **3.2**.<sup>a</sup>

Initiator	Conv. CHO (%) <sup>b</sup>	$M_n$ (kg/mol) <sup>c</sup>	$\bar{D}$
$\text{FcPF}_6$	25	4.7	3.8
<b>3.2</b>	53	32.6	1.9

<sup>a</sup>Reactions were performed in  $\text{PhCl}$  (0.17M) for 3 h at 24°C with 2 mol%  $\text{FcPF}_6$  or **3.2**.

<sup>b</sup>Determined by  $^1\text{H}$  NMR. <sup>c</sup>Determined by refractive index detector against polystyrene standards.

We examined other oxidizing reagents to find a compound that would oxidize complex **3.1** but would be unreactive with the cyclohexene oxide monomer. It should be noted that these experiments were performed in dichloromethane solvent rather than chlorobenzene as these investigations preceded solvent optimization. Silver salts such as  $\text{AgPF}_6$  ( $E^\circ = 0.65\text{V}$  vs.  $\text{Fc}^+$ )<sup>11</sup> were tested, but we found these copolymerization reactions to be even less controlled than with the oxidizing agent  $\text{FcPF}_6$  and found evidence for homopolymerization of epoxides by the silver oxidizing agent (**Table 3.5**, entry 2). Instead, we decided to use oxidizing agents more similar to  $\text{FcPF}_6$  such as

acetylferrocenium salts. Acetylferrocenium tetrafluoroborate ( $\text{AcFcBF}_4$ ,  $E^\circ = 0.27\text{V}$  vs.  $\text{Fc}^+$ )<sup>11</sup> showed much slower cyclohexene oxide polymerization rates (entry 3); however, the iron(III) complex synthesized with  $\text{AcFcBF}_4$  as an oxidizing agent did not polymerize cyclohexene oxide. Instead, acetylferrocenium  $\text{PF}_6$  was synthesized, but this oxidizing agent was also found to polymerize cyclohexene oxide rapidly (entry 4). This shows that the cyclohexene oxide is highly sensitive to the counteranions present in the reaction mixture.

**Table 3.5.** Cyclohexene oxide polymerization initiated by various oxidants in  $\text{CH}_2\text{Cl}_2$ .

Entry	Oxidant	Time (h)	Conversion (%)	$M_n$ (kg/mol)	$\bar{D}$
1	$\text{FcPF}_6$	2.5	88	16.5/0.5 <sup>b</sup>	3.70/1.16
		24	100	8.1/0.4 <sup>b</sup>	2.97/1.15
2	$\text{AgPF}_6$	2.5	96	274.9	1.56
		22	99	180.4	2.46
3	$\text{AcFcBF}_4^c$	2.5	8	4.2/0.7 <sup>b</sup>	1.48/1.15
		24	18	3.8/0.6 <sup>b</sup>	1.51/1.16
4	$\text{AcFcPF}_6^c$	3	94	7.6	4.6
5	$\text{N}(p\text{-tolyl})_3\text{PF}_6^c$	6	37	2.5	14.2

<sup>a</sup>Cyclohexene oxide polymerizations performed at room temperature in  $\text{CH}_2\text{Cl}_2$  with 0.02 mol% oxidant. <sup>b</sup>Bimodal distribution. Molecular weight data for each peak is reported.

<sup>c</sup>Reactions performed with 0.2 mol% oxidant.

Triarylammonium salts were then investigated as oxidizing agents, which were hypothesized to be inert towards epoxide polymerization. The compound  $\text{N}(p\text{-tolyl})_3\text{PF}_6$  ( $E^\circ = 0.40\text{V}$  vs  $\text{Fc}^+$ )<sup>11</sup> was added to complex **3.1** to determine whether it could efficiently be oxidized to form **3.2**. However, an additional peak in the  $^1\text{H}$  NMR spectrum was observed which indicates this oxidation reaction may not proceed cleanly. When a control reaction with  $\text{N}(p\text{-tolyl})_3$  was performed to determine whether it can perform

epoxide polymerization, it was also found to also be a competent initiator (**Table 3.5**, entry 5).

Although an ideal oxidant was not found that can effectively oxidize **3.1** to form **3.2** *in situ* and does not react with cyclohexene oxide to initiate homopolymerization, we found that by running the reactions in chlorobenzene, the side reaction of cyclohexene oxide polymerization by FcPF<sub>6</sub> is sufficiently slower than the oxidation reaction. Even if a small amount of FcPF<sub>6</sub> reacts with the epoxide monomer rather than the iron(II) complex, it will only produce a small amount of side product and does not account for all of the epoxide conversion observed during the reaction. Notably, this side reaction is much slower than it is in dichloromethane, which is another advantage of performing the reactions in this solvent.

To assess whether the oxidant was interfering with the epoxide polymerization reaction, the copolymerization was performed by adding the epoxide monomer after oxidation of the iron complex. By carrying out the polymerization in this fashion, FcPF<sub>6</sub> is consumed prior to cyclohexene oxide addition to the reaction. In the event, polymers of similar molecular weights and composition to the one-pot reaction were observed (entry 2, **Table 3.3**), which demonstrated that epoxide polymerization catalyzed by FcPF<sub>6</sub> does not interfere with the one pot copolymerization reactions. These findings imply that electron transfer is much faster than monomer enchainment, which is an important factor for redox-switchable polymerization that occurs with multiple switches.

When the copolymerization was carried out with a 5:1 ratio of CHO:L, higher incorporation of cyclohexene oxide into the copolymer was observed (entry 3, **Table 3.3**), albeit with lower yields of isolated copolymer. To further demonstrate the ability to

switch chemoselectivity upon complex oxidation, the lactide polymerization was carried out to partial completion (35%) prior to complex oxidation and subsequent epoxide polymerization (entry 4, **Table 3.3**). As expected, complex oxidation led to epoxide polymerization with no further incorporation of lactide.

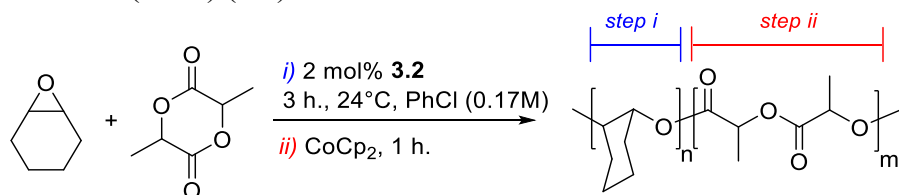
After demonstrating an effective switch from lactide to epoxide polymerization upon oxidation of the complex from iron(II) to iron(III), the reverse order was then investigated. Starting with iron(III) alkoxide complex **3.2**, a reaction containing a 1:1 mixture of the monomers underwent selective polymerization of the epoxide yielding exclusively polyether (entry 1, **Table 3.6**). As observed in lactide polymerizations, epoxide polymerization was slower compared to reactions without lactide present, a likely consequence of competitive inhibition from lactide. We were pleased to find that reduction of the iron(III) complex with CoCp<sub>2</sub> led to the rapid consumption of lactide without any further conversion of epoxide.

The chemoselectivity was once again apparent when the reaction was monitored by <sup>1</sup>H NMR spectroscopy. In the first step, only polyether is observed with no PLA present (**Figure 3.5b**). When the complex is reduced in step *ii*, polylactide appears with no further conversion of polyether (**Figure 3.5c**).

GPC analysis (RI and LS) after copolymer precipitation revealed one peak that increased in molecular weight and decreased in molecular weight distribution when CoCp<sub>2</sub> was added to the reaction (entry 1, **Table 3.6** and **Figure 3.6**). This observation was once again consistent with the production of a block copolymer. The decrease in dispersity of the copolymer product may be due to the high percentage of narrow

dispersity polylactide in the copolymer product. Precipitation of the copolymer resulted in 95% yield of the copolymer with only a small amount of homopolyether collected.

**Table 3.6.** Redox-controlled diblock copolymerization of (*rac*)-lactide (L) and cyclohexene oxide (CHO) (1:1).



After step <i>i</i>					After step <i>ii</i> and precipitation <sup>a</sup>					
	$M_n^b$	$\bar{D}$	%CHO <sup>c</sup>	%L <sup>c</sup>	$M_n^b$	$\bar{D}$	%CHO <sup>c</sup>	%L <sup>c</sup>	m:n <sup>c</sup>	%Copolymer <sup>d</sup>
<b>1</b>	1.2 (22.8)	1.9	22	0	10.6 (30.9)	1.4	22	97	9:1	95
<b>2<sup>e</sup></b>	7.4	1.8	42	0	12.5 (20.5)	1.4	42	98	9:1	84
<b>3<sup>f</sup></b>	1.2	2.0	50	0	5.8 (34.6)	1.4	51	99	3:1	53
<b>4<sup>f,g</sup></b>	2.2	2.4	21	0	11.6 (30.1)	1.4	22	98	3:1	48

<sup>a</sup>Isolated by precipitation from acetone and hexanes. <sup>b</sup> kg/mol, determined by GPC with RI detector relative to polystyrene standards; values in parentheses from LS detector. <sup>c</sup> percent conversion determined by <sup>1</sup>H NMR. <sup>d</sup>Percent copolymer determined from mass of isolated copolymer/mass of total polymer. <sup>e</sup>Lactide added in the second step after reductant. <sup>f</sup>[CHO]:[L] = 5:1 ([CHO] = 0.80M). <sup>g</sup>Step *i* carried out for 30 min.

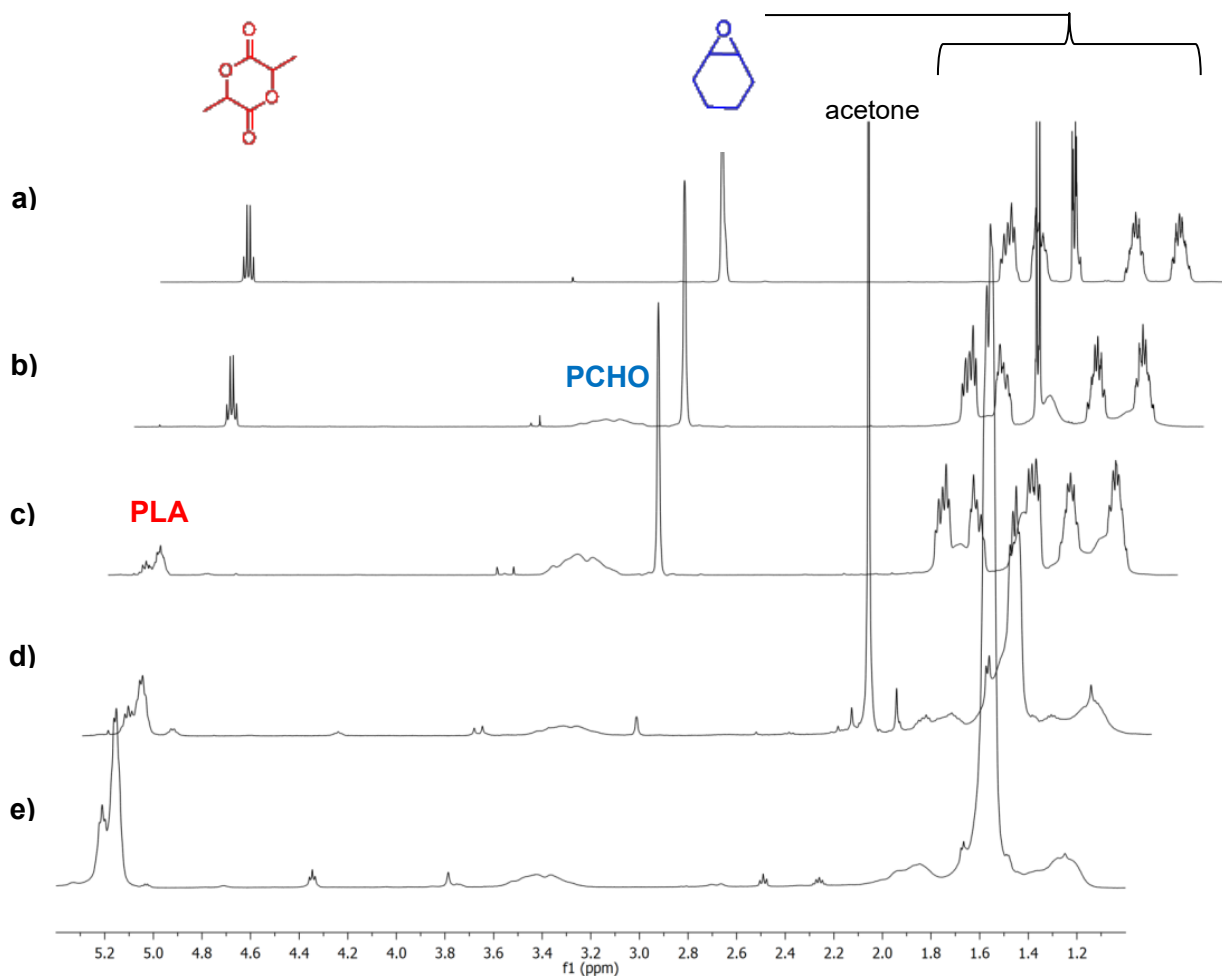


**Figure 3.5.** Representative  $^1\text{H}$  NMR spectra ( $\text{CDCl}_3$ ) of cyclohexene oxide-lactide diblock copolymerization (**Table 3.6**, entry 3) showing a) a 1:1 mixture of lactide and cyclohexene oxide for reference b) reaction mixture after step *i* ( $t = 3$  h) c) reaction mixture after step *ii* ( $t = 4$  h) d) acetone precipitation filtrate containing copolymer e) isolated copolymer from hexanes precipitation.

As was observed for the iron(II) to iron(III) switch, sequential polymerization of epoxide followed by lactide proceeded similarly as the one pot reaction with the only significant difference being higher conversion of the epoxide in the first step (entry 2, **Table 3.6**). Compared to the iron(II) to iron(III) switch, significant increases in ether content could be achieved by performing the iron(III) to iron(II) switch at higher



concentrations of cyclohexene oxide, once again at the expense of lower copolymer yields (entry 3, **Table 3.6**).

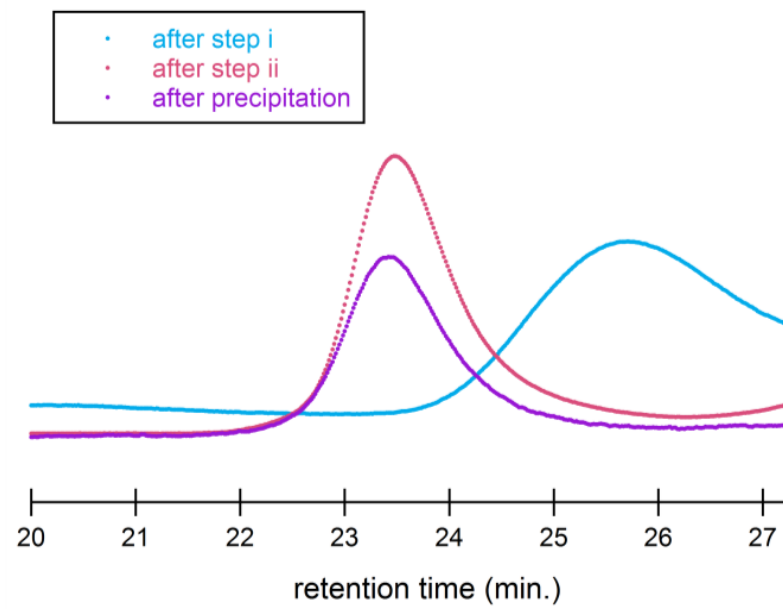


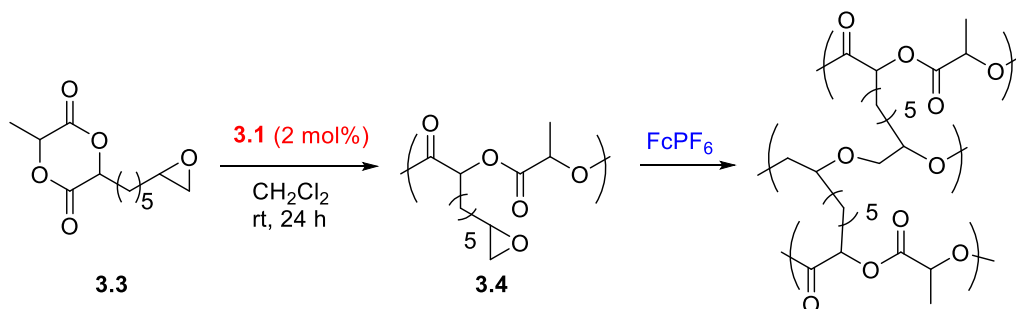
**Figure 3.6.** Representative GPC traces (RI detector) for cyclohexene oxide-lactide copolymerization (**Table 3.6**, entry 1) after step *i* (epoxide polymerization), step *ii* (lactide polymerization), and precipitation to isolate the block copolymer.

Finally, the chemoselectivity of the iron(III) to iron(II) switch was demonstrated by carrying out diblock copolymerization reactions at a CHO:L ratio of 5:1 to lower conversions prior to complex reduction (entry 4, **Table 3.6**). As expected, addition of CoCp<sub>2</sub> led to full lactide conversion without any further epoxide conversion. These results demonstrated that the chemoselectivity observed during the iron(II) to iron(III) switch was also applicable for the iron(III) to iron(II) switch, which makes it theoretically possible to carry out a multiblock copolymerization reaction involving multiple redox switches. However, we would like to improve the fidelity of the epoxide polymerization

reactions before attempting multiple redox switches to decrease the amount of homopolyether side product formed, which would complicate polymer analysis.

As a result of a collaborative project with Kayla Delle Chiaie, Lauren Yablon, Greg Michalowski, and Alex Sudyn, the redox-switching capabilities of these complexes were further utilized for redox-triggered crosslinking reactions, where both the lactide and epoxide moieties were incorporated into a single monomer **3.3** (Scheme 3.3).<sup>12</sup> When exposed to iron(II) alkoxide **3.1**, monomer **3.3** underwent chemoselective ring-opening of the cyclic diester to give epoxide-functionalized polyester (**3.4**). Oxidation of the complex with  $\text{FcPF}_6$  induced polymerization of the epoxide side chains, resulting in cross-linked polyester.

**Scheme 3.3.** Redox-triggered crosslinking polymerization.



### 3.4 Evidence for Block Copolymer Formation

Although the GPC data suggested the formation of copolymers as the major product, further experiments were carried out to rule out the possibility that the reactions yielded a mixture of homopolymers. Further support for the formation of copolymers was obtained from diffusion ordered nuclear magnetic resonance spectroscopy (DOSY-NMR). DOSY-NMR is an effective method for distinguishing block copolymers from a blend of homopolymers because it can separate polymer samples by their diffusion

coefficient.<sup>13</sup> DOSY-NMR spectra of the polymers isolated from the iron(II) to iron(III) redox switch displayed a single peak with resonances assigned to the polyester and polyether having the same diffusion coefficient ( $D = 9.5 \times 10^{-11} \text{ m}^2/\text{s}$ , **Figure 3.7a** and **Table 3.7**). Likewise, block copolymers formed from the iron(III) to iron(II) redox switch also showed signals at a single diffusion coefficient ( $D = 1.1 \times 10^{-10} \text{ m}^2/\text{s}$ , **Figure 3.7c** and **Table 3.7**). In contrast, DOSY-NMR spectra of a blend of PLA and PCHO of similar molecular weight showed two distinct diffusion coefficients at  $1.6$  and  $1.3 \times 10^{-10} \text{ m}^2/\text{s}$  (**Figure 3.7b** and **Table 3.7**) that are correlated to resonances assigned to the polyester and polyether, respectively. Combined, these data are consistent with the formation of block copolymers in both iron(II) to iron(III) and iron(III) to iron(II) redox switches.

**Table 3.7.** Diffusion coefficients determined by DOSY-NMR for copolymers and blend of homopolymers.<sup>a</sup>

Polymer	$M_n$ (kg/mol) <sup>b</sup>	$\bar{D}$	[PLA]:[PCHO] <sup>c</sup>	$D$ ( $10^{-10} \text{ m}^2/\text{s}$ )
PLA homopolymer	21.0	1.10	--	--
PCHO homopolymer	19.3	3.09	--	--
Mixture of homopolymers	20.9	2.10	79:21	1.59 1.28
Lactide-Epoxy copolymer	10.2	1.44	86:14	0.95
Epoxy-Lactide copolymer	5.8	1.42	77:23	1.06

<sup>a</sup>DOSY-NMR performed in  $\text{CDCl}_3$ . <sup>b</sup>Determined by refractive index detector referenced to polystyrene standards. <sup>c</sup>Determined by  $^1\text{H}$  NMR.

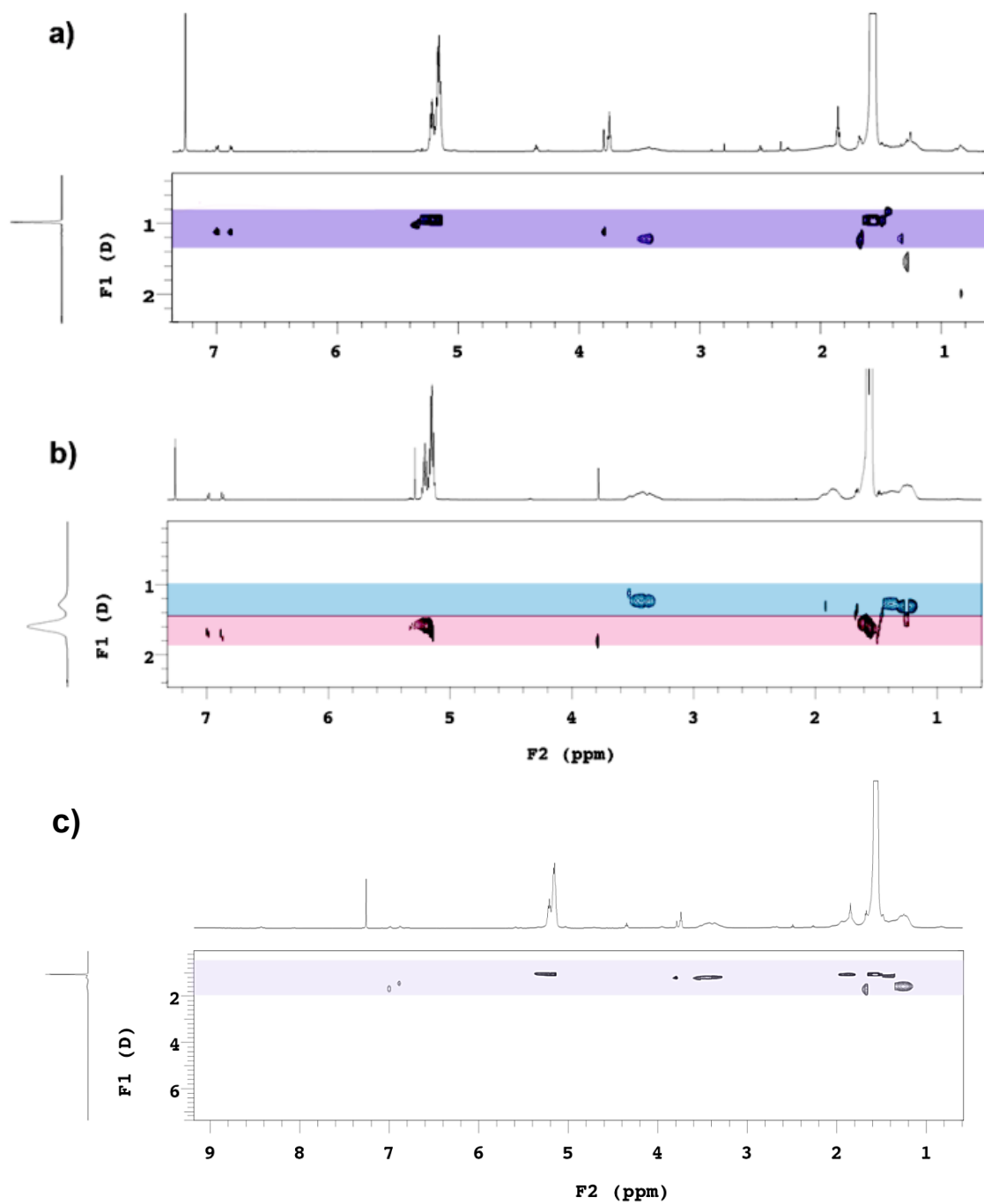
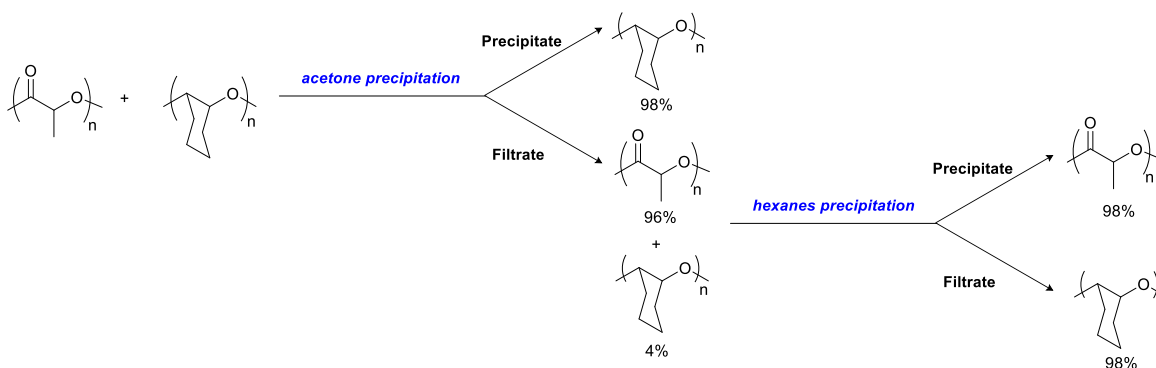


**Figure 3.7.** DOSY-NMR spectra in  $\text{CDCl}_3$  of a) lactide-epoxide block copolymer b) blend of homopolymers with similar  $M_n$  and [PLA]:[PCHO] and c) epoxide-lactide block copolymer.

**Table 3.8.** Separation of a blend of homo-PLA and homo-PCHO by precipitation.<sup>a</sup>



Entry	$M_n$ (kg/mol) <sup>b</sup>	$\bar{D}$	[PLA]:[PCHO] <sup>c</sup>
<b>Homo-PLA</b>	7.9	1.14	--
<b>Homo-PCHO</b>	14.9	2.21	--
<b>Blend</b>	15.8	2.24	1:2
<b>Acetone Filtrate</b>	8.2	1.09	21:1
<b>Acetone Precipitate</b>	20.3	2.12	1:60
<b>Hexanes Filtrate<sup>d</sup></b>	n.d.	n.d.	1:65
<b>Hexanes Precipitate</b>	7.4	1.10	58:1

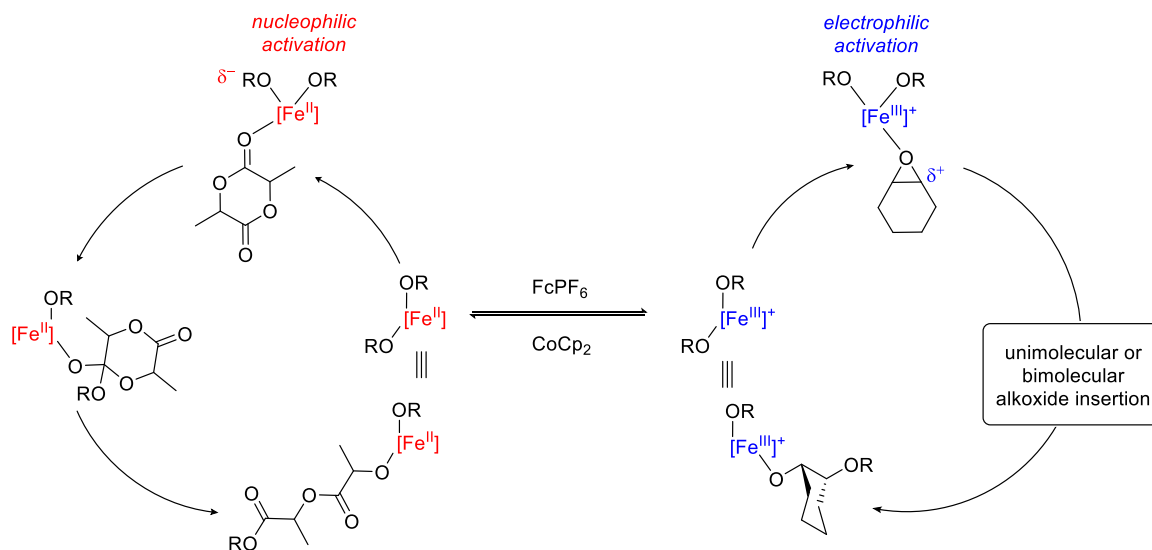
<sup>a</sup>The two homopolymers were dissolved in dichloromethane and precipitated from acetone. The material collected from the acetone filtrate was then precipitated from hexanes. <sup>b</sup>Determined by refractive index detector relative to polystyrene standards. <sup>c</sup>Determined by <sup>1</sup>H NMR. <sup>d</sup>Not determined; amount of sample collected was too small for reliable GPC measurement.

Additional support for the formation of block copolymers is the observation that the copolymer products have different solubility properties than either homopolymer. To further demonstrate this, a control experiment was performed with a mixture of the two homopolymers to show that they could be separated by the precipitation procedure used to isolate copolymer after the reaction. Poly(lactic acid) is soluble in acetone and insoluble in hexanes, while poly(cyclohexene oxide) is insoluble in acetone and soluble in hexanes. Thus, a blend of the two homopolymers can be separated from one another by sequential precipitation in acetone followed by the soluble fraction being further precipitated into hexanes: the remaining solid contains poly(lactic acid) with no evidence

for poly(cyclohexene oxide) (**Table 3.8**). In contrast, the same precipitation procedure carried out on the product from the copolymerization reactions resulted in polymer containing both poly(lactic acid) and poly(cyclohexene oxide) resonances by  $^1\text{H}$  NMR spectroscopy. Moreover, further precipitation of the copolymer in hexanes resulted in no change in polymer composition, which further suggested that polyester and polyether blocks are covalently linked.

### 3.5 Conclusions

**Scheme 3.4.** Proposed rationalization for chemoselectivity in polymerization reactions.



Cationic iron(III) bis(alkoxide) complex **3.2** was found to be an active catalyst for epoxide polymerization, while complexes in the iron(II) oxidation state were completely inactive. This trend is opposite to what was observed previously for lactide polymerization, allowing for the synthesis of redox-controlled diblock copolymers. To rationalize the switch in chemoselectivity, we hypothesize that lactide polymerization reactions benefit from nucleophilic activation of the alkoxides that are characteristic of a more electron rich iron(II) center, whereas epoxide polymerizations benefit more from

electrophilic activation that is more prevalent from the electron deficient iron(III) center (**Scheme 3.4**). While further mechanistic studies are needed to test this hypothesis, this report demonstrates for the first time that changes in oxidation state of a catalyst can lead to a complete change in the chemoselectivity of a chemical reaction.

Previously, the Diaconescu group disclosed that the composition of a polyester copolymer could be altered with the redox-controlled block copolymerization of lactide and  $\epsilon$ -caprolactone (CL).<sup>4</sup> Despite orthogonal redox control observed in homopolymerization reactions with complex **3.5** (**Figure 3.8**), the corresponding copolymerization reactions did not result in completely chemoselective reactions. Similar complications do not exist in the present system, thereby leading to formation of block copolymers with compositions that mimic sequential polymerization techniques and that feature different functional groups for each block (ester and ether). Subsequent to our report, Diaconescu and coworkers have also reported a redox-controlled synthesis of lactide or  $\beta$ -butyrolactone block copolymers with cyclohexene oxide.<sup>14</sup> When the ligand of complex **3.6** (**Figure 3.8**) is in the reduced state, the complex is active for the polymerization of lactide and  $\beta$ -butyrolactone, and in the oxidized state, is active for the polymerization of cyclohexene oxide. They also reported issues with Ferrocenium salt oxidants polymerizing cyclohexene oxide, and their ligand polymerized cyclohexene oxide in the absence of the zirconium metal. They utilized sequential monomer addition to avoid interference from the oxidant and synthesize diblock and ABA triblock copolymers.

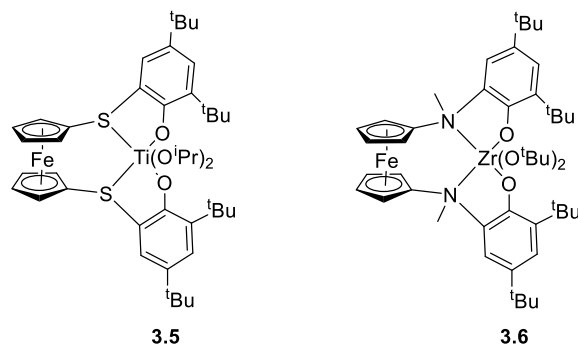


**Figure 3.8.** Complexes used by the Diaconescu group for redox-controlled copolymerization reactions.

If the oxidation could be performed electrochemically rather than from the addition of a chemical oxidant, we could avoid side reactions of the oxidant with the cyclohexene oxide. The copolymerization of cyclohexene oxide and lactide controlled by electrochemical switches is currently under investigation in our laboratory.

So as to make the redox-switchable copolymerization reactions more amenable to the production of multiblock copolymers, current work in the group is directed towards improving the fidelity of the epoxide polymerization reaction through mechanistic studies. In parallel, rapid redox-switching techniques are being explored along with the investigation of alternative monomers.

### 3.6 Experimental

**General Considerations.** Unless stated otherwise, all reactions were carried out in oven-dried glassware in a nitrogen-filled glove box or with standard Schlenk line techniques.<sup>15</sup> Solvents were used after passage through a solvent purification system under a blanket of argon and then degassed briefly by exposure to vacuum. Nuclear magnetic resonance (NMR) spectra were recorded at ambient temperature on Varian



spectrometers operating at 400-600 MHz. Gel permeation chromatography (GPC) was performed on an Agilent GPC220 in THF at 40°C with three PL gel columns (10µm) in series. Molecular weights and molecular weight distributions were determined from the signal response of the RI detector relative to polystyrene standards. Molecular weights were also determined with a light scattering detector for selected samples. Polymer products were separated with a Beckman Coulter J2-MC Centrifuge with Rotor 17.0 at 2500 RPM and 10°C for 7.0 minutes.

Lactide was obtained from Frinton Laboratories and was recrystallized from ethyl acetate followed by recrystallization from toluene and dried *in vacuo* prior to polymerization. Cyclohexene oxide was obtained from Sigma Aldrich and was dried over CaH<sub>2</sub> and distilled prior to polymerization. Chlorobenzene (Extra Dry) was obtained from Acros Organics and passed through silica prior to use. Other methods used to dry chlorobenzene led to irreproducible results in epoxide polymerization reactions. Complexes **3.1** and **3.2** were synthesized as described previously (See Chapter 2.7).

**Generic procedure for the polymerization of epoxides with complex 3.2.** In a glove box, iron(III) bis(alkoxide) complex **3.2** (0.0163 g, 0.0198 mmol) and epoxide (9.9 mmol) were added to a seven mL vial. The reaction was allowed to stir 24 hours at room temperature. Unreacted epoxide monomer was removed *in vacuo* and conversion was determined from the mass of the recovered polymer product. The reaction mixture was analyzed by GPC (RI) to determine molecular weight and molecular weight distribution of the polymers.

**Polymerization of cyclohexene oxide with complex 3.2.** In a glove box, iron(III) bis(alkoxide) complex **3.2** (0.0163 g, 0.0198 mmol) in chlorobenzene (2.0ml) was added

to a seven mL vial containing cyclohexene oxide (1.00g, 10.2 mmol) in chlorobenzene (2.0ml). The reaction was allowed to stir 24 hours at room temperature. Unreacted epoxide monomer was removed *in vacuo* and conversion was determined from the mass of the recovered polymer product. The reaction mixture was analyzed by GPC (RI) to determine molecular weight and molecular weight distribution of the polymers.

**Redox switchable polymerization of cyclohexene oxide.** In a glove box, iron(III) bis(alkoxide) complex **3.2** (0.0250 g, 0.0306 mmol) in chlorobenzene (0.8 mL) was added to a seven mL vial containing cyclohexene oxide (0.150 g, 1.53 mmol) in chlorobenzene (0.7 mL) at room temperature. After 50 min., cobaltocene (0.0058 g, 0.0306 mmol) was added to the reaction mixture and the color changed from blue to brown. At  $t = 90$  min., ferrocenium hexafluorophosphate (0.0101 g, 0.0305 mmol) was added and the reaction turned blue-brown in color. Aliquots were removed periodically from the reaction mixture and terminated by addition of wet  $\text{CDCl}_3$  outside of a glove box. Conversion was determined by  $^1\text{H}$  NMR from integrating the methine peaks of the remaining cyclohexene oxide (3.1ppm) versus the methine peaks of the polyether (3.2-3.6ppm). Each aliquot was also analyzed by GPC (RI) to determine molecular weight and molecular weight distribution of the polymers.

**Diblock copolymerization of lactide/cyclohexene oxide by an  $\text{Fe}^{\text{II}} \rightarrow \text{Fe}^{\text{III}}$  redox switch, one pot.** In a glove box, iron(II) bis(alkoxide) complex **3.1** (0.0094 g, 0.014 mmol) in chlorobenzene (2.0 mL) was added to a seven mL vial containing (*rac*)-lactide (0.10 g, 0.70 mmol) and cyclohexene oxide (0.068 g, 0.70 mmol for 1:1 [CHO]:[L], or 0.0343 g, 3.50 mmol for 5:1 [CHO]:[L]) in chlorobenzene (2.0 mL) at room temperature. After one hour, ferrocenium hexafluorophosphate (0.0050 g, 0.015 mmol) was added to

the reaction mixture and the color changed from purple-brown to blue. The reaction was allowed to stir for three hours and then was removed from a glove box and quenched with wet THF (0.5 ml). The remaining volatiles were removed *in vacuo*, and the reaction mixture was dissolved in a minimal amount of dichloromethane (2 ml) and precipitated into stirring acetone (100 mL). After stirring one hour, the turbid mixture was centrifuged and poured through a 0.02  $\mu\text{m}$  polypropylene (PP) filter membrane to collect homopolyether in the precipitate and copolymer with a small amount of low molecular weight homopolyether in the filtrate. After drying *in vacuo*, the material collected in the acetone filtrate was redissolved in minimal dichloromethane (2 ml) and precipitated into stirring hexanes (100 mL). After stirring one hour, the mixture was centrifuged and poured through a 0.02  $\mu\text{m}$  PP filter membrane to collect the copolymer in the precipitate and low molecular weight homopolyether in the filtrate.

In order to monitor the progress of the reaction, aliquots were removed periodically from the reaction mixture and terminated by addition of wet  $\text{CDCl}_3$ . Lactide conversion was determined by  $^1\text{H}$  NMR by integrating the methine peaks of the remaining lactide (5.0 ppm) versus the methine peaks of polylactide (5.2 ppm). Epoxide conversion was determined by mass of the polymer product before precipitation, taking into account the theoretical mass of polylactide and lactide. The polymers were analyzed by GPC to determine molecular weight and molecular weight distribution after each step of the reaction and each precipitation. The ratio of polylactide to polyether ([PLA]:[PCHO]) of the reaction mixtures were determined by  $^1\text{H}$  NMR by integrating the methine polyether peak (3.2-3.6 ppm) versus the methine polylactide peak (5.2 ppm). Percent copolymer was determined by copolymer mass/total polymer mass where the

“copolymer mass” is the mass of the polymer isolated in the hexanes precipitate and the “total polymer mass” is the “copolymer mass” plus any polymeric material isolated from the acetone precipitate and hexanes filtrate. Approximately 10% of polymer is lost during precipitation and handling of the polymers, so the unpurified polymer mass is not used in this calculation.

**Diblock copolymerization of lactide/cyclohexene oxide by an  $\text{Fe}^{\text{II}} \rightarrow \text{Fe}^{\text{III}}$  redox switch, sequential monomer addition.** In a glove box, iron(II) bis(alkoxide) complex **3.1** (0.0094 g, 0.014 mmol) in chlorobenzene (2.0 mL) was added to a seven mL vial containing (*rac*)-lactide (0.10g, 0.70 mmol) in chlorobenzene (2.0 mL) at room temperature. After one hour, ferrocenium hexafluorophosphate (0.0050 g, 0.015 mmol) was added to the reaction mixture at which point the reaction immediately turned from purple-brown to blue. The reaction was allowed to stir for five minutes to ensure that the oxidation reaction occurred prior to addition of the epoxide monomer. Cyclohexene oxide (0.068g, 0.70 mmol) was then added to the reaction mixture. The reaction was allowed to stir for three hours and was then removed from a glove box and quenched with wet THF (0.5ml). Chlorobenzene and unreacted cyclohexene oxide were removed *in vacuo*. Precipitations were performed as described for the one-pot polymerization to isolate copolymer products.

**Diblock copolymerization of cyclohexene oxide/lactide by an  $\text{Fe}^{\text{III}} \rightarrow \text{Fe}^{\text{II}}$  redox switch, one pot.** In a glove box, iron(III) bis(alkoxide) complex **3.2** (0.00113 g, 0.014 mmol) in chlorobenzene (2.0 mL) was added to a seven mL vial containing (*rac*)-lactide (0.10 g, 0.70 mmol) and cyclohexene oxide (0.068 g, 0.70 mmol for 1:1 [CHO]:[L], or 0.0343 g, 3.50 mmol for 5:1 [CHO]:[L]) in chlorobenzene (2.0 mL) at room temperature.

After three hours, cobaltocene (0.0026 g, 0.014 mmol) was added to the reaction mixture and the color changed from blue to brown. The reaction was allowed to stir for one hour and then was removed from a glove box and quenched with wet THF (0.5 ml). The remaining volatiles were removed *in vacuo*. The reaction mixture was dissolved in minimal dichloromethane (2 ml) and precipitated into stirring acetone (100 mL). After stirring one hour, the mixture was centrifuged and poured through a 0.02  $\mu\text{m}$  polypropylene (PP) filter membrane to collect homopolyether in the precipitate and copolymer with a small amount of low molecular weight homopolyether in the filtrate. After drying *in vacuo*, the material collected in the acetone filtrate was redissolved in minimal dichloromethane (2 ml) and precipitated into stirring hexanes (100 mL). After stirring one hour, the mixture was centrifuged and poured through a 0.02  $\mu\text{m}$  polypropylene (PP) filter membrane to collect the copolymer in the precipitate and low molecular weight homopolyether in the filtrate.

In order to monitor the progress of the reaction, aliquots were removed periodically from the reaction mixture and terminated by addition of  $\text{CDCl}_3$ . Lactide conversion was determined by  $^1\text{H}$  NMR by integrating the methine peaks of the remaining lactide (5.0 ppm) versus the methine peaks of polylactide (5.2 ppm). Epoxide conversion was determined by mass of the polymer product before precipitation, taking into account the theoretical mass of polylactide and lactide. The polymers were analyzed by GPC to determine molecular weight and molecular weight distribution after each step of the reaction and each precipitation. The ratio of polylactide to polyether ([PLA]:[PCHO]) of the reaction mixtures were determined by  $^1\text{H}$  NMR by integrating the methine polyether peak (3.2-3.6 ppm) versus the methine polylactide peak (5.2 ppm).

Percent copolymer was determined by copolymer mass/total polymer mass where the “copolymer mass” is the mass of the polymer isolated from the hexanes precipitation and the “total polymer mass” is the “copolymer mass” plus any polymeric material isolated from the acetone filtrate and hexanes precipitates. Approximately 10% of polymer is lost during precipitation and handling of the polymers, so the unpurified polymer mass is not used in this calculation.

**Diblock copolymerization of cyclohexene oxide/lactide by an  $\text{Fe}^{\text{III}} \rightarrow \text{Fe}^{\text{II}}$  redox switch, sequential monomer addition.** In a glove box, iron(III) bis(alkoxide) complex **3.2** (0.00113 g, 0.014 mmol) in chlorobenzene (2.0 mL) was added to a seven mL vial containing cyclohexene oxide (0.068 g, 0.70 mmol) in chlorobenzene (2.0 mL) at room temperature. After three hours, cobaltocene (0.0026 g, 0.014 mmol) was added to the reaction mixture at which point the reaction immediately turned from blue to brown. The reaction was allowed to stir an additional five minutes to ensure that the reduction reaction occurred prior to addition of the lactide monomer. Then (*rac*)-lactide (0.10 g, 0.70 mmol) was added to the reaction as a solid. The reaction was allowed to stir for one hour and was then removed from a glove box and quenched with wet THF (0.5 ml). The remaining volatile materials were removed *in vacuo*, and precipitations were performed as described for the one-pot polymerization to isolate copolymer products.

---

## **References**

1. Adapted with permission from Biernesser, A.B.; Delle Chiaie, K.R.; Curley, J.B.; Byers, J.A. *Angew. Chem. Int. Ed.* **2016**, 55, 5251-5254. Copyright 2016 John Wiley and Sons.
2. a) F.A. Leibfarth, K.M. Mattson, B.P. Fors, H.A. Collins, C.J. Hawker, *Angew. Chem.* **2012**, 125, 210-222; *Angew. Chem. Int. Edit.* **2012**, 52, 199-210; b) V.

- 
- Blanco, D.A. Leigh, V. Marcos, *Chem. Soc. Rev.* **2015**, *44*, 5341-5370; c) S.M. Guillaume, E. Kirillov, Y. Sarazin, J.-F. Carpentier, *Chem.–Eur. J.* **2015**, *21*, 7988-8003; d) A.J. Teator, D.N. Lastovickova, C.W. Bielawski. *Chem. Rev.* **2015**.
3. a) C.K.A. Gregson, V.C. Gibson, N.J. Long, E.L. Marshall, P.J. Oxford, A.J.P. White, *J. Am. Chem. Soc.* **2006**, *128*, 7410-7411; b) E.M. Broderick, N. Guo, C.S. Vogel, C. Xu, J. Sutter, J.T. Miller, K. Meyer, P. Mehrkhodavandi, P.L. Diaconescu, *J. Am. Chem. Soc.* **2011**, *133*, 9278-9281; c) L.A. Brown, J.L. Rhinehart, B.K. Long, *ACS Catal.* **2015**, *5*, 6057-6060.
  4. X. Wang, A. Thevenon, J.L. Brosmer, I. Yu, S.I. Khan, P. Mehrkhodavandi, P.L. Diaconescu, *J. Am. Chem. Soc.* **2014**, *136*, 11264-11267.
  5. A.B. Biernesser, B. Li, J.A. Byers, *J. Am. Chem. Soc.*, **2013**, *135*, 16553-16560.
  6. E.M. Broderick, N. Guo, T. Wu, C.S. Vogel, C. Xu, J. Sutter, J.T. Miller, K. Meyer, T. Cantat, P.L. Diaconescu, *Chem. Commun.* **2011**, *47*, 9897-9899,
  7. H.K. Cho, J.H. Cho, S.H. Jeong, D.C. Cho, J.H. Yeum, I.W. Cheong, *Arch. Pharm. Res.* **2014**, *37*, 423-434.
  8. M. Bishai, S. De, B. Adhikari, R. Banerjee, *Food Sci. Biotechnol.* **2013**, *22*, 73-77.
  9. Childers, M.I.; Longo, J.M.; Van Zee, N.J.; LaPointe, A.M.; Coates, G.W. *Chem. Rev.* **2014**, *114*, 8129-8152.
  10. We hypothesize a higher  $M_n$  than the theoretical value (7.2 kg/mol) was obtained due to a small amount of the catalyst being inactive.
  11. Connelly, G.N.; Geiger, W.E. *Chem. Rev.*, **1996**, *96*, 877.
  12. Delle Chiaie, K.R.; Yablon, L.M.; Biernesser, A.B.; Michalowski, G.R.; Sudyn, A.W.; Byers, J.A. *Polym. Chem.* **2016**, *7*, 4675.
  13. a) S. Paul, C. Romain, J. Shaw, C.K. Williams, *Macromolecules* **2015**, *48*, 6047-6056; b) S. Viel, M.I. Mazarin, R. Giordanengo, T.N.T. Phan, L. Charles, S. Caldarelli, D. Bertin, *Anal. Chim. Acta* **2009**, *654*, 45-48.
  14. Quan, S.M.; Wang, X.; Zhang, R.; Diaconescu, P.L. *Macromolecules* **2016**, *49*, 6768-6778.
  15. Burger, B. J.; Bercaw, J. E. *New Developments in the Synthesis, Manipulation and Characterization of Organometallic Compounds*; Wayda, A.L., Darensbourg, M.Y., Eds.; American Chemical Society: Washington D.C., 1987.

## Chapter 4: Exploration of Formally Iron(I) Bis(imino)pyridine Mono(alkoxide) Complexes

### 4.1 Introduction

Concern over waste disposal problems and environmental pollution has driven efforts to develop biodegradable alternatives to conventional inert polymer materials. A promising class of biodegradable materials can be derived from the ring opening polymerization of cyclic esters and carbonates, in particular, from the polymerization of lactide to form poly(lactic acid).<sup>1</sup> Although numerous catalysts for this transformation have been developed, we became interested in iron-based systems due to the biocompatibility and low toxicity of iron,<sup>2</sup> as well as the versatility and fine control of catalyst electronic structure available by oxidation state modulation. While a small number of iron complexes have been reported for the polymerization of lactide,<sup>3,4</sup> far fewer have been reported for the polymerization of lactones<sup>3c,d,5</sup> and cyclic carbonates,<sup>6</sup> many of which suffer from low activity and/or broad molecular weight distributions.

We previously reported lactide polymerization catalyzed by several bis(imino)pyridine iron(II) bis(alkoxide) complexes (**4.2**, **Figure 4.1**), and demonstrated that the polymerization was sensitive to the oxidation state and electron density of the metal center.<sup>4</sup> Lactide polymerization proceeded more rapidly with electron-rich iron(II) complexes as compared to electron-poor analogues.<sup>4,7</sup> Further, the polymerization was completely deactivated when the catalyst was oxidized to the cationic Fe(III) state (**4.3**). Conversely, epoxides displayed complementary reactivity compared to lactide, polymerizing only in Fe(III) state and were unreactive towards the Fe(II) complexes



(Figure 4.1).<sup>8</sup> The complementary reactivity of these two monomers was exploited in redox-switchable synthesis of block copolymers and redox-triggered cross-linking of polymers.<sup>8,9</sup>

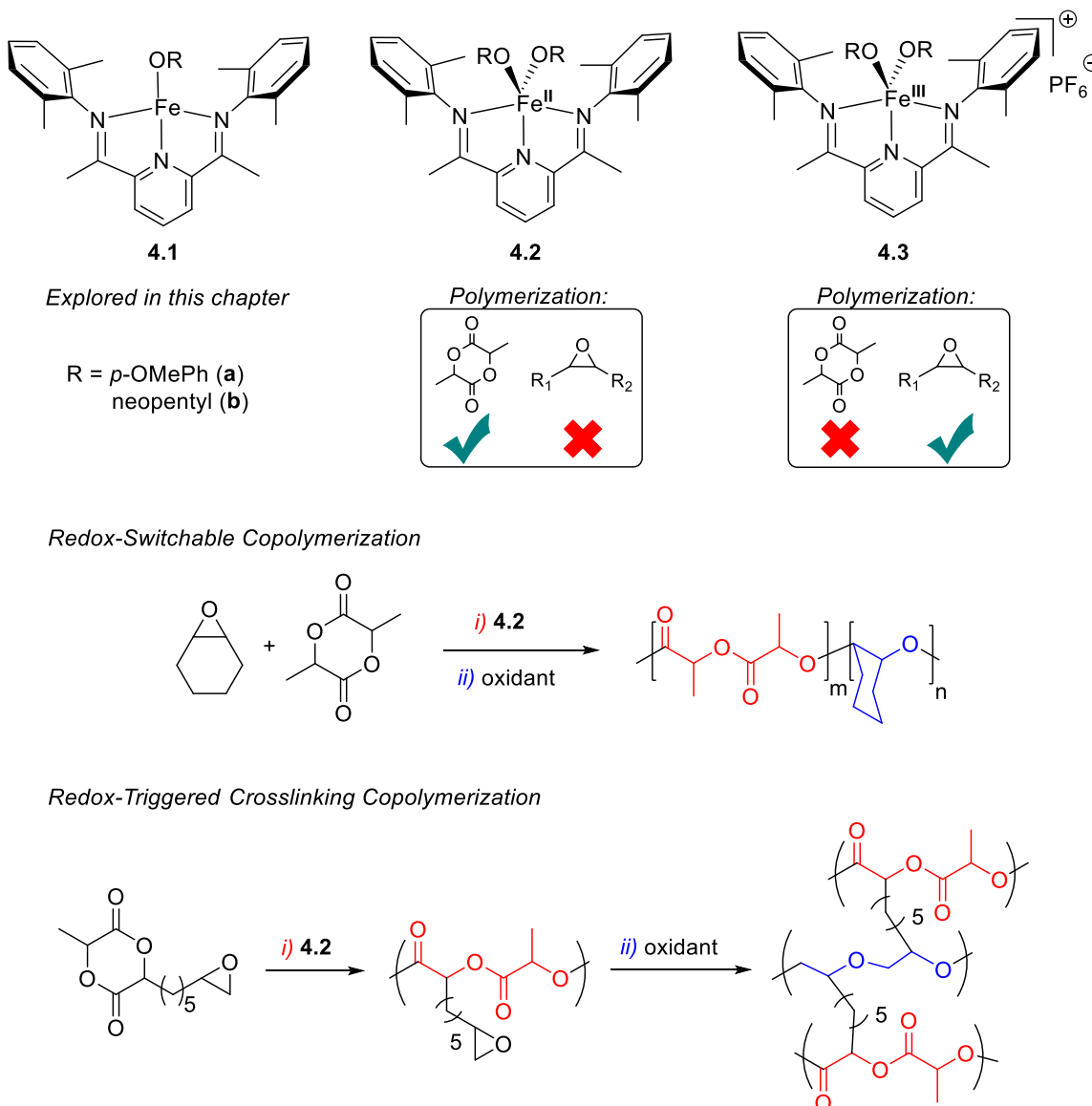
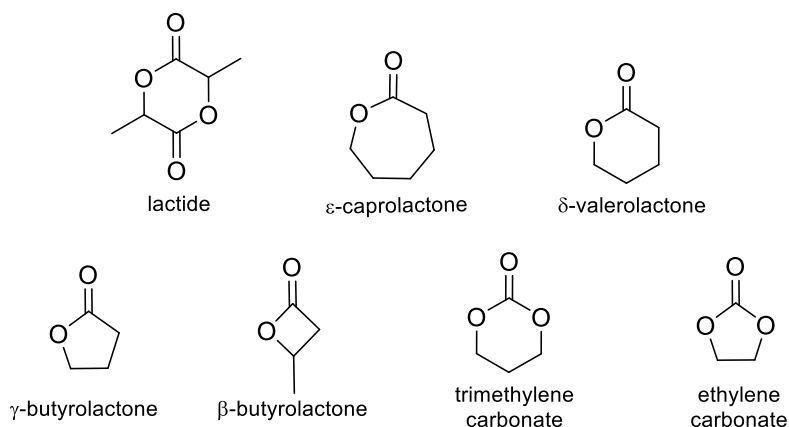


**Figure 4.1.** Different reactivities of iron bis(imino)pyridine alkoxide complexes in different oxidation states and exploitation of complementary reactivity of lactide and epoxide polymerization for the synthesis of redox-controlled copolymers.

Including our system, all reported examples of iron-based initiators for the ring-opening polymerization of cyclic esters are in the iron(II) and iron(III) oxidation

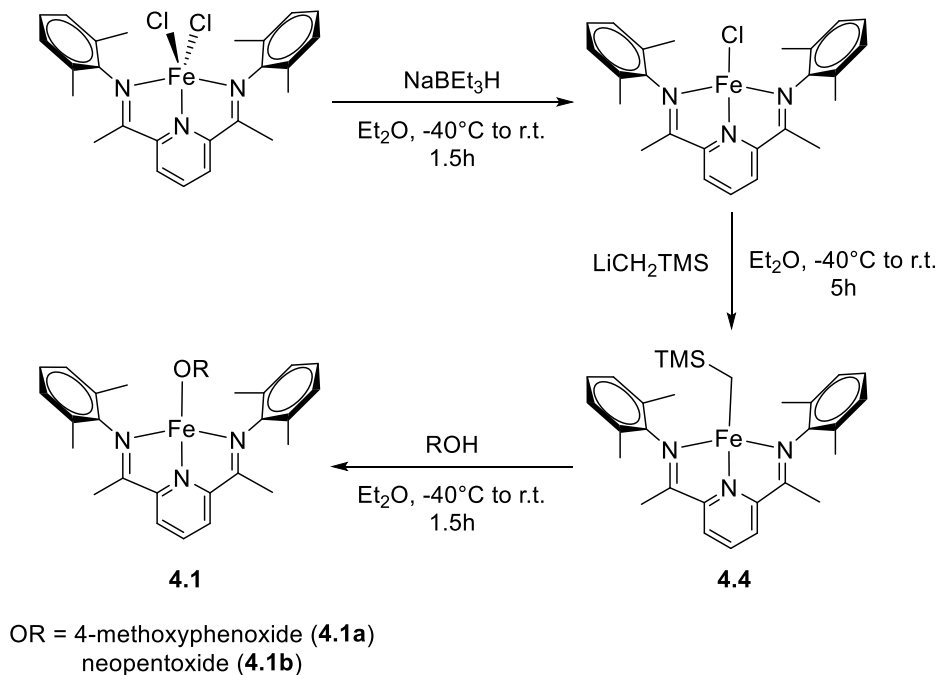
states.<sup>3,4,5,6</sup> However, iron bis(imino)pyridine complexes are highly versatile catalysts for an extensive variety of transformations, due in part to their rich redox chemistry which is facilitated by the redox non-innocent bis(imino)pyridine ligands.<sup>10</sup> Based on our results that different oxidation states manifest distinct reactivity towards polymerization and breadth of redox chemistry known on the bis(imino)pyridine ligand platform, we turned our attention towards exploring additional redox states of these complexes with the ultimate goal of extending monomer scope. There are currently not many catalysts that can polymerize a wide variety of monomers, which could be valuable for copolymerization applications. We hypothesized that an iron(I) bis(imino)pyridine alkoxide complex would be a superior catalyst for the ring-opening polymerization of cyclic esters (as compared to the ferrous and ferric complexes) due to the increased electron density at the iron center, enhancing the nucleophilicity of the alkoxide ligand. Specifically, we have undertaken the synthesis of the first examples of bis(imino)pyridine-supported formally iron(I) alkoxide complexes (**4.1**, **Figure 4.1**), characterization of their electronic structure, and initial studies on their behavior in the polymerization of a variety of cyclic esters and carbonates.

**Scheme 4.1.** Monomers investigated for ring-opening polymerization in this chapter.



## 4.2 Synthesis and Characterization of Bis(imino)pyridine Iron Mono(alkoxide) Complexes

**Scheme 4.2.** Synthesis of bis(imino)pyridine iron monoalkoxide complexes.



We have previously reported the synthesis of bis(imino)pyridine iron(II) bis(alkoxide), complexes by treating bis(imino)pyridine iron(II) bis(alkyl) complex **4.2** with a variety of alcohols.<sup>4</sup> We hypothesized that similar treatment of a bis(imino)pyridine iron mono(alkyl) would furnish the desired bis(imino)pyridine iron mono(alkoxide) complexes. Stepwise reduction of the bis(imino)pyridine iron(II) dichloride complex with NaBEt<sub>3</sub>H and alkylation with LiCH<sub>2</sub>TMS provided the reported bis(imino)pyridine iron(I) mono(alkyl) complex in good yield (**Scheme 4.2**).<sup>11</sup> The desired bis(imino)pyridine iron monoalkoxide complexes (**4.1**) were then prepared directly by protonolysis of the corresponding bis(imino)pyridine iron monoalkyl complex (**4.4**) with either *p*-methoxyphenol (**4.1a**) or neopentyl alcohol (**4.1b**), **Scheme 4.2**. In

contrast to the dark purple color of the iron(II) bis(alkoxide) complexes, the iron mono(alkoxide) complexes are distinct and dark red-brown (**Figure 4.2**).

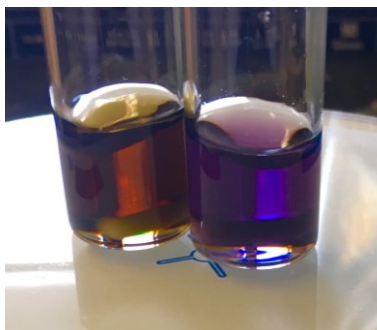


**Figure 4.2.** Picture of complex **4.1b** in a 0.0035M toluene solution (left) compared to complex **4.2b** in 0.0035M toluene solution (right).

The stoichiometry of the proteolytic reaction is critical. Addition of excess 4-methoxyphenol to complex **4.1a** instead formed the iron(II) bis(alkoxide) complex **4.2a** cleanly by  $^1\text{H}$  NMR spectroscopy. Although further investigations are required to understand the mechanism, this transformation holds promise for the possibility of an Fe(I) to Fe(II) oxidation state trigger for switchable catalysis.

Because the bis(imino)pyridine ligand is redox non-innocent, characterization of these complexes by several techniques is required to understand the electronic structure of the complex and gain information about whether this complex is reduced at the iron center or better described as an iron(II) center with a reduced bis(imino)pyridine ligand. Previously reported studies by the Chirik group describe the bis(imino)pyridine iron mono(chloride) as well as bis(imino)pyridine mono(alkyl) complexes as iron(II) centers with reduced bis(imino)pyridine ligands.<sup>12</sup>

The electron paramagnetic resonance spectrum of complex **4.1a** in a frozen toluene solution displayed a rhombic signal ( $g_{\text{eff}} = 2.01, 2.06, \text{ and } 2.36$ ), which suggests the complex possesses an  $S = 1/2$  spin state and that the singly-occupied molecular orbital (SOMO) contains significant metal character at 77 K. (**Figure 4.3**). Further support for the  $S = 1/2$  spin state can be derived from the solution magnetic moment of  $1.79 \mu_{\text{B}}$  at 298 K, which is only slightly higher than the expected spin only value for  $S = 1/2$  systems ( $1.73 \mu_{\text{B}}$ ).

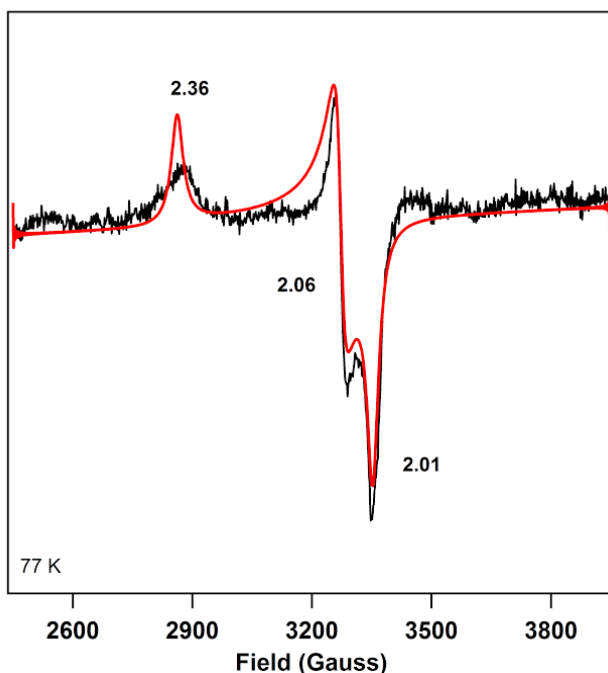


**Figure 4.3.** Frozen-toluene EPR spectrum of complex **4.1a** (unpurified) in black showing simulated spectrum in red with the parameters given in the text and a Gaussian line broadening of 15 Hz.<sup>13</sup>

Zero-field  $^{57}\text{Fe}$  Mössbauer spectroscopy was utilized to gain further information about electronic environment of iron in these complexes. The *p*-methoxyphenoxide complex **4.1a** showed a major species ( $\delta$ :  $1.04 \text{ mm/s}$ ,  $|\Delta E_{\text{Q}}|$ :  $1.79 \text{ mm/s}$ ) (**Figure 4.4**, **Table**

**4.1**, entry 1) with slightly higher isomer shift and smaller quadrupole splitting than that observed for the analogous iron(II) complex **4.2a** ( $\delta$ : 0.94 mm/s,  $|\Delta E_Q|$ : 2.19 mm/s) (entry 2).

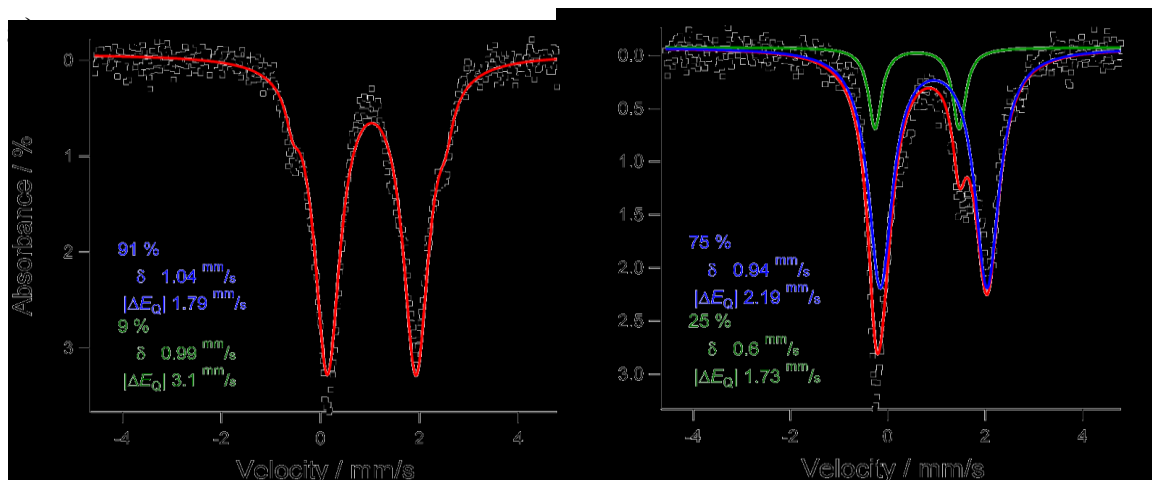


**Figure 4.4.** Zero-field  $^{57}\text{Fe}$  Mössbauer spectra at 90K for complexes a) **4.1a** and b) **4.2a**. Major species is shown in blue with the addition of an impurity in green to reproduce the experimental data. Sum of fit components is shown in red.

Although **4.1b** was recrystallized from pentane to give material that appeared pure by  $^1\text{H}$  NMR spectroscopy, the Mössbauer spectrum showed a mixture of two species both with isomer shifts and quadrupole splittings smaller than that observed for the analogous Fe(II) complex (**Figure 4.5**, **Table 4.1**, entry 3). Due to the similarity in parameters of the two components and simplicity of the  $^1\text{H}$  NMR spectrum, it is likely that the impurity is a solvent adduct of **4.1b**. Regardless, in both cases the reduction of the complex and effective loss of an alkoxide ligand decreases the quadrupole splitting from the corresponding Fe(II) species, consistent with the increase in molecular symmetry.

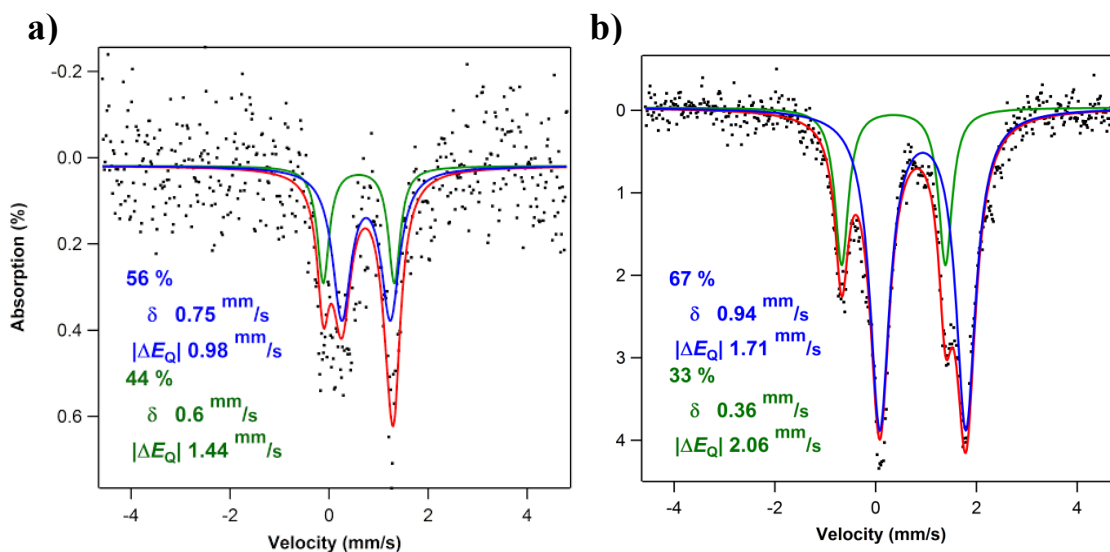


**Figure 4.5.** Zero-field  $^{57}\text{Fe}$  Mössbauer spectra at 90K for complexes a) **4.1b** and b) **4.2b**. Major species is shown in blue with the addition of an impurity in green to reproduce the experimental data. Sum of fit components is shown in red.

Although isomer shift often correlates strongly with oxidation state, these trends are manifested only when structural distortion is minimized upon oxidation/reduction of the complex, which is not true of the current family of complexes. Specifically, the isomer shift is correlated to the  $s$ -electron density at the iron center and due to both metal-ligand covalency (which directly affect  $s$ -electron density) and oxidation state (which affects shielding by the  $3d$ -electrons that interpenetrate the  $4s$  subshell of iron). Reduction increases the  $d$ -count of the iron center and will increase the isomer shift; however, removal of a ligand will enhance covalency in the resulting complex, increase the Fe  $s$ -electron density, and lower the isomer shift.<sup>14</sup> Although it is common for the latter case to outweigh the former, the unambiguous assignment of oxidation states in the present complexes is not possible without additional data.

Nevertheless, the change in isomer shift upon reduction of **4.2b** to **4.1b** demonstrates an increase in *s*-electron density at iron, counter to expectations due to its lower oxidation state. The isomer shift decrease therefore supports the notion of enhanced covalency upon loss of a strongly binding neopentyl(alkoxide) ligand, although this effect is less pronounced for the *p*-MeO(phenoxide) derivative. At present, it is not possible to exclude more complex electronic phenomena such as redox non-innocence of the bis(imino)pyridine ligand coupled with spin state changes at the metal center.

We can look at other reports in the literature on the electronic structure of formally iron(I) bis(imino)pyridine complexes and how their Mössbauer parameters compare to the analogous iron(II) complexes. For bis(imino)pyridine mono(chloride) and mono(alkyl) species, the Mössbauer isomer shifts decrease by around 0.1-0.3 mm/s from the bis(chloride) and bis(alkyl) species,<sup>12</sup> which is similar to the observed decrease in the isomer shift of complex **4.1b** as compared to complex **4.2b**. This may suggest that complex **4.1b** is also best described as an iron(II) center with a reduced bis(imino)pyridine ligand.

**Table 4.1.** Zero-field <sup>57</sup>Fe Mössbauer parameters for synthesized iron complexes.<sup>a15</sup>

Entry	Complex	δ (mm/s)	ΔE <sub>Q</sub>   (mm/s)
<b>1</b>	<b>4.1a<sup>b</sup></b>	1.04	1.79
<b>2</b>	<b>4.2a<sup>b</sup></b>	0.94	2.19
<b>3</b>	<b>4.1b</b>	0.75 (56%)	0.98
		0.60 (44%)	1.44
<b>4</b>	<b>4.2b<sup>b</sup></b>	0.94	1.71

<sup>a</sup>Spectra obtained in frozen benzene at 90K. <sup>b</sup>Samples were unpurified material and showed minor impurities in the spectra. Major species is reported.



To better determine the spin state and oxidation state of these formally Fe(I) complexes, additional EPR and Mössbauer data will be collected with cleaner, recrystallized products. The Mössbauer spectra of **4.1a** showed a minor impurity (9%), and the same sample was used for the EPR spectroscopy. Therefore, it is possible that the EPR signal observed was for the minor impurity and the signal for the major component can only be resolved at lower temperatures.

For the bis(imino)pyridine iron(I) neopentoxide complex **4.1b**, X-ray quality crystals were obtained from a concentrated solution in pentane. The solid state molecular structure reveals a slightly-distorted square planar iron center, supported by the bis(imino)pyridine ligand scaffold, with a single neopentyl alkoxide ligand. Unfortunately, the uncertainty in the ligand bond metrics obscure determination of redox activity of the bis(imido)pyridine ancillary ligand from an analysis of bond lengths.

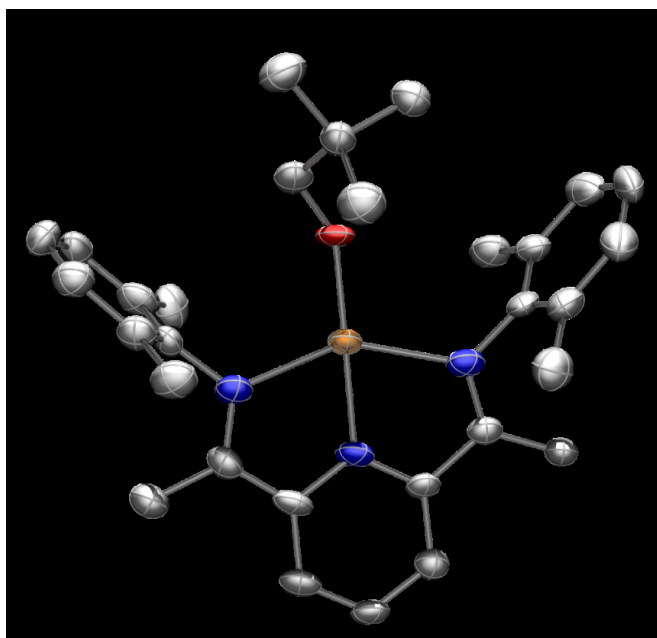


**Figure 4.6.** X-ray crystal structure of bis(imino)pyridine iron mono(neopentoxide) complex **4.1b** with thermal ellipsoids represented at the 50% probability level.<sup>16</sup> Hydrogen atoms are omitted for clarity.

In addition, computational studies are being carried out by the Cramer group at the University of Minnesota to help us better understand the electronic structure of these iron complexes.<sup>17</sup> Geometry optimization of complex **4.1a** with functional MO6-L/Def2-TZVP found good agreement for the high-spin quartet configuration with the bond metrics of the crystal structure of complex **4.1b** and was more favorable in energy than the low-spin configuration by 5.7 kcal/mol. Single point calculations on geometry optimized structures of both the high- and low-spin configurations showed that one unpaired electron resides on the ligands, so that the complex is best described as an iron(II) center. Although the high-spin configuration was found to be lower in energy for functional MO6-L, geometry optimizations performed with other functionals including OPBE-D, TPSSh-D, and MN-15 favored the low-spin configuration by 2.9-5.9 kcal/mol, although the bond distances for all low-spin configurations are much shorter than determined in the crystal structure of complex **4.1b**. The small energy differences and discrepancies observed between functionals may suggest that spin crossover events are occurring with these formally iron(I) alkoxide complexes, which will be investigated further with SQUID magnetometry.

### **4.3 Polymerization Activity of Bis(imino)pyridine Iron Aryloxide Complexes Toward Various Cyclic Esters**

#### *4.3.1 Polymerization of Lactide*

The polymerization activity of formally iron(I) complex **4.1a** was first investigated with lactide. Previously, we had determined that a more electron-donating alkoxide ligand resulted in accelerated polymerization rates compared to electron-

withdrawing alkoxides, and the iron(III) complex was completely inactive for polymerization (see Chapter 2). Therefore, we hypothesized a more electron rich iron(I) complex would give faster lactide polymerization rates compared to the iron(II) complex.

NMR experiments revealed that complex **4.1a** decomposed in CH<sub>2</sub>Cl<sub>2</sub>; however, the complex did remain stable in chlorobenzene. When lactide was exposed to 2 mol% **4.1a** in chlorobenzene, poly(lactic acid) was obtained with narrow dispersities ( $M_w/M_n = 1.1$ ) with 86% conversion after 20 minutes (**Table 4.2**). Molecular weights were higher than the theoretical values by a factor of 2.6.

**Table 4.2.** Polymerization of lactide (L) with **4.1a** and **4.2a** in chlorobenzene.<sup>a</sup>

Entry	Cat.	Cat. Loading (mol %)	[L] (M)	Time (min.)	Conv. (%)	$M_n$ (kg/mol)	$\bar{D}$	$M_n$ theor. <sup>b</sup>	$M_n$ expt./ $M_n$ theor.
1	<b>4.1a</b>	2	0.25	20	86	16.0	1.14	6.2	2.6
2	<b>4.1a</b>	1	0.43	20	86	25.7	1.16	12.4	2.1
3	<b>4.1a</b>	0.5	0.86	20	66	32.2	1.14	19.0	1.7
4	<b>4.2a</b>	2	0.25	20	94	16.1	1.15	6.8	2.4

<sup>a</sup>Reactions were performed in PhCl at room temperature. <sup>b</sup>(Lactide molecular weight)/([Fe]:[Lactide])(Conversion).

To determine whether slow initiation rates were causing molecular weights to be higher than average, lactide polymerizations were performed with increased concentrations of lactide.<sup>7</sup> Since initiation is first order in lactide, increasing the concentration of lactide in the reaction may result in an increased amount of the iron catalyst to be activated for polymerization and give molecular weights that are closer to theoretical values. When the concentration of lactide was increased in these experiments, all other parameters were kept constant, effectively decreasing the catalyst loading. When the lactide concentration was increased, the observed molecular weights were in better agreement with theoretical values (**Table 4.2**, entries 2 and 3). This suggests that slow

initiation rates are contributing to the higher than expected molecular weights, and that molecular weights close to theoretical values may be achieved by increasing the lactide concentration further. High molecular weights could also be observed due to an impurity in the reaction mixture that deactivates some of the catalyst. When polymerization of lactide with the iron(II) complex **4.2a** in chlorobenzene was studied, molecular weights were also observed to be higher than expected by a factor of 2.5 (entry 4), which may also be due to slow initiation, although varied lactide concentrations with this catalyst were not studied.

#### 4.3.2 Polymerization of $\epsilon$ -Caprolactone

Polycaprolactone is another highly useful biodegradable polymer that can be obtained through ring-opening polymerization. Although  $\epsilon$ -caprolactone is a similar cyclic ester monomer to lactide, iron(II) *p*-methoxyphenoxide complex **4.2a** is completely inactive toward  $\epsilon$ -caprolactone polymerization at room temperature and only shows moderate reactivity at 70°C (**Table 4.3**, entries 1 and 2). Interestingly, formally iron(I) complex **4.1a** is active for caprolactone polymerization at room temperature. After 24 hours, 80% conversion was observed (entry 3), with an induction period of 4 hours, suggesting the initiation rate is slow. This is consistent with the broad molecular weight distributions observed ( $\bar{M}_w/\bar{M}_n = 2.22$ ) if small amounts of active catalyst are introduced to the reaction over time.

**Table 4.3.** Polymerization of  $\epsilon$ -caprolactone with complexes **4.1a** and **4.2a**<sup>a</sup>

Entry	Cat.	Temp. (°C)	Time (h)	Conv. (%)	M <sub>n</sub> (kg/mol)	Đ
1	<b>4.2a</b>	24	24	0	--	--
2	<b>4.2a</b>	70	18	99	22.6	2.14
3	<b>4.1a</b>	24	24	80	30.6	2.22
4	<b>4.1a</b>	70	2	99	12.0	6.01

<sup>a</sup>Reactions performed with 2 mol% [Fe] in toluene (0.24M).

In order to accelerate the rate of the reaction, the polymerization was performed at elevated temperature. At 70°C in toluene, full conversion was observed after only two hours (**Table 4.3**, entry 4). An induction period was still observed (20 min.), although it was much less significant than at room temperature. Though the reaction proceeded rapidly under these conditions, broad and bimodal dispersities were obtained.

The formally iron(I) complex **4.1a** was much more active toward  $\epsilon$ -caprolactone polymerization than the analogous iron(II) complex **4.2a**, but these reactions resulted in polymers with quite broad dispersities, likely as a result of slow initiation rates. For these reasons, an iron complex with a more nucleophilic alkoxide ligand (**4.1b**) was examined for polymerization activity and is discussed in the following section.

## 4.4 Polymerization Activity of Bis(imino)pyridine Iron Neopentoxide Complexes Toward Various Cyclic Esters

### 4.4.1 Polymerization of Lactide

The formally iron(I) neopentoxide complex **4.1b** was next investigated for lactide polymerization. With the iron(II) complexes, neopentyl alcohol was found to give the fastest polymerization rates when used as the alkoxide ligand, likely due to the increased nucleophilicity of this alkoxide compared to the other ligands studied. Therefore, we

hypothesized that **4.1b** would be a superior lactide polymerization catalyst due to increased electron density at the iron center. Upon exposure of (*rac*)-lactide to **4.1b**, the polymerization was 90% converted after 10 minutes with 2 mol% catalyst loading and gave molecular weights close to theoretical values with narrow dispersities (**Table 4.4**). Linear correlation was observed for  $M_n$  vs. conversion, highlighting the living characteristics of the polymerization reaction (**Figure 4.7**). The catalyst loading could be lowered to afford higher molecular weight polymer; however, increased reaction times were required to reach high conversions (entries 2 and 3).

**Table 4.4.** Polymerization of lactide with complexes **4.1b** and **4.2b**.

Entry	Cat.	Cat. Loading (mol %)	Time (min.)	Conv. (%)	$M_n$ (kg/mol)	$M_n$ theor. (kg/mol)	$\bar{D}$
1	<b>4.1b</b>	2	10	91	9.6	6.6	1.12
2	<b>4.1b</b>	0.2	90	88	74.1	63.4	1.13
3	<b>4.1b</b>	0.05	540	84	214.1	242.1	1.18
4	<b>4.2b</b>	0.2	10	94	94.8	67.7	1.37

<sup>a</sup>Reactions were performed in toluene(0.35M) at room temperature.

Although this complex is highly active toward lactide polymerization, the analogous iron(II) complex **4.2b** was found to be more active for lactide polymerization in these conditions. With 0.2 mol% catalyst loading, the polymerization was 94% converted after 10 minutes with complex **4.2b** (**Table 4.4**, entry 4), whereas with complex **4.1b**, a reaction time of 90 minutes was required to reach high conversions. However, the observed dispersities were broader with complex **4.2b**. Because the lactide polymerization studies with the bis(imino)pyridine iron phenoxide complexes (**4.1a** and **4.2a**) were performed in chlorobenzene rather than toluene, comparisons between the neopentoxide and phenoxide complexes cannot be made at this time.

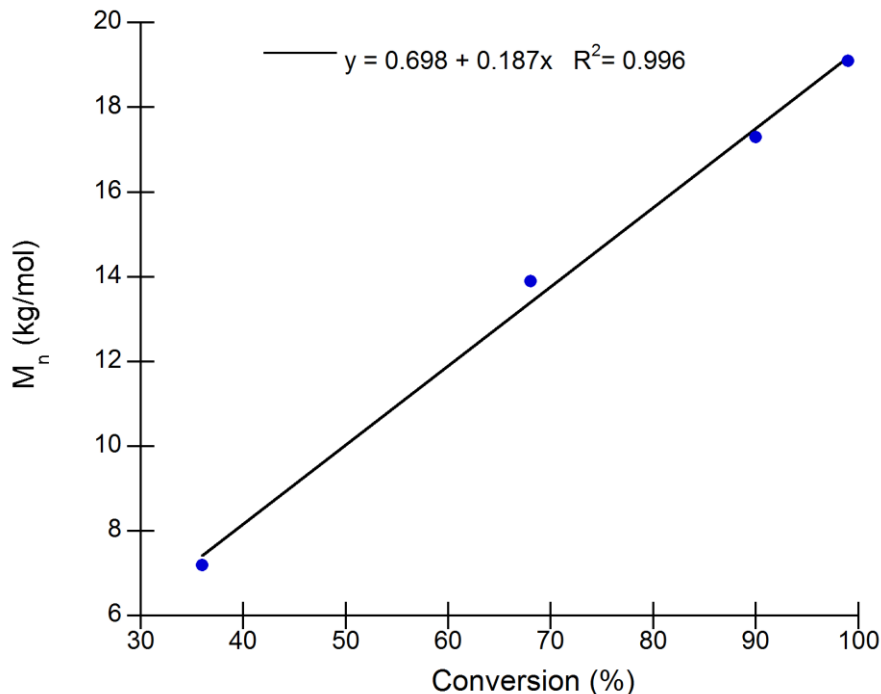


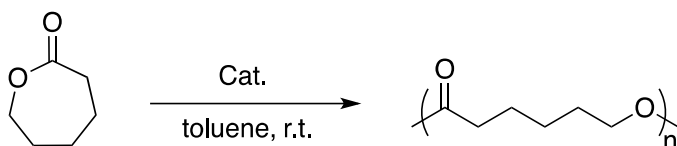
**Figure 4.7.** Molecular weight ( $M_n$ ) vs. conversion for lactide polymerization catalyzed by **4.1b**.

#### 4.4.2 Polymerization of $\epsilon$ -Caprolactone

Although formally iron(I) neopentoxide complex **4.1b** was found to be less active than the analogous iron(II) complex for lactide polymerization, we were interested in studying the activity of this complex toward other monomers. Because  $\epsilon$ -caprolactone polymerizations with complex **4.1a** seemed to suffer from slow initiation rates (section 4.3.2), we hypothesized a more nucleophilic alkoxide complex would result in faster initiation rates to give a more active catalyst and polycaprolactone with more narrow molecular weight distributions. Neopentyl alkoxide complex **4.1b** gratifyingly demonstrated rapid activity toward caprolactone polymerization at room temperature, with full conversion obtained within 10 minutes even at low catalyst loadings (0.05-2 mol%) (Table 4.5, entries 1-4). Molecular weights were higher than theoretical values,

but increased with a decrease in catalyst loading. When the catalyst loading was dropped to 0.01 mol%, only 6% conversion was observed after 24 hrs, which could be due to deactivation of the catalyst by adventitious water in the reaction solvent (entry 5). When polymerizations were performed with 0.01 mol% catalyst by increasing the monomer concentration rather than decreasing the catalyst concentration, the reaction gelled and formed high molecular weight polycaprolactone (612.2 kg/mol, entry 6).

**Table 4.5.** Polymerization of  $\epsilon$ -caprolactone (CL) with complexes **4.1b** and **4.2b**.



Entry	Cat.	Cat. Loading (mol%)	[CL] (M)	Time (min.)	Conv. (%)	M <sub>n</sub> (kg/mol)	M <sub>n</sub> theor. (kg/mol)	Đ
1	4.1b	2	0.34	10	99	24.2	5.7	1.40
2	4.1b	0.2	0.34	10	99	152.2	57.1	1.40
3	4.1b	0.1	0.34	10	99	246.2	114.1	1.41
4	4.1b	0.05	0.34	10	99	390.3	228.3	1.21
5	4.1b	0.01	0.34	1440	6	191.0	68.5	1.33
6	4.1b	0.01	1.5	20	99	612.2	1141.4	1.17
7	4.1b	0.1	0.17	10	99	237.9	114.1	1.23
8	4.1b	0.4	0.04	10	99	56.1	28.5	1.12
9	4.1b	0.2	0.04	10	99	129.3	57.1	1.19
10	4.2b	2	0.34	80	87	33.8	5.7	1.42
11	4.2b	0.2	0.34	80	89	94.9	57.1	1.33
12	4.2b	0.05	0.34	90	93	267.7	228.3	1.12

In addition to the fast reaction rates, the molecular weight distributions observed were much narrower than with complex **4.1a**, which is likely due to the accelerated initiation rates. The difference in reactivity for the iron neopentoxide complex compared to the *p*-methoxyphenoxide complex is remarkable; with one catalyst giving rapid conversion at room temperature and controlled molecular weight distributions, while the



other requires prolonged reaction periods or heating and shows bimodal molecular weight distribution. These results show the importance of the identity of the alkoxide ligand, which dictates the initiation rate of these polymerizations.

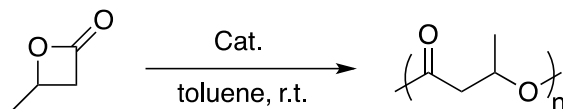
Although the *p*-methoxyphenoxide iron(II) complex **4.2a** is completely inactive for caprolactone polymerization at room temperature, the neopentoxide iron(II) complex **4.2b** is active for this transformation, again showing the importance of the identity of the alkoxide ligands for polymerization initiation. With 2 mol% of complex **4.2b**, 87% conversion of  $\epsilon$ -caprolactone was observed after 80 minutes (**Table 4.5**). Although the iron(II) neopentoxide complex is an effective catalyst for this polymerization reaction, the iron(I) complex gives more rapid polymerization rates, even at low catalyst loadings.

Attempts to study the kinetic behavior of the caprolactone polymerization with complex **4.1b** were made by lowering the concentration of caprolactone monomer in solution. However, in all attempts made (**Table 4.5**, entries 7-9), the reactions proceeded with rates that were too rapid to study by conventional means. The earliest time points for all caprolactone polymerization reactions were taken at 10 minutes, and it is likely that the reactions are complete much earlier. Attempts to study the conversion of the polymerization reaction over time by  $^1\text{H}$  NMR by performing the reaction in a J-Young tube resulted in no conversion in either toluene- $\text{d}_8$  (attempted one time at room temperature) or benzene- $\text{d}_6$  (attempted twice in frozen solution allowed to thaw) for unclear reasons.

#### 4.4.3 Polymerization of other Lactones

Because complex **4.1b** was found to be highly active toward caprolactone polymerization, it was investigated for the polymerization of other lactone monomers. Complex **4.1b** was found to react with the highly strained monomer  $\beta$ -butyrolactone, but the resulting products were low molecular weight oligomers and the reactions only proceeded to around 50% completion. Polymerizations conducted at lower catalyst loadings did not result in increased molecular weights. This polymerization must suffer from termination events that cause the molecular weights to be lower than expected. When polymerization reactions were carried out for longer reaction times (24 h), no further conversion was observed.

**Table 4.6.** Polymerization of  $\beta$ -butyrolactone ( $\beta$ BL) with complex **4.1b**.<sup>a</sup>



Entry	Cat. Loading (mol%)	Time (h)	Conv. (%)	M <sub>n</sub> (kg/mol)	D
1	2	1.5	50	1.5	1.07
2	0.2	1	47	0.7	1.08

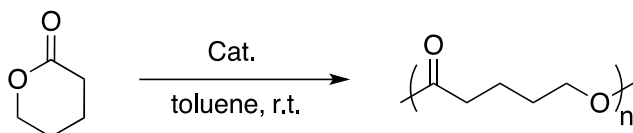
<sup>a</sup>Reactions performed at [ $\beta$ BL] = 0.34M.

Polymerization of the five-membered ring monomer  $\gamma$ -butyrolactone was unsuccessful in THF at room temperature with both complex **4.1b** and **4.2b**. This monomer is notoriously difficult to polymerize as five-membered lactones are particularly stable, and ring-opening polymerization is both enthalpically and entropically unfavorable.<sup>18</sup> In the future, polymerization studies with this monomer will be conducted

at low temperatures, which has been shown by Chen et al. to successfully overcome the unfavorable entropic penalty of this ring-opening polymerization.<sup>19</sup>

Complex **4.1b** was active for the polymerization of the 6-membered  $\delta$ -valerolactone, which has lower ring strain than  $\epsilon$ -caprolactone.<sup>20</sup> When  $\delta$ -valerolactone was exposed to 2 or 0.2 mol% **4.1b**, 85% conversion was observed within 10 minutes (Table 4.7, entries 1 and 2). Broad molecular weight distributions ( $\bar{D}$  = 1.83) were observed with 2 mol% **4.1b**, likely due to transesterification, but were much narrower ( $\bar{D}$  = 1.16 when the catalyst loading was lowered to 0.2 mol%). The observed molecular weights were only slightly higher than the theoretical values. When the polymerization reactions were carried out for longer times, no further increase in conversion was observed, which may be due to a competing depolymerization reaction in equilibrium with the forward reaction. This may also be the case for the other two ester monomers.

**Table 4.7.** Polymerization of  $\delta$ -valerolactone (VL) with complexes **4.1b** and **4.2b**.<sup>a</sup>



Entry	Cat.	Cat. Loading (mol%)	Time (min.)	Conv. (%)	$M_n$ (kg/mol)	$M_n$ theor. (kg/mol)	$\bar{D}$
1	<b>4.1b</b>	2	10	85	5.9	4.2	1.83
2	<b>4.1b</b>	0.2	10	83	47.8	41.6	1.16
3	<b>4.1b</b>	0.05	240	14	10.6	28.0	1.16
4	<b>4.2b</b>	0.2	90	80	36.4	40.1	1.47

<sup>a</sup>Reactions performed at [VL] = 0.34M.

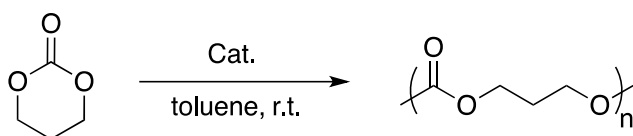
The analogous iron(II) complex **4.2b** was also competent for this transformation, but was less active than the formally iron(I) complex. At 0.2 mol% catalyst loading,

complex **4.2b** required 90 minutes to reach 80% conversion, compared to <10 minutes for complex **4.1b**.

#### 4.4.4 Polymerization of Cyclic Carbonates

Because complex **4.1b** was highly active toward the polymerization of cyclic ester monomers, reactivity toward cyclic carbonates were also investigated. Trimethylene carbonate can be derived from biomass and its ring-opening polymerization affords an elastomeric biodegradable polymer that is valuable for biomedical and industrial applications.<sup>6c</sup> The exposure of trimethylene carbonate to complex **4.1b** resulted in immediate formation of a gel precipitate in the toluene solution. <sup>1</sup>H NMR spectra showed full conversion to the polymer; however, broad, bimodal molecular weight distributions of the polymer products were observed (Table 4.8, entry 1).

**Table 4.8.** Polymerization of trimethylene carbonate (TMC) with complex **4.1b**.



Entry	Time (min.)	[TMC] (M)	Conv. (%)	M <sub>n</sub> (kg/mol)	Đ
1	10	0.35	100	5.0	6.60
2	10	0.18	100	2.7	9.45
3	10	0.07	100	1.6	13.38

We hypothesized that broad dispersities were observed due to the heterogeneity of the reaction mixture, which may be due to high substrate concentration. Dilution of the reaction mixture by adding more toluene did not improve the observed dispersities and still resulted in a gel precipitate, and actually resulted in lower molecular weight products with broader molecular weight distributions (Table 4.8, entries 2 and 3).

Polymerizations with ethylene carbonate were not successful in toluene solution and did not result in any conversion of this monomer. Similar to  $\gamma$ -butyrolactone, this monomer is extremely difficult to polymerize as it is a stable compound, and the ring-opening polymerization is entropically disfavored.<sup>18</sup> Recently, the first example of coordination-insertion ring-opening polymerization of a five-membered cyclic carbonate was reported; although a highly strained *trans*-cyclohexene carbonate monomer was utilized.<sup>21</sup> Perhaps more strained five-membered cyclic carbonate monomers would be worth investigating in the future.

#### **4.5 Copolymerization of cyclic esters with bis(imino)pyridine mono(alkoxide) complexes**

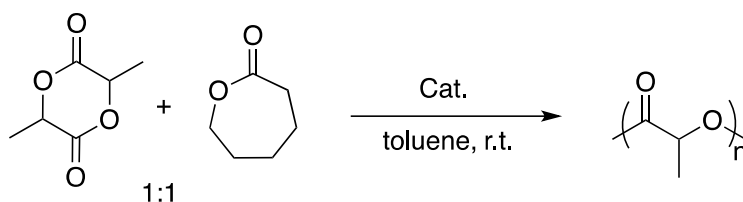
Because these formally iron(I) bis(imino)pyridine iron mono(alkoxide) complexes were highly active for a variety of polymerization reactions, copolymerizations were next investigated with these catalysts. Unlike the iron(II) and iron(III) versions of this catalyst, the iron(I) catalyst is reactive toward similar monomers to the iron(II) catalyst, so that redox-switchable copolymerizations cannot be performed with an iron(I)/iron(II) redox switch or trigger. Nevertheless, the copolymerization of different cyclic esters in one pot with the formally iron(I) catalysts can give rise to useful biodegradable polymers.

First the copolymerization of lactide and  $\epsilon$ -caprolactone was studied. When an equimolar mixture of lactide and caprolactone was exposed to **4.1a** in toluene at room temperature, full conversion of lactide was observed with no conversion of caprolactone (Table 4.9, entry 1). When the reaction temperature was raised to 70°C, caprolactone polymerization did not occur even after prolonged reaction times. When repeated with

the iron(II) complex **4.2a**, similar results were observed (entry 2). The dispersities of PLA formed in these reactions were broad and bimodal.

This copolymerization reaction was repeated with complex **4.1b** which is much more active for caprolactone polymerization, (**Table 4.9**, entry 3). Similar results were observed with this complex, but with much more narrow molecular weight distributions. Even though the homopolymerization of caprolactone is complete within 10 minutes, only poly(lactic acid) was observed after prolonged reaction periods. The species formed after lactide inserts into the iron alkoxide catalysts must not be active for the polymerization of caprolactone.

**Table 4.9.** Attempted copolymerization of lactide (L) and  $\epsilon$ -caprolactone (CL) in one pot.<sup>a</sup>

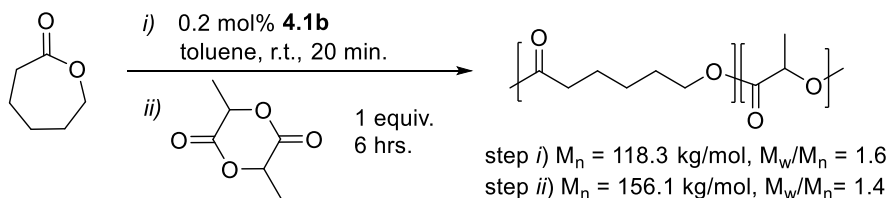


Entry	Cat.	Time (h)	Temp. (°C)	Conv. L (%)	Conv. CL (%)	M <sub>n</sub> (kg/mol)	Đ
1	4.1a	24	24	99	0	3.6	3.94
2	4.1a	24	70	99	0	2.7	4.71
3	4.2a	24	70	99	0	5.8	2.78
4	4.1b <sup>b</sup>	9	24	95	0	85.0	1.40

<sup>a</sup>Reactions performed in toluene at 2 mol% catalyst loading. [Lactide] = [ $\epsilon$ -caprolactone] = 0.34M. <sup>b</sup>Reaction performed with 0.2 mol% catalyst loading.

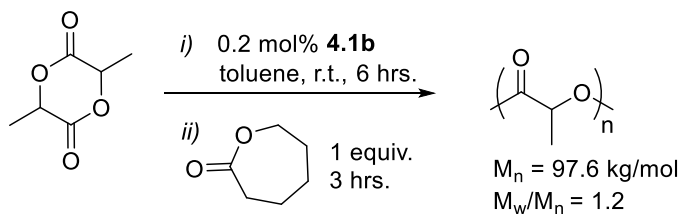
Copolymerization of caprolactone and lactide was also attempted by sequential addition of the two monomers with complex **4.1b** (**Scheme 4.3**). When lactide was added to a reaction mixture after caprolactone polymerization had been carried out to completion, full conversion of lactide and an increase in molecular weight was observed (118.3 to 156.1 kg/mol), suggesting a block copolymer was synthesized.

**Scheme 4.3.** Diblock copolymerization of  $\epsilon$ -caprolactone and lactide by sequential addition of lactide to caprolactone polymerization.



Conversely, when the sequential addition copolymerization is performed with lactide followed by caprolactone addition, no conversion of caprolactone is observed (**Scheme 4.4**). The lactide polymerization step was carried out for 6 hours to ensure that the lactide polymerization had proceeded to full conversion to rule out the possibility that the presence of lactide monomer inhibits the polymerization of caprolactone. This result also shows that the active species formed during lactide polymerization is not active for the insertion of caprolactone.

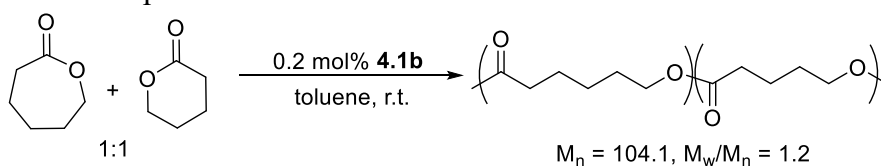
**Scheme 4.4.** Sequential addition of caprolactone to lactide polymerization catalyzed by **4.1b**.



When another lactone monomer,  $\delta$ -valerolactone, was utilized for copolymerizations with lactide, similar results were observed. When complex **4.1b** (0.2mol%) was exposed to an equimolar mixture of lactide and  $\delta$ -valerolactone were allowed to stir for 24 hours, only polymerization of lactide was observed ( $M_n = 24.3$  kg/mol,  $\bar{D} = 1.27$ ), with no conversion of  $\delta$ -valerolactone.

Although the copolymerization of lactone and lactide monomers resulted only in the synthesis of PLA, the one-pot copolymerization of two lactone monomers,  $\epsilon$ -caprolactone and  $\delta$ -valerolactone, resulted in a copolymer that incorporated both monomers. When an equimolar mixture of the two monomers was exposed to 0.2 mol% **4.1b** in toluene, both poly(caprolactone) and poly(valerolactone) were observed by  $^1\text{H}$  NMR (Table 4.10). Although **4.1b** seemed to be more active toward caprolactone than valerolactone in homopolymerization experiments indicated by faster reaction rates at low catalyst loadings, the two monomers appeared to have similar conversion rates in the copolymerization experiment. Although reactivity ratios have not been determined, this preliminary data suggests the copolymer structure is somewhat random. Interestingly,  $\delta$ -valerolactone reached higher ultimate conversion than was observed in the homopolymerization reactions (93% compared to 83%), which suggests the depolymerization reaction is not as accessible under the copolymerization conditions.

**Table 4.10.** Copolymerization of  $\epsilon$ -caprolactone (CL) and  $\delta$ -valerolactone (VL) with complex **4.1b** in one pot.



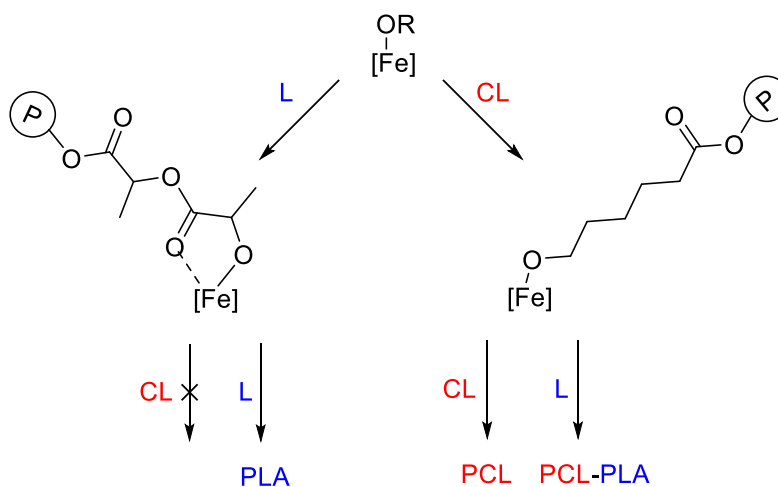
Entry	Time (min.)	Conv. CL (%)	Conv. VL (%)
1	10	72	81
2	20	84	89
3	40	94	93

Although the formally iron(I) complex **4.1b** is highly active for the polymerization of both lactide and lactone monomers, only lactide polymerization is



observed when a mixture of the monomers is simultaneously exposed to the iron complex. While the overall polymerization rate for  $\epsilon$ -caprolactone homopolymerization is faster than that observed for lactide homopolymerization, the lactide polymerization may proceed with a faster initiation rate. Caprolactone/lactide copolymerizations often manifest preferential lactide insertion resulting in gradient or block copolymers, which may be due to the superior coordination ability of lactide.<sup>22</sup> Once lactide inserts into the iron alkoxide bond, the growing polymer chain may chelate to the iron center with an adjacent ester functionality, creating a favorable five-membered ring structure as shown in **Scheme 4.5**, left.

**Scheme 4.5.** Proposed explanation for the inability to polymerize caprolactone (CL) following lactide (L) polymerization. P = growing polymer chain.



We suggest that lactide polymerization can continue to propagate from this species; however, the  $\epsilon$ -caprolactone monomer is not able to displace this chelate, bind to the iron center, and initiate polymerization. Conversely, the growing poly(lactone) chain (derived from  $\epsilon$ -caprolactone initiation, **Scheme 4.5**, right) cannot form a similar chelate

structure, leaving the iron center open for coordination by either monomer. In this manner, initiation of lactide polymerization is selective for lactide propagation, while initiation of caprolactone polymerization allows for either monomer to propagate. This selectivity effectively promotes lactide homo-polymerization even from a mixture of monomers. A similar explanation could be posited for the inability to polymerize  $\delta$ -valerolactone following lactide propagation.

## 4.6 Conclusions

Two formally iron(I) bis(imino)pyridine iron mono(alkoxide) complexes were synthesized, characterized, and investigated for polymerization activity in the ring-opening polymerization of various monomers. Preliminary EPR studies and solution magnetometry are suggestive of an  $S = 1/2$  spin state, and zero-field  $^{57}\text{Fe}$  Mössbauer spectroscopy is consistent with a more reduced metal center compared to the iron(II) analogues. However, definitive determination of the redox state of the iron atom requires additional support as current data is not sufficient to exclude the possibility of either a neutral bis(imino)pyridine-supported iron(I) complex or an anionic bis(imido)pyridine-supported iron(II) complex. An X-ray crystal structure of the iron mono(neopentoxide) complex was determined; however, the bond metrics could not be utilized for assignment of a reduced or neutral bis(imino)pyridine ligand due to high standard deviations of the relevant structural metrics. Further EPR and Mössbauer studies with more highly purified material, as well as computational modelling will be carried out to help us better understand the electronic structure of these iron complexes.

The formally iron(I) and iron(II) aryloxide complexes are active for the polymerization of lactide with similar reaction rates. However, these complexes showed different reactivities toward  $\epsilon$ -caprolactone. While the iron(II) complex **4.2a** is completely inactive for  $\epsilon$ -caprolactone polymerization at room temperature, the formally iron(I) complex **4.1a** showed moderate activity, although with broad molecular weight distributions.

The iron complexes with neopentoxide ligands were generally superior catalysts to their aryloxide congeners, due to the more nucleophilic nature of the alkyl alkoxide ligand. The formally iron(I) complex **4.1b** was found to be one of the most active iron-based catalysts reported for the polymerization of the lactone monomers  $\epsilon$ -caprolactone and  $\delta$ -valerolactone, and afforded accelerated polymerization rates compared to the analogous iron(II) complex **4.2b**. Complex **4.1b** was also investigated for  $\beta$ -butyrolactone polymerization, but resulted in low molecular weight oligomers and reactions that did not reach full conversion. Polymerization of trimethylene carbonate was also rapid with complex **4.1b**, although broad bimodal molecular weight distributions were obtained. Finally, **4.1b** was highly active for the polymerization of lactide, although at a slower rate than for the analogous iron(II) complex **4.2b**.

Our initial hypothesis was that the more electron rich iron center of complex **4.1b** would make it a superior catalyst for lactide polymerization, but perhaps a chelating interaction as described in Scheme 4.5 occurs during lactide polymerization. This chelation would be stronger with more electron rich complexes due to increased  $\pi$ -backdonation, making it more difficult to be displaced by an incoming lactide monomer and continue chain propagation. However, the formally iron(I) complexes were found to

be superior for the ring-opening polymerization of lactones compared to the iron(II) complexes. For lactone polymerization, this type of chelating interaction would not be as favorable and therefore, the nucleophilicity of the alkoxide ligand may be the governing factor in determining the reaction rate.

Although the formally iron(I) and iron(II) complexes showed different reaction rates toward different substrates, they were both able to polymerize the same classes of cyclic ester monomers. This is unlike the cationic iron(III) complex, which is not competent for the polymerization of cyclic esters, and has only been found to react with epoxides thus far. It is possible that these complexes react toward similar classes of monomers because they share an iron(II) oxidation state, but as mentioned above, further characterization is required to better understand the electronic nature of the iron mono(alkoxide) complexes.

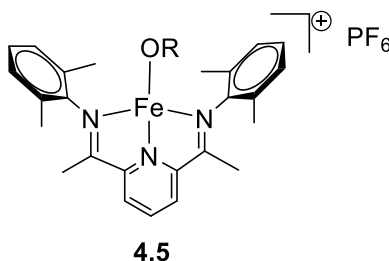
The attempted copolymerization of lactide with lactone monomers in one reaction vessel resulted only in the formation of poly(lactic acid). This is likely due to the propensity of lactide to bind to metals compared to lactones, and a possible chelating species that may prevent lactone monomers from being able to initiate polymerization. Copolymerization of two lactones,  $\epsilon$ -caprolactone and  $\delta$ -valerolactone, in one pot resulted in full conversion of both monomers, which polymerized at comparable rates.

Future investigations will involve  $\gamma$ -butyrolactone and ethylene carbonate monomers, which are notoriously challenging to polymerize, as well as other types of monomers for ring-opening. Ideally, one of the monomers will show activity only in the iron(I) oxidation state and show no activity in the iron(II) oxidation state, which would

allow for redox-switching copolymerization techniques to be extended to the iron(I) oxidation state.

Additionally, investigations of a cationic bis(imino)pyridine iron(II) mono(alkoxide) complex may help decipher what factors are important for ring opening polymerization of epoxides. Preliminary studies indicate the successful synthesis of **4.5** upon exposure of **4.1a** or **4.1b** to one equivalent of ferrocenium hexafluorophosphate, although further characterization is required (**Scheme 4.6**). For the epoxide polymerization, we hypothesize that a more electrophilic iron center is required to activate the epoxide monomer. Studying the activity of **4.5** could provide insight on whether the oxidation state of the iron center or the cationic nature of the iron complex determines activity toward epoxide polymerization.

**Scheme 4.6.** Formally iron(II) bis(imino)pyridine mono(alkoxide) complex.



## 4.7 Experimental

**General Considerations.** Unless stated otherwise, all reactions were carried out in oven-dried glassware in a nitrogen-filled glove box or with standard Schlenk line techniques.<sup>23</sup> Solvents were used after passage through a solvent purification system under a blanket of argon and then degassed briefly by exposure to vacuum. Nuclear magnetic resonance (NMR) spectra were recorded at ambient temperature on Varian

spectrometers operating at 400-600 MHz. Magnetic moments were determined by Evans' method<sup>24</sup> in THF by means of a procedure published by Gibson and coworkers.<sup>25</sup> Gel permeation chromatography (GPC) was performed on an Agilent GPC220 in THF at 40°C with three PL gel columns (10µm) in series. Molecular weights and molecular weight distributions were determined from the signal response of the RI detector relative to polystyrene standards. EPR spectra were obtained on a Bruker EleXsys E-500 CW-EPR spectrometer. Spectra were measured as frozen toluene glasses at a microwave power of 0.6325–2 mW. Effective g-values were obtained from spectral simulations of  $S = 1/2$  systems with the program Easyspin.<sup>26</sup> Zero-field <sup>57</sup>Fe Mössbauer spectra were measured with a constant acceleration spectrometer (SEE Co, Minneapolis, MN) at 90K. Isomer shifts are quoted relative to Fe foil at room temperature. Data was analyzed and simulated with Igor Pro 6 software (WaveMetrics, Portland, OR) by means of Lorentzian fitting functions. Samples were prepared by freezing a solution of 20-30 mg compound in benzene.

The monomer (*rac*)-lactide was recrystallized from ethyl acetate followed by recrystallization from toluene and dried *in vacuo* prior to polymerization. The monomers ε-caprolactone, ö-valerolactone, β-butyrolactone, and γ-valerolactone were dried over CaH<sub>2</sub> and distilled prior to polymerization. Trimethylene carbonate and ethylene carbonate were dried *in vacuo* prior to polymerization. Complexes **4.2a**, **4.2b**, and **4.4** were synthesized as described previously.<sup>4,11</sup>

**Synthesis of Complex 4.1a.** In a glove box, a solution of 4-methoxyphenol (0.0249g, 0.201mmol) in Et<sub>2</sub>O (10ml) was cooled to -40°C and added to a solution of **4.4** (0.100g, 0.196mmol) in Et<sub>2</sub>O (5ml) that had also been cooled to -40°C. It was allowed to

stir at room temperature for one hour, and the red mixture was filtered through celite and solvent was removed from the filtrate to yield a dark red solid (96%).  $^1\text{H}$  NMR (ppm,  $\text{C}_6\text{D}_6$ , broad singlets): 90.3, 16.5, -3.9, -12.9, -24.6, -63.9.

**Synthesis of Complex 4.1b.** In a glove box, a solution of neopentyl alcohol (0.0220g, 0.250 mmol) in  $\text{Et}_2\text{O}$  (2ml) was cooled to  $-40^\circ\text{C}$  and added to a solution of **4.4** (0.1301g, 0.2538mmol) in  $\text{Et}_2\text{O}$  (6ml) that had also been cooled to  $-40^\circ\text{C}$ . It was allowed to stir at room temperature for 30 minutes, and then solvent was removed from the reaction. It was lyophilized in frozen benzene. The mixture was then dissolved in pentane and filtered through celite, and the solvent was removed from the filtrate to yield a dark red solid (82%). Crystallization in pentane at  $-40^\circ\text{C}$  afforded crystals suitable for X-ray analysis.  $^1\text{H}$  NMR (ppm,  $\text{C}_6\text{D}_6$ , broad singlets): 67.5, 50.6, -10.0, -15.9, -50.0.

**Polymerization of (*rac*)-lactide with aryloxide complexes 4.1a and 4.2a.** At room temperature in a glove box, iron aryloxide complex **4.1a** or **4.2a** (0.007 mmol) in chlorobenzene (0.9 mL) was added to a seven mL vial containing (*rac*)-lactide (0.050g, 0.35 mmol) in chlorobenzene (0.5 mL). Aliquots were removed periodically from the reaction mixture and terminated by exposing them to air. Solvent was removed *in vacuo* and conversion was determined by  $^1\text{H}$  NMR in  $\text{CDCl}_3$  by integrating the methine peak of the remaining lactide versus the methine peak of poly(lactic acid). The aliquots were also analyzed by GPC to determine molecular weight and molecular weight distribution of the polymers.

**Polymerization of  $\epsilon$ -caprolactone with aryloxide complexes 4.1a and 4.2a.** At room temperature in a glove box, iron aryloxide complex **4.1a** or **4.2a** (0.014 mmol) in toluene (1.8 mL) was added to a seven mL vial containing  $\epsilon$ -caprolactone (0.080g, 0.70

mmol) in toluene (1.0 mL). Aliquots were removed periodically from the reaction mixture and terminated by exposing them to air. Solvent was removed *in vacuo* and conversion was determined by  $^1\text{H}$  NMR in  $\text{CDCl}_3$  by integrating the  $\alpha$ -methylene peak of the remaining  $\epsilon$ -caprolactone versus the  $\alpha$ -methylene peak of poly(caprolactone). The aliquots were also analyzed by GPC to determine molecular weight and molecular weight distribution of the polymers.

**Polymerization of (*rac*)-lactide with neopentoxide complexes **4.1b** and **4.2b**.**

At room temperature in a glove box, the desired amount of iron neopentoxide complex **4.1b** or **4.2b** in toluene (1.0 mL) was added to a seven mL vial containing (*rac*)-lactide (0.10 g, 0.7mmol) in toluene (1.0 mL). Aliquots were removed periodically from the reaction mixture and terminated by exposing them to air. Solvent was removed *in vacuo* and conversion was determined by  $^1\text{H}$  NMR in  $\text{CDCl}_3$  by integrating the methine peak of the remaining lactide versus the methine peak of poly(lactic acid). The aliquots were also analyzed by GPC to determine molecular weight and molecular weight distribution of the polymers.

**Polymerization of  $\epsilon$ -caprolactone with neopentoxide complexes **4.1b** and **4.2b**.** Most polymerization reactions were performed at 0.34M [CL]: At room temperature in a glove box, the desired amount of iron neopentoxide complex **4.1a** or **4.2a** in toluene (1.0 mL) was added to a seven mL vial containing  $\epsilon$ -caprolactone (0.080g, 0.70 mmol) in toluene (1.0 mL). Aliquots were removed periodically from the reaction mixture and terminated by exposing them to air. Solvent was removed *in vacuo* and conversion was determined by  $^1\text{H}$  NMR in  $\text{CDCl}_3$  by integrating the  $\alpha$ -methylene peak of the remaining  $\epsilon$ -caprolactone versus the  $\alpha$ -methylene peak of poly(caprolactone).



The aliquots were also analyzed by GPC to determine molecular weight and molecular weight distribution of the polymers. Reactions performed at higher concentrations were carried out by increasing the amount of  $\epsilon$ -caprolactone added and reactions performed at lower concentrations were performed by increasing the amount of toluene added.

**Polymerization of  $\delta$ -valerolactone with neopentoxide complexes 4.1b and 4.2b.** At room temperature in a glove box, the desired amount of iron neopentoxide complex **4.1a** or **4.2a** in toluene (1.0 mL) was added to a seven mL vial containing  $\delta$ -valerolactone (0.070g, 0.70 mmol) in toluene (1.0 mL). Aliquots were removed periodically from the reaction mixture and terminated by exposing them to air. Solvent was removed *in vacuo* and conversion was determined by  $^1\text{H}$  NMR in  $\text{CDCl}_3$  by integrating the  $\alpha$ -methylene peak of the remaining  $\delta$ -valerolactone versus the  $\alpha$ -methylene peak of poly(valerolactone). The aliquots were also analyzed by GPC to determine molecular weight and molecular weight distribution of the polymers.

**Polymerization of  $\beta$ -butyrolactone with neopentoxide complexes 4.1b and 4.2b.** At room temperature in a glove box, the desired amount of iron neopentoxide complex **4.1a** or **4.2a** in toluene (1.0 mL) was added to a seven mL vial containing  $\beta$ -butyrolactone (0.070g, 0.70 mmol) in toluene (1.0 mL). Aliquots were removed periodically from the reaction mixture and terminated by exposing them to air. Solvent was removed *in vacuo* and conversion was determined by  $^1\text{H}$  NMR in  $\text{CDCl}_3$  by integrating the  $\alpha$ -methylene peak of the remaining  $\beta$ -butyrolactone versus the  $\alpha$ -methylene peak of poly(butyrolactone). The aliquots were also analyzed by GPC to determine molecular weight and molecular weight distribution of the polymers.

**Attempted polymerization of  $\gamma$ -butyrolactone with neopentoxide complexes 4.1b and 4.2b.** At room temperature in a glove box, the desired amount of iron neopentoxide complex **4.1a** or **4.2a** (0.007mmol) in THF (0.9 mL) was added to a seven mL vial containing  $\gamma$ -butyrolactone (0.070g, 0.70 mmol) in THF (1.0 mL). The reaction was allowed to stir 24 hours at room temperature. No conversion was observed by  $^1\text{H}$  NMR.

**Polymerization of trimethylene carbonate with neopentoxide complex 4.1b.** At room temperature in a glove box, the desired amount of iron neopentoxide complex **4.1b** in toluene (0.5 mL) was added to a seven mL vial containing trimethylene carbonate (0.036g, 0.35 mmol) in toluene (0.5 mL). A gel-like precipitate formed immediately. The reaction mixture was allowed to stir for 10 minutes and was quenched by exposing to air. Solvent was removed *in vacuo* and conversion was determined by  $^1\text{H}$  NMR in  $\text{CDCl}_3$  by integrating the  $\alpha$ -methylene peak of the remaining  $\beta$ -butyrolactone versus the  $\alpha$ -methylene peak of poly(butyrolactone). The aliquots were also analyzed by GPC to determine molecular weight and molecular weight distribution of the polymers.

**Attempted polymerization of ethylene carbonate with neopentoxide complexes 4.1b and 4.2b.** At room temperature in a glove box, the desired amount of iron neopentoxide complex **4.1b** or **4.2b** in THF (0.9 mL) was added to a seven mL vial containing ethylene carbonate (0.032g, 0.36 mmol) in toluene (0.5 mL). The reaction mixture was allowed to stir at room temperature for 24 hours. No conversion was observed by  $^1\text{H}$  NMR.

**Attempted copolymerization of lactide and  $\epsilon$ -caprolactone in one reaction pot.** At room temperature in a glove box, the desired amount of iron alkoxide complex

**4.1a, 4.1b** or **4.2a** in toluene (1.0 mL) was added to a seven mL vial containing (*rac*)-lactide (0.10 g, 0.70mmol) and  $\epsilon$ -caprolactone (0.080g, 0.70mmol) in toluene (1.0 mL). Aliquots were removed periodically from the reaction mixture and terminated by exposing them to air. Solvent was removed *in vacuo* and conversion of lactide was determined by  $^1\text{H}$  NMR in  $\text{CDCl}_3$  by integrating the methine peak of the remaining lactide versus the methine peak of poly(lactic acid). No conversion of  $\epsilon$ -caprolactone was observed by  $^1\text{H}$  NMR. The aliquots were also analyzed by GPC to determine molecular weight and molecular weight distribution of the polymers.

**Attempted copolymerization of lactide and  $\epsilon$ -caprolactone by sequential lactide-caprolactone addition.** At room temperature in a glove box, iron alkoxide complex **4.1b** (350 $\mu\text{L}$  of a 0.0040M solution in toluene, 0.0014mmol) was added to a seven mL vial containing (*rac*)-lactide (0.10 g, 0.7mmol) in toluene (2.0 mL). The reaction was allowed to stir at room temperature for six hours, and then  $\epsilon$ -caprolactone (0.080g, 0.70mmol) was added. Aliquots were removed periodically from the reaction mixture and terminated by exposing them to air. Solvent was removed *in vacuo* and conversion of lactide was determined by  $^1\text{H}$  NMR in  $\text{CDCl}_3$  by integrating the methine peak of the remaining lactide versus the methine peak of poly(lactic acid). No conversion of  $\epsilon$ -caprolactone was observed by  $^1\text{H}$  NMR. The aliquots were also analyzed by GPC to determine molecular weight and molecular weight distribution of the polymers.

**Block copolymerization of lactide and  $\epsilon$ -caprolactone by sequential caprolactone-lactide addition.** At room temperature in a glove box, complex **4.1b** (350 $\mu\text{L}$  of a 0.0040M solution in toluene, 0.0014mmol) was added to a seven mL vial containing  $\epsilon$ -caprolactone (0.080g, 0.7mmol) in toluene (2.0 mL). The reaction was

allowed to stir at room temperature for 20 minutes, and then (*rac*)-lactide (0.10g, 0.70mmol) was added. Aliquots were removed periodically from the reaction mixture and terminated by exposing them to air. Solvent was removed *in vacuo* and conversion of lactide was determined by  $^1\text{H}$  NMR in  $\text{CDCl}_3$  by integrating the methine peak of the remaining lactide versus the methine peak of poly(lactic acid). Conversion of  $\epsilon$ -caprolactone was determined by  $^1\text{H}$  NMR in  $\text{CDCl}_3$  by integrating the  $\alpha$ -methylene peak of the remaining  $\epsilon$ -caprolactone versus the  $\alpha$ -methylene peak of poly(caprolactone). The aliquots were also analyzed by GPC to determine molecular weight and molecular weight distribution of the polymers.

**Attempted copolymerization of lactide and  $\delta$ -valerolactone in one reaction pot.** At room temperature in a glove box, the desired amount of iron alkoxide complex complex **4.1b** (350 $\mu\text{L}$  of a 0.0040M solution in toluene, 0.0014mmol) was added to a seven mL vial containing (*rac*)-lactide (0.10 g, 0.70mmol) and  $\delta$ -valerolactone (0.080g, 0.70mmol) in toluene (2.0 mL). Aliquots were removed periodically from the reaction mixture and terminated by exposing them to air. Solvent was removed *in vacuo* and conversion of lactide was determined by  $^1\text{H}$  NMR in  $\text{CDCl}_3$  by integrating the methine peak of the remaining lactide versus the methine peak of poly(lactic acid). No conversion of  $\delta$ -valerolactone was observed by  $^1\text{H}$  NMR. The aliquots were also analyzed by GPC to determine molecular weight and molecular weight distribution of the polymers.

**Copolymerization of  $\epsilon$ -caprolactone and  $\delta$ -valerolactone in one reaction pot.** At room temperature in a glove box, the desired amount of iron alkoxide complex complex **4.1b** (350 $\mu\text{L}$  of a 0.0040M solution in toluene, 0.0014mmol) was added to a seven mL vial containing  $\epsilon$ -caprolactone (0.080 g, 0.70mmol) and  $\delta$ -valerolactone

(0.080g, 0.70mmol) in toluene (2.0 mL). Aliquots were removed periodically from the reaction mixture and terminated by exposing them to air. Solvent was removed *in vacuo* and conversions of both monomers were determined by  $^1\text{H}$  NMR in  $\text{CDCl}_3$  by integrating the  $\alpha$ -methylene peak of the remaining lactone monomer versus the  $\alpha$ -methylene peak of poly(lactone). The aliquots were also analyzed by GPC to determine molecular weight and molecular weight distribution of the polymers.

---

### **References**

1. a) Dove, A.P. *Chem. Commun.* **2008**, 48, 6446-6470. b) Dechy-Cabaret, O.; Martin-Vaca, B.; Bourissou, D. *Chem. Rev.* **2004**, 104, 6147-6176. c) Mehta, R.; Kumar, V.; Bhunia, H.; Upadhyay, S.N. *J. Macromol. Sci. Polymer Rev.* **2005**, 45, 325-349.
2. Hoppe, J. O.; Agnew Marcelli, M. G.; Tainter, M. L. *Am. J. Med. Sci.* **1955**, 230, 558-571.
3. a) Stolt, M.; Södergård, A. *Macromolecules* **1999**, 32, 6412-6417. b) O'Keefe, B. J.; Monnier, S. M.; Hillmyer, M. A.; Tolman, W. B. *J. Am. Chem. Soc.* **2000**, 123, 339-340. c) O'Keefe, B. J.; Breyfogle, L. E.; Hillmyer, M. A.; Tolman, W. B. *J. Am. Chem. Soc.* **2002**, 124, 4384-4393. d) Gibson, V. C.; Marshall, E. L.; Navarro-Llobet, D.; White, A. J. P.; Williams, D. J. *J. Chem. Soc., Dalton Trans.* **2002**, 4321-4322. e) McGuinness, D. S.; Marshall, E. L.; Gibson, V. C.; Steed, J. W. *J. Polym. Sci. A Polym. Chem.* **2003**, 41, 3798-3803. f) Wang, X.; Liao, K.; Quan, D.; Wu, Q. *Macromolecules* **2005**, 38, 4611-4617. g) Idage, B. B.; Idage, S. B.; Kasegaonkar, A. S.; Jadhav, R. V. *Mater. Sci. Eng., B*, **2010**, 168, 193-198. h) Södergård, A.; Stolt, M. *Macromol. Symp.* **1998**, 130, 393-402. i) Arvanitoyannis, I.; Nakayama, A.; Psomiadou, E.; Kawasaki, N.; Yamamoto, N. *Polymer* **1996**, 37, 651-660. j) Kricheldorf, H.R.; Boettcher, C. *Die Makromol. Chem.* **1993**, 194, 463-473. k) Kricheldorf, H.R.; Damrau, D.-O. *Macromol. Chem. Phys.* **1997**, 198, 1767-1774.
4. Biernesser, A.B.; Li, B.; Byers, J.A. *J. Am. Chem. Soc.*, **2013**, 135, 16553-16560.
5. a) Arbaoui, A.; Redshaw, C.; Elsegood, M.R.J.; Wright, V.E.; Yohsizawa, A.; Yamato, T. *Chem. Asian J.* **2010**, 5, 621-623. b) Gowda, R.R.; Chakraborty, D. *J. Mol. Catal. A Chem.* **2009**, 301, 84-92. c) Chen, M.-Z.; Sun, H.-M.; Li, W.-F.; Wang, Z.-G.; Shen, Q.; Zhang, Y. *J. Organomet. Chem.* **2006**, 691, 2489-2494. d)

- 
- Geng, C.; Peng, Y.; Wang, L.; Roesky, H.W.; Liu, K. *Dalton Trans.* **2016**, *45*, 15779-15782. e) Hege, C.S.; Schiller, S.M. *Green Chem.* **2014**, *16*, 1410-1416. f) Estrina, G.A.; Grishchuk, A.A.; Karateyev, A.M.; Rozenberg, B.A. *Polym. Sci. U.S.S.R.* **1988**, *30*, 615-620. g) Fang, Y.-Y.; Gong, W.-J.; Shang, X.-J.; Li, H.-X.; Gao, J.; Lang, J.-P. *Dalton Trans.* **2014**, *43*, 8282-8289.
6. a) Dobrzynski, P.; Pastusiak, M.; Bero, M. *J. Poly. Sci. A. Polym. Chem.* **2005**, *43*, 1913-1922. b) Kricheldorf, H. R.; Lee, S.; Weegen-Shultz, B. *Macromol. Chem. Phys.* **1996**, *197*, 1043-1054. c) Helou, M.; Miserque, O.; Brusson, J.-M.; Carpentier, J.-F.; Guillaume, S.M. *Adv. Synth. Catal.* **2009**, *351*, 1312-1324.
7. Manna, C.; Kaplan, H.Z.; Li, B.; Byers, J.A. *Polyhedron* **2014**, *84*, 160-167.
8. Biernesser, A.B.; Delle Chiaie, K.R.; Curley, J.B.; Byers, J.A. *Angew. Chem. Int. Ed.* **2016**, *55*, 5251-5254.
9. Delle Chiaie, K.R.; Yablon, L.M.; Biernesser, A.B.; Michalowski, G.R.; Sudyn, A.W.; Byers, J.A. *Polym. Chem.* **2016**, *7*, 4675.
10. a) Small, B. L.; Brookhart, M.; Bennett, A. M. A. *J. Am. Chem. Soc.* **1998**, *120*, 4049-4050. b) Britovsek, G. J. P.; Bruce, M.; Gibson, V. C.; Kimberley, B. S.; Maddox, P. J.; Mastroianni, S.; McTavish, S. J.; Redshaw, C.; Solan, G. A.; Strömberg, S.; White, A. J. P.; Williams, D. J. *J. Am. Chem. Soc.* **1999**, *121*, 8728-8740. c) Trovitch, R. J.; Lobkovsky, E.; Bill, E.; Chirik, P. J. *Organometallics* **2008**, *27*, 1470-1478; Monfette, S.; d) Turner, Z. R.; Semproni, S. P.; Chirik, P. J. *J. Am. Chem. Soc.*, **2012**, *134*, 4561-4564; e) Tondreau, A. M.; Atienza, C. C. H.; Weller, K. J.; Nye, S. A.; Lewis, K. M.; Delis, J. G. P.; Chirik, P. J. *Science*, **2012**, *335*, 567-570. f) Russell, S. K.; Lobkovsky, E.; Chirik, P. J. *J. Am. Chem. Soc.*, **2011**, *133*, 8858-8861.
11. Bouwkamp, M.W.; Bart, S.C.; Hawrelak, E.J.; Trovitch, R.J.; Lobkovsky, E.; Chirik, P.J. *Chem. Commun.* **2005**, 3406-3408.
12. a) Bart, S.C.; Chlopek, K.; Bill, E.; Bouwkamp, M.W.; Lobkovsky, E.; Neese, F.; Weighardt, K.; Chirik, P.J. *J. Am. Chem. Soc.* **2006**, *128*, 13901-13912. b) Tondreau, A.M.; Milsman, C.; Patrick, A.D.; Hoyt, H.M.; Lobkovsky, E.; Wieghardt, K.; Chirik, P.J. *J. Am. Chem. Soc.* **2010**, *132*, 15046-15059.
13. EPR spectroscopy and data simulation performed by Dr. Matt Wilding of Professor Ted Betley's group at Harvard University.
14. Gütlich, P.; Bill, E.; Trautwein, A.X. *Mössbauer Spectroscopy and Transition Metal Chemistry*, Springer-Verlag: Berlin Heidelberg, 2011.
15. Mössbauer spectroscopy performed by Dr. Matt Wilding and Diana Iovan in Professor Ted Betley's laboratory at Harvard University.

- 
16. X-ray crystal structure determined by Dr. Bo Li at the X-ray Crystallography Center of Boston College.
  17. Calculations performed by Manuel A. Ortuño and Büsra Dereli in Professor Chris Cramer's research group at the University of Minnesota.
  18. Myers, D.; Cyriac, A.; Williams, C.K. *Nature Chem.* **2016**, 8, 3-4.
  19. Hong, M.; Chen, E.Y.X. *Nature Chem.* **2016**, 8, 42-49.
  20. Saiyasombat, W.; Molloy, R.; Nicholson, T.M.; Johnson, A.F.; Ward, I.M.; Pshyachinda, S. *Polymer* **1998**, 39, 5581-5585.
  21. Guerin, W.; Diallo, A.K.; Kirilov, E.; Helou, M.; Slawinski, M.; Brusson, J.-M.; Carpentier, J.-F.; Guillaume, S.M. *Macromolecules* **2014**, 47, 4230-4235.
  22. a) Nomura, N.; Akita, A.; Ishii, R.; Mizuno, M. *J. Am. Chem. Soc.* **2010**, 132, 1750-1751. b) Vion, J.-M.; Jerome, R.; Teyssie, P. *Macromolecules* **1986**, 19, 1828-1838.
  23. Burger, B. J.; Bercaw, J. E. *New Developments in the Synthesis, Manipulation and Characterization of Organometallic Compounds*; Wayda, A.L., Darensbourg, M.Y., Eds.; American Chemical Society: Washington D.C., 1987.
  24. a) Evans, D. F. *J. Chem. Soc.* **1959**, 2003-2005. b) Schubert, E. M. *J. Chem. Educ.* **1992**, 69, 62.
  25. Britovsek, G. J. P.; Gibson, V. C.; Spitzmesser, S. K.; Tellmann, K. P.; White, A. J. P.; Williams, D. J. *J. Chem. Soc., Dalton Trans.* **2002**, 1159-1171.
  26. Stoll, S.; Schweiger, A. *J. Magn. Reson.* **2006**, 178, 42-55.

## Appendix A: X-ray Crystal Structure Data

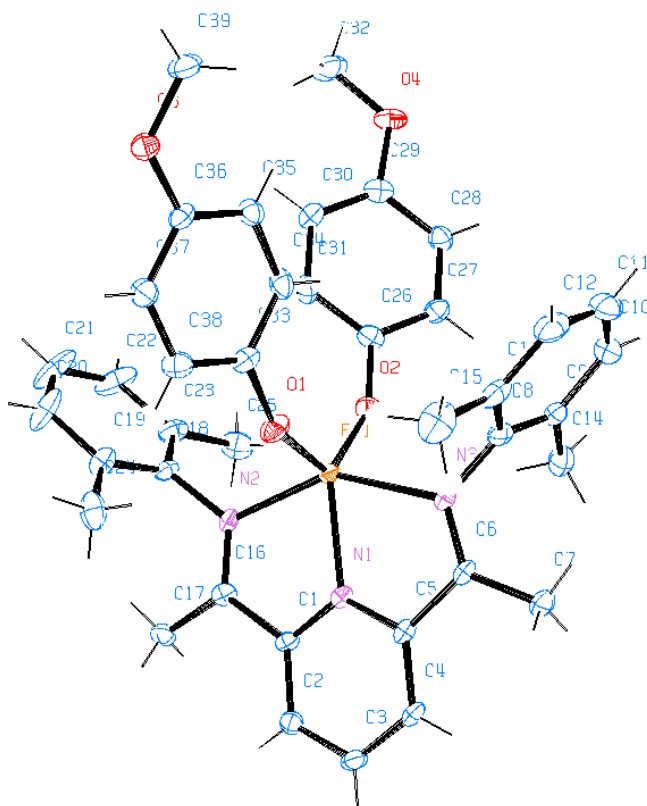
### A.1 X-ray crystal structure data from Chapter 2

**Table A.1.** Crystal data and structure refinement for [Fe(PDI)(4-methoxyphenoxide)<sub>2</sub>]<sup>+</sup>PF<sub>6</sub><sup>-</sup> (**2.5**)

Identification code	C <sub>45</sub> H <sub>47</sub> F <sub>6</sub> FeN <sub>3</sub> O <sub>4</sub> P
Empirical formula	C <sub>45</sub> H <sub>47</sub> F <sub>6</sub> FeN <sub>3</sub> O <sub>4</sub> P
Formula weight	894.67
Temperature	100(2) K
Wavelength	1.54178 Å
Crystal system	Monoclinic
Space group	P 21/c
Unit cell dimensions	a = 24.1694(15) Å    α = 90°. b = 11.6266(9) Å    β = 102.859(4)°. c = 15.5172(9) Å    γ = 90°.
Volume	4251.1(5) Å <sup>3</sup>
Z	4
Density (calculated)	1.398 Mg/m <sup>3</sup>
Absorption coefficient	3.828 mm <sup>-1</sup>
F(000)	1860
Crystal size	0.100 x 0.020 x 0.010 mm <sup>3</sup>
Theta range for data collection	1.875 to 67.381°.
Index ranges	-28 ≤ h ≤ 28, -13 ≤ k ≤ 13, -18 ≤ l ≤ 14
Reflections collected	23734
Independent reflections	7213 [R(int) = 0.1156]
Completeness to theta = 67.679°	93.8 %
Absorption correction	Semi-empirical from equivalents
Max. and min. transmission	0.7532 and 0.4680
Refinement method	Full-matrix least-squares on F <sup>2</sup>
Data / restraints / parameters	7213 / 168 / 549
Goodness-of-fit on F <sup>2</sup>	0.993
Final R indices [I > 2σ(I)]	R1 = 0.0571, wR2 = 0.1250
R indices (all data)	R1 = 0.0970, wR2 = 0.1449
Largest diff. peak and hole	0.879 and -0.458 e.Å <sup>-3</sup>



**Table A.2.** Bond lengths [Å] and angles [°] for [Fe(PDI)(4-methoxyphenoxide)<sub>2</sub>]<sup>+</sup>PF<sub>6</sub><sup>-</sup> (2.5)



Fe(1)-O(1)	1.816(3)	C(7)-H(7C)	0.9800
Fe(1)-O(2)	1.820(3)	C(8)-C(13)	1.386(6)
Fe(1)-N(1)	2.089(3)	C(8)-C(9)	1.398(6)
Fe(1)-N(2)	2.172(3)	C(9)-C(10)	1.394(5)
Fe(1)-N(3)	2.197(3)	C(9)-C(14)	1.500(6)
O(1)-C(33)	1.348(5)	C(10)-C(11)	1.389(7)
O(2)-C(26)	1.350(5)	C(10)-H(10)	0.9500
O(3)-C(36)	1.380(5)	C(11)-C(12)	1.367(7)
O(3)-C(39)	1.426(5)	C(11)-H(11)	0.9500
O(4)-C(29)	1.390(5)	C(12)-C(13)	1.406(6)
O(4)-C(32)	1.418(6)	C(12)-H(12)	0.9500
N(1)-C(1)	1.339(4)	C(13)-C(15)	1.496(7)
N(1)-C(5)	1.341(5)	C(14)-H(14A)	0.9800

---

N(2)-C(16)	1.283(5)	C(14)-H(14B)	0.9800
N(2)-C(18)	1.449(5)	C(14)-H(14C)	0.9800
N(3)-C(6)	1.275(5)	C(15)-H(15A)	0.9800
N(3)-C(8)	1.442(4)	C(15)-H(15B)	0.9800
C(1)-C(2)	1.378(5)	C(15)-H(15C)	0.9800
C(1)-C(16)	1.495(5)	C(16)-C(17)	1.493(5)
C(2)-C(3)	1.378(6)	C(17)-H(17A)	0.9800
C(2)-H(2)	0.9500	C(17)-H(17B)	0.9800
C(3)-C(4)	1.390(5)	C(17)-H(17C)	0.9800
C(3)-H(3)	0.9500	C(18)-C(19)	1.388(6)
C(4)-C(5)	1.379(5)	C(18)-C(23)	1.390(6)
C(4)-H(4)	0.9500	C(19)-C(20)	1.385(6)
C(5)-C(6)	1.487(5)	C(19)-C(24)	1.499(6)
C(6)-C(7)	1.489(5)	C(20)-C(21)	1.378(8)
C(7)-H(7A)	0.9800	C(20)-H(20)	0.9500
C(7)-H(7B)	0.9800	C(21)-C(22)	1.363(8)
C(21)-H(21)	0.9500	C(39)-H(39C)	0.9800
C(22)-C(23)	1.396(6)	P(1)-F(6)	1.584(3)
C(22)-H(22)	0.9500	P(1)-F(3)	1.587(3)
C(23)-C(25)	1.503(6)	P(1)-F(1)	1.593(2)
C(24)-H(24A)	0.9800	P(1)-F(2)	1.602(2)
C(24)-H(24B)	0.9800	P(1)-F(4)	1.604(3)
C(24)-H(24C)	0.9800	P(1)-F(5)	1.606(3)
C(25)-H(25A)	0.9800	C(1S)-C(6S)	1.379(7)
C(25)-H(25B)	0.9800	C(1S)-C(2S)	1.383(7)
C(25)-H(25C)	0.9800	C(1S)-H(1S)	0.9500
C(26)-C(27)	1.385(6)	C(2S)-C(3S)	1.367(7)
C(26)-C(31)	1.387(6)	C(2S)-H(2S)	0.9500
C(27)-C(28)	1.378(5)	C(3S)-C(4S)	1.379(7)
C(27)-H(27)	0.9500	C(3S)-H(3S)	0.9500
C(28)-C(29)	1.385(6)	C(4S)-C(5S)	1.363(7)
C(28)-H(28)	0.9500	C(4S)-H(4S)	0.9500
C(29)-C(30)	1.372(6)	C(5S)-C(6S)	1.369(7)
C(30)-C(31)	1.395(6)	C(5S)-H(5S)	0.9500
C(30)-H(30)	0.9500	C(6S)-H(6S)	0.9500

---

---

C(31)-H(31)	0.9500		
C(32)-H(32A)	0.9800	O(1)-Fe(1)-O(2)	118.30(13)
C(32)-H(32B)	0.9800	O(1)-Fe(1)-N(1)	116.09(12)
C(32)-H(32C)	0.9800	O(2)-Fe(1)-N(1)	125.58(13)
C(33)-C(38)	1.388(6)	O(1)-Fe(1)-N(2)	97.28(12)
C(33)-C(34)	1.394(5)	O(2)-Fe(1)-N(2)	100.77(12)
C(34)-C(35)	1.386(6)	N(1)-Fe(1)-N(2)	73.73(11)
C(34)-H(34)	0.9500	O(1)-Fe(1)-N(3)	99.38(12)
C(35)-C(36)	1.391(6)	O(2)-Fe(1)-N(3)	96.03(12)
C(35)-H(35)	0.9500	N(1)-Fe(1)-N(3)	73.43(11)
C(36)-C(37)	1.383(5)	N(2)-Fe(1)-N(3)	147.05(11)
C(37)-C(38)	1.393(6)	C(33)-O(1)-Fe(1)	148.7(3)
C(37)-H(37)	0.9500	C(26)-O(2)-Fe(1)	144.8(3)
C(38)-H(38)	0.9500	C(36)-O(3)-C(39)	117.6(3)
C(39)-H(39A)	0.9800	C(29)-O(4)-C(32)	116.4(3)
C(39)-H(39B)	0.9800	C(1)-N(1)-C(5)	119.8(3)
C(1)-N(1)-Fe(1)	120.2(2)	C(10)-C(9)-C(8)	117.4(4)
C(5)-N(1)-Fe(1)	120.0(2)	C(10)-C(9)-C(14)	120.6(4)
C(16)-N(2)-C(18)	120.6(3)	C(8)-C(9)-C(14)	121.9(3)
C(16)-N(2)-Fe(1)	118.2(3)	C(11)-C(10)-C(9)	120.4(4)
C(18)-N(2)-Fe(1)	120.9(2)	C(11)-C(10)-H(10)	119.8
C(6)-N(3)-C(8)	120.8(3)	C(9)-C(10)-H(10)	119.8
C(6)-N(3)-Fe(1)	117.9(2)	C(12)-C(11)-C(10)	120.7(4)
C(8)-N(3)-Fe(1)	121.2(2)	C(12)-C(11)-H(11)	119.7
N(1)-C(1)-C(2)	121.6(3)	C(10)-C(11)-H(11)	119.7
N(1)-C(1)-C(16)	112.8(3)	C(11)-C(12)-C(13)	121.2(4)
C(2)-C(1)-C(16)	125.6(3)	C(11)-C(12)-H(12)	119.4
C(1)-C(2)-C(3)	118.9(3)	C(13)-C(12)-H(12)	119.4
C(1)-C(2)-H(2)	120.6	C(8)-C(13)-C(12)	116.9(4)
C(3)-C(2)-H(2)	120.6	C(8)-C(13)-C(15)	121.4(4)
C(2)-C(3)-C(4)	119.6(3)	C(12)-C(13)-C(15)	121.5(4)
C(2)-C(3)-H(3)	120.2	C(9)-C(14)-H(14A)	109.5
C(4)-C(3)-H(3)	120.2	C(9)-C(14)-H(14B)	109.5
C(5)-C(4)-C(3)	118.5(3)	H(14A)-C(14)-H(14B)	109.5
C(5)-C(4)-H(4)	120.8	C(9)-C(14)-H(14C)	109.5

---

---

C(3)-C(4)-H(4)	120.8	H(14A)-C(14)-H(14C)	109.5
N(1)-C(5)-C(4)	121.6(3)	H(14B)-C(14)-H(14C)	109.5
N(1)-C(5)-C(6)	113.4(3)	C(13)-C(15)-H(15A)	109.5
C(4)-C(5)-C(6)	124.9(3)	C(13)-C(15)-H(15B)	109.5
N(3)-C(6)-C(5)	115.1(3)	H(15A)-C(15)-H(15B)	109.5
N(3)-C(6)-C(7)	126.0(3)	C(13)-C(15)-H(15C)	109.5
C(5)-C(6)-C(7)	118.9(3)	H(15A)-C(15)-H(15C)	109.5
C(6)-C(7)-H(7A)	109.5	H(15B)-C(15)-H(15C)	109.5
C(6)-C(7)-H(7B)	109.5	N(2)-C(16)-C(17)	125.9(3)
H(7A)-C(7)-H(7B)	109.5	N(2)-C(16)-C(1)	115.0(3)
C(6)-C(7)-H(7C)	109.5	C(17)-C(16)-C(1)	119.1(3)
H(7A)-C(7)-H(7C)	109.5	C(16)-C(17)-H(17A)	109.5
H(7B)-C(7)-H(7C)	109.5	C(16)-C(17)-H(17B)	109.5
C(13)-C(8)-C(9)	123.3(4)	H(17A)-C(17)-H(17B)	109.5
C(13)-C(8)-N(3)	119.4(4)	C(16)-C(17)-H(17C)	109.5
C(9)-C(8)-N(3)	117.3(3)	H(17A)-C(17)-H(17C)	109.5
H(17B)-C(17)-H(17C)	109.5	C(28)-C(27)-H(27)	119.7
C(19)-C(18)-C(23)	123.0(4)	C(26)-C(27)-H(27)	119.7
C(19)-C(18)-N(2)	116.6(3)	C(27)-C(28)-C(29)	120.2(4)
C(23)-C(18)-N(2)	120.3(3)	C(27)-C(28)-H(28)	119.9
C(20)-C(19)-C(18)	117.7(4)	C(29)-C(28)-H(28)	119.9
C(20)-C(19)-C(24)	120.6(4)	C(30)-C(29)-C(28)	120.1(4)
C(18)-C(19)-C(24)	121.6(4)	C(30)-C(29)-O(4)	124.8(4)
C(21)-C(20)-C(19)	120.4(4)	C(28)-C(29)-O(4)	115.1(4)
C(21)-C(20)-H(20)	119.8	C(29)-C(30)-C(31)	119.7(4)
C(19)-C(20)-H(20)	119.8	C(29)-C(30)-H(30)	120.2
C(22)-C(21)-C(20)	121.0(4)	C(31)-C(30)-H(30)	120.2
C(22)-C(21)-H(21)	119.5	C(26)-C(31)-C(30)	120.4(4)
C(20)-C(21)-H(21)	119.5	C(26)-C(31)-H(31)	119.8
C(21)-C(22)-C(23)	121.0(5)	C(30)-C(31)-H(31)	119.8
C(21)-C(22)-H(22)	119.5	O(4)-C(32)-H(32A)	109.5
C(23)-C(22)-H(22)	119.5	O(4)-C(32)-H(32B)	109.5
C(18)-C(23)-C(22)	117.0(4)	H(32A)-C(32)-H(32B)	109.5
C(18)-C(23)-C(25)	122.0(4)	O(4)-C(32)-H(32C)	109.5
C(22)-C(23)-C(25)	121.0(4)	H(32A)-C(32)-H(32C)	109.5

---

---

C(19)-C(24)-H(24A)	109.5	H(32B)-C(32)-H(32C)	109.5
C(19)-C(24)-H(24B)	109.5	O(1)-C(33)-C(38)	119.1(3)
H(24A)-C(24)-H(24B)	109.5	O(1)-C(33)-C(34)	121.9(4)
C(19)-C(24)-H(24C)	109.5	C(38)-C(33)-C(34)	119.0(4)
H(24A)-C(24)-H(24C)	109.5	C(35)-C(34)-C(33)	120.7(4)
H(24B)-C(24)-H(24C)	109.5	C(35)-C(34)-H(34)	119.7
C(23)-C(25)-H(25A)	109.5	C(33)-C(34)-H(34)	119.7
C(23)-C(25)-H(25B)	109.5	C(34)-C(35)-C(36)	119.5(4)
H(25A)-C(25)-H(25B)	109.5	C(34)-C(35)-H(35)	120.2
C(23)-C(25)-H(25C)	109.5	C(36)-C(35)-H(35)	120.2
H(25A)-C(25)-H(25C)	109.5	O(3)-C(36)-C(37)	115.3(4)
H(25B)-C(25)-H(25C)	109.5	O(3)-C(36)-C(35)	124.2(3)
O(2)-C(26)-C(27)	119.3(4)	C(37)-C(36)-C(35)	120.5(4)
O(2)-C(26)-C(31)	121.7(4)	C(36)-C(37)-C(38)	119.5(4)
C(27)-C(26)-C(31)	119.0(4)	C(36)-C(37)-H(37)	120.2
C(28)-C(27)-C(26)	120.5(4)	C(38)-C(37)-H(37)	120.2
C(33)-C(38)-C(37)	120.7(4)	C(3S)-C(4S)-H(4S)	119.6
C(33)-C(38)-H(38)	119.6	C(4S)-C(5S)-C(6S)	119.6(5)
C(37)-C(38)-H(38)	119.6	C(4S)-C(5S)-H(5S)	120.2
O(3)-C(39)-H(39A)	109.5	C(6S)-C(5S)-H(5S)	120.2
O(3)-C(39)-H(39B)	109.5	C(5S)-C(6S)-C(1S)	119.9(4)
H(39A)-C(39)-H(39B)	109.5	C(5S)-C(6S)-H(6S)	120.0
O(3)-C(39)-H(39C)	109.5	C(1S)-C(6S)-H(6S)	120.0
H(39A)-C(39)-H(39C)	109.5		
H(39B)-C(39)-H(39C)	109.5		
F(6)-P(1)-F(3)	90.63(16)		
F(6)-P(1)-F(1)	90.45(15)		
F(3)-P(1)-F(1)	178.34(16)		
F(6)-P(1)-F(2)	90.86(15)		
F(3)-P(1)-F(2)	90.62(15)		
F(1)-P(1)-F(2)	90.63(15)		
F(6)-P(1)-F(4)	90.56(15)		
F(3)-P(1)-F(4)	89.20(15)		
F(1)-P(1)-F(4)	89.53(14)		
F(2)-P(1)-F(4)	178.56(16)		

---

---

F(6)-P(1)-F(5)	179.72(17)
F(3)-P(1)-F(5)	89.63(15)
F(1)-P(1)-F(5)	89.29(14)
F(2)-P(1)-F(5)	89.25(14)
F(4)-P(1)-F(5)	89.33(14)
C(6S)-C(1S)-C(2S)	120.5(5)
C(6S)-C(1S)-H(1S)	119.8
C(2S)-C(1S)-H(1S)	119.8
C(3S)-C(2S)-C(1S)	119.0(5)
C(3S)-C(2S)-H(2S)	120.5
C(1S)-C(2S)-H(2S)	120.5
C(2S)-C(3S)-C(4S)	120.1(5)
C(2S)-C(3S)-H(3S)	119.9
C(4S)-C(3S)-H(3S)	119.9
C(5S)-C(4S)-C(3S)	120.8(5)
C(5S)-C(4S)-H(4S)	119.6

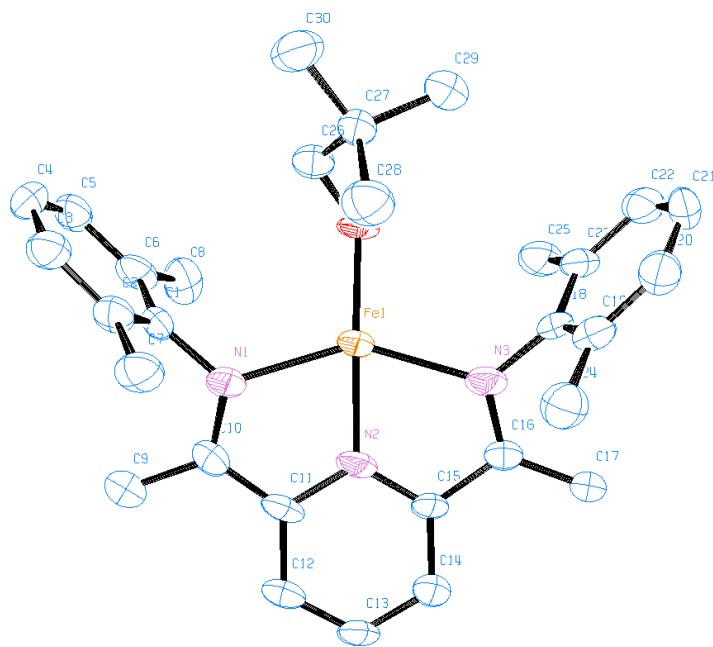
---

## A.2 X-ray crystal structure data from Chapter 4

**Table A.3.** Crystal data and structure refinement for Fe(PDI)(neopentoxide) (4.1b)

Identification code	C <sub>30</sub> H <sub>38</sub> FeN <sub>3</sub> O
Empirical formula	C <sub>30</sub> H <sub>38</sub> Fe N <sub>3</sub> O
Formula weight	512.48
Temperature	100(2) K
Wavelength	1.54178 Å
Crystal system	Triclinic
Space group	P-1
Unit cell dimensions	a = 9.6160(6) Å      α = 80.409(4)°. b = 15.1762(8) Å      β = 89.607(4)°. c = 18.9657(11) Å      γ = 89.916(4)°.
Volume	2729.0(3) Å <sup>3</sup>
Z	4
Density (calculated)	1.247 Mg/m <sup>3</sup>
Absorption coefficient	4.624 mm <sup>-1</sup>
F(000)	1092
Crystal size	0.200 x 0.080 x 0.070 mm <sup>3</sup>
Theta range for data collection	2.363 to 67.771°.
Index ranges	-11 ≤ h ≤ 11, -18 ≤ k ≤ 18, -21 ≤ l ≤ 22
Reflections collected	31006
Independent reflections	9543 [R(int) = 0.0732]
Completeness to theta = 67.679°	98.4 %
Absorption correction	Semi-empirical from equivalents
Max. and min. transmission	0.7528 and 0.4940
Refinement method	Full-matrix least-squares on F <sup>2</sup>
Data / restraints / parameters	9543 / 0 / 650
Goodness-of-fit on F <sup>2</sup>	1.230
Final R indices [I > 2σ(I)]	R1 = 0.1087, wR2 = 0.2768
R indices (all data)	R1 = 0.1365, wR2 = 0.3238
Largest diff. peak and hole	2.156 and -1.485 e.Å <sup>-3</sup>

**Table A.4.** Bond lengths [ $\text{\AA}$ ] and angles [ $^\circ$ ] for Fe(PDI)(neopentoxide) (**4.1b**)



Fe(1)-O(1)	1.842(5)	C(13)-C(14)	1.377(13)
Fe(1)-N(2)	1.991(7)	C(13)-H(13)	0.9500
Fe(1)-N(1)	2.143(7)	C(14)-C(15)	1.405(12)
Fe(1)-N(3)	2.147(8)	C(14)-H(14)	0.9500
O(1)-C(26)	1.411(11)	C(15)-C(16)	1.459(12)
N(1)-C(10)	1.309(12)	C(16)-C(17)	1.473(12)
N(1)-C(1)	1.428(10)	C(17)-H(17A)	0.9800
N(2)-C(15)	1.356(11)	C(17)-H(17B)	0.9800
N(2)-C(11)	1.378(12)	C(17)-H(17C)	0.9800
N(3)-C(16)	1.326(11)	C(18)-C(19)	1.394(15)
N(3)-C(18)	1.439(12)	C(18)-C(23)	1.401(13)
C(1)-C(6)	1.395(13)	C(19)-C(20)	1.371(15)
C(1)-C(2)	1.398(13)	C(19)-C(24)	1.487(15)
C(2)-C(3)	1.387(13)	C(20)-C(21)	1.415(16)
C(2)-C(7)	1.512(13)	C(20)-H(20)	0.9500
C(3)-C(4)	1.397(14)	C(21)-C(22)	1.350(18)
C(3)-H(3)	0.9500	C(21)-H(21)	0.9500
C(4)-C(5)	1.366(14)	C(22)-C(23)	1.398(15)



---

C(4)-H(4)	0.9500	C(22)-H(22)	0.9500
C(5)-C(6)	1.394(13)	C(23)-C(25)	1.493(16)
C(5)-H(5)	0.9500	C(24)-H(24A)	0.9800
C(6)-C(8)	1.529(13)	C(24)-H(24B)	0.9800
C(7)-H(7A)	0.9800	C(24)-H(24C)	0.9800
C(7)-H(7B)	0.9800	C(25)-H(25A)	0.9800
C(7)-H(7C)	0.9800	C(25)-H(25B)	0.9800
C(8)-H(8A)	0.9800	C(25)-H(25C)	0.9800
C(8)-H(8B)	0.9800	C(26)-C(27)	1.526(16)
C(8)-H(8C)	0.9800	C(26)-H(26A)	0.9900
C(9)-C(10)	1.475(14)	C(26)-H(26B)	0.9900
C(9)-H(9A)	0.9800	C(27)-C(29)	1.505(13)
C(9)-H(9B)	0.9800	C(27)-C(28)	1.523(13)
C(9)-H(9C)	0.9800	C(27)-C(30)	1.547(13)
C(10)-C(11)	1.420(13)	C(28)-H(28A)	0.9800
C(11)-C(12)	1.415(12)	C(28)-H(28B)	0.9800
C(12)-H(12)	0.9500	C(28)-H(28C)	0.9800
C(29)-H(29A)	0.9800	C(39)-H(39A)	0.9800
C(29)-H(29B)	0.9800	C(39)-H(39B)	0.9800
C(29)-H(29C)	0.9800	C(39)-H(39C)	0.9800
C(30)-H(30A)	0.9800	C(40)-C(41)	1.453(13)
C(30)-H(30B)	0.9800	C(41)-C(42)	1.365(12)
C(30)-H(30C)	0.9800	C(42)-C(43)	1.378(15)
Fe(2)-O(2)	1.811(7)	C(42)-H(42)	0.9500
Fe(2)-N(5)	1.985(7)	C(43)-C(44)	1.379(15)
Fe(2)-N(6)	2.144(7)	C(43)-H(43)	0.9500
Fe(2)-N(4)	2.147(7)	C(44)-C(45)	1.393(12)
O(2)-C(56)	1.393(12)	C(44)-H(44)	0.9500
N(4)-C(40)	1.304(11)	C(45)-C(46)	1.437(13)
N(4)-C(31)	1.455(11)	C(46)-C(47)	1.516(13)
N(5)-C(45)	1.369(13)	C(47)-H(47A)	0.9800
N(5)-C(41)	1.385(12)	C(47)-H(47B)	0.9800
N(6)-C(46)	1.323(11)	C(47)-H(47C)	0.9800
N(6)-C(48)	1.428(12)	C(48)-C(53)	1.403(13)
C(31)-C(36)	1.369(15)	C(48)-C(49)	1.409(13)

---

C(31)-C(32)	1.413(13)	C(49)-C(50)	1.396(13)
C(32)-C(33)	1.393(15)	C(49)-C(54)	1.501(13)
C(32)-C(37)	1.508(17)	C(50)-C(51)	1.394(15)
C(33)-C(34)	1.390(18)	C(50)-H(50)	0.9500
C(33)-H(33)	0.9500	C(51)-C(52)	1.349(15)
C(34)-C(35)	1.359(15)	C(51)-H(51)	0.9500
C(34)-H(34)	0.9500	C(52)-C(53)	1.399(14)
C(35)-C(36)	1.398(16)	C(52)-H(52)	0.9500
C(35)-H(35)	0.9500	C(53)-C(55)	1.491(14)
C(36)-C(38)	1.528(14)	C(54)-H(54A)	0.9800
C(37)-H(37A)	0.9800	C(54)-H(54B)	0.9800
C(37)-H(37B)	0.9800	C(54)-H(54C)	0.9800
C(37)-H(37C)	0.9800	C(55)-H(55A)	0.9800
C(38)-H(38A)	0.9800	C(55)-H(55B)	0.9800
C(38)-H(38B)	0.9800	C(55)-H(55C)	0.9800
C(38)-H(38C)	0.9800	C(56)-C(57)	1.540(12)
C(39)-C(40)	1.511(13)	C(56)-H(56A)	0.9900
C(56)-H(56B)	0.9900	C(1)-C(2)-C(7)	120.8(8)
C(57)-C(60)	1.491(17)	C(2)-C(3)-C(4)	119.0(9)
C(57)-C(59)	1.504(18)	C(2)-C(3)-H(3)	120.5
C(57)-C(58)	1.544(16)	C(4)-C(3)-H(3)	120.5
C(58)-H(58A)	0.9800	C(5)-C(4)-C(3)	121.1(8)
C(58)-H(58B)	0.9800	C(5)-C(4)-H(4)	119.4
C(58)-H(58C)	0.9800	C(3)-C(4)-H(4)	119.4
C(59)-H(59A)	0.9800	C(4)-C(5)-C(6)	120.7(9)
C(59)-H(59B)	0.9800	C(4)-C(5)-H(5)	119.6
C(59)-H(59C)	0.9800	C(6)-C(5)-H(5)	119.6
C(60)-H(60A)	0.9800	C(5)-C(6)-C(1)	118.6(9)
C(60)-H(60B)	0.9800	C(5)-C(6)-C(8)	120.7(9)
C(60)-H(60C)	0.9800	C(1)-C(6)-C(8)	120.7(9)
		C(2)-C(7)-H(7A)	109.5
O(1)-Fe(1)-N(2)	163.7(3)	C(2)-C(7)-H(7B)	109.5
O(1)-Fe(1)-N(1)	107.8(3)	H(7A)-C(7)-H(7B)	109.5
N(2)-Fe(1)-N(1)	75.3(3)	C(2)-C(7)-H(7C)	109.5
O(1)-Fe(1)-N(3)	105.3(3)	H(7A)-C(7)-H(7C)	109.5

---

N(2)-Fe(1)-N(3)	75.6(3)	H(7B)-C(7)-H(7C)	109.5
N(1)-Fe(1)-N(3)	145.6(3)	C(6)-C(8)-H(8A)	109.5
C(26)-O(1)-Fe(1)	131.9(5)	C(6)-C(8)-H(8B)	109.5
C(10)-N(1)-C(1)	120.4(8)	H(8A)-C(8)-H(8B)	109.5
C(10)-N(1)-Fe(1)	115.7(6)	C(6)-C(8)-H(8C)	109.5
C(1)-N(1)-Fe(1)	122.2(5)	H(8A)-C(8)-H(8C)	109.5
C(15)-N(2)-C(11)	119.2(7)	H(8B)-C(8)-H(8C)	109.5
C(15)-N(2)-Fe(1)	120.2(6)	C(10)-C(9)-H(9A)	109.5
C(11)-N(2)-Fe(1)	119.8(6)	C(10)-C(9)-H(9B)	109.5
C(16)-N(3)-C(18)	120.0(7)	H(9A)-C(9)-H(9B)	109.5
C(16)-N(3)-Fe(1)	115.1(6)	C(10)-C(9)-H(9C)	109.5
C(18)-N(3)-Fe(1)	124.1(5)	H(9A)-C(9)-H(9C)	109.5
C(6)-C(1)-C(2)	120.7(8)	H(9B)-C(9)-H(9C)	109.5
C(6)-C(1)-N(1)	119.5(8)	N(1)-C(10)-C(11)	115.1(8)
C(2)-C(1)-N(1)	119.8(8)	N(1)-C(10)-C(9)	122.6(8)
C(3)-C(2)-C(1)	119.9(8)	C(11)-C(10)-C(9)	122.3(8)
C(3)-C(2)-C(7)	119.2(9)	N(2)-C(11)-C(12)	120.1(9)
N(2)-C(11)-C(10)	113.1(7)	C(21)-C(22)-C(23)	121.2(10)
C(12)-C(11)-C(10)	126.8(9)	C(21)-C(22)-H(22)	119.4
C(13)-C(12)-C(11)	119.4(9)	C(23)-C(22)-H(22)	119.4
C(13)-C(12)-H(12)	120.3	C(22)-C(23)-C(18)	117.2(11)
C(11)-C(12)-H(12)	120.3	C(22)-C(23)-C(25)	120.9(9)
C(14)-C(13)-C(12)	120.3(8)	C(18)-C(23)-C(25)	121.9(9)
C(14)-C(13)-H(13)	119.9	C(19)-C(24)-H(24A)	109.5
C(12)-C(13)-H(13)	119.9	C(19)-C(24)-H(24B)	109.5
C(13)-C(14)-C(15)	119.1(8)	H(24A)-C(24)-H(24B)	109.5
C(13)-C(14)-H(14)	120.5	C(19)-C(24)-H(24C)	109.5
C(15)-C(14)-H(14)	120.5	H(24A)-C(24)-H(24C)	109.5
N(2)-C(15)-C(14)	121.5(8)	H(24B)-C(24)-H(24C)	109.5
N(2)-C(15)-C(16)	113.5(7)	C(23)-C(25)-H(25A)	109.5
C(14)-C(15)-C(16)	124.9(8)	C(23)-C(25)-H(25B)	109.5
N(3)-C(16)-C(15)	113.4(7)	H(25A)-C(25)-H(25B)	109.5
N(3)-C(16)-C(17)	125.1(8)	C(23)-C(25)-H(25C)	109.5
C(15)-C(16)-C(17)	121.3(7)	H(25A)-C(25)-H(25C)	109.5
C(16)-C(17)-H(17A)	109.5	H(25B)-C(25)-H(25C)	109.5

---

C(16)-C(17)-H(17B)	109.5	O(1)-C(26)-C(27)	114.3(8)
H(17A)-C(17)-H(17B)	109.5	O(1)-C(26)-H(26A)	108.7
C(16)-C(17)-H(17C)	109.5	C(27)-C(26)-H(26A)	108.7
H(17A)-C(17)-H(17C)	109.5	O(1)-C(26)-H(26B)	108.7
H(17B)-C(17)-H(17C)	109.5	C(27)-C(26)-H(26B)	108.7
C(19)-C(18)-C(23)	122.4(9)	H(26A)-C(26)-H(26B)	107.6
C(19)-C(18)-N(3)	119.3(8)	C(29)-C(27)-C(28)	109.5(8)
C(23)-C(18)-N(3)	118.2(9)	C(29)-C(27)-C(26)	110.0(8)
C(20)-C(19)-C(18)	118.5(10)	C(28)-C(27)-C(26)	111.0(8)
C(20)-C(19)-C(24)	120.8(10)	C(29)-C(27)-C(30)	109.2(8)
C(18)-C(19)-C(24)	120.7(9)	C(28)-C(27)-C(30)	109.0(9)
C(19)-C(20)-C(21)	119.8(11)	C(26)-C(27)-C(30)	108.2(8)
C(19)-C(20)-H(20)	120.1	C(27)-C(28)-H(28A)	109.5
C(21)-C(20)-H(20)	120.1	C(27)-C(28)-H(28B)	109.5
C(22)-C(21)-C(20)	120.8(10)	H(28A)-C(28)-H(28B)	109.5
C(22)-C(21)-H(21)	119.6	C(27)-C(28)-H(28C)	109.5
C(20)-C(21)-H(21)	119.6	H(28A)-C(28)-H(28C)	109.5
H(28B)-C(28)-H(28C)	109.5	C(34)-C(33)-C(32)	121.6(10)
C(27)-C(29)-H(29A)	109.5	C(34)-C(33)-H(33)	119.2
C(27)-C(29)-H(29B)	109.5	C(32)-C(33)-H(33)	119.2
H(29A)-C(29)-H(29B)	109.5	C(35)-C(34)-C(33)	119.1(11)
C(27)-C(29)-H(29C)	109.5	C(35)-C(34)-H(34)	120.4
H(29A)-C(29)-H(29C)	109.5	C(33)-C(34)-H(34)	120.4
H(29B)-C(29)-H(29C)	109.5	C(34)-C(35)-C(36)	121.7(12)
C(27)-C(30)-H(30A)	109.5	C(34)-C(35)-H(35)	119.2
C(27)-C(30)-H(30B)	109.5	C(36)-C(35)-H(35)	119.2
H(30A)-C(30)-H(30B)	109.5	C(31)-C(36)-C(35)	118.8(10)
C(27)-C(30)-H(30C)	109.5	C(31)-C(36)-C(38)	121.3(10)
H(30A)-C(30)-H(30C)	109.5	C(35)-C(36)-C(38)	119.9(10)
H(30B)-C(30)-H(30C)	109.5	C(32)-C(37)-H(37A)	109.5
O(2)-Fe(2)-N(5)	148.8(3)	C(32)-C(37)-H(37B)	109.5
O(2)-Fe(2)-N(6)	106.7(3)	H(37A)-C(37)-H(37B)	109.5
N(5)-Fe(2)-N(6)	75.8(3)	C(32)-C(37)-H(37C)	109.5
O(2)-Fe(2)-N(4)	109.6(3)	H(37A)-C(37)-H(37C)	109.5
N(5)-Fe(2)-N(4)	75.6(3)	H(37B)-C(37)-H(37C)	109.5

---

N(6)-Fe(2)-N(4)	143.5(3)	C(36)-C(38)-H(38A)	109.5
C(56)-O(2)-Fe(2)	137.1(7)	C(36)-C(38)-H(38B)	109.5
C(40)-N(4)-C(31)	119.3(7)	H(38A)-C(38)-H(38B)	109.5
C(40)-N(4)-Fe(2)	116.2(6)	C(36)-C(38)-H(38C)	109.5
C(31)-N(4)-Fe(2)	123.2(5)	H(38A)-C(38)-H(38C)	109.5
C(45)-N(5)-C(41)	120.2(8)	H(38B)-C(38)-H(38C)	109.5
C(45)-N(5)-Fe(2)	119.7(6)	C(40)-C(39)-H(39A)	109.5
C(41)-N(5)-Fe(2)	119.8(6)	C(40)-C(39)-H(39B)	109.5
C(46)-N(6)-C(48)	119.1(7)	H(39A)-C(39)-H(39B)	109.5
C(46)-N(6)-Fe(2)	114.6(6)	C(40)-C(39)-H(39C)	109.5
C(48)-N(6)-Fe(2)	125.5(6)	H(39A)-C(39)-H(39C)	109.5
C(36)-C(31)-C(32)	121.5(9)	H(39B)-C(39)-H(39C)	109.5
C(36)-C(31)-N(4)	120.1(8)	N(4)-C(40)-C(41)	114.5(8)
C(32)-C(31)-N(4)	118.3(9)	N(4)-C(40)-C(39)	123.7(8)
C(33)-C(32)-C(31)	117.3(10)	C(41)-C(40)-C(39)	121.9(8)
C(33)-C(32)-C(37)	122.3(9)	C(42)-C(41)-N(5)	119.7(9)
C(31)-C(32)-C(37)	120.4(9)	C(42)-C(41)-C(40)	127.3(8)
N(5)-C(41)-C(40)	112.9(7)	C(51)-C(52)-H(52)	118.9
C(41)-C(42)-C(43)	120.2(9)	C(53)-C(52)-H(52)	118.9
C(41)-C(42)-H(42)	119.9	C(52)-C(53)-C(48)	118.7(9)
C(43)-C(42)-H(42)	119.9	C(52)-C(53)-C(55)	121.4(9)
C(42)-C(43)-C(44)	120.2(9)	C(48)-C(53)-C(55)	119.9(8)
C(42)-C(43)-H(43)	119.9	C(49)-C(54)-H(54A)	109.5
C(44)-C(43)-H(43)	119.9	C(49)-C(54)-H(54B)	109.5
C(43)-C(44)-C(45)	119.3(10)	H(54A)-C(54)-H(54B)	109.5
C(43)-C(44)-H(44)	120.3	C(49)-C(54)-H(54C)	109.5
C(45)-C(44)-H(44)	120.3	H(54A)-C(54)-H(54C)	109.5
N(5)-C(45)-C(44)	119.6(9)	H(54B)-C(54)-H(54C)	109.5
N(5)-C(45)-C(46)	113.1(7)	C(53)-C(55)-H(55A)	109.5
C(44)-C(45)-C(46)	127.2(9)	C(53)-C(55)-H(55B)	109.5
N(6)-C(46)-C(45)	115.1(8)	H(55A)-C(55)-H(55B)	109.5
N(6)-C(46)-C(47)	122.4(8)	C(53)-C(55)-H(55C)	109.5
C(45)-C(46)-C(47)	122.5(8)	H(55A)-C(55)-H(55C)	109.5
C(46)-C(47)-H(47A)	109.5	H(55B)-C(55)-H(55C)	109.5
C(46)-C(47)-H(47B)	109.5	O(2)-C(56)-C(57)	114.1(9)

---

H(47A)-C(47)-H(47B)	109.5	O(2)-C(56)-H(56A)	108.7
C(46)-C(47)-H(47C)	109.5	C(57)-C(56)-H(56A)	108.7
H(47A)-C(47)-H(47C)	109.5	O(2)-C(56)-H(56B)	108.7
H(47B)-C(47)-H(47C)	109.5	C(57)-C(56)-H(56B)	108.7
C(53)-C(48)-C(49)	120.3(8)	H(56A)-C(56)-H(56B)	107.6
C(53)-C(48)-N(6)	119.8(8)	C(60)-C(57)-C(59)	112.4(12)
C(49)-C(48)-N(6)	119.3(8)	C(60)-C(57)-C(56)	112.6(9)
C(50)-C(49)-C(48)	117.9(9)	C(59)-C(57)-C(56)	108.5(10)
C(50)-C(49)-C(54)	121.9(9)	C(60)-C(57)-C(58)	107.8(11)
C(48)-C(49)-C(54)	120.3(8)	C(59)-C(57)-C(58)	108.7(11)
C(51)-C(50)-C(49)	121.9(10)	C(56)-C(57)-C(58)	106.6(9)
C(51)-C(50)-H(50)	119.1	C(57)-C(58)-H(58A)	109.5
C(49)-C(50)-H(50)	119.1	C(57)-C(58)-H(58B)	109.5
C(52)-C(51)-C(50)	119.0(9)	H(58A)-C(58)-H(58B)	109.5
C(52)-C(51)-H(51)	120.5	C(57)-C(58)-H(58C)	109.5
C(50)-C(51)-H(51)	120.5	H(58A)-C(58)-H(58C)	109.5
C(51)-C(52)-C(53)	122.2(10)	H(58B)-C(58)-H(58C)	109.5
C(57)-C(59)-H(59A)	109.5		
C(57)-C(59)-H(59B)	109.5		
H(59A)-C(59)-H(59B)	109.5		
C(57)-C(59)-H(59C)	109.5		
H(59A)-C(59)-H(59C)	109.5		
H(59B)-C(59)-H(59C)	109.5		
C(57)-C(60)-H(60A)	109.5		
C(57)-C(60)-H(60B)	109.5		
H(60A)-C(60)-H(60B)	109.5		
C(57)-C(60)-H(60C)	109.5		
H(60A)-C(60)-H(60C)	109.5		
H(60B)-C(60)-H(60C)	109.5		

---

## Appendix B: NMR and $^{57}\text{Fe}$ Mössbauer Spectra

### B.1 NMR Spectra from Chapter 2

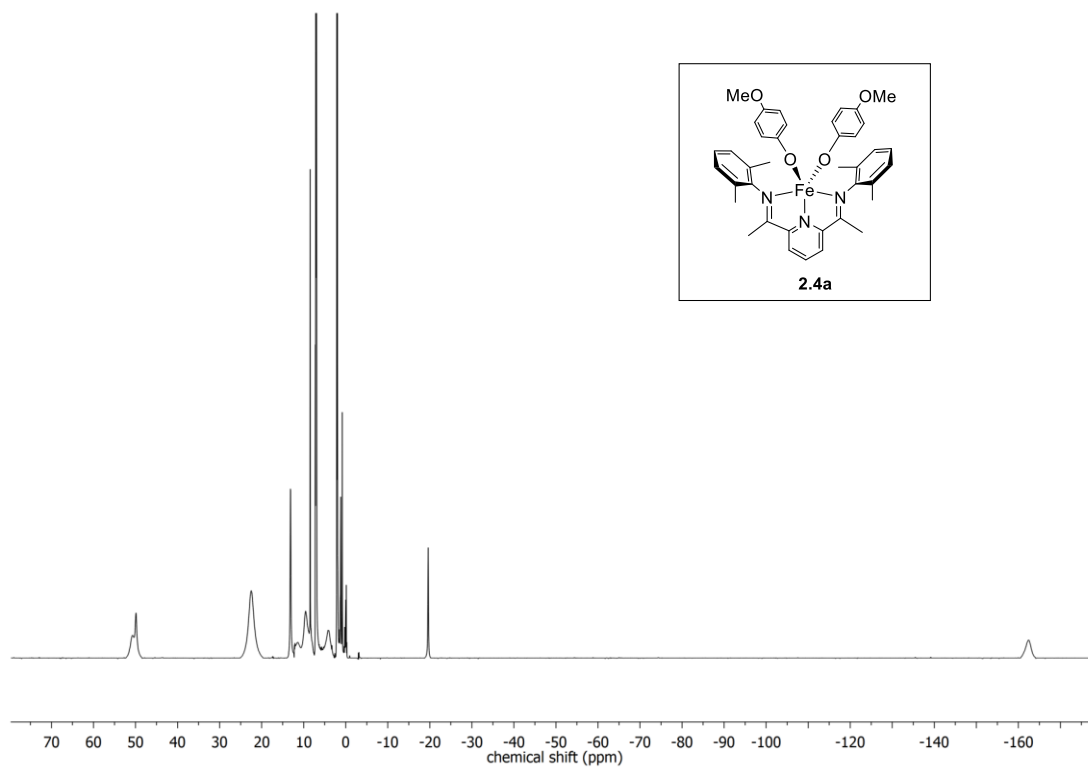


**Figure B.1.**  $^1\text{H}$  NMR spectrum of  $\text{Fe}(\text{PDI})(4\text{-methoxyphenoxide})_2$  (**2.4a**) in  $\text{C}_6\text{D}_6$  (25°C, 500 MHz).

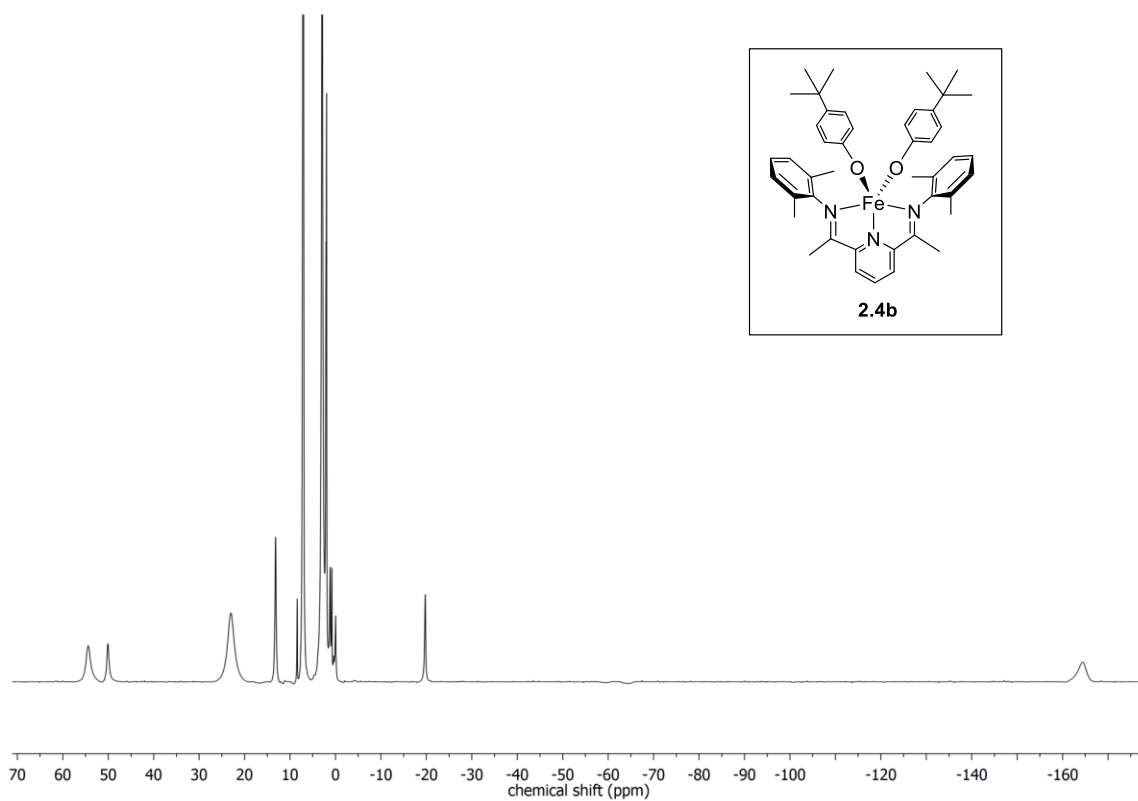


**Figure B.2.**  $^1\text{H}$  NMR spectrum of  $\text{Fe}(\text{PDI})(4\text{-}t\text{-butylphenoxide})_2$  (**2.4b**) in  $\text{C}_6\text{D}_6$  (25°C, 500 MHz).



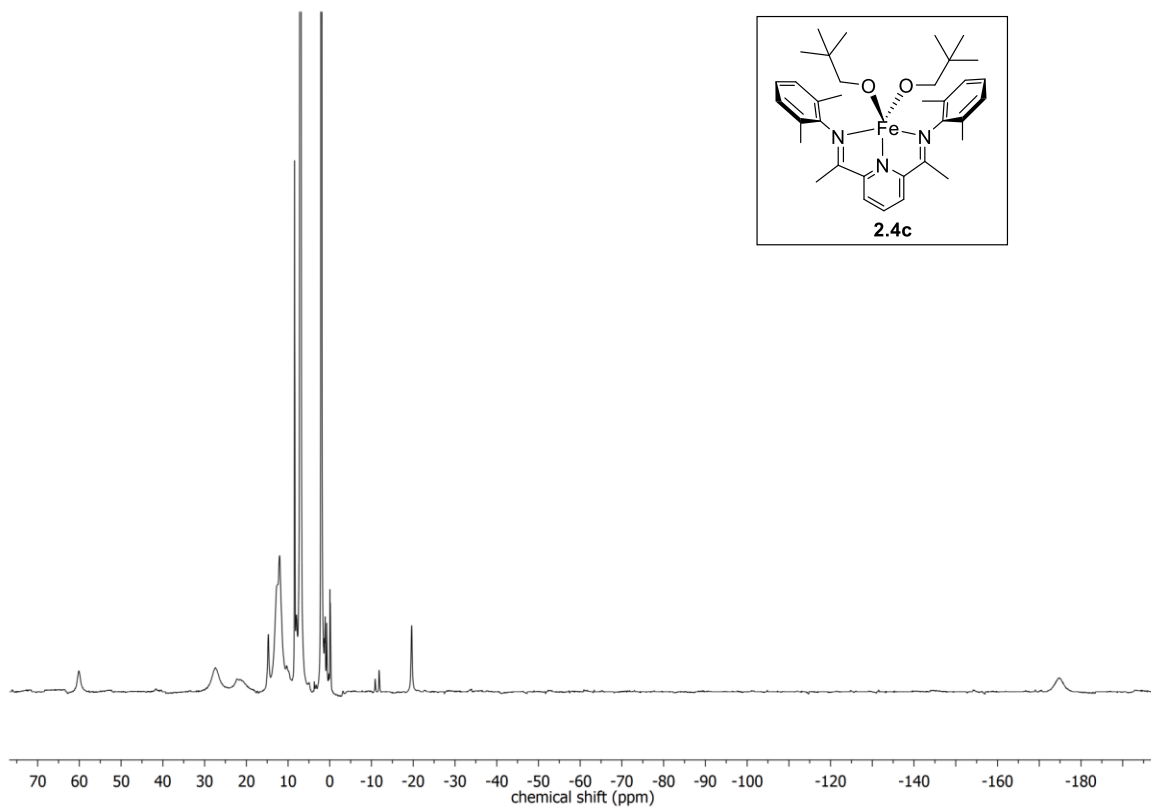


**Figure B.3.**  $^1\text{H}$  NMR spectrum of  $\text{Fe}(\text{PDI})(\text{neopentoxide})_2$  (**2.4c**) in  $\text{C}_6\text{D}_6$  ( $25^\circ\text{C}$ , 500 MHz).

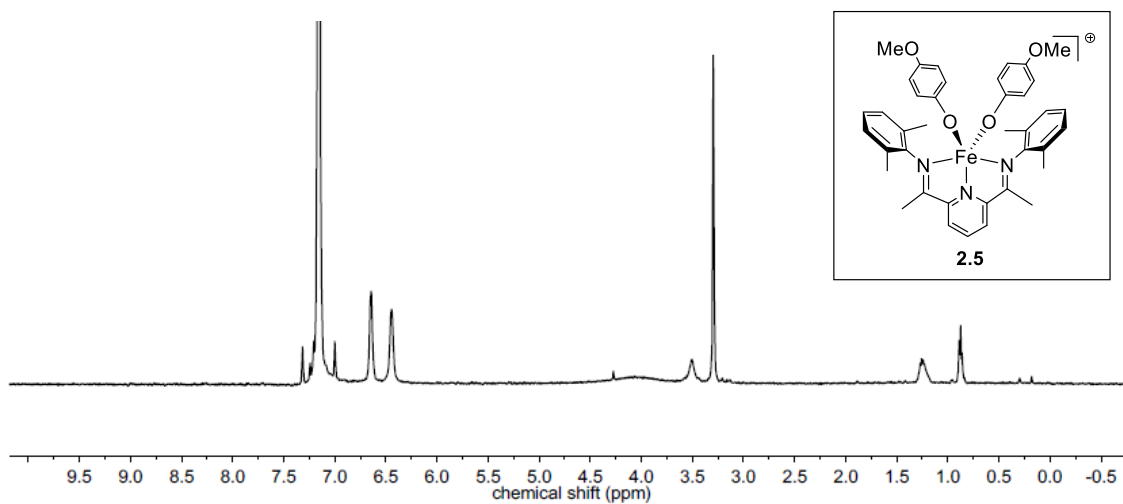


**Figure B.4.**  $^1\text{H}$  NMR spectrum of  $[\text{Fe}(\text{PDI})(4\text{-methoxyphenoxide})_2][\text{PF}_6]$  (**2.5**) in  $\text{C}_6\text{D}_6$  ( $25^\circ\text{C}$ , 500 MHz).



## B.2 NMR Spectra from Chapter 4

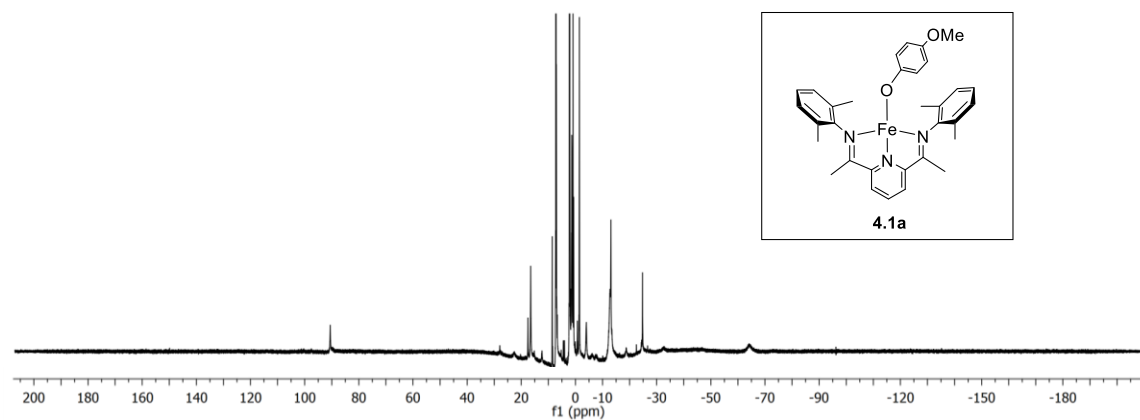


**Figure B.10.**  $^1\text{H}$  NMR of Fe(PDI)(4-methoxyphenoxide) (**4.1a**) in  $\text{C}_6\text{D}_6$  (25°C, 500 MHz).

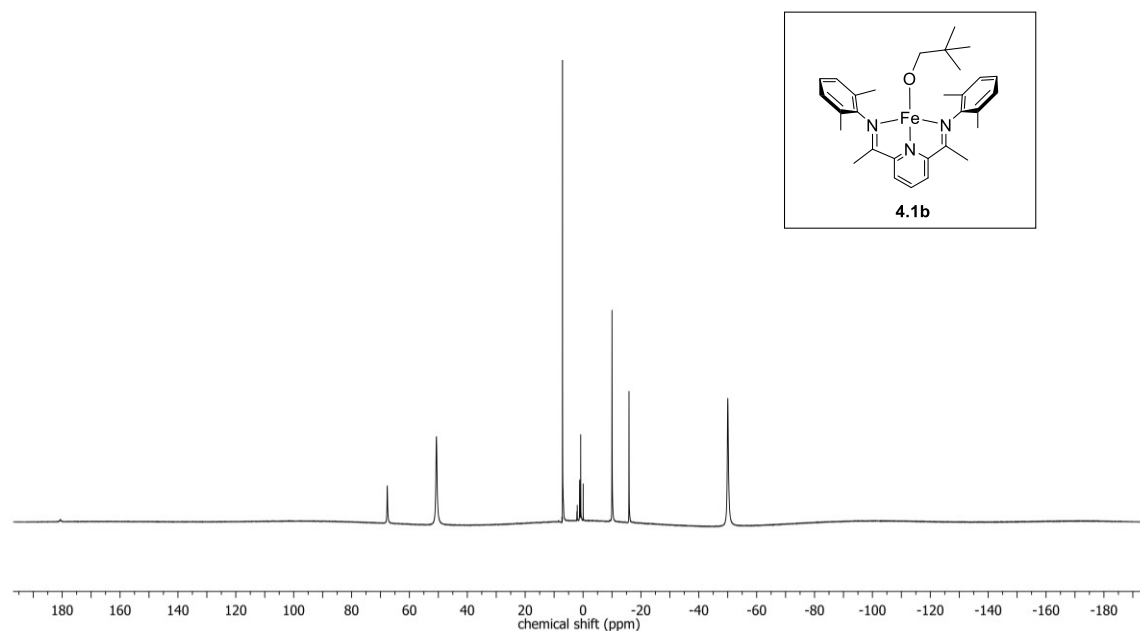


**Figure B.11.**  $^1\text{H}$  NMR spectrum of Fe(PDI)(neopentoxide) (**4.1b**) in  $\text{C}_6\text{D}_6$  (25°C, 500 MHz).

## Appendix C: Additional Polymer Molecular Weight Data

### C.1 Cyclohexene oxide polymerization molecular weight data from Chapter 3

**Table C.1.** Molecular weight and dispersities over time for redox-switching cyclohexene oxide (CHO) polymerization.

Time (min.)	CHO conv. (%)	$M_n$ (kg/mol) <sup>a</sup>	$\bar{D}^b$
10	14	17.2	2.41
20	21	20.0	2.24
30	25	21.1	2.24
40	31	20.1	2.18
50	36	18.9	1.94
(CoCp <sub>2</sub> added)			
60	38	22.7	2.03
70	38	27.4	1.72
80	38	21.4	2.09
90	38	29.0	1.91
(FcPF <sub>6</sub> added)			
100	42	28.2	1.70
110	45	21.9	2.12
120	47	25.0	1.94
140	50	22.5	2.04

<sup>a</sup>Molecular weights were determined by GPC relative to polystyrene standards. <sup>b</sup>PDI =  $M_w/M_n$ .

## C.2 Lactide-epoxide copolymerization data from Chapter 3

**Table C.2.** Lactide-epoxide copolymerization data with a 1:1 monomer ratio<sup>a</sup> (Table 3.3, entry 1)

Entry	$M_n$ (kg/mol) <sup>b</sup>	$M_w/M_n$	[PLA]:[PCHO] <sup>c</sup>	Mass recov. (%)
After step <i>i</i>	11.9	1.21	--	--
After step <i>ii</i> (unpurified)	6.0	2.20	1:1	--
Acetone filtrate	8.8	1.77	2:1	96
Acetone ppt.	8.9	1.74	0:1	4
Hexanes filtrate	0.7	6.89	1:27	29
Hexanes ppt.	10.2	1.52	7:1	67

<sup>a</sup>The reaction mixture was precipitated from acetone to remove homopolyether. The material collected from the acetone filtrate was then precipitated from hexanes to isolate copolymer and remove some low molecular weight homopolyether. <sup>b</sup>Determined by refractive index detector relative to polystyrene standards. <sup>c</sup>Determined by <sup>1</sup>H NMR.

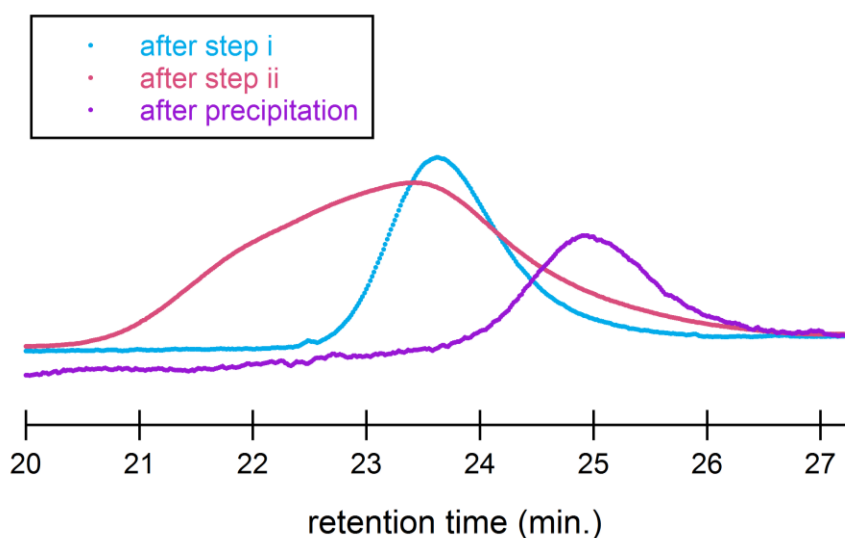


**Figure C.1.** GPC traces for lactide-cyclohexene oxide copolymerization with [lactide]:[cyclohexene oxide] = 1:5 (Table 3.3, entry 3) after step *i* (lactide polymerization), step *ii* (epoxide polymerization), and precipitation to isolate the block copolymer.

**Table C.3.** Lactide-epoxide copolymerization data with a 5:1 [L]:[CHO] ratio<sup>a</sup> (Table 3.3, entry 3)

Entry	M <sub>n</sub> (kg/mol) <sup>b</sup>	M <sub>w</sub> /M <sub>n</sub>	[PLA]:[PCHO] <sup>c</sup>	Mass recov. (%)
After step <i>i</i>	10.0	1.17	--	--
After step <i>ii</i> (unpurified)	10.3	2.68	1:1	--
Acetone filtrate	7.3	2.13	1:2	54
Acetone ppt.	14.9	2.21	1:23	35
Hexanes filtrate	5.0	2.50	1:12	58
Hexanes ppt.	3.5	1.39	5:1	37

<sup>a</sup>The reaction mixture was precipitated from acetone to remove homopolyether. The material collected from the acetone filtrate was then precipitated from hexanes to isolate copolymer and remove some low molecular weight homopolyether. <sup>b</sup>Determined by refractive index detector relative to polystyrene standards. <sup>c</sup>Determined by <sup>1</sup>H NMR.

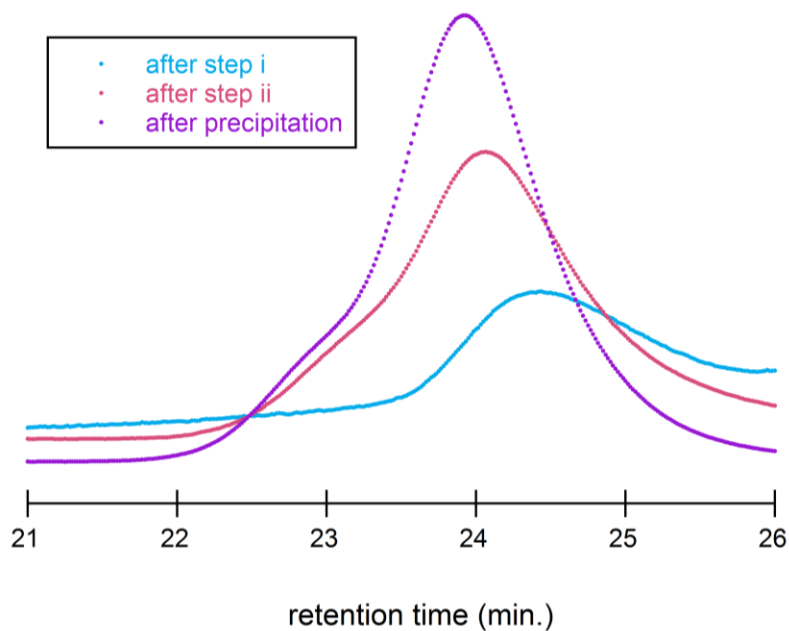


**Figure C.2.** GPC traces for lactide-cyclohexene oxide copolymerization with [lactide]:[cyclohexene oxide] = 1:1 where lactide polymerization was switched off before full conversion was reached (Table 3.3, entry 4) after step *i* (lactide polymerization), step *ii* (epoxide polymerization), and precipitation to isolate the block copolymer.

**Table C.4.** Lactide-epoxide copolymerization data with a 1:1 monomer ratio where the lactide polymerization is switched off before full conversion is reached<sup>a</sup> (Table 3.3, entry 4)

Entry	M <sub>n</sub> (kg/mol) <sup>b</sup>	M <sub>w</sub> /M <sub>n</sub>	[PLA]:[PCHO] <sup>c</sup>	Mass recov. (%)
After step <i>i</i>	4.5	1.3	--	--
After step <i>ii</i> (unpurified)	3.4	1.6	1:2	--
Acetone filtrate	1.7	2.1	1:2	81
Acetone ppt.	1.8	3.6	1:8	2
Hexanes filtrate	0.8	3.2	1:9	58
Hexanes ppt.	1.7	2.0	4:1	28

<sup>a</sup>The reaction mixture was precipitated from acetone to remove homopolyether. The material collected from the acetone filtrate was then precipitated from hexanes to isolate copolymer and remove some low molecular weight homopolyether. <sup>b</sup>Determined by refractive index detector relative to polystyrene standards. <sup>c</sup>Determined by <sup>1</sup>H NMR.

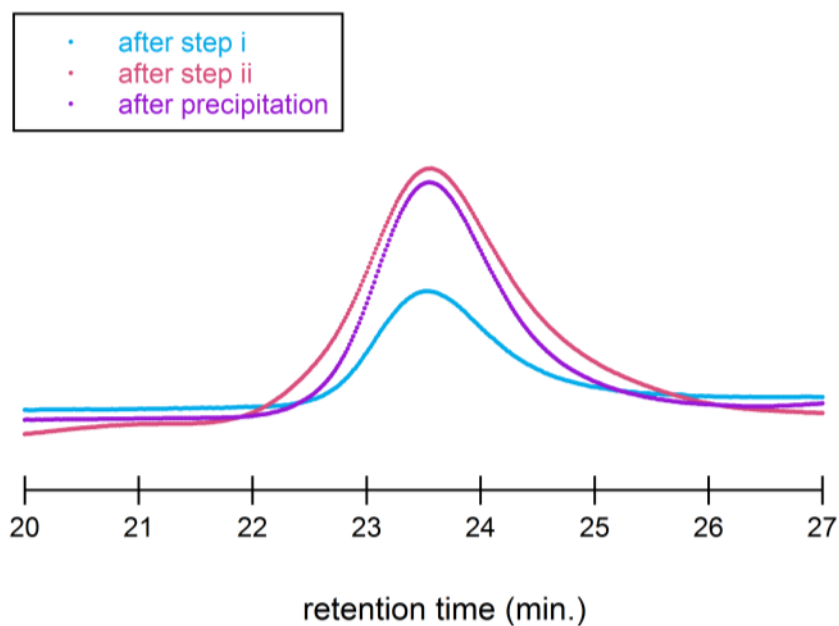


**Figure C.3.** GPC traces for sequential lactide-cyclohexene oxide copolymerization with [lactide]:[cyclohexene oxide] = 1:1 (Table 3.3, entry 2) after step *i* (lactide polymerization), step *ii* (epoxide polymerization), and precipitation to isolate the block copolymer.

**Table C.5.** Sequential lactide-epoxide copolymerization data with a 1:1 monomer ratio<sup>a</sup> (Table 3.3, entry 2)

Entry	M <sub>n</sub> (kg/mol) <sup>b</sup>	M <sub>w</sub> /M <sub>n</sub>	[PLA]:[PCHO] <sup>c</sup>	Mass recov. (%)
After step <i>i</i>	11.2	1.2	--	--
After step <i>ii</i> (unpurified)	7.7	1.9	3:1	--
Acetone filtrate	8.0	1.7	2:1	86
Acetone ppt.	8.9	1.6	1:100	2
Hexanes filtrate	1.2	18.6	1:20	32
Hexanes ppt.	9.2	1.4	7:1	63

<sup>a</sup>The reaction mixture was precipitated from acetone to remove homopolyether. The material collected from the acetone filtrate was then precipitated from hexanes to isolate copolymer and remove some low molecular weight homopolyether. <sup>b</sup>Determined by refractive index detector relative to polystyrene standards. <sup>c</sup>Determined by <sup>1</sup>H NMR.

**Table C.6.** Lactide-Epoxy Copolymer molecular weight data by GPC and <sup>1</sup>H NMR.

Entry	After step <i>i</i>			After step <i>ii</i> and precipitation <sup>a</sup>			
	M <sub>n</sub> (GPC-RI) <sup>b</sup>	M <sub>n</sub> (GPC-LS) <sup>c</sup>	M <sub>n</sub> (NMR) <sup>d</sup>	M <sub>n</sub> (GPC-RI) <sup>b</sup>	M <sub>n</sub> (GPC-LS) <sup>c</sup>	M <sub>n</sub> (NMR) <sup>d</sup>	[PLA]: [PCHO] <sup>e</sup>
<b>1</b>	11.9	n.d.	9.0	11.2	37.5	10.6	7:1
<b>2<sup>f</sup></b>	11.2	12.1	8.0	9.2	27.2	9.3	7:1
<b>3<sup>g</sup></b>	10.0	n.d.	8.5	3.5	20.1	9.1	5:1
<b>4<sup>h</sup></b>	4.5	n.d.	n.d.	1.7	27.0	1.3	4:1

<sup>a</sup>Isolated by precipitation from acetone and hexanes. <sup>b</sup>kg/mol, determined by GPC relative to refractive index detector relative to polystyrene standards. <sup>c</sup>kg/mol, determined by GPC with light scattering detector <sup>d</sup>kg/mol, determined by <sup>1</sup>H NMR integration ratio of methine peaks of polymer and aromatic peaks of 4-methoxyphenoxide end groups multiplied by molecular weight of monomer. <sup>e</sup>Determined by <sup>1</sup>H NMR. <sup>f</sup>Epoxide added in step *ii* after FcPF<sub>6</sub>. <sup>g</sup>[CHO]:[L] = 5:1 ([CHO] = 0.80M). <sup>h</sup>Step *i* carried out for 15 min.



### C.3 Cyclohexene oxide-lactide copolymerization molecular weight data from Chapter 3

**Table C.7.** Epoxide-lactide copolymerization data with a 1:1 monomer ratio<sup>a</sup> (Table 3.6, entry 1)

Entry	M <sub>n</sub> (kg/mol) <sup>b</sup>	M <sub>w</sub> /M <sub>n</sub>	[PLA]:[PCHO] <sup>c</sup>	Mass recov. (%)
After step <i>i</i>	1.2	1.9	--	--
After step <i>ii</i> (unpurified)	9.7	1.4	8:1	--
Acetone filtrate	8.9	1.4	8:1	93
Acetone ppt.	n.d. <sup>d</sup>	n.d. <sup>d</sup>	0:1	2
Hexanes filtrate	1.0	4.1	1:98	4
Hexanes ppt.	10.6	1.4	9:1	96

<sup>a</sup>The reaction mixture was precipitated from acetone to remove homopolyether. The material collected from the acetone filtrate was then precipitated from hexanes to isolate copolymer and remove some low molecular weight homopolyether. <sup>b</sup>Determined by refractive index detector relative to polystyrene standards. <sup>c</sup>Determined by <sup>1</sup>H NMR. <sup>d</sup>Not determined; not enough sample collected to observe a response by GPC.

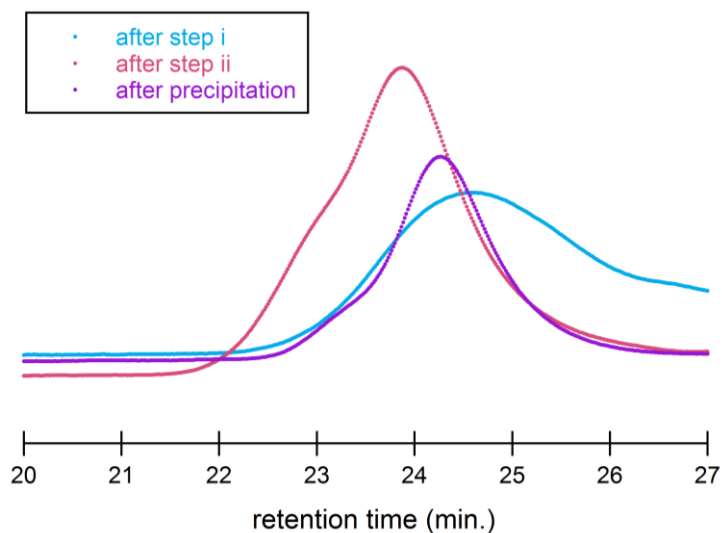


**Figure C.4.** GPC traces for cyclohexene oxide-lactide copolymerization with [lactide]:[cyclohexene oxide] = 5:1 (Table 3.6, entry 3) after step *i* (epoxide polymerization), step *ii* (lactide polymerization), and precipitation to isolate the block copolymer.

**Table C.8.** Epoxide-lactide copolymerization data with a 5:1 [L]:[CHO] ratio<sup>a</sup> (Table 3.6, entry 3)

Entry	M <sub>n</sub> (kg/mol) <sup>b</sup>	M <sub>w</sub> /M <sub>n</sub>	[PLA]:[PCHO] <sup>c</sup>	Mass recov. (%)
After step <i>i</i>	1.2	2.0	--	--
After step <i>ii</i> (unpurified)	7.1	1.8	1:3	--
Acetone filtrate	7.1	1.7	1:1	66
Acetone ppt.	12.8	1.4	1:99	19
Hexanes filtrate	8.4	2.0	1:11	31
Hexanes ppt.	5.8	1.4	3:1	65

<sup>a</sup>The reaction mixture was precipitated from acetone to remove homopolyether. The material collected from the acetone filtrate was then precipitated from hexanes to isolate copolymer and remove some low molecular weight homopolyether. <sup>b</sup>Determined by refractive index detector relative to polystyrene standards. <sup>c</sup>Determined by <sup>1</sup>H NMR.

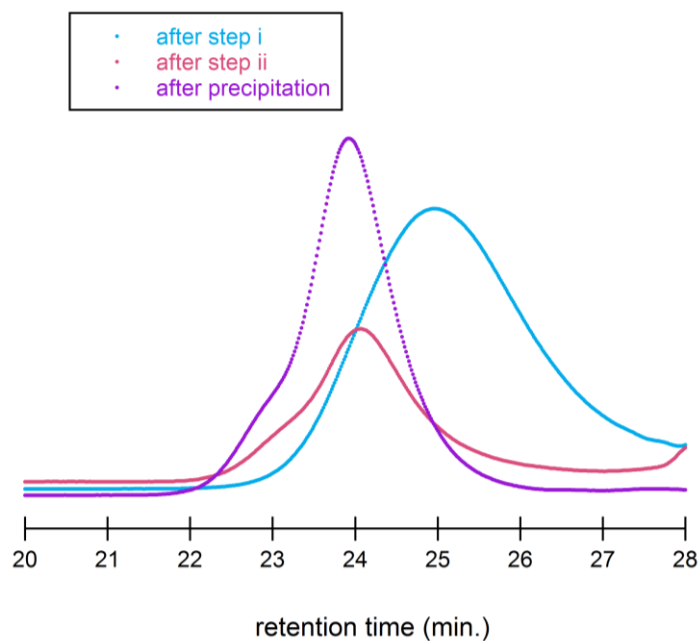


**Figure C.5.** GPC traces for cyclohexene oxide-lactide copolymerization with [lactide]:[cyclohexene oxide] = 5:1 where epoxide polymerization was switched off before full conversion was reached (Table 3.6, entry 4) after step *i* (epoxide polymerization), step *ii* (lactide polymerization), and precipitation to isolate the block copolymer.

**Table C.9.** Epoxide-lactide copolymerization data with a 5:1 [L]:[CHO] ratio where the lactide polymerization is switched off before full conversion is reached<sup>a</sup> (Table 3.6, entry 4)

Entry	M <sub>n</sub> (kg/mol) <sup>b</sup>	M <sub>w</sub> /M <sub>n</sub>	[PLA]:[PCHO] <sup>c</sup>	Mass recov. (%)
After step <i>i</i>	2.2	2.4	--	--
After step <i>ii</i> (unpurified)	8.8	1.4	1:3	--
Acetone filtrate	7.4	1.5	1:3	96
Acetone ppt.	9.3	1.5	1:42	2
Hexanes filtrate	8.0	2.0	1:7	37
Hexanes ppt.	11.6	1.4	3:1	44

<sup>a</sup>The reaction mixture was precipitated from acetone to remove homopolyether. The material collected from the acetone filtrate was then precipitated from hexanes to isolate copolymer and remove some low molecular weight homopolyether. <sup>b</sup>Determined by refractive index detector relative to polystyrene standards. <sup>c</sup>Determined by <sup>1</sup>H NMR.

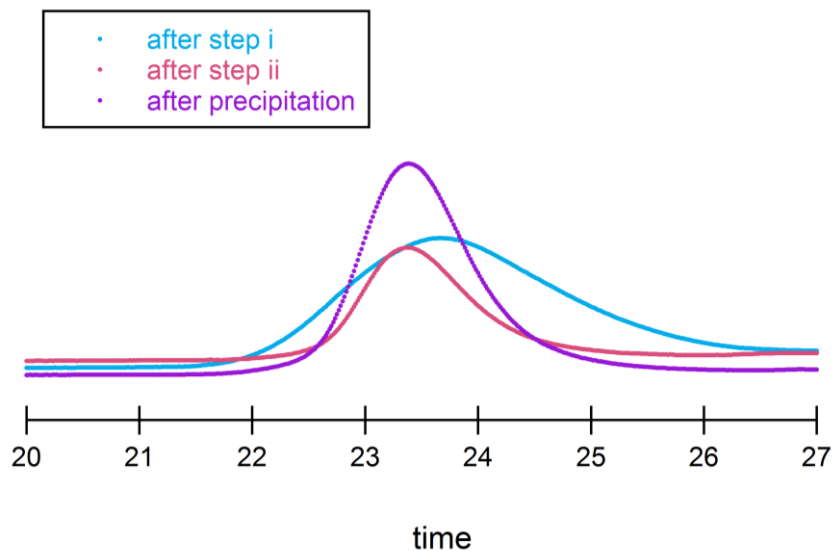


**Figure C.6.** GPC traces for sequential cyclohexene oxide-lactide copolymerization with [lactide]:[cyclohexene oxide] = 1:1 (Table 3.6, entry 2) after step *i* (epoxide polymerization), step *ii* (lactide polymerization), and precipitation to isolate the block copolymer.

**Table C.10.** Sequential epoxide-lactide copolymerization data with a 1:1 monomer ratio<sup>a</sup> (Table 3.6, entry 2)

Entry	M <sub>n</sub> (kg/mol) <sup>b</sup>	M <sub>w</sub> /M <sub>n</sub>	[PLA]:[PCHO] <sup>c</sup>	Mass recov. (%)
After step <i>i</i>	7.4	1.8	--	--
After step <i>ii</i> (unpurified)	12.5	1.4	7:1	--
Acetone filtrate	12.3	1.4	7:1	93
Acetone ppt.	15.2	2.0	1:20	2
Hexanes filtrate	1.5	4.2	1:14	15
Hexanes ppt.	11.5	1.3	9:1	85

<sup>a</sup>The reaction mixture was precipitated from acetone to remove homopolyether. The material collected from the acetone filtrate was then precipitated from hexanes to isolate copolymer and remove some low molecular weight homopolyether. <sup>b</sup>Determined by refractive index detector relative to polystyrene standards. <sup>c</sup>Determined by <sup>1</sup>H NMR.

**Table C.11.** Copolymer molecular weight data by GPC and <sup>1</sup>H NMR.

Entry	After step <i>i</i>			After step <i>ii</i> and precipitation <sup>a</sup>			
	M <sub>n</sub> (GPC-RI) <sup>b</sup>	M <sub>n</sub> (GPC-LS) <sup>c</sup>	M <sub>n</sub> (NMR) <sup>d</sup>	M <sub>n</sub> (GPC-RI) <sup>b</sup>	M <sub>n</sub> (GPC-LS) <sup>c</sup>	M <sub>n</sub> (NMR) <sup>d</sup>	[PLA]: [PCHO] <sup>e</sup>
<b>1</b>	1.2	22.8	n.d.	10.6	30.9	10.3	9:1
<b>2<sup>g</sup></b>	7.4	n.d.	n.d.	12.5	20.5	13.3	9:1
<b>3<sup>f</sup></b>	1.2	n.d.	n.d.	5.8	34.6	17.9	3:1
<b>4<sup>f,h</sup></b>	2.2	n.d.	n.d.	11.6	30.1	11.5	3:1

<sup>a</sup>Isolated by precipitation from acetone and hexanes. <sup>b</sup>kg/mol, determined by GPC with refractive index detector relative to polystyrene standards. <sup>c</sup>kg/mol, determined by GPC with light scattering detector <sup>d</sup>kg/mol, determined by <sup>1</sup>H NMR integration ratio of methine peaks of polymer and aromatic peaks of 4-methoxyphenoxide end groups multiplied by molecular weight of monomer. <sup>e</sup>Determined by <sup>1</sup>H NMR. <sup>f</sup>[CHO]:[L] = 5:1 ([CHO] = 0.80M). <sup>g</sup>Lactide added in step *ii* after CoCp<sub>2</sub>. <sup>h</sup>Step *i* carried out for 30 min.